# CONDITIONING OF MESENCHYMAL STEM CELLS INITIATES CARDIOGENIC DIFFERENTIATION AND INCREASES FUNCTION IN INFARCTED HEARTS

A Dissertation

Submitted to the Faculty of the

WORCESTER POLYTECHNIC INSTITUTE

In partial fulfillment of the requirements for the Degree of

Doctorate of Philosophy in Biomedical Engineering

November 23rd, 2011

By

Jacques Paul Guyette

Approved by:

**ACKNOWLEDGEMENTS**

In the completion of this work, I owe a great deal of gratitude to those who have aided me in my personal and scientific growth. First and foremost, I must thank Glenn R. Gaudette, Ph.D., for all of his help and mentorship. Whether he is getting his hands dirty in the lab, advising on various aspects of a project, or providing professional guidance, Glenn has been an instrumental force throughout my graduate experience. He has provided me the tremendous opportunity to do high-impact work in the field of cardiac regeneration, which had been a goal of mine long before I entered graduate school. Through his mentoring, I have grown as a scientist to continually develop a strong knowledgebase, critical-eye, and work ethic. By allowing me the freedom to try new ideas and creative approaches, he has instilled in me a professional level of self-confidence. I am certain that his mentoring has prepared for the next stages of my scientific career, and I am deeply grateful.

I would also like to thank my dissertation committee, my advisors, the WPI BME department, as well as the WPI BME and Life Sciences faculty. Their passion for biomedical engineering and science is palpable, as they are truly committed to the "Lehr and Kunst" philosophy of WPI. Through their teaching and guidance, they have challenged me to think, grow, and become a better researcher. In addition, I am grateful to have developed several lasting relationships that will remain strong once I leave WPI.

I could not have accomplished this body of work without the many "helping-hands" of the WPI community. I would like to extend my thanks to staff members who facilitated me with preparation and implementation of several aspects of my project such as staining & histology, surgery preparation, animal care in the vivarium, and microscopy analysis. In addition, I would like to thank fellow graduate students and collaborating labs for their continued support and help, whether it was a quick question in passing, a debate over data, or showing my how to implement new techniques. I would also like to thank fellow Gaudette Lab members and undergraduate volunteers who helped in my project, for their willingness to take on difficult tasks as well as their dedication and commitment to see them through. All of you have challenged me to think differently, to broaden my approach to scientific problems, and to become a better leader.

Lastly, but certainly not least, I would like to thank my family and friends. Your support and patience has been invaluable, and has allowed me to keep an "even keel" throughout my graduate school process.

**TABLE OF CONTENTS**

**TABLE OF FIGURES**

**TABLE OF TABLES**

**ABBREVIATIONS**

ACE – angiotensin-converting enzyme
ACTN2 – gene corresponding with sarcomeric α-Actinin; cardiac-specific marker
AHA – American Heart Association
ANOVA – analysis of variance
ATP – adenosine triphosphate
BMCs – bone marrow cells
BMP-4 – bone morphogenetic protein 4; signaling protein
BOOST – BOne marrOw transfer to enhance ST-elevation infarct regeneration; title of a clinical trial
$Ca^{2+}$ - calcium ion, calcium
CaCNA1C – L-type calcium channel α1C subunit
CaCNA1D – L-type calcium channel α1D subunit
CaCNA1S – L-type calcium channel α1S subunit
CASI – computer aided speckle interferometry
cDNA – complimentary deoxyribonucleic acid
CHD – coronary heart disease
$CO_2$ – carbon dioxide
CSCs – cardiac stem cells
cTnI – cardiac troponin I; cardiac-specific marker
cTnT – cardiac troponin T; cardiac-specific marker
DMEM – Dulbecco's Modified Eagle's Medium
DNA – deoxyribonucleic acid
dNTPs – deoxyribonucleotides triphosphates
dP/dt – change in ventricular pressure over change in time
EBs – embryoid bodies
ECHO – echocardiography
ECM – extracellular matrix
EDA – end diastolic area
EDV – end diastolic volume
EF – ejection fraction
EGFP – enhanced green fluorescent protein
EKG – electrocardiogram
ELISA – enzyme linked immunosorbent assay
ESA – end systolic area
ESCs – embryonic stem cells
ESPVR – end systolic pressure-volume relationship
ESV – end systolic volume
FGF-2 – Fibroblast growth factor 2
GAPDH – glyceraldehyde-3-phosphate dehydrogenase
GATA-4 – cardiac transcription factor
GFP – green fluorescent protein
HDM – high density mapping
HF – heart failure
Hg – mercury; element, unit of pressure
HGF – hepatocyte growth factor
hMSCs – human mesenchymal stem cells
IC – intracoronary
ICC – immunocytochemistry
IHC – immunohistochemistry
IM – intramyocardial

iPSCs – induced pluripotent stem cells
IV – intravenous
LAD – Left Anterior Descending coronary artery
LV – left ventricle, or left ventricular
LVEDP – left ventricular end-diastolic pressure
MEF2C – myocyte enhancement factor 2C, cardiac transcription factor
MESP1 – cardiac transcription factor
mg – milligram
MHCβ – myosin heavy chain beta; cardiac-specific marker
MI – myocardial infarction
mL – milliliter
MRI – magnetic resonance imaging
MSCGM – Mesenchymal Stem Cell Growth Media
MSCs – mesenchymal stem cells
MYLC2A – myosin light chain 2A subunit; cardiac-specific marker
MYLC2V – myosin light chain 2V subunit; cardiac-specific marker
$N_2$ – nitrogen
ng – nanogram
Nkx2.5 – cardiac transcription factor
nm – nanometer
$O_2$ – oxygen
P – pressure, or ventricular pressure
PBS – phosphate buffered saline
PDGF – platelet derived growth factor; signaling protein
PDs – population doublings
pg – picogram
PI3K – phophatidylinositol 3-kinase; intracellular effector protein
pM – picomolar, picomoles
PRSW – preload recruitable stroke work
QDs – quantum-dots; referring to quantum-dot nanoparticles
RNA – ribonucleic acid
rpm – rotations per minute
RSW – regional stroke work
RT-PCR – reverse transcriptase polymerase chain reaction
SAC – systolic area contraction
STI – speckle tracking imaging
SV – stroke volume
SW – stroke work
TBX5 – T-box transcription factor 5, cardiac transcription factor
TGF-β – transforming growth factor beta; signaling protein
μg – microgram
μL – microliter
μm – micrometer, micron
μM – micromolar

## ABSTRACT

Current treatment options are limited for patients with myocardial infarction or heart failure. Cellular cardiomyoplasty is a promising therapeutic strategy being investigated as a potential treatment, which aims to deliver exogenous cells to the infarcted heart, for the purpose of restoring healthy myocardial mass and mechanical cardiac function. While several cell types have been studied for this application, only bone marrow cells and human mesenchymal stem cells (hMSCs) have been shown to be safe and effective for improving cardiac function in clinical trials. In both human and animal studies, the delivery of hMSCs to infarcted myocardium decreased inflammatory response, promoted cardiomyocyte survival, and improved cardiac functional indices.

While the benefits of using hMSCs as a cell therapy for cardiac repair are encouraging, **the desired expectation of cardiomyoplasty is to increase cardiomyocyte content that will contribute to active cardiac mechanical function.** Delivered cells may increase myocyte content by several different mechanisms such as differentiating to a cardiomyocyte lineage, secreting paracrine factors that increase native stem cell differentiation, or secreting factors that increase native myocyte proliferation. Considerable work suggests that hMSCs can differentiate towards a cardiomyocyte lineage based on measured milestones such as cardiac-specific marker expression, sarcomere formation, ion current propagation, and gap junction formation. However, current methods for cardiac differentiation of hMSCs have significant limitations. Current differentiation techniques are complicated and tedious, signaling pathways and mechanisms are largely unknown, and only a small percentage of hMSCs appear to exhibit cardiogenic traits.

In this body of work, we developed a simple strategy to initiate cardiac differentiation of hMSCs *in vitro*. Incorporating environmental cues typically found in a myocardial infarct (e.g. decreased oxygen tension and increased concentrations of cell-signaling factors), our novel *in vitro* conditioning regimen combines reduced-$O_2$ culture and hepatocyte growth factor (HGF) treatment. Reduced-$O_2$ culturing of hMSCs has shown to enhance differentiation, tissue formation, and the release of cardioprotective signaling factors. HGF is a pleiotropic cytokine involved in several biological processes including developmental cardiomyogenesis, through its interaction with the tyrosine kinase receptor c-Met. We hypothesize that applying a combined conditioning treatment of reduced-$O_2$ and HGF to hMSCs *in vitro* will enhance cardiac-specific gene and protein expression. Additionally, the transplantation of conditioned hMSCs into an *in vivo* infarct model will result in differentiation of delivered hMSCs and improved cardiac mechanical function.

In testing our hypothesis, we show that reduced-$O_2$ culturing can enhance hMSC growth kinetics and total c-Met expression. Combining reduced-$O_2$ culturing with HGF treatment, hMSCs can be conditioned to express cardiac-specific genes and proteins *in vitro*. Using small-molecule inhibitors to target specific effector proteins in a proposed HGF/c-Met signaling pathway, treated reduced-$O_2$/HGF hMSCs show a decrease in cardiac gene expression. When implanted into rat infarcts *in vivo*, reduced-$O_2$/HGF conditioned hMSCs increase regional cardiac mechanics within the infarct region at 1 week and 1 month. Further analysis from the *in vivo* study showed a significant increase in the retention of reduced-$O_2$/HGF conditioned hMSCs. Immunohistochemistry showed that some of the reduced-$O_2$/HGF conditioned hMSCs express cardiac-specific proteins *in vivo*. These results suggest that a combined regimen of reduced-$O_2$ and HGF conditioning increases cardiac-specific marker expression in hMSCs *in vitro*. In addition, the implantation of reduced-$O_2$/HGF conditioned hMSCs into an infarct significantly improves cardiac function, with contributing factors of improved cell retention and possible increases in myocyte content. Overall, we developed a simple *in vitro* conditioning regimen to improve cardiac differentiation capabilities in hMSCs, in order to enhance the outcomes of using hMSCs as a cell therapy for the diseased heart.

# CHAPTER 1: Overview

## 1.1. Introduction

According to the 2011 heart disease statistics published by the American Heart Association, an estimated 16.3 million Americans ≥20 years of age are living with coronary heart disease (CHD), which is reported as the most prevalent cause of death of American men and women.[1] As a leading indication of CHD, 7.2 million of these American adults have also experienced a myocardial infarction (MI), or heart attack.[1] Though the severity of MIs can vary, all MIs result in the death of cardiomyocytes, which compromises the heart's functional capability and endangers one's survival. Current treatment options are limited for MI patients. Despite novel surgical and pharmaceutical interventions aiming to treat scarred myocardium, they fail to address the fundamental need to replace the necrotic cardiomyocytes with new contractile cells in order to restore active cardiac mechanical function.[2] Currently, heart transplantation is the only viable treatment for the replacement of necrotic myocardium. However, less than 2,200 hearts are donated per year,[1,3] which does not satisfy the demand of MI patients in need. Developing methods and techniques for generating new cardiomyocytes, which can replace necrotic myocardium and be made available to a wider audience of patients, will have a significant impact on the long-term survival of millions of Americans.

Over the past decade, a strong focus in regenerative medicine has aimed to develop strategies that treat the diseased heart. Cardiomyocytes were once thought to be a post-mitotic cell-type, incapable of self-regeneration. However, new endogenous and exogenous cell therapies for myocardial regeneration have emerged from an increasing understanding of cardiac development, cardiomyocyte cell biology, stem cell biology, and cardiomyoplasty. Recent data suggests that 1-4% of cardiomyocytes are capable of proliferation *in vivo*,[4,5] the heart can recruit the body's own endogenous stem cells to regions of myocardial injury,[6,7] and the heart may also contain its own resident population of stem cells that can aid in self-repair.[8,9] Studies involving exogenous strategies have found that a small percentage of biopsied cardiomyocytes can be coerced to proliferate under specific conditions *in vitro*, and several different types of stem cells (i.e. mesenchymal stem cells, embryonic stem cells, cardiac stem cells, and induced

pluripotent stem cells) can differentiate towards a cardiac lineage.[10-14] While the achieved progress of endogenous methodologies warrants continued research, it has been shown that only 4% of the approximated 3 billion native cardiomyocytes in the left ventricle undergo proliferation.[5] With an estimated loss of about 1 billion cardiomyocytes during a severe MI,[15] it is unlikely that the new cardiomyocytes generated *in situ* from the 4% proliferative native myocytes can significantly improve or sustain function. Conversely, exogenous strategies for cardiomyocyte regeneration, by *in vitro* stem cell differentiation and cell expansion, have shown that it may be possible to generate enough new cardiomyocytes to replace the amount lost during an MI.[16-20]

Since exogenously generated cardiomyocytes are developed *in vitro*, the cells must be implanted in the heart for therapeutic applications. Cardiomyoplasty is a surgical approach which aims to deliver cells to the infarcted heart, for the ultimate purpose of restoring healthy myocardial mass and mechanical cardiac function. Delivered cells may restore myocardial mass by differentiating into cardiomyocytes that contribute mechanical function; however, delivered cells can also restore myocardial mass by secreting paracrine factors that can enhance native cardiomyocyte survival,[21] promote native myocyte proliferation,[10,22] recruit endogenous stem cells to the infarct area,[6,23,24] and possibly differentiate endogenous stem cells to cardiac phenotypes. While several cell types have been studied for this application,[13,14] only bone marrow cells (BMCs) and human mesenchymal stem cells (hMSCs) have been shown to be safe and effective for improving cardiac function in clinical trials.[25] In both human and animal studies, it has been shown that delivering hMSCs (and the subsequent paracrine factors) to infarcted myocardium decreases inflammation,[26-28] promotes cardiomyocyte survival,[21,29] and improves cardiac functional indices such as left ventricular systolic pressure, volume, and ejection fraction.[12,25,30-32] While the benefits of using hMSCs as a cell therapy for cardiac repair are encouraging, the desired expectation of cardiac cell therapy is to deliver new contractile cardiomyocytes that will contribute to active cardiac mechanical function. A considerable body of work suggests that hMSCs can differentiate towards a cardiomyocyte lineage based on measured milestones such as cardiac-specific marker

expression, sarcomere formation, ion current propagation, and gap junction formation (assessed and reviewed by Schuldt *et al*.).[13]

Despite the achievements of hMSC cardiac differentiation, however, these studies demonstrate considerable limitations. Only a small percentage of the cells express cardiac markers and it remains unclear if hMSCs can generate a mature, contractile cardiomyocyte phenotype. Since Anversa's initial study in 2001 suggesting that bone marrow cells could regenerate infarcted myocardium,[12] several groups have dedicated substantial time and resources to study the potential of bone marrow cells and bone marrow stem cells in cardiac repair. And while many of these researchers believe in the promise of cellular therapy for treating the diseased heart, conflicting results and reports raise a concern of whether bone marrow cells or hMSCs are appropriate cell-types for the task.[33] However, hMSCs remain a plentiful autologous cell source, which have been shown to be safe and effective for short-term improvement of ejection fraction for MI patients in clinical studies.[25] Herein lies the current controversy over the use of hMSCs as a cell therapy for cardiac repair. While some researchers have dismissed hMSCs in favor of new cell types and strategies, others continue to study hMSCs for new cardiac repair mechanisms and differentiation techniques.

In 2010, Behfar *et al*. showed that bone-marrow derived hMSCs harvested from coronary artery patients could be conditioned with a cocktail of recombinant factors for guided cardiopoiesis.[16] Treating hMSCs with transforming growth factor β1, bone morphogenetic protein-4, Activin A, retinoic acid, insulin-like growth factor-1, fibroblast growth factor-2, alpha-thrombin, and interleukin-6, they were able to increase expression of cardiac transcription factors such as Nkx 2.5, TBX5, MESP1, and MEF2C *in vitro*. Implanting these treated hMSCs into infarcted mouse hearts demonstrated an increased functional output, with sarcomeric and gap junction marker expression co-localized with human nuclear staining. These outcomes suggest that pre-emptive conditioning of hMSCs for cardiac lineage specification may improve their therapeutic benefit, claiming increased cardiomyocyte content from hMSCs and improved cardiac mechanical function.

Behfar *et al.*'s work is the latest study to suggest that hMSCs derived from adult bone marrow may have the capacity to regenerate myocardium.[16] However, this work iterates a unique paradigm in cell therapy: primitive multipotent cells, which have been conditioned to express fundamental organ-specific genes and proteins, can further differentiate into mature phenotypes once implanted *in vivo*, by being equipped with the appropriate cellular "machinery" to respond and adapt to the organ's microenvironmental cues. In 2008, our lab also used this paradigm to describe how mechanical manipulation of hMSCs by hanging drops could partially differentiate hMSCs towards a cardiomyocyte lineage to show cardiac marker expression and L-type calcium channel currents *in vitro*, while also improving mechanical function *in vivo*.[34] The paradigm certainly concedes that we do not fully understand the possible mechanisms involved in hMSC cardiac differentiation, but the idea of pre-conditioning hMSCs for early cardiopoiesis prior to implantation is gaining popularity.[35,36] A recent review by Marban and Malliaras, suggests that conditioning hMSCs in a "boot camp" of natural and embryonic signaling factors prior to implantation may improve both direct and indirect mechanisms of cardiac repair.[36] A simplistic strategy with fewer steps and factors for hMSC cardiac differentiation is likely to be more clinically applicable as it would simplify the FDA approval process and be easier to implement. In addition, a facile hMSC differentiation strategy is likely to garner industry support due to ease, decreased incubation time, and reduced resources. Exploring new conditioning regimens may help to overcome the current limitations of hMSC cardiac differentiation, and thereby improve hMSC cell therapy for the diseased heart.

### 1.2. Overall Goal and Hypothesis

The overall goal of this project is to enhance the effectiveness of using hMSCs for cardiomyoplasty by analyzing the effects of a unique *in vitro* conditioning regimen on hMSC growth kinetics, c-Met receptor expression, cardiac marker expression, HGF/c-Met pathway involvement in cardiac marker expression, and the changes in cardiac mechanical function when conditioned hMSCs are implanted into MIs *in vivo*.

**We hypothesize that applying a combined conditioning treatment of reduced-$O_2$ and HGF to hMSCs *in vitro* will enhance cardiac-specific gene and protein expression. Additionally, the transplantation of conditioned hMSCs into an *in vivo* MI model will result in cardiac specific differentiation of delivered hMSCs and improved cardiac mechanical function.**

In this study, early cardiac differentiation is defined as the expression or upregulation of cardiac genes, as well as the expression and localization of cardiac proteins. The expected outcome of this thesis is a novel and simplistic conditioning regimen to initiate cardiogenic differentiation of hMSCs *in vitro*, which allows for more mature cardiomyocyte differentiation *in vivo* and contribution to cardiac mechanical function. To systematically test this hypothesis, this thesis was separated into three parts, with five objectives.

### 1.3. Part I: Evaluation of reduced-$O_2$ conditions on mesenchymal stem cell function

#### 1.3.1. Objective 1: Determine effect of reduced-$O_2$ on hMSC growth kinetics and c-Met expression

Culturing hMSCs in a reduced-$O_2$ environment challenges the normal convention of traditional hMSC cell culture, which typically employs atmospheric $O_2$ concentrations. However, reduced-$O_2$ culturing of hMSCs has been shown to have a significant effect on signaling and response mechanisms that can affect proliferation, differentiation, and tissue formation.[21,28,37-40] In Chapter 3 of this thesis, we evaluated the effects of reduced-$O_2$ conditions on the growth potential of hMSCs. In addition, as HGF has been implicated in cardiac differentiation, we evaluate the expression of its receptor, c-Met tyrosine kinase. By defining a 7-day passaging parameter and controlling for the cell-seeding concentration at each passage, we systematically quantified the growth rate of hMSCs cultured in reduced-$O_2$ versus normal-$O_2$ conditions. Taking the average of multiple cell counts at each 7-day growth period, initial and final cell concentrations were used in an exponential function to calculate the number of population doublings. We

found that reduced-$O_2$ conditions significantly increased the total number of population doublings, doubling rate, and the number of passages before the cells become senescent. Additionally, we analyzed the expression of total c-Met in hMSCs over a time-course of reduced-$O_2$ culture. Quantifying expression by ELISA normalized to total protein, we found that expression for total c-Met was significantly increased at day 7 compared to other time points. Comparing the two oxygen conditions, reduced-$O_2$ cultured hMSCs also showed a significant increase in total c-Met expression at day 7. The growth results of this study serve to support a debated contention that reduced-$O_2$ can increase MSC proliferation, while the findings on c-Met expression help to define a parameter for our conditioning regimen to increase the number of receptors available for HGF binding and HGF/c-Met signaling.

## 1.4. Part II: Conditioning of hMSCs with reduced-$O_2$ and HGF to express cardiac markers

### 1.4.1. Objective 2A: Determine effect of combined conditioning on cardiac marker expression

Previous studies suggest that hMSCs have the potential to express cardiac markers. However, tedious mechanical manipulation or complicated growth factor treatments, with unknown differentiation mechanisms, can only produce a small percentage of cardiogenic hMSCs. For the purpose of exploring novel methods that will initiate cardiac-differentiation of hMSCs and improve upon current limitations, we developed a simplistic *in vitro* conditioning regimen based on two aspects described in the MSC literature. In Chapter 4 of this thesis, we evaluated the effects of a combined treatment of reduced-$O_2$ and HGF conditioning on the expression of cardiac markers in hMSCs *in vitro*. Based on the c-Met expression results from Objective 1, hMSCs were first conditioned in reduced-$O_2$ with growth medium for 7 days to increase the c-Met receptor expression. On day 7, growth medium was removed and replaced with DMEM supplemented with only HGF (20 ng/mL), and hMSCs were cultured for another 7 days. Using different plating formats depending on post-treatment analysis; cells were either harvested for RNA isolation or fixed in preparation for immunocytochemical analysis for cardiogenic protein expression. By RT-PCR, we found that a combined reduced-$O_2$/HGF conditioning regimen increased or elicited the expression of several cardiac genes including transcription factors, sarcomeric components,

and L-type calcium channel subunits. By immunocytochemistry, we found that conditioned cells also expressed cardiac proteins, which were localized to the appropriate cellular regions. These results indicate that a simplistic conditioning regimen using reduced-$O_2$ and HGF can initiate cardiac differentiation of hMSCs *in vitro*.

#### 1.4.2. Objective 2B: Evaluate the role of HGF/c-Met signaling in cardiac marker expression

In an effort to determine the involvement of HGF/c-Met signaling in the activation of downstream gene transcription for cardiac differentiation, we sought to analyze a proposed HGF signaling pathway. We treated reduced-$O_2$/HGF conditioned hMSCs with two small-molecule inhibitors that interact with specific targets in the HGF pathway. Each small-molecule inhibitor was tested separately with concentrations comparable to what is reported in the literature. Small molecule inhibitor PHA-665752 was used to block phosphorylation of the intracellular domain of c-Met. Small molecule inhibitor LY294002 was used to selectively inhibit the activity of phophatidylinositol 3-kinase (PI3K). Separate inhibitor-treated samples were harvested for RNA isolation and analyzed by RT-PCR for cardiac-specific genes. Results from this study suggest that inhibition of multiple points in the HGF signaling pathway causes decreased cardiac marker expression.

### 1.5. Part III: Implantation of conditioned hMSCs into a myocardial infarct model

#### 1.5.1. Objective 3A: Evaluate regional cardiac function of cell-treated MIs

Although we have investigated the effects of reduced-$O_2$/HGF conditioning on cardiac-specific marker expression of hMSCs *in vitro*, we were also interested in delivering reduced-$O_2$/HGF conditioned hMSCs to acute MIs *in vivo* to assess the effects on cardiac function. In this study, we delivered conditioned cells to MIs created in male athymic rats, and determined cardiac function at 1 week and 1 month time points. Cell therapy strategies for cardiac regeneration aims to overcome the chief limitation of current MI treatments by replacing necrotic cardiomyocytes with viable cells that can restore cardiac mechanics. Several different cell types that have been delivered to the heart in clinical and pre-clinical

studies have been shown to regenerate cardiac mechanical function. This leads to a fundamental question of whether the delivered cells increase active function by adding contractile elements, or whether they improve passive function by increasing the compliance within the region of the developed scar. [2,41] Using techniques to study regional mechanical cardiac function, however, it is possible to study small defined areas in the heart. And by using a high spatial-resolution imaging technique called high density mapping (HDM), it is possible to determine area deformation within small infarct regions with a high degree of accuracy, precision, and repeatability.[42] By correlating measured changes in area with measured intracavitary pressure over the course of a heartbeat, we used HDM to calculate regional stroke work (RSW) and systolic area contraction (SAC) as indicators of active function in cell-treated MIs. Results from this study indicate that MIs treated with reduced-$O_2$/HGF conditioned cells significantly improved both RSW and SAC after 1 week, compared to untreated MIs and all other cell treatments. In addition, MIs treated with reduced-$O_2$/HGF conditioned cells could significantly improve both RSW and SAC after 1 month. Further analysis indicated that there was no significant change in RSW or SAC in any of the treatment groups from 1 week to 1 month. These results indicate that the implantation reduced-$O_2$/HGF conditioned cells can improve mechanical function of infarcted hearts.

### 1.5.2. Objective 3B: Determine retention and cardiac differentiation of delivered cells

Since our novel conditioning regimen was partially designed to mimic some known MI environmental cues, hMSCs that are pre-conditioned with reduced-$O_2$/HGF *in vitro* prior to implantation *in vivo* may able to adapt more easily to MIs than traditionally cultured hMSCs. In effect, implanting cells that can adapt and survive more easily in an MI will improve cell retention. By treating hMSCs to express cardiac-specific markers *in vitro* prior to implantation, cells are primed with the physiological and organ-appropriate cellular machinery, which may be more suitable for suitable for survival, mature differentiation, tissue incorporation, and function.[36] Transplanting “cardiogenic” hMSCs into a cardiac-niche may allow for further cardiac differentiation, which may include enhanced cardiac protein expression and mature sarcomere formation. Furthermore, implanting hMSCs that have only been

partially differentiated towards a cardiac lineage may allow cells to commit to region-specific cardiac cell types.[34] To determine the retention and cardiac differentiation of delivered cells, we analyzed cell-treated MIs of male athymic rats after the 1-week time point. Results from this study indicate that there was a significantly higher retention of reduced-$O_2$/HGF conditioned hMSCs than unconditioned, normal-$O_2$/MSCGM hMSCs. In addition, some of the retained reduced-$O_2$/HGF conditioned hMSCs were found to express sarcomeric α-actinin or myosin heavy chain proteins.

## 1.6. References


1 Roger, V. L. *et al.* Heart disease and stroke statistics--2011 update: a report from the American Heart Association. *Circulation* **123**, e18-e209, (2011).

2 Gaudette, G. R. & Cohen, I. S. Cardiac regeneration: materials can improve the passive properties of myocardium, but cell therapy must do more. *Circulation* **114**, 2575-2577, (2006).

3 Rosamond, W. *et al.* Heart disease and stroke statistics--2008 update: a report from the American Heart Association Statistics Committee and Stroke Statistics Subcommittee. *Circulation* **117**, e25-146, (2008).

4 Bergmann, O. *et al.* Evidence for cardiomyocyte renewal in humans. *Science* **324**, 98-102, (2009).

5 Beltrami, A. P. *et al.* Evidence that human cardiac myocytes divide after myocardial infarction. *N Engl J Med* **344**, 1750-1757, (2001).

6 Abbott, J. D. *et al.* Stromal cell-derived factor-1alpha plays a critical role in stem cell recruitment to the heart after myocardial infarction but is not sufficient to induce homing in the absence of injury. *Circulation* **110**, 3300-3305, (2004).

7 Schenk, S. *et al.* Monocyte chemotactic protein-3 is a myocardial mesenchymal stem cell homing factor. *Stem Cells* **25**, 245-251, (2007).

8 Beltrami, A. P. *et al.* Adult cardiac stem cells are multipotent and support myocardial regeneration. *Cell* **114**, 763-776, (2003).

9 Oh, H. *et al.* Cardiac progenitor cells from adult myocardium: homing, differentiation, and fusion after infarction. *Proc Natl Acad Sci U S A* **100**, 12313-12318, (2003).

10 Bersell, K., Arab, S., Haring, B. & Kuhn, B. Neuregulin1/ErbB4 signaling induces cardiomyocyte proliferation and repair of heart injury. *Cell* **138**, 257-270, (2009).

11 Kuhn, B. *et al.* Periostin induces proliferation of differentiated cardiomyocytes and promotes cardiac repair. *Nat Med* **13**, 962-969, (2007).

12 Orlic, D. *et al.* Bone marrow cells regenerate infarcted myocardium. *Nature* **410**, 701-705, (2001).

13 Schuldt, A. J., Rosen, M. R., Gaudette, G. R. & Cohen, I. S. Repairing damaged myocardium: evaluating cells used for cardiac regeneration. *Curr Treat Options Cardiovasc Med* **10**, 59-72, (2008).

14 Guyette, J. P., Cohen, I. S. & Gaudette, G. R. Strategies for regeneration of heart muscle. *Crit Rev Eukaryot Gene Expr* **20**, 35-50, (2010).

15 Laflamme, M. A. & Murry, C. E. Regenerating the heart. *Nat Biotechnol* **23**, 845-856, (2005).

16 Behfar, A. *et al.* Guided cardiopoiesis enhances therapeutic benefit of bone marrow human mesenchymal stem cells in chronic myocardial infarction. *J Am Coll Cardiol* **56**, 721-734, (2010).

17 Laflamme, M. A. *et al.* Cardiomyocytes derived from human embryonic stem cells in pro-survival factors enhance function of infarcted rat hearts. *Nat Biotechnol* **25**, 1015-1024, (2007).

18 Mauritz, C. *et al.* Generation of functional murine cardiac myocytes from induced pluripotent stem cells. *Circulation* **118**, 507-517, (2008).

19 Kreutziger, K. L. & Murry, C. E. Engineered human cardiac tissue. *Pediatr Cardiol* **32**, 334-341, (2011).

20 Laflamme, M. A. & Murry, C. E. Heart regeneration. *Nature* **473**, 326-335, (2011).

21 Sadat, S. *et al.* The cardioprotective effect of mesenchymal stem cells is mediated by IGF-I and VEGF. *Biochem Biophys Res Commun* **363**, 674-679, (2007).

22 Virag, J. A. *et al.* Fibroblast growth factor-2 regulates myocardial infarct repair: effects on cell proliferation, scar contraction, and ventricular function. *The American journal of pathology* **171**, 1431-1440, (2007).

23 Neuss, S., Becher, E., Woltje, M., Tietze, L. & Jahnen-Dechent, W. Functional expression of HGF and HGF receptor/c-met in adult human mesenchymal stem cells suggests a role in cell mobilization, tissue repair, and wound healing. *Stem Cells* **22**, 405-414, (2004).

24 Ceradini, D. J. & Gurtner, G. C. Homing to hypoxia: HIF-1 as a mediator of progenitor cell recruitment to injured tissue. *Trends Cardiovasc Med* **15**, 57-63, (2005).

25 Hare, J. M. *et al.* A randomized, double-blind, placebo-controlled, dose-escalation study of intravenous adult human mesenchymal stem cells (prochymal) after acute myocardial infarction. *J Am Coll Cardiol* **54**, 2277-2286, (2009).

26 Guo, J., Lin, G. S., Bao, C. Y., Hu, Z. M. & Hu, M. Y. Anti-inflammation role for mesenchymal stem cells transplantation in myocardial infarction. *Inflammation* **30**, 97-104, (2007).

27 Wang, M., Crisostomo, P. R., Herring, C., Meldrum, K. K. & Meldrum, D. R. Human progenitor cells from bone marrow or adipose tissue produce VEGF, HGF, and IGF-I in response to TNF by a p38 MAPK-dependent mechanism. *Am J Physiol Regul Integr Comp Physiol* **291**, R880-884, (2006).

28 Wang, M. *et al.* STAT3 mediates bone marrow mesenchymal stem cell VEGF production. *J Mol Cell Cardiol* **42**, 1009-1015, (2007).
29 Guo, Y. *et al.* Locally overexpressing hepatocyte growth factor prevents post-ischemic heart failure by inhibition of apoptosis via calcineurin-mediated pathway and angiogenesis. *Arch Med Res* **39**, 179-188, (2008).
30 Assmus, B. *et al.* Transplantation of Progenitor Cells and Regeneration Enhancement in Acute Myocardial Infarction (TOPCARE-AMI). *Circulation* **106**, 3009-3017, (2002).
31 Janssens, S. *et al.* Autologous bone marrow-derived stem-cell transfer in patients with ST-segment elevation myocardial infarction: double-blind, randomised controlled trial. *Lancet* **367**, 113-121, (2006).
32 Wang, C. C. *et al.* Direct intramyocardial injection of mesenchymal stem cell sheet fragments improves cardiac functions after infarction. *Cardiovasc Res* **77**, 515-524, (2008).
33 Sussman, M. A. & Murry, C. E. Bones of contention: marrow-derived cells in myocardial regeneration. *J Mol Cell Cardiol* **44**, 950-953, (2008).
34 Potapova, I. A. *et al.* Enhanced recovery of mechanical function in the canine heart by seeding an extracellular matrix patch with mesenchymal stem cells committed to a cardiac lineage. *Am J Physiol Heart Circ Physiol* **295**, H2257-2263, (2008).
35 Cohen, I. S. & Gaudette, G. R. Regenerating the heart: new progress in gene/cell therapy to restore normal mechanical and electrical function. *Dialogues in Cardiovascular Medicine* **14**, 19, (2009).
36 Marban, E. & Malliaras, K. Boot camp for mesenchymal stem cells. *J Am Coll Cardiol* **56**, 735-737, (2010).
37 Tang, Y. L. *et al.* Hypoxic preconditioning enhances the benefit of cardiac progenitor cell therapy for treatment of myocardial infarction by inducing CXCR4 expression. *Circ Res* **104**, 1209-1216, (2009).
38 Rosova, I., Dao, M., Capoccia, B., Link, D. & Nolta, J. A. Hypoxic Preconditioning Results in Increased Motility and Improved Therapeutic Potential of Human Mesenchymal Stem Cells. *Stem Cells*, (2008).
39 Grayson, W. L., Zhao, F., Bunnell, B. & Ma, T. Hypoxia enhances proliferation and tissue formation of human mesenchymal stem cells. *Biochem Biophys Res Commun* **358**, 948-953, (2007).
40 Chacko, S. M. *et al.* Hypoxic preconditioning induces the expression of prosurvival and proangiogenic markers in mesenchymal stem cells. *Am J Physiol Cell Physiol* **299**, C1562-1570, (2010).
41 Wall, S. T., Walker, J. C., Healy, K. E., Ratcliffe, M. B. & Guccione, J. M. Theoretical impact of the injection of material into the myocardium: a finite element model simulation. *Circulation* **114**, 2627-2635, (2006).
42 Kelly, D. J., Azeloglu, E. U., Kochupura, P. V., Sharma, G. S. & Gaudette, G. R. Accuracy and reproducibility of a subpixel extended phase correlation method to determine micron level displacements in the heart. *Med Eng Phys* **29**, 154-162, (2007).

# CHAPTER 2: Background

## 2.1. Introduction

### 2.1.1. The Heart

The heart is a complex and vital organ, which functions as an electromechanical pump to drive the body's circulatory system. Under normal healthy conditions, synchronous contraction of the cardiac muscle maintains the homeostatic, rhythmic beating of the heart with the primary objective of delivering blood throughout the body.[1] The human heart resides in the thoracic cavity, located posterior to the sternum and lungs, and anterior to the vertebral column. It is encased in a fluid filled bi-layered sac called the pericardium, which serves to support the anatomical position, protect the heart from other organs, and provide lubrication needed to maintain mechanical function.[2] Anatomically, the major vasculature attaches to the superior end of the heart, which is often referred to as the "base" of the heart. The free, inferior end of the heart is often referred to as the "apex".

The heart consists of four chambers, having two atria sitting superior to two ventricles. With respect to functionality, the heart is also considered to have a right side and a left side, with both sides having an atrium and a ventricle.[2] The right side of the heart is primarily responsible for pulmonary circulation, by collecting circulated deoxygenated blood from the body and pumping it to the lungs to be re-oxygenated. The left side of the heart is primarily responsible for systemic circulation, by collecting re-oxygenated blood from the lungs and pumping it to all organs and tissues within the body. The atria are thin-walled, low-pressure chambers, which contribute about 10-15% of the total cardiac output by collecting blood and pumping it to their respective ventricles.[1] The ventricles are thick-walled, high-pressure chambers that drive the blood to either pulmonary or systemic circulation. The ventricles are much larger and thicker than the atria because of the additional muscle mass needed to pump blood throughout the body.[1] In addition, the left ventricle is typically thicker and more muscular than the right ventricle because it must develop more force to deliver blood to all bodily organs and extremities,[1] whereas the right ventricle only pumps blood proximally to the lungs located within the thoracic cavity.

Two types of cardiac valves aid in the unidirectional flow of blood through the heart. Atrioventricular valves separate the atria from the ventricles, and semilunar valves separate the ventricles from their respective major arteries (the aorta and the pulmonary artery). The valves consist of two-leaflet or three-leaflet cusps composed of endothelium-covered fibrous tissue. Valve cusps are convex in the direction of blood flow to allow forward progression, and concave in the opposite direction to prevent back-flow of blood once a valves close.

The heart, itself, is an oxygen and nutrient dependent organ that requires a substantial blood supply to maintain normal healthy function. Therefore, perhaps it is inherently deliberate that the first two blood vessels to branch off of the aorta are the coronary arteries. The coronary arteries supply re-oxygenated blood to the cardiac tissue. The left main coronary artery divides into the left anterior descending coronary artery and circumflex coronary artery branches to supply the left side of the heart, whereas the right main coronary artery supplies the right side of the heart.

Cardiac tissue consists of several cell-types (e.g. muscle cells, fibroblasts, conducting pacemaker cells, and possibly resident cardiac stem cells), which function within an extracellular matrix (ECM) that serves as a complex lattice of interacting proteins (e.g. collagen I, collagen III, laminin, elastin, and fibronectin). The muscular walls of the atria and ventricles are largely composed of cardiac muscle cells, called cardiomyocytes. Cardiomyocytes can attach to other cardiomyocytes or to the ECM, and form branched muscle fibers. Muscle fibers are separated by intercalated disks, which contain gap junctions composed of connexin proteins that facilitate conduction of action potentials throughout the myocardium. This structure allows cardiac muscle to function as a syncytium, so that stimulus applied to any one part of the cardiac muscle results in synchronized contraction of the entire heart.

### 2.1.2. Cardiomyocyte Structure and Sarcomere Function

Cardiomyocytes contain several contractile protein units called myofibrils, which are composed of bundles of both thick myosin filaments and thin actin filaments (Figure 2.1A). Myofibrils can be further subdivided into sarcomeres (Figure 2.1B), which are the most basic contractile structures that repeat

throughout each cardiomyocyte and give their signature striated phenotype. Sarcomeres are denoted by the overlapping actin and myosin filaments between two Z-lines (Figure 2.1B), which form cross-bridges that function to shorten and lengthen cardiomyocytes.

To sustain repeated contraction and relaxation of the heart during one's lifetime, cardiomyocytes also contain a large number of mitochondria. Mitochondria contain the necessary enzymes and proteins that allow for oxidative phosphorylation, which is a process that oxidizes substrates for the synthesis of adenosine triphosphate (ATP). An increased number of mitochondria allows for increased oxidative phosphorylation, which generates enough ATP to meet the metabolic energy demands of the myocardium. However, in order to supply the heart with enough oxygen and substrate so that the mitochondria can produce ATP, the myocardium also contains a unique capillary bed called the transverse tubular system. The transverse tubular system localizes intimately with myofibrils for short diffusion distances between cardiomyocytes and the blood supply, which allows for gas exchange ($O_2$ and $CO_2$), nutrient delivery, calcium diffusion, and waste removal. The transverse tubular system is thought to be a deep extension of the sarcolemma. The sarcolemma is another unique feature of cardiac and skeletal striated muscle types, which surrounds and envelops groups of myofibrils to also facilitate gas exchange, nutrient delivery, and waste removal.

As stated above, sarcomeres are the basic contractile structures in cardiomyocytes, which contain overlapping filaments of actin and myosin. Thick myosin filaments are endowed with globular heads that ratchet along binding positions located on the thin actin filaments. In order for this movement to take place, the cross-bridges cycle between relaxed and active states to shorten sarcomeres. In the relaxed state, ATP is partially hydrolyzed and myosin remains unattached to actin. As calcium enters the cell through the sarcolemma and transverse tubules, the globular heads of myosin attach to their binding sites on the actin filaments to activate the cross-bridge cycle. As the ATP becomes completely hydrolyzed, a conformational change to the myosin causes the globular head to pull the actin filament closer to the center of the sarcomere. A new ATP molecule is then required to bind to myosin for cross-bridge release. Partial hydrolysis of the ATP molecule reconfigures the relaxed position of the globular head, so that the

cycle can repeat. During contraction, myosin globular heads ratchet along actin filaments, which decreases the distance between Z-lines by essentially pulling the Z-lines closer towards the M-line (Figure 2.1B). Contraction also decreases the widths of the I-bands and H-zones (Figure 2.1B), while widths of the A-bands remain the same.

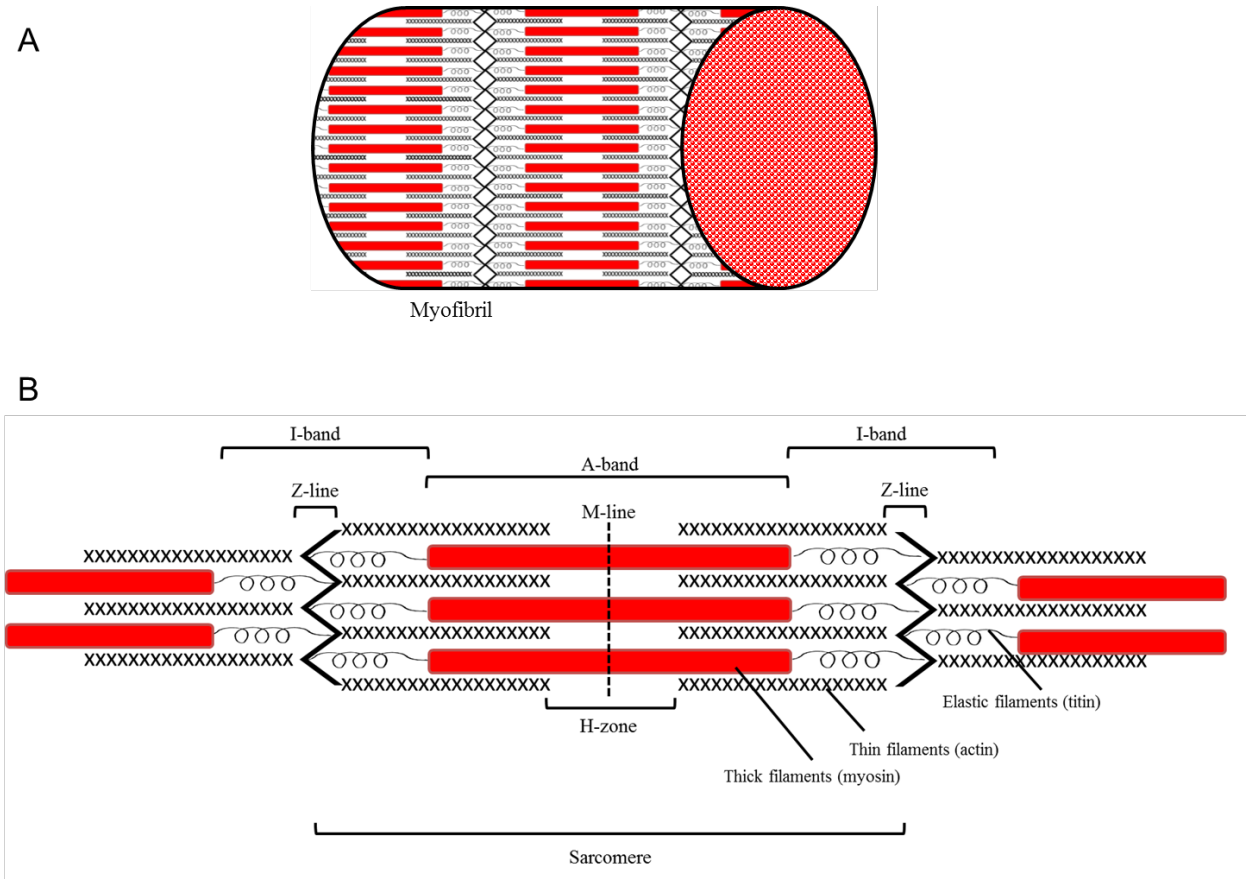


**Figure 2.1. Cardiac muscle structure.** (A) Cardiomyocytes contain several long, branched strands of myofibrils, which are composed of sarcomeres that give a striated appearance. (B) Sarcomeres are the basic contractile unit of cardiac muscle, which are organized into overlapping thick and thin filaments. During contraction, myosin globular heads attach to and pull the thin actin filaments, causing a shortening of the sarcomere. During shortening, the distance between Z-lines decreases, and the widths of the I-bands and H-zones decrease as well.

## 2.2. Heart Disease

Coronary Heart Disease (CHD) presents as a narrowing of the coronary arteries that supply the heart with blood and oxygen. Recognized as one of the leading causes of death worldwide, CHD cases resulted

in 7.6 million deaths globally in 2005 and are projected to reach 11.1 million by 2020.[3,4] As the single most common cause of death in Europe, CHD accounts for 1.92 million deaths each year, with 741,000 of those deaths occurring in the European Union.[3] The American Heart Association (AHA) reports that 16.8 million Americans suffer from CHD, and projects an incidence of 785,000 new cases each year.[5]

Myocardial ischemia results when narrowing coronary arteries inhibit delivery of oxygen-rich blood to a region of the heart, failing to meet the metabolic demand of the myocardial tissue. Such ischemic events can lead to cardiomyocyte cell-death called myocardial infarction (MI, heart attack), resulting in a region of necrotic heart muscle. Of the 16.8 million Americans living with CHD, the AHA reports that 7.9 million have also experienced an MI.[5] In 2008 alone, the AHA estimated that CHD contributed to approximately 1 million MIs and 451,000 deaths.[4,6] Though severity can range, the consequences of an MI can be dire as necrotic myocardium impairs cardiac performance. This can lead to the onset of heart failure (HF) as myocardial necrosis reduces the heart's function as a rhythmic pump, thereby inhibiting the delivery of sufficient blood flow to the rest of the body organs.[4,7,8] With CHD and MI as major contributors, 5.7 million Americans suffer from HF, with an incidence rate of 1/100 people over the age of 65 that surmounts to about 500,000 deaths annually.[5] The frequency of new HF cases has increased by 159% over the last decade without improvement in reducing the mortality rate, driving associated medical costs for Americans to an estimated $37.2 billion in 2009.[5,7]

### 2.3. Current Therapeutic Strategies

Once a patient exhibits HF, his or her long-term survival is significantly jeopardized.[9-11] Despite considerable advancements in many areas of cardiovascular disease, the current treatment options for HF have shown limited improvements in the discouraging survival rate of this progressive disease.[11] For patients suffering from end-stage HF, the only viable treatment is transplantation in which the damaged heart is surgically replaced with a functional donor heart. With roughly two thousand transplants in the U.S. each year,[5] however, this option is only available for a small fraction of HF patients. Devices such

as implantable cardioverter-defibrillators, cardiac resynchronization pacemakers, and heart pumps offer an alternative to transplantation. However, these options aim to correct or sustain the electrical and mechanical functions of the heart without treating the cause of reduced function. Current pharmacological treatments such as ACE inhibitors, beta blockers, and diuretics are prescribed to address the associated physiologic consequences of HF (i.e. high blood pressure, increased water retention), but again offer limited or no treatment for the damaged myocardium.

The chief limitation of current treatments is the failure to address the need to replace the lost contractile myocytes that are responsible for normal cardiac mechanical function. In order to effectively treat MI and HF patients, functional myocytes must be regenerated to restore the lost contractile mass. Recent research advancements in both gene and cell therapies have been proposed to target this need. While these treatments are in their infancy as therapeutic approaches, they provide optimism for generating new contractile myocytes. Herein, we review the strategies of these regenerative therapies with consideration to the milestones achieved and the challenges that lie ahead.

### 2.4. Cardiac Regeneration

Regenerative medicine has emerged to the forefront of cardiac research, marrying discoveries in both basic science and engineering to develop viable therapeutic approaches for treating the diseased heart. Significant advancements in gene therapy, stem cell biology, and cardiomyoplasty provide new optimism for regenerating damaged myocardium. Exciting new strategies for endogenous and exogenous regeneration have been proposed, however questions remain as to whether these approaches can provide enough new myocyte mass to sufficiently restore mechanical function to the heart. Here, we consider the mechanisms of endogenous cardiomyocyte regeneration and exogenous cell differentiation (with respect to myoblasts, stem cells, and induced pluripotent cells being researched for cell therapies). We review some of the cues being harnessed in strategies of gene/cell therapy for regenerating myocardium. We also consider some of the technical challenges that remain in determining new myocyte generation, tracking delivered cells *in vivo*, and correlating new myocyte contractility with cardiac function.

Strategies for regenerating the heart are being realized as both animal and clinical trials suggest that these new approaches provide short-term improvement of cardiac function. However, a more complete understanding of the underlying mechanisms and applications is necessary to sustain longer-term therapeutic success.

Adult human cardiac myocytes have long been thought to be a terminally differentiated cell type that also lacks the ability to proliferate. Support for this traditional theory lies in the fact that the heart is unable to fully repair itself or restore function post-infarction, nor do cardiomyocytes expand in culture once they are harvested from biopsies. However, Bergmann and colleagues recently demonstrated that cardiomyocyte turnover does in fact occur over the human lifespan, with a decrease in renewal as one ages.[12] The likely mechanisms by which myocardium is regenerated are either native myocyte proliferation or stem cell differentiation. While a complete approach for cardiac regeneration is still uncertain, it may be possible to exploit aspects of these two likely regeneration strategies to establish viable therapies. Given a more complete understanding of the cues responsible for native myocyte turnover, it may be possible to elicit these responses for greater renewal following an MI. In addition, many animal and clinical studies have demonstrated improved mechanical function in hearts receiving stem cell therapy.[8,13,14] If mechanisms of cardiac regeneration could be identified and developed into clinical therapies, it would give realistic hope in extending the life expectancy for millions of patients suffering from HF, which are projected to have a mortality rate of greater than 60% within 5 years of diagnosis.[15]

### 2.4.1. Endogenous Repair

***Myocyte Proliferation***

Traditionally, the heart was believed to be incapable of regeneration upon injury.[7,8,16-18] This is to say that cardiomyocytes were thought to be a terminally differentiated cell type lacking the ability to proliferate, further complicating the prognoses for patients suffering from MI or cardiomyopathy. However, recent work in cardiac regeneration suggests that cardiomyocytes may have a limited ability to

enter the cell cycle following MI.[19,20] Anversa's laboratory found evidence of cell-cycle protein expression in cardiomyocytes cultured from biopsies of heart transplant patients.[21] The same laboratory then reported that a small number of adult cardiac myocytes lying within the peripheral border-zone of an infarct stained positive for the cell-cycle marker Ki-67.[19] Results from these studies challenge traditional dogma, suggesting that human cardiomyocytes may hold limited proliferative capacity.

Myocyte proliferation has also been noted in many other species, including zebrafish,[22] mice,[23] rats[24] and dogs.[25] Zebrafish are able to regenerate myocardium through myocyte proliferation after amputation of 20% of their ventricle.[22] The MRL mouse, which has a reduced scarring response, appears to regenerate myocardium through proliferation after MI.[23] Progenitor cells may release factors to induce native myocytes to enter the cell cycle in the rat heart.[24] We recently documented the expression of cell cycle markers in the canine heart implanted with an extracellular matrix (ECM) isolated from the porcine urinary bladder.[25] The ECM has previously been shown to attract bone marrow derived cells,[26] which may include mesenchymal stem cells. However, a definitive relationship between the release of factors from stem or progenitor cells and myocyte proliferation has yet to be demonstrated.

The use of myocyte proliferation to restore function to the heart lies with either inducing myocyte proliferation *in vivo* or expanding adult myocytes in culture *in vitro* before delivering them to the heart. Biopsied cardiomyocytes have shown expression of cell-cycle markers *in vitro,* which have previously been shown to regulation the proliferation of non-cardiomyocyte cells. For example, transfecting cardiomyocytes isolated from 21-day old rats with a gene to over-express cyclin D2, a cell cycle protein, induces myocyte proliferation.[27] Inhibition of p38 MAP kinase also increases proliferation in 21-day old rat cardiomyocytes *in vitro*.[28] However, it has yet to be determined whether genetic manipulation or interference with regulation of specific genes can target effector myocytes in the border-zone of an MI to induce site-specific myocyte proliferation.

Instead of using factors to induce myocytes to proliferate *in vivo*, a small population of cardiac myocytes can be biopsied, as is currently done with heart transplant recipients. Cardiac myocytes could be isolated from the tissue, expanded in culture and returned to the heart. A similar procedure has been

proposed for growing cardiac stem cells.[29] Given the death of approximately 1 billion myocytes in infarct mediated heart failure, however, a large quantity of myocytes need to be grown in culture.

### 2.4.2. Exogenous Repair

***Cardiomyoplasty***

Since the 1990s, the field of regenerative medicine has been exploring methods for regenerating the heart via cell therapy. Cellular cardiomyoplasty is an experimental surgical intervention, in which newly differentiated functional cardiomyocytes are delivered to the infarcted heart as a therapeutic technique to restore mechanical function. Several cell-types have been considered as possible cell-therapy candidates for cardiomyoplasty, including skeletal myoblasts, embryonic stem cells, bone marrow stem cells, cardiac stem cells, and induced pluripotent stem cells.[30,31] In addition, several biological techniques have been employed to elicit cardiac differentiation in these different cell types. In a recent review article, we have defined a set of criteria for assessing the different cell-therapy approaches based on milestones of cardiomyocyte differentiation and achieved improvements in mechanical cardiac function.[30] With regards to differentiation *in vitro* and *in vivo*, the criteria outline a succession of events that help to determine if the key cardiomyocyte characteristics are being met (i.e. cardiac protein expression, mature sarcomere formation, functional contractility, cardiac action potentials, and electrical integration). *In vitro* characterization provides proof of concept and easier methods for measuring degree of differentiation. However, the *in vivo* assessment determines if the cardiomyocytes retain their characteristics and integrate with native myocardium when they are delivered to the heart. Importantly, *in vivo* studies also can provide higher-order milestones of improved regional and global cardiac function, though a correlation between new myocyte number and functional improvement has yet to be determined. To complement this previous work, this section considers the cell types that have been used for cardiomyoplasty, the current state of the field, and the limitations that need to be overcome.

### 2.4.3. Cell Types and Milestones

#### *Skeletal Myoblasts*

Skeletal myoblasts were one of the first isolated cell types used clinically to regenerate mechanical function in the infarcted heart.[32] Skeletal myocyte progenitor cells can differentiate into striated muscle cells and have been afforded considerable attention for their availability, ease of culturing, work potential, and graft potential.[33-35] When delivered to the heart, these cells have been shown to improve mechanical function in infarcted animals. However, skeletal myoblasts do not appear to express gap junction proteins after differentiation into myotubes, and are thus unlikely to contract in sync with the native myocardium.[36] This lack of integration may be responsible for arrhythmias reported with skeletal myoblast therapy.[37,38] Due to the high incidence of ventricular arrhythmias, internal cardiac defibrillators are implanted in patients receiving skeletal myoblasts.

#### *Embryonic Stem Cells*

Embryonic stem cells (ESCs) harvested from the inner cell mass of blastocyst-stage embryos of both mice and humans appear to have the strongest capacity for cardiomyocyte differentiation.[30,39-41] Their unique pluripotent nature provides them with the potential to differentiate into cell-types derived from all three germ layers, including cardiomyocytes, without genetic manipulation. While it is clear that harvested ESCs will not develop as an embryo in culture, the environmental cues and cell signaling that ESCs encounter during culture and differentiation may have commonalities to those in fetal organ development. [42]

*In vitro* differentiation of ESCs by aggregated embryoid body (EB) formation has produced differentiated cells that upregulate cardiac-specific genes and proteins (i.e. Nkx2.5, GATA-4, Wnt3A, MEF2C, sarcomeric α-Actinin, myosin heavy chain, and cardiac Troponin I) with a subsequent loss of "stemness" markers such as Oct-4.[39,40,42,43] In addition, ESC-derived cardiomyocytes display myofibril formation and can spontaneously contract in culture.[39,40,44,45] Connexin-43 protein expression suggests that the differentiated ESCs form gap-junction proteins important for cardiomyocyte cell-cell attachment

and propagation of cardiac action potentials. Further investigation of ESC-derived cardiomyocytes has shown that they have the ability to generate action potentials of different cardiac phenotypes, and even develop specific cardiac ion currents (e.g. $I_{to1}$, $I_{Kr}$, $I_f$, $I_{K1}$, $I_{Ca,L}$, and $I_{Na+}$) over prolonged periods of differentiation.[39,44] While the expression of cardiac ion currents is encouraging, ESC-derived cardiomyocytes have mixed action potentials, with some cells expressing nodal like action potentials and others expressing ventricular like action potentials, which could leave the heart prone to fibrillation when implanted together.[39,40]

One of the major caveats of the EB differentiation method, however, is the limited number of cardiomyocytes that can be purified from a mixed batch of ESCs. Initial studies reported using 5 million ESCs to form sets of EBs, with cardiomyocyte differentiation efficiencies of <10%.[40,46] Under the best circumstances, this method produced $5x10^5$ ESC-derived cardiomyocytes, amongst a variety of other differentiated ESC-derived cell-types. Current work on *in vitro* ESC-cardiomyocyte strategies has focused on improving the differentiation efficiency, in order to produce enough myocytes to meet the needs for treating an MI. Recent cardiomyocyte-purification methods by Percoll density separation or cardiac marker detection have increased the efficiency to >30%.[41,47,48] Novel direct differentiation strategies based on cues from developmental cardiogenesis, such as the Activin-A/BMP-4 treatment method, have also improved efficiency to >30%. [41,42] Even more intriguing is the combination of direct differentiation and separation methods with reported yields of >70% differentiation efficiency based on starting cell numbers. [41]

Another strategy for increasing the number of cells available for cardiomyoplasty may lie in one of the definitive differences between mouse and human ESC-derived cardiomyocytes. Human ESC-cardiomyocytes are capable of proliferation, whereas mouse ESC-cardiomyocytes do not appear to have a proliferative ability.[49-51] Recent work by McDevitt *et al*. has identified the IGF/PI 3-kinase/Akt signaling pathway as one of the major regulators of human ESC-cardiomyocyte proliferation, though a complete understanding has not been achieved.[52] Strategies regulating cardiomyocyte proliferation may prove to be delicate, as proliferation may be beneficial for improving cardiomyocyte number *in vitro*, but could be

detrimental during *in vivo* applications unless proliferation can be terminated when the appropriate number of myocytes has been regenerated.

Despite these significant improvements, a complete strategy that recapitulates all of the complexities involved in developmental cardiomyogenesis remains elusive. While these studies are exciting, there are scientific concerns that need to be investigated before ESC-derived cardiomyocytes can be implanted into patients. One of the most pressing scientific concerns is being able to deliver a pure population of cardiomyocytes to the heart, as it has been shown that delivering undifferentiated ESCs *in vivo* will form teratomas.[53] Another concern is being able to control the proliferation of ESC-derived cardiomyocytes, in which uncontrolled proliferation may cause hypertrophic cardiomyopathy *in vivo*. Yet another serious medical concern is that ESC-derived cardiomyocytes may elicit a strong immune response, based on the compatibility of ABO blood-group antigens or embryo-specific antigens between delivered cells and host systems.[54,55] In addition to scientific concerns, ethical barriers regarding the origin of ESCs and limited knowledge about medical consequences has slowed the progression of the use of these cells in clinical studies.

***Bone Marrow Derived Stem Cells***

Since the late 1990's, multipotent stem cells isolated from adult bone marrow have gained considerable attention for their ability to transdifferentiate into several cell types including endothelium, lung, neural, liver, and bone.[56-60] In 2001, a study by Orlic *et al*. suggested that the delivery of bone marrow cells (BMCs) could regenerate ischemic myocardium.[8] By delivering $Lin^-$, c-$kit^+$ mouse BMCs carrying enhanced green fluorescent protein (EGFP) to a murine infarct model, they demonstrated regeneration of new myocytes in the infarct zone and improved ventricular function after nine days. This initial report suggested considerable promise for the use of BMCs in myocardial repair; however, additional studies have not been able to repeat these results.[61,62] Despite controversy, BMCs remain an attractive candidate for cardiomyoplasty as they can be obtained from autologous sources and expanded easily in culture. *In vitro* cardiomyocyte differentiation and *in vivo* heart applications remain a focus of

continued research on BMCs, as the full extent of their multipotency and therapeutic value have yet to be determined.

### *Differentiation – In Vitro*

Since the landmark study by Orlic *et al*., several groups have tried to determine possible mechanisms for transdifferentiating BMCs into cardiomyocytes *in vitro*. Studies based on separation of the c-kit$^+$ BMC subpopulation showed partial cardiac differentiation in experiments with rat neonatal cardiomyocyte co-culture and BMP4/TGF-β treatment methods.[63] Results showed that transdifferentiated cells expressed cardiac markers (i.e. MEF2C, GATA-4, sarcomeric α-Actinin), but lacked the ability to form gap junctions and generate action potentials characteristic of fully differentiated cardiomyocytes. Subpopulations of both bone-marrow derived mesenchymal stem cells (MSCs) and stromal cells, however, have been able to form gap junctions and elicit cardiac action potentials.[64-67] *In vitro* treatment of marrow stromal cells (containing a high fraction of MSCs) with 5-azacytadine, a DNA demethylation agent, induced about 30% of the cells to differentiate towards a cardiac lineage, with expression of cardiac markers, evidence of mature sarcomeres, and propagation of cardiac-specific action potentials (nodal and ventricular) for spontaneous contractions.[65] Based on literature from fetal heart development and ESC-derived cardiomyocytes, other groups have experimented with cardiac-inducing cytokine treatments (i.e. retinoic acid, hepatocyte growth factor, and platelet derived growth factor) to show partial cardiac differentiation by gene and protein expression.[68-71] Our laboratory has employed three-dimensional aggregation of human MSCs for spheroid formation (similar to EB formation) to show that 50% of the hMSCs can differentiate towards a cardiac lineage detected by protein expression within 2 weeks.[67] Patch-clamping analysis of these "cardiogenic" cells indicate that 16% of the differentiated hMSCs display large L-type $Ca^{2+}$ currents, indicating that some of the differentiated hMSCs may be capable of producing cardiac-specific action potentials. Using specific milestones for *in vitro* cardiac differentiation, BMCs and BMC-subpopulations have demonstrated the capacity for protein expression, sarcomere organization, cardiac electrical currents, electrical integration by gap junctions, and functional

contractility (Figure 2.2).[30] These results provide optimism that BMCs have the potential to become fully-differentiated cardiomyocytes, even though BMCs do not differentiate as readily as ESCs. Greater success in *in vitro* differentiation of BMCs may lie in defining all the necessary factors for complete differentiation.

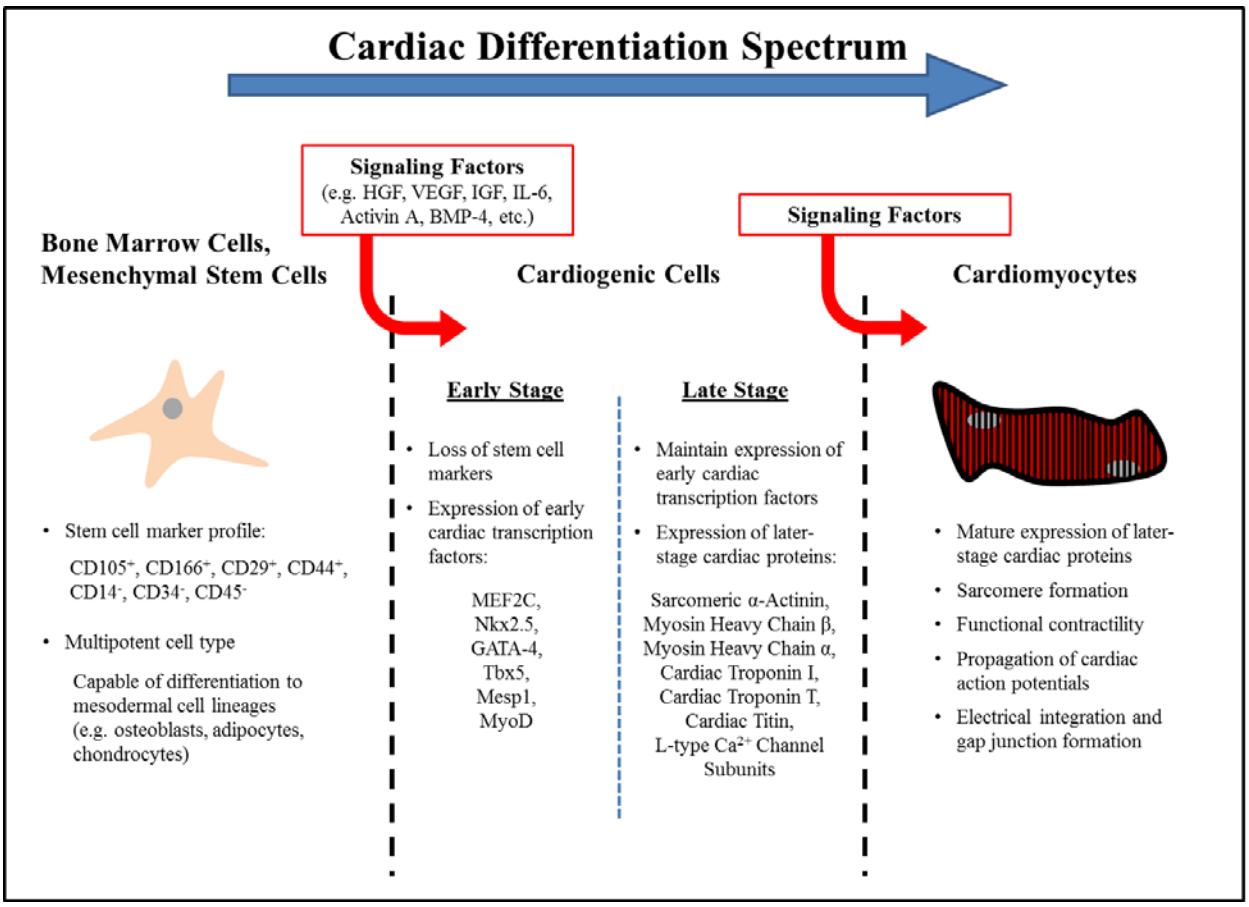


**Figure 2.2. Cardiac Differentiation Spectrum.** A schematic depicting the cardiac differentiation spectrum as bone marrow cells or marrow-derived mesenchymal stem cells differentiate towards a cardiomyocyte lineage. Stages indicate changes in cell characteristics. As multipotent stem cells differentiate towards a cardiomyocyte lineage, stem cell markers are lost as early cardiac transcription factors start to be expressed. Early cardiac transcription factors function to further differentiate cardiogenic cells, to elicit later-stage cardiac proteins. Fully differentiated cardiomyocytes arrange later-stage cardiac proteins to form sarcomeres with electromechanical functionality.

### *Cardiac Applications In Vivo*

Delivering BMCs (including MSCs) as a cell therapy for *in vivo* applications has been shown to improve wound healing in several tissue types by homing to injury sites, secreting therapeutic cytokines

and growth factors, and differentiating into injured-tissue phenotypes.[72-78] The study by Orlic *et al*. suggested that the delivery of undifferentiated BMCs *in vivo* to a murine infarct model resulted in the generation of new cardiomyocytes and improved cardiac function.[8] Since then, BMC delivery for cell therapy to the heart in both animal and clinical trials have focused on the local therapeutic benefits of delivered BMC signaling, the possibility of *in vivo* BMC-cardiomyocyte differentiation, and the restorative effects on regional and global cardiac function. The delivery of MSCs to infarcts has shown to increase paracrine signaling that mediates inflammation, enhances angiogenesis, promotes cardiomyocyte survival, and aids in maintaining cardiomyocyte contractile function.[77-83] These regional signaling factors indicate that the BMCs provide cardio-protective benefits to the infarcted heart, which may limit cardiomyocyte loss and help to generate new vasculature for reperfusion of ischemic myocardium.

With respect to *in vivo* cardiomyocyte differentiation, recent studies have reported cardiac-specific protein expression by delivered BMCs.[8,67,84,85] However, additional studies report that delivered BMCs fail to exhibit cardiac proteins.[61,62,86,87] A contributing cause of uncertainty is that most cell-types used in cardiomyoplasty can fuse with cardiac myocytes, making it difficult to distinguish delivered BMCs from native cardiomyocytes which frequently are multinucleated.[38,86,88] Due to apparent autofluorescence of heart tissue and challenges with tracking delivered cells, evaluation of *in vivo* differentiation of BMCs remains difficult. Our laboratory has recently experimented with quantum-dot (Q-dot) nano-particle cell tracking for identification of delivered BMCs.[89] Q-dots were passively loaded into the cytoplasm of MSCs by endocytosis before *in vivo* delivery, which provided greater contrast for cell tracking by co-localizing the Q-dot signal with cardiac-marker expression when visualized under a fluorescent microscope. Using this tracking method, our results suggest that delivered cardiogenic cells derived from spheroid-treated MSCs can express cardiac markers with mature sarcomeres.[67] In terms of further milestones of *in vivo* cardiac-differentiation, there is limited evidence to definitively determine if delivered BMCs or MSCs can generate action potentials, form gap junctions with native cardiomyocytes, or functionally contract.[30]

While *in vivo* cardiac differentiation of BMCs is still being studied for these measures, evidence from animal and clinical trials suggest that BMCs delivered to MIs can improve both regional and global cardiac function.[8,67,84,90-94] Though overall functional improvement has shown to be positive, studies disagree on the level of therapeutic effect.[14,91-93,95] Some studies report significant functional improvement from BMC cell therapy within a short-term period of 6 months, whereas other studies of the same duration do not. The only longer-term study to evaluate cardiac function for 18 months after BMC delivery, the BOOST (Bone marrow transfer to enhance ST-elevation infarct regeneration) trial also indicated therapeutic inconsistency over time.[96] While results at 6 months indicated enhanced left ventricular ejection fraction, results at 18 months did not appear to sustain the short-term functional improvements compared to the controls. Importantly, the data from these clinical trials supported the safety of BMC cell therapy for MIs. There may be several confounding factors contributing to the differences reported for cardiac function.[30] Since *in vivo* studies have been performed with both mixed BMCs and isolated BMC subpopulations (i.e. MSCs and mononuclear marrow cells), it remains unclear as to which BMC population is better for improvement of function. Furthermore, BMC population characteristics can differ based upon handling and preparation prior to delivery, which may also affect cell fate *in vivo* and potential therapeutic benefits.[67,93,94] Further, while BMC dosage does not appear to correlate with functional outcome, results from the 18 month BOOST study suggest that repeated cell doses over time may help to sustain therapeutic benefits.[14,92,96] Improved tracking and evaluation methods will aid in determining if delivered BMCs can fully differentiate into new contractile cardiomyocytes, and if the presence of new myocytes quantitatively correlates with increased cardiac function. These methods may also provide further understanding of the cardio-protective mechanisms of BMCs, which may also play a role in improving function immediately post-MI.[77-83] While it is clear that clinical studies have demonstrated short-term efficacy and increased function, studies carried out over greater durations are needed to demonstrate longer-term benefits of delivering BMCs as a cell therapy for MIs.

***Cardiac Stem Cells***

Though the heart was initially thought to be an unlikely source of progenitor cells, evidence suggests that populations of resident cardiac stem cells (CSCs) can be isolated from myocardium. First described by Beltrami *et al* in 2003, a population of adult rat heart cells displaying a $Lin^-/c\text{-}kit^+$ profile were shown to be self-renewing and multipotent.[97] These cells were detected in both the atrial and ventricular myocardium, and could partially differentiate into cardiomyocytes, endothelial cells, and smooth muscle cells *in vitro* and *in vivo*. Administering $Lin^-/c\text{-}kit^+$ CSCs to a rat infarct model by both direct intramyocardial and intracoronary injection has been shown to regenerate cardiomyocytes in the infarcted heart and improve left ventricular function.[97,98] However, the morphological presentation of the newly generated myocytes has been questioned, and new myocyte contractility was not correlated with ventricular function.[30,38]

Shortly after the discovery of $Lin^-/c\text{-}kit^+$ progenitors, Oh *et al* isolated a second population of CSCs from adult mouse hearts that displayed a $Sca\text{-}1^+$ profile (also found to be $c\text{-}kit^-$).[99] While the isolated $Sca\text{-}1^+$ cells did not express cardiac-specific markers, upregulation of cardiac genes were induced by DNA demethylation with 5'-azacytidine. However, this differentiation method failed to produce functionally contracting myocytes *in vitro*. Intravenous delivery of $Sca\text{-}1^+$ CSCs *in vivo* were shown to home to the infarcted mouse heart, express cardiac-specific proteins, and demonstrate cardiac differentiation through fusion with native myocardium. A third population of CSCs called "side population cells" has been isolated from mouse hearts by Hoechst dye exclusion.[100,101] Side population CSCs have been described as $Sca\text{-}1^+$ with low-level c-kit expression, and are reportedly capable of cardiomyocyte differentiation by co-culture with rat cardiomyocytes through intercellular coupling mechanisms (not fusion).[101] A fourth CSC population isolated from neonatal mouse hearts was identified by $Isl\text{-}1^+$ expression ($Sca\text{-}1^-$ and $c\text{-}kit^-$), which is a marker previously described for cells that contribute to heart formation during development.[102] Isl-1, or islet-1, was originally discovered during embryogenesis of pancreatic islets of Langerhans, but was recently found to be a marker of the second heart field during mammalian cardiogenesis.[103] $Isl\text{-}1^+$ CSCs showed expression of cardiac-specific transcription factors (i.e. Nkx2.5 and GATA-4), along with

the capability of cardiac-differentiation *in vitro* and *in vivo* displaying sarcomere formation, action potentials, and calcium currents.

Due to the minimal regenerative potential exhibited by the heart, it is surprising that the heart is a source of multiple populations of progenitor cells. Even more confounding is why these progenitors remain seemingly unresponsive to myocardial injury. However, it is speculated that CSCs may be involved slower repair mechanisms, which could account for the recent reports describing the heart's limited potential for myocyte turnover.[12,19,30,46] While the evidence of CSCs is significant, there are still several concerns that must be addressed prior to their use in clinical applications. Each of the distinct CSC populations indicates partial levels of cardiac-differentiation potential, while their efficacy for generating new functional myocytes is uncertain. Of the four candidates, $Lin^-/c\text{-}kit^+$ CSCs appear to be the most well characterized, but a more complete understanding of their electrophysiological properties is necessary. While it appears that both $Sca\text{-}1^+$ and $Lin^-/c\text{-}kit^+$ CSCs can improve global cardiac function when delivered to MI models, additional *in vivo* studies are needed to determine the effects of side population cells and postnatal $isl\text{-}1^+$ CSCs on this experimental measure. The $isl\text{-}1^+$ population are the only CSCs that have been shown to generate action potentials, which are comparable to neonatal cardiomyocytes.[102] However, it remains to be determined if $isl\text{-}1^+$ CSCs can generate mature action potentials, or if they can be isolated from adult hearts.

In addition to efficacy, another major caveat regarding CSCs is their limited availability. With reported isolation efficiencies from cardiac biopsies ranging from 0.001-0.03%, CSCs are considered to be a rare cell-type.[30,97,99] Recently, Messina *et al* have tried to overcome this limitation by separating "phase-bright cells" from mouse and human myocardium to form cardiospheres that could be expanded in culture.[104] Additional work with cardiospheres has shown that they can generate cardiac action potentials when co-cultured with neonatal rat cardiomyocytes *in vitro*, and also improve ventricular function when delivered to the infarcted heart.[29] However, it remains unclear if human cardiospheres can generate new myocytes. Given the limited availability of CSCs from biopsies, extensive *in vitro* expansion will be

necessary to generate the number of cardiomyocytes needed to replace the contractile mass lost due to infarction.

### *Induced Pluripotent Stem Cells*

Transdifferentiation is a phenomena used to describe how cells committed to one lineage may be induced to express the phenotype of a lineage originating from a different germ layer.[46] As an example of normal differentiation, multipotent mesodermal BMCs naturally become various blood cell types, as well as fat, cartilage, and bone. However, transdifferentiation occurs when BMCs are encouraged to differentiate to alternate lineages, such endodermal epithelial cells or ectodermal neural cells.[56,59] Though mechanisms for these transitions are not completely understood, one hypothesis is that differentiated cells may be able to de-differentiate to a more pluripotent state and then re-differentiate into other cell-types. In 2007, a landmark study by Takahashi *et al*. demonstrated that human somatic cells can be reprogrammed to exhibit ESC-like properties.[31] By transfecting human dermal fibroblasts with Oct3/4, Klf4, Sox2, and c-Myc, they were able to induce the expression of several ESC-specific markers. Further studies revealed that the ESC-like fibroblasts could differentiate into cell types arising from all three germ layers, as well as form teratomas when delivered *in vivo* (a hallmark indication of ESCs). The combination of these results suggested that human dermal fibroblasts could seemingly be de-differentiated towards an ESC-like state, as induced pluripotent stem cells (iPS cells).

As part of their evidence for ESC-like pluripotency, Takahashi *et al*. used an established ESC-dervied cardiomyocyte differentiation protocol, treating with Activin-A/BMP4 to show that iPS cells could express cardiac markers (i.e. Nkx2.5, MEF2C, cTnT, MYL2A, and MYHCβ) and spontaneously contract after 12 days. Other studies have applied differentiation methods to iPS cells based on established methods adopted from ESC-derived cardiomyocyte literature (e.g. EB formation). Co-culture of iPS cells with OP9 stromal cells was found to enhance cardiac-specific markers and show organized striated phenotypes, with some of the cells producing nodal-like action potentials.[105] Using an EB-like differentiation process, iPS cell aggregates were able to express cardiac proteins, form sarcomeres,

contract *in vitro*, express gap junction proteins, and exhibit functional electrical coupling.[106] Most recently, Ieda *et al*. showed that retroviral transduction of a combination of three developmental transcription factors (Gata-4, Mef2C, and Tbx5) could directly and efficiently reprogram dermal fibroblasts to cardiomyocyte-like cells, without passing through an intervening pluripotent state.[107] Directly induced cardiomyocytes (iCMs) have a higher efficiency of cardiomyocyte differentiation, and have shown further cardiac cell maturation in successive weeks by sarcomere organization, increased contractility, and developed electrical properties.

One of the major questions that must be addressed regarding iPS cells is which genes are required to induce pluripotency and whether different combinations induce essentially the same pluripotent cell types. In addition, the work done with iCMs raises the question of whether it is necessary to reprogram cells back to a pluripotent state, or whether a more direct reprogramming approach is more effective for a cardiac cell types. The identification of specific factors responsible for reprogramming cells to exhibit ESC-like "stemness" is a marked achievement, however the viral vectors employed may cause unpredictable genetic dysfunctions. In addition, regulating the expression of these factors and their downstream effects may prove to be both difficult and problematic. This aspect of iPS cell research has encouraged groups to explore alternative methods for initiating these effective pluripotency mechanisms. Some groups have experimented with different gene delivery mechanisms, such as the use of removable transposons to deliver a multi-protein expression vector to minimize genetic modification.[108] Other groups suggest that iPS cells can be generated without genetic manipulation, by delivering "reprogramming proteins" fused to cell-penetrating peptides.[109] Recent studies have also suggested that fibroblast growth factor in low oxygen culture conditions increases nuclear expression of stem cell factors in adult human fibroblast.[110] Differentiation of adult human cells without genetic manipulation is likely to reduce the potential for mutagenic effects. Though these studies did not look for cardiogenic differentiation, they showed that their respective iPS cells can generate cell types that arise from all three germ layers. Another major concern with iPS cells is their propensity to form teratomas *in vivo*, even

though this is a well-recognized indication of true ESC-like pluripotency. As with ESCs, further studies are needed to show the safety and efficacy of differentiated iPS cells before they can be used in the clinic.

### 2.5. Mechanical Cardiac Function

Myocardial infarction (MI) and heart failure (HF) result in cardiomyocyte cell-death; thereby eliciting a remodeling cascade that not only reduces the number of contractile units, but also generates a scar that compromises both the integrity and compliance of the myocardial wall. With respect to the heart as an electromechanical pump, healthy cardiomyocytes respond to cyclic electrical impulses to shorten their sarcomeres. Synchronous action by cardiomyocytes permits the contraction of the myocardial walls, which act to pressurize atrial and ventricular cavities to pump blood for systemic circulation. Cardiomyocyte cell-death reduces active contraction within a region of the heart due to the decrease of working sarcomeres, impairing the heart's function as a mechanical pump. Necrosis and scarring within the affected region changes the material properties of the myocardial wall, creating a stiff area that may not comply with the dynamics of either surrounding contractile cardiomyocytes or developed pressures within heart cavities. Aiming to improve these outcomes, the ultimate goal of cardiac regeneration for the treatment of myocardial infarction and heart failure is to restore mechanical function to the injured heart.

Consequently, the effectiveness of any novel therapy for the improvement of myocardial function must be based on the resulting changes it demonstrates on mechanical function. Currently, there are several techniques that can be applied for measuring global or regional mechanical cardiac function, which have been used in either clinical or pre-clinical studies. In addition there are several parameters that can be measured as indicators of cardiac function, but inevitably the chosen technique can often limit the parameters that can be measured. Unfortunately, resource availability can present logistical challenges in choosing an appropriate technique. Oftentimes, investigators are limited by equipment expense or availability. In addition, the need for technological expertise may limit the experimental approach or flexibility in choosing unfamiliar methods. Knowing the capabilities of different

measurement techniques and the metrics that can be determined from acquired data should allow investigators to better interpret their findings regarding myocardial function.

### 2.6. Techniques for Measuring Mechanical Cardiac Function

Clinically, echocardiography and magnetic resonance imaging are the most commonly used techniques to assess cardiac mechanical function in patients.[111-122] Both methods provide options that are non- or minimally invasive, and have also been applied in experimental and pre-clinical studies. While studies on smaller animals require the appropriate equipment and procedure, the data acquisition and analysis methods are most similar to what clinicians use on human patients.

Echocardiography (ECHO) is a cardiac ultrasound technique, which employs a system to send and receive high-frequency sound waves to create either 2D or 3D images of the heart. The system requires the use of a probe to send sound across the chest cavity, which then reflects off of internal tissue. The reflection signature is then received by a transducer and translated to visualize the structure and motion of the tissue. The probe used for ECHO can either be placed externally on the outside of the chest for transthoracic signaling, or inserted down the esophagus for a transesophageal approach. These applications can be used to examine both the shape and velocity of the heart tissue in real time, allowing for the determination of wall movement, wall thickness, and blood velocity. While ECHO is a relatively inexpensive technique, it does have experimental limitations. The spatial resolution of ECHO has been reported to be on the order of 5 mm with a temporal resolution of 15 milliseconds, which is more suited for evaluating global function (compared to regional function) for short term cardiac-cycle analysis.[123] However, technological advances are continually improving upon these spatial and temporal constraints. ECHO is also subject to processing limitations, such as “noise” resulting from interference or image-variability depending on probe orientation.[123,124] While transthoracic ECHO is a less invasive approach, some regions of the ventricle can be difficult to image.[125] And though transesophageal ECHO may provide better access for tissue imaging, it is a slightly more invasive procedure.

Magnetic resonance imaging (MRI) is another non-invasive technique used to determine cardiac function, commonly used by radiologists to visualize detailed structure and function of internal body tissues. In this system, an MRI machine uses a radio frequency transmitter to energize photons to a resonance frequency, creating an electromagnetic field.[126] When a patient lies within the machine, the energized photons re-orient the spin of aligned hydrogen protons in water molecules within myocardial tissue.[126] When the machine is turned off, the protons return to their natural spin state, releasing energy in the form of photons which can be detected by a scanner to generate images of the heart.[126] Tagged MRI can provide more regional information than shape and size data obtained with conventional MRI. This technique uses intersecting "presaturation" planes that form "tag lines" throughout the myocardial tissue, in which intersections serve as markers that move with the heart wall. The movements of the intersections can be tracked, allowing for the determination of three-dimensional deformation and the enhancement of region-specific analysis. Despite these improvements, the data acquisition process for this technique can be time consuming as usually only one plane can be imaged at a time. After the data is acquired for one plane, the procedure is then repeated for the next plane (usually orthogonal to the base-apex axis). As a result, the total amount of time for data acquisition can take 35-40 minutes.[127] The spatial resolution of the technique (as defined as the distance between tags) is generally on the order of 5 mm. Improvements in image detail are limited, as better resolution comes at the risk of the MRI tags disappearing before the end of the diastolic/systolic interval being examined.[118] In addition to laborious data acquisition, data analysis is also complicated and time-consuming. Due to the required equipment and expertise needed, MRI can be very expensive. Despite the limitations, however, MRI is routinely used to evaluate hearts in pre-clinical studies of mice and rats, as well as clinical studies.[92,95,96,128,129]

Another clinical technique gaining popularity involves the electromechanical mapping of the heart with magnetic fields, through the use of a NOGA system (originally developed as the NOGA Cardiac Navigational System by Biosense Webster Inc. in 1997). In this system, a catheter is inserted into the ventricular cavity through the ventricular wall. A magnetic pad lying underneath the patient is used to generate a low level magnetic field, providing a three-dimensional orientation for guiding the catheter.

The catheter can then be positioned to sample several different points on the endocardial surface of the ventricle. The point measurements are then used to create a map of the endocardial surface, detailing information regarding mechanical deformation and unipolar voltage. With a spatial resolution of 1 mm, this technique is very useful for determining the movement of the ventricular wall at multiple locations and defined regions.

In the animal laboratory setting, sonomicrometry is commonly used to determine regional function of the heart *in-vivo*.[117,130-133] Sonomicrometry is a uni-axial technique involving the use of ultrasonic transducers, in which one transducer sends a sound wave to another transducer that receives the signal. The distance between the two transducers is proportional to the time it takes for the sound to travel, thereby providing a continuous measure of the distance between the two transducers as the heart expands and contracts. The transducer crystals must be implanted or sutured into the heart wall and the tissue should be homogeneous to sound waves for the signal to pass correctly. Sonomicrometry assumes a homogenous deformation between the transducers (~7-20 mm) and can only determine function along this axis. One pair of transducers provides distance measure along one axis, while two pairs of transducers can be used along two orthogonal axes to measure area deformation. If three pairs of transducers are used at three orthogonal axes, the volume of the ventricle can be calculated making the assumption the ventricle is an ellipsoidal in shape. In a regional setting, sonomicrometry can be used to determine changes in distance surrounding a specific area of the myocardium (e.g. an infarct region). This method is commonly used to determine ventricular volume, regional area, segment length, and wall thickening.

A major limitation of sonomicrometry, however, is that the implantation of the transducer crystals is more invasive and consequently more “fixed” in terms of region. To measure multiple regions would require either re-implanting the transducers to new locations or implanting more transducers, both of which result in more invasiveness and possible damage to the heart wall. As myocardial infarction usually results in a region (or regions) of the heart becoming dysfunctional, a technique to determine regional function over many regions (whole field) in the heart may be more helpful. To determine whole

field function, Prinzen et al. used 40-60 paper markers (1.5 mm diameter) arranged on the epicardium to determine epicardial wall displacements.[134] By tracking the markers, they were able to determine 2D wall displacements. And while using several markers, they could generate mechanical deformation data at multiple locations on the heart surface for whole field analysis.

To improve the spatial resolution of the epicardial-marker technique, an innovative phase correlation algorithm called Computer Aided Speckle Interferometry (CASI) was developed.[135] In this system, silicon carbide particles (40 μm in diameter) are applied to the epicardium, which are then illuminated with white light to create a speckled contrast for particle tracking (Figure 2.3). The phase correlation algorithm allows for increased computational efficiency compared to conventional particle tracking or digital correlation techniques. This algorithm has been shown to determine uni-axial strain that is equivalent to what can be obtained with sonomicrometry in isolated rabbit hearts.[135] Unlike sonomicrometry, however, CASI is a whole field technique that is able to determine two dimensional deformations with high spatial resolution.

Further improvements to the accuracy and precision of CASI were made by incorporating a sub-pixel algorithm called High Density Mapping (HDM), based on a method proposed by Foroosh and Zerubia.[136] In order to determine regional function over the course of a heartbeat, measured displacements must be summed between many images. HDM is used to model the result of CASI phase correlation as a sinc function, which is interpolated to determine subpixel motion. The sinc function, or cardinal sine function, is used to interpolate bandlimited discrete-time signals with respect to sampling rate and time by using uniformly spaced samples of each signal. To determine the accuracy of HDM, images of the heart were digitally shifted resulting in a 0.25, 0.50, or 0.75 pixel displacement. HDM was able to determine the pixel shift with an accuracy of 0.09 pixels, a precision of 0.04 pixels, and repeatability of measuring regional work loops in the beating heart of 0.04 mm Hg (normalized to end diastolic area).[137] These results demonstrate the ability of the technique to accurately, precisely, and repeatably determine regional deformation.

In order to determine regional function with HDM, the heart must be exposed to allow for a region to be imaged. A region of interest is then divided into subimages, with the displacement of each subimage being determined between consecutive images through Fourier transform. Through this algorithm, displacement can be determined at hundreds of locations, providing a whole field measurement (Figure 2.4). Regional stroke work can then be determined in very small regions based on the change in area between four neighboring points. So instead of constructing a work loop out of every four neighboring points, the average change in a sub-region consisting of 16-25 different areas is used. This method determines function in regions of less than 10 $mm^2$, as opposed to sonomicrometry in which the regional areas are generally greater than 100 $mm^2$. This technique has been used to determine regional function in the isolated rabbit heart, the *in vivo* porcine heart, and the *in vivo* canine heart.[25,67,138-140]

While the methods described herein provide data for both systolic and diastolic function, there are several limitations to them as well. Both MRI and ECHO require expensive equipment to image the heart. Along with this equipment, a lot of time is invested to collect data using MRI. The spatial resolution of both methods is less than optimal. Sonomicrometry and optical methods require exposure of the heart leading to an invasive procedure. In addition, optical methods generally require placement of non-sterile tracking markers making it useful only during the terminal phases of an experiment.

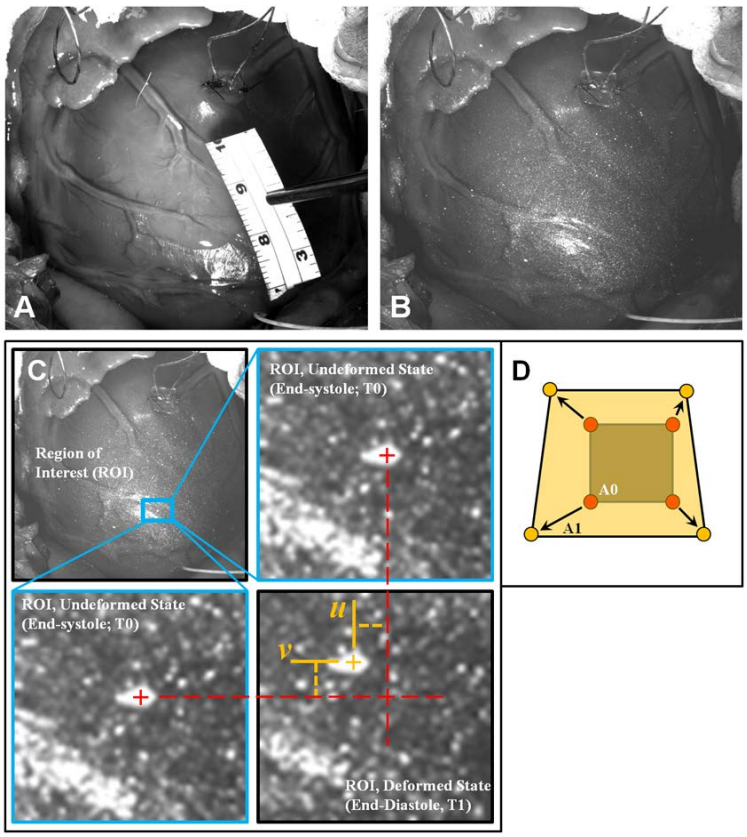


**Figure 2.3. Determination of regional cardiac function using High Density Mapping (HDM).** (A) Representative image of a porcine heart containing region of interest (ROI) (B) Image containing ROI, same area from (A), prepared with silicon carbide particles and retroreflective beads, creating speckled contrast for particle-tracking. (C) An identified ROI outlined in blue in the upper-left quadrant. An enlargement of the ROI in the undeformed state at $T_0$ is shown in the upper-right and lower-left quadrants (the same image is used for *u*, *v* reference points), with the location of a particle marked in red. An enlargement of the ROI in the deformed state at $T_1$, with the location of a particle marked in yellow, shown in the lower-right quadrant, indicating the shift of speckle particles throughout the cardiac cycle. (D) Schematic drawing of how several areas within the ROI can be tracked through the cardiac cycle. As the heart expands during diastole, regions of normal functioning myocardium also expand. By applying this algorithm to several areas in the ROI, regional mechanical function can be determine in a whole field manner, with high spatial resolution. (JP Guyette and GR Gaudette chapter, "Assessing Regional Mechanical Function after Stem Cell Delivery" in the text, *Regenerating the Heart*)[141]

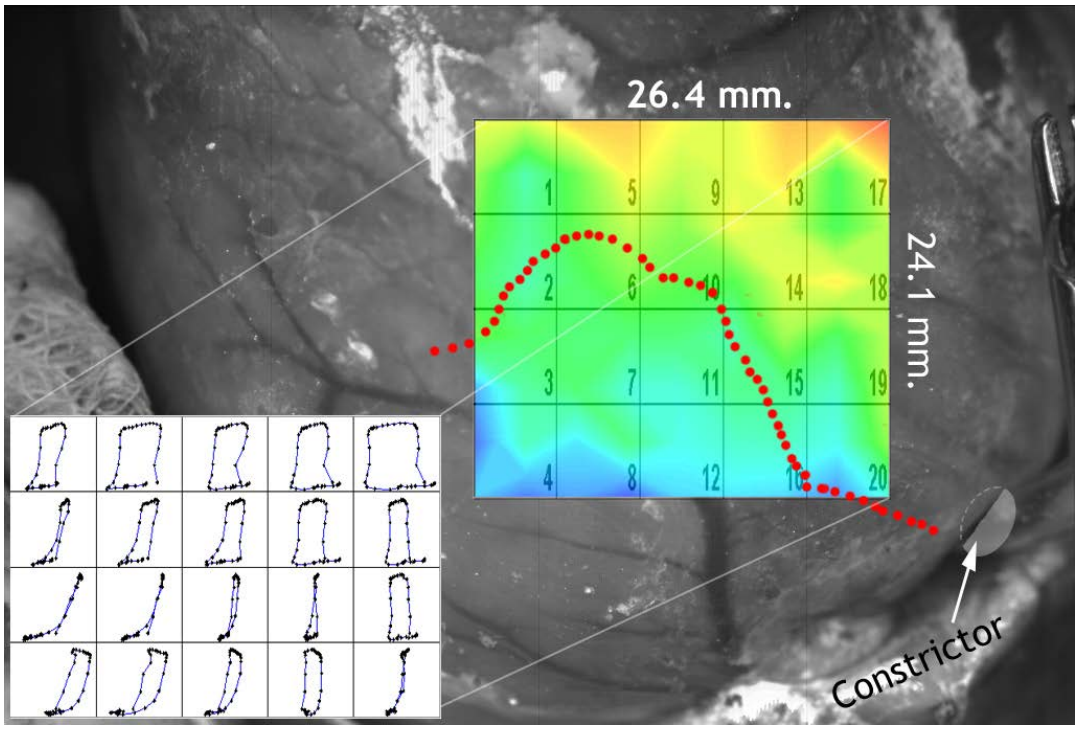


**Figure 2.4. Regional stroke work in the regionally ischemic porcine heart for whole field measurement.** The color map denotes the change in regional stroke work across the ischemic border (orange represents the highest function, whereas blue represents the lowest function). The insert in the lower left corner shows some of the regional work loops determined with HDM in the region of interest. For clarity, only 20 out of the 60 regional work loops computed in the region of interest are shown. Notes: 1) This assessment was taken on the epicardial surface of the left ventricle, in an ischemic porcine heart; 2) The loops in the lower left are actually reversed in direction (clockwise), denoting negative regional work; 3) The dotted line represents the ischemic border. (JP Guyette and GR Gaudette chapter, "Assessing Regional Mechanical Function after Stem Cell Delivery" in the text, *Regenerating the Heart*)[141]

## 2.7. Parameters for Assessing Mechanical Cardiac Function

Having discussed the clinical and experimental techniques used for analyzing heart structure and function, it is also necessary to review the relevant parameters that can be measured or calculated as functional indicators of cardiac mechanics. As the heart operates as an electromechanical pump, it functions to perpetuate and control circulation. While the right ventricle pumps deoxygenated blood to the lungs (within relatively close proximity in the chest), the left ventricle pumps oxygenated blood throughout the body (accessing all internal and extremity tissues/organs). Consequently, the left ventricle performs more work than the right ventricle and has a thicker wall due to increased muscularity. There are several measures that can be used to assess the function of the heart as a whole, though most are measures of left ventricular function in consideration of its vital purpose. The functional measures include stroke volume, stroke work, ejection fraction, tau ($\tau$), maximum change in pressure over time ($dP/dt_{max}$), and minimum change in pressure as a function of time ($dP/dt_{min}$).

In describing these measures, it is useful to review the basic physiological dynamics that constitute a cardiac cycle. A cardiac cycle involves the complete succession of one phase of ventricular contraction known as systole, followed by one phase of ventricular relaxation known as diastole (Figure 2.5A). Ventricular systole begins as the mitral valve closes at the end of atrial contraction, and consists of two main stages known as isovolumic contraction and ejection (Figure 2.5A, point "A"). Isovolumic contraction is the brief period of time between the onset of systole and the opening of the aortic valve, during which the ventricular volume remains constant as the ventricular pressure increases sharply. As pressure continues to increase within the ventricle, the aortic valve opens (at ~80 mmHg in a healthy heart), marking the end of isovolumic contraction and the onset of ejection. Ventricular pressure continues to rise during rapid ejection, forcing blood from the ventricle to the aorta as myocardium contracts and ventricular volume decreases. As pressure between the ventricle and aorta becomes more equalized, pressure within the ventricle begins to decrease for reduced ejection. When the ventricle fully contracts to a minimum volume and the aortic pressure is greater than that of the ventricle, the aortic valves close to mark the end of the contraction phase (called end-systole; Figure 2.5A, point "B"). End-

systole also signifies the onset of the diastolic ventricular relaxation phase. Diastole begins with isovolumic relaxation, in which ventricular pressure decreases sharply as ventricular volume remains steady. During this period, the atria are reaching maximum volume and pressure as they fill with blood. The isovolumic relaxation stage ends as the mitral valve opens, signifying the start of diastolic filling. During the filling stage, ventricular volume rapidly increases, allowing the ventricular pressure to remain low for efficient blood flow from the high-pressure atrium. When the ventricle is fully relaxed and the ventricular pressure exceeds atrial pressure, the mitral valve closes to mark the end of the relaxation phase (called end-diastole; Figure 2.5A, point "A"), thus completing the cycle.

Another key concept of cardiac physiology is the effective preload and afterload on cardiac muscle. Preload can be described as the stretching of cardiomyocytes that make up the intact heart, effectively represented by the end-diastolic ventricular volume at the end of filling. Several conditions can either increase or decrease preload, thereby having a direct effect on end-diastolic volume and the amount of blood filling the ventricle. Afterload can be described as the amount of pressure that must be generated by the left ventricle in order to overcome aortic pressure, which is necessary for the ejection of blood into the aorta. Just as with preload, there are a number of conditions that can either increase or decrease afterload. And while preload and afterload do not directly effect each other, there is a well-known relationship in which the heart can change its contractile force in response to venous return of blood. This phenomenon is known as the Frank-Starling mechanism. Venous return affects ventricular filling, thereby affecting left ventricular end-diastolic pressure (LVEDP, or preload). Ventricular filling also affects end-diastolic volume (preload), and changes in sarcomere length affect force generation in the form of stroke volume (SV). The Frank-Starling mechanism can be represented by plotting SV as a function of LVEDP (Figure 2.5B). The dynamic relationship shows how increases in LVEDP can increase SV and decreases in LVEDP can decrease SV (Figure 2.5B). The relationship can also have a significant effect on cardiac cycle pressure-volume work loops. Afterload can be controlled in experimental settings using animal models in order to study cardiac mechanics. Herein, this section will focus on measured parameters with reference to the described cardiac cycle and physiologic phenomenon.

Stroke volume (SV) is a practical volumetric measure, defined as the amount of blood that can be pumped to the aorta in one cardiac contraction (Equation 1). Stroke volume is calculated by subtracting the end-systolic volume (ESV; the minimum ventricular volume) from the end-diastolic volume (EDV; the maximum ventricular volume).

$$SV = EDV - ESV \tag{1}$$

Also considered to be a measure of the contractility of the heart, stroke volume can be used for calculating additional cardiac functional parameters.[142] For example, integrating stroke volume with respect to ventricular pressure (P) yields stroke work (SW) as shown in equation 2.

$$SW = \int SV \cdot dP \tag{2}$$

Stroke work is the amount of work performed by the ventricle as it ejects blood to the aorta in one cycle, or beat.[142] As a dynamic measure that can change based on metabolism, the generated kinetic energy can range from ~5% during rest to ~50% during high exertion. Stroke work can also change with the presentation of cardiomyopathies (e.g. myocardial infarction), resulting from physiological changes in ventricular volume and/or pressure.

Many clinical and experimental studies have also used ejection fraction as a measure of contractility. Ejection fraction (EF) is the ratio of the volume of blood ejected into the aorta in one cycle (i.e. end-diastolic volume *EDV* minus end-systolic volume *ESV*, which is equivalent to stroke volume *SV*) to the end-diastolic volume, as shown in equation 3.

$$EF = \frac{EDV - ESV}{EDV} = \frac{SV}{EDV} \tag{3}$$

Different from stroke volume, ejection fraction provides an indication of contractile efficiency by calculating the percentage of blood pumped out of the ventricle with respect to the maximal ventricular volume.

Parameters such as stroke volume, stroke work, and ejection fraction are relatively easy to determine in the clinic with commonly available equipment. This advantage allows the same variable to be measured at multiple testing sites and times. In addition, it offers a way to assess patients and compare the effects of potential treatment options. However, these parameters can be altered by ventricular aneurysms, valve incompetence, or changes in the overall ventricular size. In addition, changes in the passive properties of infarcted myocardium can lead to improved diastolic filling without improving the active contractile properties of the ventricle. Measurements of regional parameters that are synced with the ventricular pressure or EKG are better for determining improved contractile function.

Wall thickening, regional strain and systolic contraction can be acquired clinically to provide information on the contractile status of the ventricular wall. It is important to determine if the wall is contracting in synchrony with the rest of the ventricle. A passive material in the heart that is loaded with intracavitary pressure will decrease in thickness, whereas a contractile material will increase in thickness (which leads to the increase in intracavitary pressure).[143] A material that decreases in thickness will tend to be less compliant in that it cannot withstand intracavitary pressure, which may eventually lead to ventricular aneurysm. A material that increases in thickness could also be less compliant in that it may become too stiff, and may therefore impede the normal contractile force of the ventricle.

Animal models provide more opportunity for measuring independent of variables that are not easy to control in the clinic (e.g. heart rate and afterload). Preload recruitable stroke work (PRSW) has been used to evaluate the global function of the heart. PRSW, the linear relationship of the stroke work to end diastolic volume, is independent of heart rate and afterload.[1] Measurements such as end systolic volume, end systolic pressure-volume relationship (ESPVR), change in ventricular pressure over time (dP/dt), can

provide valuable information on the contractile status in the global heart, but can also be dependent on heart rate and aortic pressure (Figure 2.5 C, D).

While many techniques focus on systolic function, diastolic function also plays an important role in heart failure as stiffness and wall thickness can affect relaxation and filling. Diastolic function has commonly been assessed based on a global measurement of the time constant of isovolumic pressure decay, tau ($\tau$). The isovolumic relaxation constant was determined by Weiss et. al by assessing pressure fall during isovolumic beats.[144] They found pressure fall, dP/dt, was exponential during isovolumic relaxation and was characterized by a time constant of relaxation, $\tau$. More recently, apical recoil or untwisting and the temporal change in this variable, have been used to assess diastolic function of the ventricle.[145] As this can be measured at different locations within the ventricle, it can be used to define regional diastolic function.

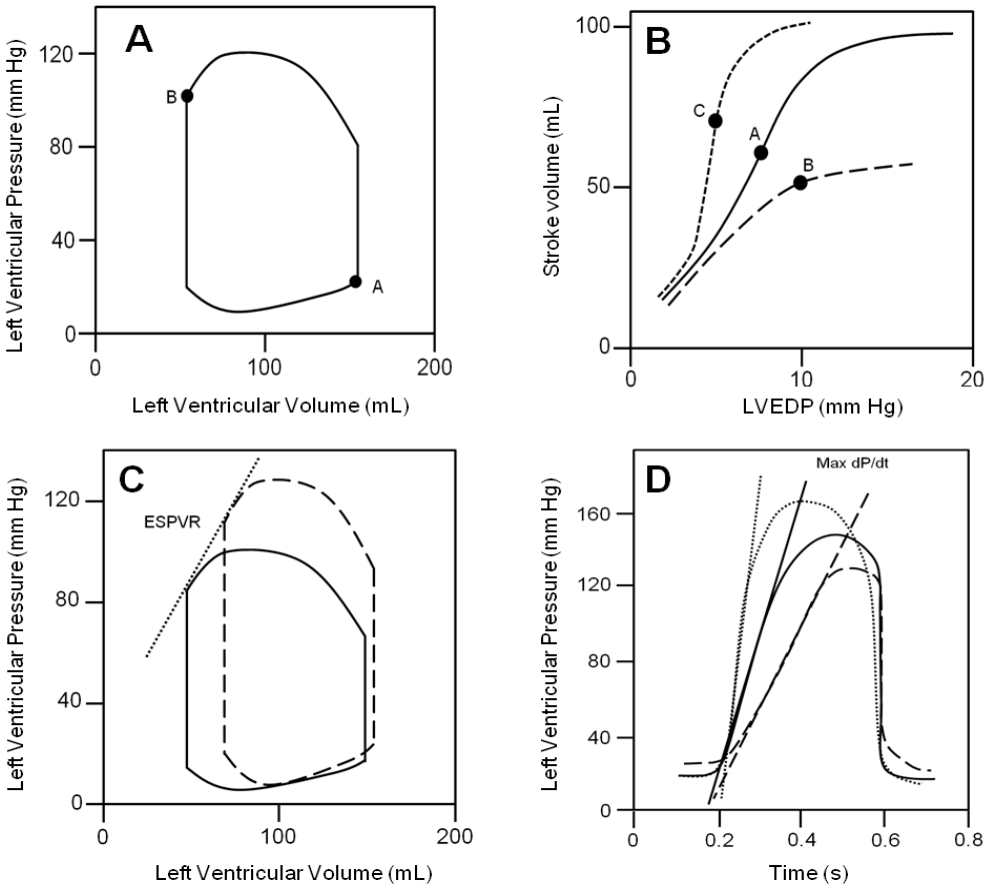


**Figure 2.5. Variables used in determining regional function in the heart.** (A) Pressure-volume work loop of the left ventricle through one cardiac cycle. Point A indicates "end-diastole" and Point B indicates "end-systole". Integrating for the area within the loop provides the amount of work done by the left ventricle over the course of one cardiac cycle. By substituting regional area for left ventricular volume, a regional stroke work loop is constructed, with regional stroke work being determined from the integral of left ventricular volume with respect to regional area. (B) Frank-Starling curves show the effects that preload can have on stroke volume, which is directly related to stretching during diastolic filling. Line A indicates a normal operating curve, whereas Line B indicates a decreased contractility and Line C indicates increased contractility. (C) End systolic pressure volume relationship (ESPVR) is determined by plotting this point for several different sized work loops. The size of the work loop can be altered by changing the preload on the ventricle. Preload recruitable stroke work, the linear relationship between stroke work and end-diastolic volume, can also be determined with the information from this plot. (D) Maximum (or minimum) dP/dt (change in pressure per change in time) can be obtained by plotting the left ventricular pressure as a function of time. This relationship can be altered, providing a measure of the mechanical function in the left ventricle. (JP Guyette and GR Gaudette chapter, "Assessing Regional Mechanical Function after Stem Cell Delivery" in the text, *Regenerating the Heart*)[141]

## 2.8. Regional Cardiac Mechanics

Myocardial defects such as smaller myocardial infarctions can occur within definite, localized regions of the heart. In order to study these effects and potential treatments, it is necessary to be able to determine the mechanical function in the defined regions. Clinically, these measurements can be taken with several techniques including MRI, ECHO, and NOGA. Tagged MRI is a method that can noninvasively measure the internal motions within the heart wall.[146,147] As mentioned, tagged MRI is advantageous because it can be used to determine 3D measurements of both stroke volume and stroke work. It can also be used for local strain measurements to determine function in regions of the myocardium that may be damaged from ischemia, hypertrophy, or infarction.[148-151] Dong et. al. have also used tagged MRI on canines to measure the angle displacement of the base of the heart relative to the apex.[152] The displacement angles were indicative of the twisting of the heart due to an applied force in the circumferential direction, resulting in ventricular torsion. Torsion measurements determined during diastole could then be correlated to the global measure of the diastolic relaxation time constant, tau, during isovolumic relaxation. [152]

ECHO is also used to determine regional changes in wall size, wall movements, wall stiffness, and cavity size. Most recently, ECHO has been used to determine strain and strain rate in the myocardium. A new method of ECHO called ultrasound speckle tracking imaging (STI) has been employed, which uses B-scan ultrasound to give the appearance of speckle patterns within the tissue. Motion analysis can then be done on the speckles to determine strain and ventricular torsion.[153]

Using the aforementioned methods, deformation can be determined in the beating heart leading to the determination of engineering strain, defined in the uni-axial case as the change in length divided by the original undeformed length. The heart is exposed to three dimensional deformations, leading to strain along 3 axes and shear stress acting on orthogonal planes. There exists an orientation in which there is no shear strain. In this orientation, the maximum and minimum strain exists. The maximal strain is the principal strain in the 1 direction and the minimal strain I s the principal strain in the 2 direction which is orthogonal to the 1 direction.

The strain in the 1 direction is the expansion of the myocardium during systole. Since the myocardium is incompressible and hence the volume needs to be conserved, expansion has to be coupled with contraction in a different direction in the wall. Principal strain changes in both magnitude and angle resulting from cardiac events.[154-156] Using MRI to measure principal strain changes in mice with heart failure Hankiewicz et. al. found that the principal strain in the 1 direction decreased with advancement of heart failure compared to controls.[155] In addition, they detected decreases in principal strains prior to dilation of the ventricle.[155] Cupps and colleagues[156] used MRI to measure the principal strain orientation in the normal human left ventricle. Their results suggested that principal strain in the maximal contraction direction occurs in the circumferential-longitudinal plane that aligns with the apex to base axis of the heart.[156] Their work shows that orienting displacement data along the apex to base cardiac axis will provide the maximal contractile strain for the heart.

### 2.9. Active and Passive Mechanical Function

Mechanical function in the heart consists of both active and passive components, both of which are potential targets for regenerative therapy. The active function is manifested by the contraction of cardiomyocytes, which is primarily responsible for the systolic phase of the cardiac cycle. Active function (i.e. systolic contraction) decreases during myocardial infarction and heart failure, due to the loss or dysfunction of cardiomyocytes. Just as important as active function, the passive function of the ventricle also plays an important role by providing a compliant structure. In the cardiac cycle, the compliance of the myocardium allows for maximal shortening during systolic contraction and maximal expansion during diastolic relaxation.

Myocardium is a complex tissue type, comprised of contractile cardiomyocytes that interact with each other and several other cell types (e.g. vascular smooth muscle cells, endothelial cells, fibroblasts, etc.) in an extracellular matrix (ECM) composed of structural proteins (e.g. collagen, elastin, laminin, and fibronectin). While cardiomyocytes are responsible for active function, the interactions of cells and ECM are responsible for passive function. Cell-ECM interactions provide the structural network for anchoring

cardiomyocytes and translating the sarcomeric shortening of individual myocytes into organized myocardial contraction. The network also provides elasticity and integrity during diastole, allowing for maximal expansion while preventing overstretching or rupture.

Active and passive function can both be compromised during myocardial infarction (MI). During an MI, the heart undergoes a wound response that typically includes inflammation, cellular turnover, and extracellular matrix remodeling. Dead or afflicted cells (including cardiomyocytes) are replaced with new cellular components such as fibroblasts and vascular cells. The content and organization of the cardiac extracellular matrix is remodeled by both reparative and reactive fibrosis, causing the degradation of normal matrix and increasing the deposition of collagen.[157] The resulting scar is stiffer than healthy cardiac extracellular matrix and leaves the affected area devoid of cardiomyocytes. Not only does the infarct region lose contractile elements necessary for active function, but passive function is also impaired as the stiffer matrix is more difficult to deform during systolic contraction and diastolic expansion. Considering the spared cardiomyocytes at the border-zone of an MI or in the case of a non-transmural MI, cell-infarct interactions compromise systolic contraction as myocytes have a more difficult time shortening when anchored to a non-compliant substrate.

To repair the outcomes of an MI and restore mechanical function, regenerative therapies can be targeted to improve active function, passive function, or both.[143] Adding contractile elements to the infarct may increase active contraction. Whether delivering exogenous cells (i.e. stem cell derived cardiomyocytes), or recruiting endogenous cells to home and differentiate to cardiomyocytes, it may be possible to restore contractile function.[4] Alternatively, improving the compliance of the infarct region may increase passive function.[143] Whether surgically replacing the infarct with a more compliant biomaterial, or delivering/recruiting cells that improve cardiac tissue remodeling, it may be possible to decrease stiffness or increase elasticity for improved passive function. Implanting a more-compliant biomaterial seeded with cardiomyocytes, or implanting a biomaterial that actively recruits cardiomyocytes, may combine efforts to improve both active and passive mechanical function.[143]

It is difficult to distinguish the active contractile properties from the passive properties *in vivo*. In normal myocardium, the increase in intracavitary pressure results from the contraction of myocytes. If one were to look at a cross-section of left ventricle, the area of this region would decrease with increased load such as intracavitary pressure (Figure 2.6). However, if a material void of cells and contractile properties is implanted in the heart, it will expand under an increase intracavitary load. This is similar to what happens when an elastic balloon is filled with water; the balloon expands as the pressure inside the balloon increases. If the balloon was composed of a stiff material, the balloon would still increase, however the increase may be microscopic. When an accelluar compliant scaffold, such as isolated porcine urinary bladder ECM, is implanted in the ventricular wall, the area of the scaffold will increase with intracavitary pressure (Figure 2.6). Most biological materials are non-linear in the elastic range. If the scaffold is a stiff material, such as Dacron, the load is not enough to cause a significant change in the area of the implanted scaffold. Hence, changes in intracavitary pressure do not deform the scaffold, similar to the effects of a stiff scarred region. Therefore, a more compliant scaffold tends to improve function by allowing for passive properties such as expansion and elasticity, whereas stiff scaffolds do not offer much functional benefit beyond the originals scar.

If contractile cells begin to populate the implanted region, they must be able to deform the scaffold prior to performing useful mechanical work that contributes to pump function. If the material is expanding during contraction (Figure 2.6), then the contractile cells in this region must generate enough force to balance the tensile forces due to the increased intracavitary load. If the region is stiff, as is often the case in collagen populated infarcts, the contractile cells must be able to deform the region in order to contribute to a decreased systolic volume in the heart. For example, contracting embryoid bodies are able to deform surrounding attached cells, but they do not deform the stiff cell culture dish. Thus, if a small number of myocytes were regenerated in a stiff infarcted region of the heart, they could not generate enough force to improve contraction in the heart. Thus, there appears to be a critical number of new myocytes that needed to contribute to active function in the heart. And this critical number of myocytes may be dependent on the passive mechanical properties of the region. [158]

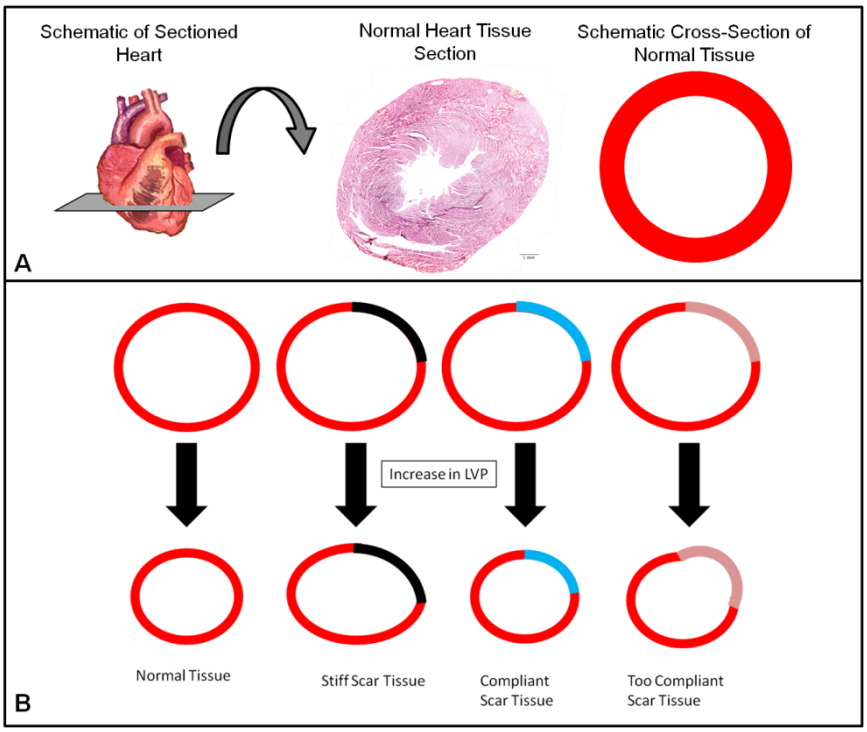


**Figure 2.6. Variable tissue properties of a passive region can lead to changes in ventricular function.** For a region that is passive, that is one that does not have any contractile elements, its deformation is dictated by the intracavitary pressure. Unlike normal myocardium, which contracts with increasing intracavitary pressure, passive materials will elongate (resulting in a thinner wall) under intracavitary loads. (A) The normal cross sectional area of the left ventricle is schematically demonstrated as a red circle on the right of the panel. (B) If the mechanical properties of a region of the heart are altered (e.g. myocardial infarct, scar, scaffold implantation), the shape of the cross section of the ventricle can be altered. As the pressure increases in the normal heart, the entire cross section of the ventricle contracts (far left). In the case of a stiff scar, the region cannot contract, leading to a region of the ventricle that does not change in shape (second from left). If the scar is compliant, it will deform with the ventricle, although it will not contract if it is passive (second from right). However, if the scar is thin and very compliant, it will balloon out as the pressure inside the ventricle (far right). (JP Guyette and GR Gaudette chapter, "Assessing Regional Mechanical Function after Stem Cell Delivery" in the text, *Regenerating the Heart*)[141]

## 2.10. Regional Mechanical Function in the Diseased Heart

Most animal models used to evaluate cell therapy aim to develop a well-defined region of dysfunction. However, mechanical function in ischemic or infarcted hearts is generally heterogeneous. For example, Figure 2.4 demonstrates work loops from regions within the ischemic porcine heart. Mechanical function in the border zone, the region between infarcted tissue and normally perfused tissue, is very different compared to normally perfused tissue or tissue in the center of the ischemic zone. The work loops from the border zones (Regions 2, 6, 11, 15 and 20 in Figure 2.4) in general show very little work, as evident by the lack of any significant area within the work loop. Regions within the ischemic zone (regions 4, 8, 12, and 16 in Figure 2.4) show reversed work loops, suggesting the contraction of these regions is out of sync with ventricular contraction. While regions of normally perfused tissue are contracting, resulting in increased intracavitary pressure, the ischemic regions are dyskinetic and expanding due to the increased load on the tissue. Therefore, the ventricle (as a whole) is producing less contractile force, which thereby causes an increased end-systolic volume during the cardiac cycle and a decreased ejection fraction.

Similar to myocardial ischemia, various ranges of dysfunction can occur within the infarcted myocardium depending on the severity of the infarct, the time of recovery and the location (Fomovsky & Holmes, 2009). For more details on the mechanical properties of myocardial infarcts, see Holmes, Borg & Covell, 2007.

In order to evaluate the effects of cell therapy in the dysfunctional heart, the region of cell delivery must first be identified. Delivery by intravenous or intracoronary methods can lead to dispersion of cells throughout the heart, making the location of cells difficult to identify. To clearly identify the delivery region, we have employed the use of a cell seeded myocardial patch composed of an extracellular matrix.[67] When this patch is used to replace a full thickness defect in the ventricular wall, a region for mechanical analysis is well defined. Using HDM (previously described) allowed for determination of function in regions approximately 5 x 5 mm. Upon implantation of unseeded scaffold, there is no contractile function. As the load inside the ventricle increases, the scaffold passively deforms increasing

in area. Such a response is expected of any compliant, passive material when it is exposed to an increase in intracavitary pressure. A stiff material, such as Dacron, is also a passive material and does not demonstrate any deformation when the heart contracts.[158] The deformation is limited due to the stiff (non-compliant) nature of the material. Eight weeks after implantation of scaffolds seeded with human mesenchymal stem cells, regional stroke work is positive. This suggests that the scaffold region is contracting in sync with the rest of the heart because the scaffold region is contracting while the intracavitary pressure is increasing.

### 2.11. Challenges with Cellular Therapy for the Heart

Despite the initial successes with cell therapy, there are still many issues facing the field. Cell retention in the beating heart remains a challenge. Intravenous and intracoronary delivery of cells results in low engraftment in the heart. Cell retention is increased with intramyocardial injections, but 3-11% retention rates are still very inefficient.[159,160] Delivery of cells by applying a cell seeded scaffold onto the epicardial surface of the heart can further increase cell engraftment, but this requires a more invasive procedure.[161] In addition, only a small percentage of cells migrate through the heart wall to the endocardium, where most clinical myocardial infarctions reside.[161] Novel methods of cell delivery include loading cells on biological sutures that can then be delivered to the heart wall.[162] However, much work needs to be done to determine how many cells can be delivered with this method.

Tracking delivered cells can also be an issue. Injured myocardial tissue is known to be highly auto-fluorescent leading to difficulties when using green fluorescent proteins to track cells.[38] Iron oxide labeled cells can be tracked with MRI but it is difficult to track small numbers in the whole heart. Accurate determination of the numbers of engrafted cells will be important in evaluating the dose response curves of different cell types. Engraftment rates are also important in determining if improved regional function correlates with the number of cells retained by the heart. Regional mechanical function can be determined by a number of techniques, but few offer the high spatial resolution needed to assess function in the small region surrounding cell delivery sites.

The expression of cardiac specific proteins has been documented in many different differentiated cells. However, the organization of cardiac specific proteins into functionally relevant sarcomere formations is unclear or questionable. The ability of a cell to express cardiac proteins is an important initial step in differentiation, but formation of sarcomeres and other functionally essential apparatus in the cell are necessary for improved function.[30] While the addition of non-contractile cells may improve mechanical function in the heart, full regeneration will require the contractile elements.[143]

Many studies have demonstrated "proof of principle" for the benefits of cardiac cell therapy, by increasing cardiomyocyte content by either myocyte proliferation or stem cell differentiation. Both methods have their advantages and there is no evidence to suggest the two methods cannot be used synergistically to regenerate function at a higher rate than either alone. Success with either or both of these approaches will improve the prognosis for millions of Americans suffering from myocardial infarction and/or heart failure.

### 2.12. Mechanical Function Post Stem Cell Delivery

A number of clinical trials have been initiated to assess the resultant function of various cell therapies delivered to the heart. The results from trials have been mixed, with some trials indicating improved left ventricular EF ranging from 2.5 to 6.0 percentage points with BMCs at 4-6 months compared to controls,[163-165] and others showing no effect from cell therapy (treatment effect of +0.6 and +1.0 percentage points on LVEF).[152,166] Despite short-term improvements in function, it is unclear whether long term enhancement in EF can be sustained as another study showed loss of improvements at 18 months after cell delivery.[167] In order to make these measurements in small animals such as mice and rats, echocardiography and MRI are frequently used. Both of these techniques are able to determine global volume of the heart, allowing assessment of global function in the heart. However, the limited spatial resolution of the techniques decreases the ability to accurately assess regional function in the heart of small animals. In addition to echocardiography and MRI, sonomicrometry, conductance catheters[168] and digital imaging techniques have been used in large animal models.

One major limitation facing the field is that the use of different parameters (e.g. ejection fraction, stroke work, developed pressure, wall thickness, etc.) makes it difficult to compare different studies. Therefore, it is difficult to compare the various cell types being used (as described throughout this text), which confounds the determination of an optimal cell type for cardiomyoplasty. Another major limitation that is often not considered is the use of human cells in animal models, whose hearts beat much faster than human hearts (e.g. 60 bpm in humans, and ~400 bpm in rats). It remains to be determined if human cells delivered in the human heart will engraft with similar efficiency and improve functional parameters similar to that of animal models. As mentioned previously, it is also difficult to separate the passive component versus the active component of cardiac mechanical function. Moving forward, more studies are needed to correlate the improvement of mechanical function with the evidence of increased contractile mass. This correlation will help to distinguish whether the improvements can be attributed to regenerated, actively contracting cardiomyocytes, or whether the improvements are due to more optimal tissue-compliance with the delivered cellular mass.

## 2.13. References


1 Mathew N. Levy, M. a. A. J. P., PhD. in *The Mosby Physiology Monograph Series* (ed William Schmitt) 269 (Mosby Elsevier, Philadelphia, PA, 2007).

2 Robert M. Berne, M. N. L., Bruce M. Koeppen, Bruce A. Stanton 1014 (Mosby, an affiliate of Elsevier, Inc., St. Louis, MO, 2004).

3 AHA. *American Heart Association: International Cardiovascular Disease Statistics*, <http://www.americanheart.org/downloadable/heart/12362040121112INTL.pdf> (2009).

4 Cohen, I. S. & Gaudette, G. R. Regenerating the heart: new progress in gene/cell therapy to restore normal mechanical and electrical function. *Dialogues in Cardiovascular Medicine* **14**, 19, (2009).

5 Lloyd-Jones, D. *et al.* Heart disease and stroke statistics--2009 update: a report from the American Heart Association Statistics Committee and Stroke Statistics Subcommittee. *Circulation* **119**, e21-181, (2009).

6 Rosamond, W. *et al.* Heart disease and stroke statistics--2008 update: a report from the American Heart Association Statistics Committee and Stroke Statistics Subcommittee. *Circulation* **117**, e25-146, (2008).

7 Jessup, M. & Brozena, S. Heart failure. *N Engl J Med* **348**, 2007-2018, (2003).

8 Orlic, D. *et al.* Bone marrow cells regenerate infarcted myocardium. *Nature* **410**, 701-705, (2001).

9 Buxton, A. E. Should everyone with an ejection fraction less than or equal to 30% receive an implantable cardioverter-defibrillator? Not everyone with an ejection fraction < or = 30% should receive an implantable cardioverter-defibrillator. *Circulation* **111**, 2537-2549; discussion 2537-2549, (2005).

10 Moss, A. J. Should everyone with an ejection fraction less than or equal to 30% receive an implantable cardioverter-defibrillator? Everyone with an ejection fraction < or = 30% should receive an implantable cardioverter-defibrillator. *Circulation* **111**, 2537-2549; discussion 2537-2549, (2005).

11 Risk stratification and survival after myocardial infarction. *N Engl J Med* **309**, 331-336, (1983).

12 Bergmann, O. *et al.* Evidence for cardiomyocyte renewal in humans. *Science* **324**, 98-102, (2009).

13 Strauer, B. E. *et al.* Repair of infarcted myocardium by autologous intracoronary mononuclear bone marrow cell transplantation in humans. *Circulation* **106**, 1913-1918, (2002).

14 Schachinger, V. *et al.* Intracoronary bone marrow-derived progenitor cells in acute myocardial infarction. *N Engl J Med* **355**, 1210-1221, (2006).

15 Ko, D. T. *et al.* Life expectancy after an index hospitalization for patients with heart failure: a population-based study. *American heart journal* **155**, 324-331, (2008).

16 Dorfman, J. *et al.* Myocardial tissue engineering with autologous myoblast implantation. *J Thorac Cardiovasc Surg* **116**, 744-751, (1998).

17 Taylor, D. A. *et al.* Regenerating functional myocardium: improved performance after skeletal myoblast transplantation. *Nat Med* **4**, 929-933, (1998).

18 Wang, C. C. *et al.* Direct intramyocardial injection of mesenchymal stem cell sheet fragments improves cardiac functions after infarction. *Cardiovasc Res* **77**, 515-524, (2008).

19 Beltrami, A. P. *et al.* Evidence that human cardiac myocytes divide after myocardial infarction. *N Engl J Med* **344**, 1750-1757, (2001).

20 Meckert, P. C. *et al.* Endomitosis and polyploidization of myocardial cells in the periphery of human acute myocardial infarction. *Cardiovasc Res* **67**, 116-123, (2005).

21 Beltrami, C. A. *et al.* Proliferating cell nuclear antigen (PCNA), DNA synthesis and mitosis in myocytes following cardiac transplantation in man. *J Mol Cell Cardiol* **29**, 2789-2802, (1997).

22 Poss, K. D., Wilson, L. G. & Keating, M. T. Heart regeneration in zebrafish. *Science* **298**, 2188-2190, (2002).

23 Leferovich, J. M. *et al.* Heart regeneration in adult MRL mice. *Proc Natl Acad Sci U S A* **98**, 9830-9835, (2001).

24 Schuster, M. D. *et al.* Myocardial neovascularization by bone marrow angioblasts results in cardiomyocyte regeneration. *Am J Physiol Heart Circ Physiol* **287**, H525-532, (2004).

25 Kelly, D. J. *et al.* Increased Myocyte Content and Mechanical Function Within a Tissue-Engineered Myocardial Patch Following Implantation. *Tissue Eng Part A*, (2009).

26 Badylak, S. F., Park, K., Peppas, N., McCabe, G. & Yoder, M. Marrow-derived cells populate scaffolds composed of xenogeneic extracellular matrix. *Exp Hematol* **29**, 1310-1318, (2001).

27 Busk, P. K. *et al.* Cyclin D2 induces proliferation of cardiac myocytes and represses hypertrophy. *Exp Cell Res* **304**, 149-161, (2005).

28 Engel, F. B. *et al.* p38 MAP kinase inhibition enables proliferation of adult mammalian cardiomyocytes. *Genes Dev*, (2005).

29 Smith, R. R. *et al.* Regenerative potential of cardiosphere-derived cells expanded from percutaneous endomyocardial biopsy specimens. *Circulation* **115**, 896-908, (2007).
30 Schuldt, A. J., Rosen, M. R., Gaudette, G. R. & Cohen, I. S. Repairing damaged myocardium: evaluating cells used for cardiac regeneration. *Curr Treat Options Cardiovasc Med* **10**, 59-72, (2008).
31 Takahashi, K. *et al.* Induction of pluripotent stem cells from adult human fibroblasts by defined factors. *Cell* **131**, 861-872, (2007).
32 Menasche, P. in *Rebuilding the Infarcted Heart* (eds K C Wollert & L J Field) 181-194 (Informa Healthcare, 2007).
33 Hauschka, S. D. Clonal analysis of vertebrate myogenesis. II. Environmental influences upon human muscle differentiation. *Dev Biol* **37**, 329-344, (1974).
34 Mannion, J. D., Bitto, T., Hammond, R. L., Rubinstein, N. A. & Stephenson, L. W. Histochemical and fatigue characteristics of conditioned canine latissimus dorsi muscle. *Circ Res* **58**, 298-304, (1986).
35 Stevens, K. R. *et al.* Chemical dimerization of fibroblast growth factor receptor-1 induces myoblast proliferation, increases intracardiac graft size, and reduces ventricular dilation in infarcted hearts. *Hum Gene Ther* **18**, 401-412, (2007).
36 Leobon, B. *et al.* Myoblasts transplanted into rat infarcted myocardium are functionally isolated from their host. *Proc Natl Acad Sci U S A* **100**, 7808-7811, (2003).
37 Coppen, S. R. *et al.* A factor underlying late-phase arrhythmogenicity after cell therapy to the heart: global downregulation of connexin43 in the host myocardium after skeletal myoblast transplantation. *Circulation* **118**, S138-144, (2008).
38 Laflamme, M. A. & Murry, C. E. Regenerating the heart. *Nat Biotechnol* **23**, 845-856, (2005).
39 He, J. Q., Ma, Y., Lee, Y., Thomson, J. A. & Kamp, T. J. Human embryonic stem cells develop into multiple types of cardiac myocytes: action potential characterization. *Circ Res* **93**, 32-39, (2003).
40 Kehat, I. *et al.* Human embryonic stem cells can differentiate into myocytes with structural and functional properties of cardiomyocytes. *J Clin Invest* **108**, 407-414, (2001).
41 Laflamme, M. A. *et al.* Cardiomyocytes derived from human embryonic stem cells in pro-survival factors enhance function of infarcted rat hearts. *Nat Biotechnol* **25**, 1015-1024, (2007).
42 Lev, S., Kehat, I. & Gepstein, L. Differentiation pathways in human embryonic stem cell-derived cardiomyocytes. *Ann N Y Acad Sci* **1047**, 50-65, (2005).
43 Nakamura, T., Sano, M., Songyang, Z. & Schneider, M. D. A Wnt- and beta -catenin-dependent pathway for mammalian cardiac myogenesis. *Proc Natl Acad Sci U S A* **100**, 5834-5839, (2003).
44 Sartiani, L. *et al.* Developmental changes in cardiomyocytes differentiated from human embryonic stem cells: a molecular and electrophysiological approach. *Stem Cells* **25**, 1136-1144, (2007).
45 Satin, J. *et al.* Mechanism of spontaneous excitability in human embryonic stem cell derived cardiomyocytes. *J Physiol* **559**, 479-496, (2004).
46 Murry, C. E., Reinecke, H. & Pabon, L. M. Regeneration gaps: observations on stem cells and cardiac repair. *J Am Coll Cardiol* **47**, 1777-1785, (2006).
47 Xu, C., Police, S., Hassanipour, M. & Gold, J. D. Cardiac bodies: a novel culture method for enrichment of cardiomyocytes derived from human embryonic stem cells. *Stem cells and development* **15**, 631-639, (2006).
48 Yang, L. *et al.* Human cardiovascular progenitor cells develop from a KDR+ embryonic-stem-cell-derived population. *Nature* **453**, 524-528, (2008).
49 Klug, M. G., Soonpaa, M. H. & Field, L. J. DNA synthesis and multinucleation in embryonic stem cell-derived cardiomyocytes. *Am J Physiol* **269**, H1913-1921, (1995).
50 Snir, M. *et al.* Assessment of the ultrastructural and proliferative properties of human embryonic stem cell-derived cardiomyocytes. *Am J Physiol Heart Circ Physiol* **285**, H2355-2363, (2003).
51 Xu, C., Police, S., Rao, N. & Carpenter, M. K. Characterization and enrichment of cardiomyocytes derived from human embryonic stem cells. *Circ Res* **91**, 501-508, (2002).
52 McDevitt, T. C., Laflamme, M. A. & Murry, C. E. Proliferation of cardiomyocytes derived from human embryonic stem cells is mediated via the IGF/PI 3-kinase/Akt signaling pathway. *J Mol Cell Cardiol* **39**, 865-873, (2005).
53 Hentze, H. *et al.* Teratoma formation by human embryonic stem cells: evaluation of essential parameters for future safety studies. *Stem cell research* **2**, 198-210, (2009).
54 Chidgey, A. P., Layton, D., Trounson, A. & Boyd, R. L. Tolerance strategies for stem-cell-based therapies. *Nature* **453**, 330-337, (2008).

55 Drukker, M. & Benvenisty, N. The immunogenicity of human embryonic stem-derived cells. *Trends in biotechnology* **22**, 136-141, (2004).
56 Jiang, Y. *et al.* Pluripotency of mesenchymal stem cells derived from adult marrow. *Nature* **418**, 41-49, (2002).
57 Lagasse, E. *et al.* Purified hematopoietic stem cells can differentiate into hepatocytes in vivo. *Nat Med* **6**, 1229-1234, (2000).
58 Wang, X. *et al.* Kinetics of liver repopulation after bone marrow transplantation. *The American journal of pathology* **161**, 565-574, (2002).
59 Brazelton, T. R., Rossi, F. M., Keshet, G. I. & Blau, H. M. From marrow to brain: expression of neuronal phenotypes in adult mice. *Science (New York, N.Y* **290**, 1775-1779, (2000).
60 Weimann, J. M., Charlton, C. A., Brazelton, T. R., Hackman, R. C. & Blau, H. M. Contribution of transplanted bone marrow cells to Purkinje neurons in human adult brains. *Proc Natl Acad Sci U S A* **100**, 2088-2093, (2003).
61 Balsam, L. B. *et al.* Haematopoietic stem cells adopt mature haematopoietic fates in ischaemic myocardium. *Nature* **428**, 668-673, (2004).
62 Murry, C. E. *et al.* Haematopoietic stem cells do not transdifferentiate into cardiac myocytes in myocardial infarcts. *Nature* **428**, 664-668, (2004).
63 Lagostena, L. *et al.* Electrophysiological properties of mouse bone marrow c-kit+ cells co-cultured onto neonatal cardiac myocytes. *Cardiovasc Res* **66**, 482-492, (2005).
64 Beeres, S. L. *et al.* Human adult bone marrow mesenchymal stem cells repair experimental conduction block in rat cardiomyocyte cultures. *J Am Coll Cardiol* **46**, 1943-1952, (2005).
65 Makino, S. *et al.* Cardiomyocytes can be generated from marrow stromal cells in vitro. *J Clin Invest* **103**, 697-705, (1999).
66 Xu, M. *et al.* Differentiation of bone marrow stromal cells into the cardiac phenotype requires intercellular communication with myocytes. *Circulation* **110**, 2658-2665, (2004).
67 Potapova, I. A. *et al.* Enhanced recovery of mechanical function in the canine heart by seeding an extracellular matrix patch with mesenchymal stem cells committed to a cardiac lineage. *Am J Physiol Heart Circ Physiol* **295**, H2257-2263, (2008).
68 Koninckx, R. *et al.* Human bone marrow stem cells co-cultured with neonatal rat cardiomyocytes display limited cardiomyogenic plasticity. *Cytotherapy*, 1-15, (2009).
69 Poh, K. K. *et al.* Repeated direct endomyocardial transplantation of allogeneic mesenchymal stem cells: safety of a high dose, "off-the-shelf", cellular cardiomyoplasty strategy. *Int J Cardiol* **117**, 360-364, (2007).
70 Forte, G. *et al.* Hepatocyte growth factor effects on mesenchymal stem cells: proliferation, migration, and differentiation. *Stem Cells* **24**, 23-33, (2006).
71 Xaymardan, M. *et al.* Platelet-derived growth factor-AB promotes the generation of adult bone marrow-derived cardiac myocytes. *Circ Res* **94**, E39-45, (2004).
72 Ciulla, M. M. *et al.* Assessment of selective homing and contribution to vessel formation of cryopreserved peripherally injected bone marrow mononuclear cells following experimental myocardial damage. *Cardiovasc Hematol Disord Drug Targets* **6**, 141-149, (2006).
73 Ye, J., Lee, S. Y., Kook, K. H. & Yao, K. Bone marrow-derived progenitor cells promote corneal wound healing following alkali injury. *Graefes Arch Clin Exp Ophthalmol* **246**, 217-222, (2008).
74 Sasaki, M. *et al.* Mesenchymal stem cells are recruited into wounded skin and contribute to wound repair by transdifferentiation into multiple skin cell type. *J Immunol* **180**, 2581-2587, (2008).
75 Chen, L., Tredget, E. E., Wu, P. Y. & Wu, Y. Paracrine factors of mesenchymal stem cells recruit macrophages and endothelial lineage cells and enhance wound healing. *PLoS ONE* **3**, e1886, (2008).
76 Wu, Y., Chen, L., Scott, P. G. & Tredget, E. E. Mesenchymal stem cells enhance wound healing through differentiation and angiogenesis. *Stem Cells* **25**, 2648-2659, (2007).
77 Guo, J., Lin, G. S., Bao, C. Y., Hu, Z. M. & Hu, M. Y. Anti-inflammation role for mesenchymal stem cells transplantation in myocardial infarction. *Inflammation* **30**, 97-104, (2007).
78 Guo, Y. *et al.* Locally overexpressing hepatocyte growth factor prevents post-ischemic heart failure by inhibition of apoptosis via calcineurin-mediated pathway and angiogenesis. *Arch Med Res* **39**, 179-188, (2008).
79 Wang, M., Crisostomo, P. R., Herring, C., Meldrum, K. K. & Meldrum, D. R. Human progenitor cells from bone marrow or adipose tissue produce VEGF, HGF, and IGF-I in response to TNF by a p38 MAPK-dependent mechanism. *Am J Physiol Regul Integr Comp Physiol* **291**, R880-884, (2006).

80 Wang, M. *et al.* STAT3 mediates bone marrow mesenchymal stem cell VEGF production. *J Mol Cell Cardiol* **42**, 1009-1015, (2007).
81 Wang, Y., Ahmad, N., Wani, M. A. & Ashraf, M. Hepatocyte growth factor prevents ventricular remodeling and dysfunction in mice via Akt pathway and angiogenesis. *J Mol Cell Cardiol* **37**, 1041-1052, (2004).
82 Sadat, S. *et al.* The cardioprotective effect of mesenchymal stem cells is mediated by IGF-I and VEGF. *Biochem Biophys Res Commun* **363**, 674-679, (2007).
83 Giordano, F. J. *et al.* A cardiac myocyte vascular endothelial growth factor paracrine pathway is required to maintain cardiac function. *Proc Natl Acad Sci U S A* **98**, 5780-5785, (2001).
84 Amado, L. C. *et al.* Cardiac repair with intramyocardial injection of allogeneic mesenchymal stem cells after myocardial infarction. *Proc Natl Acad Sci U S A* **102**, 11474-11479, (2005).
85 Yoon, Y. S. *et al.* Clonally expanded novel multipotent stem cells from human bone marrow regenerate myocardium after myocardial infarction. *J Clin Invest* **115**, 326-338, (2005).
86 Nygren, J. M. *et al.* Bone marrow-derived hematopoietic cells generate cardiomyocytes at a low frequency through cell fusion, but not transdifferentiation. *Nat Med* **10**, 494-501, (2004).
87 Mollmann, H. *et al.* Bone marrow-derived cells contribute to infarct remodelling. *Cardiovasc Res* **71**, 661-671, (2006).
88 Alvarez-Dolado, M. *et al.* Fusion of bone-marrow-derived cells with Purkinje neurons, cardiomyocytes and hepatocytes. *Nature* **425**, 968-973, (2003).
89 Rosen, A. B. *et al.* Finding fluorescent needles in the cardiac haystack: tracking human mesenchymal stem cells labeled with quantum dots for quantitative in vivo three-dimensional fluorescence analysis. *Stem Cells* **25**, 2128-2138, (2007).
90 Potapova, I. A. *et al.* Replacing damaged myocardium. *J Electrocardiol* **40**, S199-201, (2007).
91 Assmus, B. *et al.* Transplantation of Progenitor Cells and Regeneration Enhancement in Acute Myocardial Infarction (TOPCARE-AMI). *Circulation* **106**, 3009-3017, (2002).
92 Janssens, S. *et al.* Autologous bone marrow-derived stem-cell transfer in patients with ST-segment elevation myocardial infarction: double-blind, randomised controlled trial. *Lancet* **367**, 113-121, (2006).
93 Lunde, K. *et al.* Intracoronary injection of mononuclear bone marrow cells in acute myocardial infarction. *N Engl J Med* **355**, 1199-1209, (2006).
94 Schachinger, V. *et al.* Improved clinical outcome after intracoronary administration of bone-marrow-derived progenitor cells in acute myocardial infarction: final 1-year results of the REPAIR-AMI trial. *European heart journal* **27**, 2775-2783, (2006).
95 Wollert, K. C. *et al.* Intracoronary autologous bone-marrow cell transfer after myocardial infarction: the BOOST randomised controlled clinical trial. *Lancet* **364**, 141-148, (2004).
96 Meyer, G. P. *et al.* Intracoronary bone marrow cell transfer after myocardial infarction: eighteen months' follow-up data from the randomized, controlled BOOST (BOne marrOw transfer to enhance ST-elevation infarct regeneration) trial. *Circulation* **113**, 1287-1294, (2006).
97 Beltrami, A. P. *et al.* Adult cardiac stem cells are multipotent and support myocardial regeneration. *Cell* **114**, 763-776, (2003).
98 Dawn, B. *et al.* Cardiac stem cells delivered intravascularly traverse the vessel barrier, regenerate infarcted myocardium, and improve cardiac function. *Proc Natl Acad Sci U S A* **102**, 3766-3771, (2005).
99 Oh, H. *et al.* Cardiac progenitor cells from adult myocardium: homing, differentiation, and fusion after infarction. *Proc Natl Acad Sci U S A* **100**, 12313-12318, (2003).
100 Martin, C. M. *et al.* Persistent expression of the ATP-binding cassette transporter, Abcg2, identifies cardiac SP cells in the developing and adult heart. *Dev Biol* **265**, 262-275, (2004).
101 Pfister, O. *et al.* CD31- but Not CD31+ cardiac side population cells exhibit functional cardiomyogenic differentiation. *Circ Res* **97**, 52-61, (2005).
102 Laugwitz, K. L. *et al.* Postnatal isl1+ cardioblasts enter fully differentiated cardiomyocyte lineages. *Nature* **433**, 647-653, (2005).
103 Laugwitz, K. L., Moretti, A., Caron, L., Nakano, A. & Chien, K. R. Islet1 cardiovascular progenitors: a single source for heart lineages? *Development* **135**, 193-205, (2008).
104 Messina, E. *et al.* Isolation and expansion of adult cardiac stem cells from human and murine heart. *Circ Res* **95**, 911-921, (2004).
105 Narazaki, G. *et al.* Directed and systematic differentiation of cardiovascular cells from mouse induced pluripotent stem cells. *Circulation* **118**, 498-506, (2008).

106 Mauritz, C. *et al.* Generation of functional murine cardiac myocytes from induced pluripotent stem cells. *Circulation* **118**, 507-517, (2008).
107 Ieda, M. *et al.* Direct reprogramming of fibroblasts into functional cardiomyocytes by defined factors. *Cell* **142**, 375-386, (2010).
108 Kaji, K. *et al.* Virus-free induction of pluripotency and subsequent excision of reprogramming factors. *Nature* **458**, 771-775, (2009).
109 Kim, D. *et al.* Generation of human induced pluripotent stem cells by direct delivery of reprogramming proteins. *Cell stem cell* **4**, 472-476, (2009).
110 Page, R. L. *et al.* Induction of stem cell gene expression in adult human fibroblasts without transgenes. *Cloning and stem cells* **11**, 417-426, (2009).
111 Stoylen, A. *et al.* Strain rate imaging by ulrasonography in the diagnosis of coronary artery disease. *Journal of the American Society of Echocardiography* **13**, 1053-1064, (2000).
112 Spencer, K. T. *et al.* The role of echocardiographic harmonic imaging and contrast enhancement for improvement of endocardial border delineation. *Journal of the American Society of Echocardiography* **13**, 131-138, (2000).
113 Voigt, J. U. *et al.* Assessment of regional longitudinal myocardial strain rate derived from doppler myocardial imaging indexes in normal and infarcted myocardium. *Journal of the American Society of Echocardiography* **13**, 588-598, (2000).
114 Trambaiolo, P., Tonti, G., Salustri, A., Fedele, F. & Sutherland, G. New insights into regional systolic and diastolic left ventricular funtion with tissue doppler echocardiography: from qualitative analysis to a quantitative approach. *Journal of the American Society of Echocardiography* **14**, 85-96., (2001).
115 Heimdal, A., Stoylen, A., Torp, H. & Skjaerpe, T. Real-time strain rate imaging of the left ventricle by ultrasound. *Journal of the American Society of Echocardiography* **11**, 1013-1019, (1998).
116 Derumeaux, G. *et al.* Doppler tissue imaging quantitates regional wall motion during myocardial ischemia and reperfusion. *Circulation* **97**, 1970-1977., (1998).
117 Urheim, S., Edvardsen, T., Torp, H., Angelsen, B. & Smiseth, O. A. Myocardial strain by Doppler echocardiography. Validation of a new method to quantify regional myocardial function. *Circulation* **102**, 1158-1164., (2000).
118 Moulton, M. J. *et al.* Spline surface interpolation for calculating 3-D ventricular strains from MRI tissue tagging. *American Journal of Physiology* **270**, H281-H297, (1996).
119 Gotte, M. J. *et al.* Recognition of infarct localization by specific changes in intramural myocardial mechanics. *American Heart Journal* **138**, 1038-1045, (1999).
120 McVeigh, E. Regional myocardial function. *Cardiology Clinics* **16**, 189-206, (1998).
121 Scott, C. H. *et al.* Effect of dobutamine on regional left ventricular function measured by tagged magnetic resonance imaging in normal subjects. *American Journal of Cardiology* **83**, 412-417, (1999).
122 Bogaert, J. *et al.* Remote myocardial dysfunction after acute anterior myocardial infarction: impact of left ventricular shape on regional function: a magnetic resonance myocardial tagging study. *Journal of the American College of Cardiology* **35**, 1525-1534, (2000).
123 Stoylen, A. *et al.* Strain rate imaging by ultrasonography in the diagnosis of coronary artery disease. *J Am Soc Echocardiogr* **13**, 1053-1064., (2000).
124 Castro, P. L., Greenberg, N. L., Drinko, J., Garcia, M. J. & Thomas, J. D. Potential pitfalls of strain rate imaging: angle dependency. *Biomed Sci Instrum* **36**, 197-202, (2000).
125 Spencer, K. T. *et al.* The role of echocardiographic harmonic imaging and contrast enhancement for improvement of endocardial border delineation. *J Am Soc Echocardiogr* **13**, 131-138., (2000).
126 Joseph P. Hornak, P. (Interactive Learning Software, Henietta, NY, 1996-2011).
127 Sayad, D. E., Willett, D. L., Hundley, W. G., Grayburn, P. A. & Peshock, R. M. Dobutamine magnetic resonance imaging with myocardial tagging quantitatively predicts improvement in regional function after revascularization. *American Journal of Cardiology* **82**, 1149-1151, (1998).
128 Fernandes, S. *et al.* Human embryonic stem cell-derived cardiomyocytes engraft but do not alter cardiac remodeling after chronic infarction in rats. *J Mol Cell Cardiol* **49**, 941-949, (2010).
129 Chacko, V. P., Aresta, F., Chacko, S. M. & Weiss, R. G. MRI/MRS assessment of in vivo murine cardiac metabolism, morphology, and function at physiological heart rates. *Am J Physiol Heart Circ Physiol* **279**, H2218-2224, (2000).
130 Cohen, M. V., Yang, X. M., Neumann, T., Heusch, G. & Downey, J. M. Favorable remodeling enhances recovery of regional myocardial function in the weeks after infarction in ischemically preconditioned hearts. *Circulation* **102**, 579-583., (2000).

131 Atkins, B. Z. *et al.* Myogenic cell transplantation improves in vivo regional performance in infarcted rabbit myocardium. *Journal of Heart & Lung Transplantation* **18**, 1173-1180, (1999).
132 von Degenfeld, G., Giehrl, W. & Boekstegers, P. Targeting of dobutamine to ischemic myocardium without systemic effects by selective suction and pressure-regulated retroinfusion. *Cardiovascular Research* **35**, 233-240, (1997).
133 Bufkin, B. L. *et al.* Preconditioning during simulated MIDCABG attenuates blood flow defects and neutrophil accumulation. *Annals of Thoracic Surgery* **66**, 726-731, (1998).
134 Prinzen, F. W., Arts, T., Hoeks, A. P. G. & Reneman, R. S. Discrepancies between myocardial blood flow and fiber shortening in the ischemic border zone as assessed with video mapping of epicardial deformation. *Phlugers. Arc (Europ. J. Physiol.)* **415**, 220-229, (1989).
135 Gaudette, G. R., Todaro, J., Krukenkamp, I. B. & Chiang, F. P. Computer aided speckle interferometry: a technique for measuring deformation of the surface of the heart. *Ann Biomed Eng* **29**, 775-780., (2001).
136 Foroosh, H. & Zerubia, J. Extension of phase correlation to subpixel registration. *IEEE Transactions on Image Processing* **11**, 188-200, (2002).
137 Kelly, D. J., Azeloglu, E. U., Kochupura, P. V., Sharma, G. S. & Gaudette, G. R. Accuracy and reproducibility of a subpixel extended phase correlation method to determine micron level displacements in the heart. *Med Eng Phys* **29**, 154-162, (2007).
138 Gaudette, G. R. *et al.* Determination of regional area stroke work with high spatial resolution in the heart. *Cardiovascular Engineering: An International Journal* **2**, 129-137, (2002).
139 Azeloglu, E. U. *et al.* High resolution mechanical function in the intact porcine heart: mechanical effects of pacemaker location. *J Biomech* **39**, 717-725, (2006).
140 Kochupura, P. V. *et al.* Tissue-engineered myocardial patch derived from extracellular matrix provides regional mechanical function. *Circulation* **112**, I144-149, (2005).
141 *Regenerating the Heart*. (Humana Press, part of Springer Science+Business Media, 2011).
142 Levy, M. N., Pappano, A. J. & Berne, R. M. *Cardiovascular physiology*. 9th edn, (Mosby Elsevier, 2007).
143 Gaudette, G. R. & Cohen, I. S. Cardiac regeneration: materials can improve the passive properties of myocardium, but cell therapy must do more. *Circulation* **114**, 2575-2577, (2006).
144 Weiss, J. L., Frederiksen, J. W. & Weisfeldt, M. L. Hemodynamic determinants of the time-course of fall in canine left ventricular pressure. *J Clin Invest* **58**, 751-760, (1976).
145 Dong, S. J. *et al.* Independent effects of preload, afterload, and contractility on left ventricular torsion. *Am J Physiol* **277**, H1053-1060, (1999).
146 Axel, L. & Dougherty, L. Heart wall motion: improved method of spatial modulation of magnetization for MR imaging. *Radiology* **172**, 349-350, (1989).
147 Axel, L. & Dougherty, L. MR imaging of motion with spatial modulation of magnetization. *Radiology* **171**, 841-845, (1989).
148 Kraitchman, D. *et al.* Myocardial perfusion and function in dogs with moderate coronary stenosis. *Magn Reson Med* **35**, 771-780, (1996).
149 Kuijpers, D., Ho, K., van Dijkman, P., Vliegenthart, R. & Oudkerk, M. Dobutamine cardiovascular magnetic resonance for the detection of myocardial ischemia with the use of myocardial tagging. *Circulation* **107**, 1592-1597, (2003).
150 Young, A., Kramer, C., Ferrari, V., Axel, L. & Reichek, N. Three-dimensional left ventricular deformation in hypertrophic cardiomyopathy. *Circulation* **90**, 854-867, (1994).
151 Kramer, C. *et al.* Regional differences in function within noninfarcted myocardium during left ventricular remodeling. *Circulation* **88**, 1279-1288, (1993).
152 Dong, S. J., Hees, P. S., Siu, C. O., Weiss, J. L. & Shapiro, E. P. MRI assessment of LV relaxation by untwisting rate: a new isovolumic phase measure of tau. *Am J Physiol Heart Circ Physiol* **281**, H2002-2009, (2001).
153 Notomi, Y. *et al.* Measurement of ventricular torsion by two-dimensional ultrasound speckle tracking imaging. *J Am Coll Cardiol* **45**, 2034-2041, (2005).
154 Hankiewicz, J. & Lewandowski, E. Improved cardiac tagging resolution at ultra-high magnetic field elucidates transmural differences in principal strain in the mouse heart and reduced stretch in dilated cardiomyopathy. *J Cardiovasc Magn Reson* **9**, 883-890, (2007).
155 Hankiewicz, J., Goldspink, P., Buttrick, P. & Lewandowski, E. Principal strain changes precede ventricular wall thinning during transition to heart failure in a mouse model of dilated cardiomyopathy. *Am J Physiol Heart Circ Physiol* **294**, H330-336, (2008).

156 Cupps, B. *et al.* Principal strain orientation in the normal human left ventricle. *Ann Thorac Surg* **79**, 1338-1343, (2005).
157 Swynghedauw, B. Molecular mechanisms of myocardial remodeling. *Physiol Rev* **79**, 215-262, (1999).
158 Kelly, D. J. *et al.* Increased myocyte content and mechanical function within a tissue-engineered myocardial patch following implantation. *Tissue Eng Part A* **15**, 2189-2201, (2009).
159 Hou, D. *et al.* Radiolabeled cell distribution after intramyocardial, intracoronary, and interstitial retrograde coronary venous delivery: implications for current clinical trials. *Circulation* **112**, I150-156, (2005).
160 Wolf, D. *et al.* Dose-dependent effects of intravenous allogeneic mesenchymal stem cells in the infarcted porcine heart. *Stem cells and development* **18**, 321-329, (2009).
161 Simpson, D., Liu, H., Fan, T. H., Nerem, R. & Dudley, S. C., Jr. A tissue engineering approach to progenitor cell delivery results in significant cell engraftment and improved myocardial remodeling. *Stem Cells* **25**, 2350-2357, (2007).
162 Proulx, M. K. *et al.* Fibrin microthreads support mesenchymal stem cell growth while maintaining differentiation potential. *J Biomed Mater Res A* **96**, 301-312, (2011).
163 Kuijpers, D., Ho, K. Y., van Dijkman, P. R., Vliegenthart, R. & Oudkerk, M. Dobutamine cardiovascular magnetic resonance for the detection of myocardial ischemia with the use of myocardial tagging. *Circulation* **107**, 1592-1597, (2003).
164 Young, A. A., Kramer, C. M., Ferrari, V. A., Axel, L. & Reichek, N. Three-dimensional left ventricular deformation in hypertrophic cardiomyopathy. *Circulation* **90**, 854-867, (1994).
165 Kramer, C. M. *et al.* Regional differences in function within noninfarcted myocardium during left ventricular remodeling. *Circulation* **88**, 1279-1288, (1993).
166 Notomi, Y. *et al.* Measurement of ventricular torsion by two-dimensional ultrasound speckle tracking imaging. *J Am Coll Cardiol* **45**, 2034-2041, (2005).
167 Hankiewicz, J. H. & Lewandowski, E. D. Improved cardiac tagging resolution at ultra-high magnetic field elucidates transmural differences in principal strain in the mouse heart and reduced stretch in dilated cardiomyopathy. *J Cardiovasc Magn Reson* **9**, 883-890, (2007).
168 Kim, B. O. *et al.* Cell transplantation improves ventricular function after a myocardial infarction: a preclinical study of human unrestricted somatic stem cells in a porcine model. *Circulation* **112**, I96-104, (2005).

## CHAPTER 3: Effects of reduced-$O_2$ on hMSC growth kinetics and c-Met expression

### 3.1. Introduction

Traditional conditions for culturing adult, bone marrow derived hMSCs typically employ a conventional gas composition consisting of 95% atmospheric air (containing ~19% $O_2$ and ~76% $N_2$) and 5% $CO_2$, maintained at 37°C. However, recent studies suggest that culturing hMSCs in reduced oxygen concentrations (reduced-$O_2$) is more appropriate for mimicking physiological conditions of cells and tissues *in vivo*.[1-4] Physiological ventilation and perfusion relationships support this argument, as oxygen concentrations decrease from when it enters the body, circulates in the bloodstream, and diffuses into bodily tissues. The partial pressure of $O_2$ in ambient air is ~160 mm Hg (~21% of normal atmospheric air pressure, 760 mm Hg), but decreases to ~150 mm Hg (~19% $O_2$) as it mixes with water vapor in the mouth and trachea.[5] When inspired gas reaches the alveoli of the lungs, $O_2$ is transported across alveolar membrane into the blood and $CO_2$ is transported from the capillaries to the alveoli. Gas exchange causes a flux of decreasing $O_2$ and increasing $CO_2$ fractions in the alveoli, causing changes in the partial pressure of $O_2$ in the alveoli. Using the alveolar gas equation to account for this physiological phenomenon, the partial pressure of $O_2$ in the alveoli has been calculated to be ~102 mm Hg (~13% $O_2$).[5] During transport into systemic circulation, oxygen mixes with relatively constant physiological levels of $CO_2$ ($pCO_2$ = 40 mm Hg), $H_2O$ ($pH_2O$ at 37°C = 47 mm Hg), and $N_2$ ($pN_2$ = 571 mm Hg). In combination, these gases must maintain a homeostatic balance with atmospheric pressure of 760 mm Hg, which causes the partial pressure of $O_2$ in systemic arterial blood to drop to ~90 mm Hg (~12% $O_2$).[5]

The rationale for culturing hMSCs in reduced-$O_2$ is further supported by consideration of both the hMSC niche environment (i.e. bone marrow) and the target tissues where hMSCs are implanted for cell therapy (e.g. myocardial infarcts). Studies estimate that the oxygen tension within bone tissue is in the range of 1-12% $O_2$, with estimates of $O_2$ levels in the bone marrow in the range of 1-7%.[4,6,7] Furthermore, a pre-clinical study done on rat myocardial infarcts detected the $pO_2$ of the infarcted tissue to be 3 mm Hg (~0.4% $O_2$) at day 0 and 13 mm Hg (~1.7% $O_2$) after 4 weeks.[8] Taken together, these data suggest that reduced-$O_2$ culturing of hMSCs might be more "normal" in terms of physiological relevance than the

conventional norm of culturing hMSCs in atmospheric $O_2$. However, the idea and practice of reduced-$O_2$ conditioning is still a relatively new paradigm, and the effects of reduced-$O_2$ conditioning on hMSCs are not well understood.

Several groups have begun to study the effects of reduced-$O_2$ conditions on mesenchymal stem cells (MSCs), using a range of oxygen concentrations spanning 0.5-5.0% $O_2$.[1-4,6,7,9-14] Some studies report that reduced-$O_2$ conditioning can increase MSC proliferation,[3,4,9] while other studies report reduced-$O_2$ decreases MSC proliferation,[6,13,14] and yet others report that reduced-$O_2$ has no effect on MSC self-renewal.[1] In addition, some studies report that reduced-$O_2$ conditioning can increase MSC differentiation potential,[9,10,14] while other studies report reduced-$O_2$ decreases MSC differentiation potential,[7,13] and yet others report that reduced-$O_2$ conditioning of MSCs can elicit the expression of de-differentiation markers such as Oct-4 and Rex-1.[3,4] Upon further analysis, it was found that reduced-$O_2$ conditioning of MSCs can increase prosurvival marker expression (e.g. Akt, HIF-1α, and survivin),[1,10,11] growth factor secretion (e.g. VEGF, HGF, and FGF-2),[2,11,15] and growth factor/cytokine receptor expression (e.g. VEGFR1, c-Met, and CXCR4).[1,6,11,12] In vitro and in vivo studies have also shown that reduced-$O_2$ conditioned MSCs can increase tissue formation,[4] enhance motility/homing to injury sights,[1] improve engraftment/retention in injured tissue,[2,6] and upregulate angiogenesis;[1,2] all of which would be advantageous in therapeutic applications for tissue regeneration and wound healing.

Despite the therapeutic potential, inconsistent results plague the field, and continued research is required for a more comprehensive understanding of the effects involved in reduced-$O_2$ conditioning on MSCs. Discrepancies in the literature may be largely due to the use of different MSC species (e.g. human,[1,3,4,7,14] rat,[9-11,15] and mouse[2,12,13]), different cell sources (e.g. tibial bone marrow,[7] iliac crest bone marrow,[1,3,4] and adipose[13,14]), different oxygen concentrations (0.5-5.0% $O_2$), varying durations of reduced-$O_2$ exposure (hours vs. days), and different applications. In sifting through the literature, we sought to draw from and build upon studies that were relevant to our MSC species, source, and application.

We are using human MSCs (hMSCs) derived from bone marrow harvested from iliac crests of adult donors, for cell therapy applications in myocardial infarcts where oxygen tension ranges from 0.4-1.7% $O_2$.[8] Keying in on three specific studies that used hMSCs from iliac crest bone marrow, several beneficial cellular and therapeutic effects have been found when conditioning these cells in 1-3% $O_2$,[1,3,4] with one study concluding that culturing hMSCs at 2% demonstrated a "switch" in metabolic pathways and enhanced proliferation potential.[3] As 2% $O_2$ appeared to elicit advantageous effects without adversely affecting hMSC growth, it was also close to the physiological oxygen tension found in myocardial infarcts. Therefore, we selected 2% $O_2$ for our reduced-$O_2$ conditioning studies. To create a 2% $O_2$ environment, we used an incubator system that allowed for an increased nitrogen intake to displace ambient oxygen, as described further in the materials and methods below. Once the reduced-$O_2$ conditioning system was established, we examined the effects of our system on hMSC growth kinetics and c-Met expression. Recently, c-Met has been shown to elicit cardiac specific markers in mouse MSCs, by interacting with its pleiotropic cytokine HGF.[16] In addition, c-Met has been shown to be an important factor in the motility and migration of hMSCs to sites of injured tissue.[1,16] As recent studies suggest that reduced-$O_2$ conditioning can increase c-Met receptor expression in hMSCs,[1] we are interested in determining if we can do the same in order to exploit the therapeutic potential or cardiac differentiation mechanisms in hMSCs.

### 3.1.1. Determining the effects of reduced-$O_2$ on hMSC growth kinetics

For a more complete understanding of how reduced-$O_2$ conditioning affects hMSC growth kinetics over time, we evaluated cumulative population doublings and doubling rate of hMSCs maintained in either normal-$O_2$ (20% $O_2$) or reduced-$O_2$ (2% $O_2$) conditions. Since there are conflicting results in the literature as to whether reduced-$O_2$ conditioning increases,[3,4] decreases,[6] or has no effect[1] on hMSC proliferation, we sought to conduct our own controlled study to better understand our reduced-$O_2$ system and contribute to the body of literature. Again, reported discrepancies regarding reduced-$O_2$ effects on hMSC growth kinetics may lie in the parameters chosen in the study set-up (e.g. reduced-$O_2$ exposure

duration, length of the study, or treatment with/without serum) and the methods used to evaluate (e.g. cell cycle analysis, cell counts, fold-expansion, or colony formation). From experience, we know that hMSCs cultured in normal-$O_2$ conditions have an approximate doubling-time of ~7 days, and they remain viable and proliferative until ~passage 10. Using the 7-day doubling-time as a benchmark parameter, we compared hMSC growth in reduced-$O_2$ versus normal-$O_2$, seeding all flasks from the same initial vial of cells and taking cell counts at each passage (every 7 days). Data obtained from cell counts were used to calculate population doublings at each passage. Population doublings were compared across cell-passages to evaluate doubling rate over time. In addition, population doublings were compounded at each successive passage to evaluate total doublings over time.

### 3.1.2. Determining the effects of reduced-$O_2$ on c-Met expression

In support of our hypothesis that reduced-$O_2$/HGF conditioning can initiate cardiac differentiation of hMSCs, it has been previously shown that HGF interacts with its c-Met receptor to activate signaling pathways that may be involved in downstream cardiac marker expression.[16,17] In addition, previous studies suggest reduced-$O_2$ conditioning of both human and rat MSCs may increase c-Met receptor expression,[1,11] but the methods used to evaluate this phenomenon have been either qualitative or semi-quantitative analyses of early-stage time points. If we can better understand this phenomenon, we may be able to exploit the increase in c-Met expression to enhance HGF/c-Met signaling, which we can then test as a possible cardiogenic differentiation strategy in hMSCs. To improve upon the scope of previous studies, we determined the effect of reduced-$O_2$ conditioning on the c-Met expression of hMSCs cultured in reduced-$O_2$ for a broader range of time durations (1, 3, 7, 10, and 14 days). And to improve upon the methods previously used, c-Met expression was determined by ELISA for a more quantitative and comparable evaluation. In addition we compared the c-Met expression of hMSCs cultured in normal-$O_2$ versus reduced-$O_2$ at days 3, 7, and 10. A more comprehensive evaluation suggests that longer-term reduced-$O_2$ conditioning may increase c-Met expression in hMSCs.

## 3.2. Materials and Methods

### 3.2.1. Implementation of reduced-$O_2$ culture environment

To implement a reduced-$O_2$ cell culture system, we used a HERAcell® 150 incubator (Thermo Electron Corporation, #51022545, Langenselbold, Germany) with both carbon dioxide ($CO_2$) and nitrogen ($N_2$) gas-intake valves. $CO_2$ supplied by a compressed gas reserve was maintained at 5% by a sensor-regulated intake valve. $N_2$ gas was supplied by a high-pressure liquid nitrogen reserve that was connected to a Heraeus system gauge (Thermo Electron Corporation, #50059043, Langenselbold, Germany), which incorporates an automatic switch to a back-up compressed $N_2$ tank in case of emergencies. The $N_2$ composition was increased and maintained at 93%, displacing the $O_2$ composition to only 2%. $O_2$ gas levels were maintained and checked with both a HERAcell® $O_2$ Sensor Set (internal to the HERAcell® 150 incubator, Thermo Electron Corporation, Langenselbold, Germany) and a FYRITE® Gas Analyzer (Bacharach, Inc., Test Kit #10-5053, New Kingston, PA).

### 3.2.2. General techniques for culturing human mesenchymal stem cells

Human mesenchymal stem cells (hMSCs) isolated from human adult bone marrow were purchased from Lonza, Inc. (#PT-2501, Walkersville, MD). Cryo-preserved vials arrived as passage-2 hMSCs, which had been pre-characterized by the manufacturer. Upon thawing, passage-3 hMSCs were plated with a seeding density of 500,000 cells per T-75 flask and were cultured in mesenchymal stem cell growth medium (MSCGM, Lonza's proprietary hMSC growth media, includes 10% fetal bovine serum; Lonza, Inc., #PT-3001). Multiple flasks originating from the same vial were segregated to either normal-$O_2$ (20%) or reduced-$O_2$ (2%) conditions. Cells were maintained at 37°C, growth media was changed every 2 days, and cells were passaged when growth reached approximately 80-90% confluency. Successive cell-passages were maintained in their pre-designated oxygen concentrations, and passage 4-9 hMSCs were used for experimentation.

### 3.2.3. Culturing hMSCs for growth kinetics

A fresh vial of hMSCs (Lonza, Inc., #PT-2501, Walkersville, MD) was thawed and immediately reconstituted in 5 mL of warm MSCGM (Includes 10% fetal bovine serum; Lonza, Inc., #PT-3001, Walkersville, MD) in a drop-wise fashion in a 15 mL conical tube. The tube was centrifuged at 1,000 rpm for 5 minutes to form a pellet, the media was aspirated, the pellet was resuspended in 1 mL of fresh warm MSCGM, and a cell count was taken using a hemocytometer (Hausser Scientific Co., #3200, Horsham, PA). The resuspended hMSCs were used to seed six T-25 vented tissue culture flasks (Becton Dickinson Labware, #35-3108, Franklin Lakes, NJ), with a cell-density of 167,000 cells per flask. Three of the T-25 flasks were conditioned in normal-$O_2$ conditions, and the remaining 3 T-25 flasks were cultured in reduced-$O_2$ conditions. Cells were cultured in MSCGM for the duration of experiment, media was changed every 2 days, and cells were passaged every 7 days (upon reaching 80-90% confluence). Successive cell-passages were maintained in their pre-designated oxygen concentrations. At each passaging period, pellets were resuspended in 1 mL of fresh MSCGM, and 2 cell counts were performed for each cell suspension. For each cell count, 20 µL of suspension was mixed with 20 µL of Trypan Blue, and then 10 µL of the cell/Trypan mixture was seeded onto a hemocytometer. For each analysis, enough hemocytometer-areas were evaluated to count more than 100 cells, and cell counts were back-calculated to determine the total cell number in each suspension. Based on the cell concentration of each suspension, aliquoted volumes containing 167,000 cells were then re-plated into new T-25 flasks to perpetuate the fidelity of each culture/experiment. During each passaging period, 6 new T-25 flasks were generated from the previous 6 flasks (3 in normal-$O_2$ and 3 in reduced-$O_2$), to be evaluated over the next passage.

### 3.2.4. Calculation of population doublings

To assess hMSC growth kinetics, population doublings were calculated for each flask at every passage. During passaging, the cells in each T-25 flask were trypsynized and centrifuged at 1,000 rpm for 5 minutes. Old media was aspirated and cell pellets were resuspended in 0.5 mL of DMEM

supplemented with 10% FBS. For each cell suspension, 2 cell counts were taken using a hemocytometer, making sure to count at least 100 cells for each cell count to satisfy the limits of the hemocytometer chamber. The 2 cell counts were then averaged as a single metric for the cell concentration of each cell suspension. Total cell number was back-calculated based on the measured cell concentration and the 0.5 mL resuspension volume. The following equation was then applied to calculate the population doubling for each cell suspension:

$$p = p_o \cdot 2^d \quad \rightarrow \quad d = \frac{\ln\left(\frac{p}{p_o}\right)}{\ln(2)}$$

$p$ = total cell number (calculated)
$p_o$ = initial-seeding cell number (167,000 cells)
$d$ = # of doublings

Once population doublings were calculated for each cell suspension, the triplicate of population doublings for each $O_2$ concentration were averaged (n=3 for normal-$O_2$ and n=3 for reduced-$O_2$).

### 3.2.5. Culturing hMSCs for c-Met expression

A fresh vial of hMSCs (PT-2501, Lonza, Inc., Walkersville, MD) was thawed, reconstituted, centrifuged, resuspended, and then plated into T-75 vented tissue culture flasks (Becton Dickinson Labware, #35-3136, Franklin Lakes, NJ) at a concentration of 500,000 cells per flask. At least one T-75 flask was placed into normal-$O_2$ conditions, and at least one T-75 flask was placed into reduced-$O_2$ conditions. Cells were fed with MSCGM every 2 days, and passaged when they were between 80-90% confluent. When passaged, cells were re-plated with a seeding density of 500,000 cells per flask, and successive passages were maintained in their pre-determined oxygen conditions. At passage 5, three or more T-75 flasks were seeded with 500,000 cells per flask for each time point in both oxygen conditions, and then returned to their appropriate incubators. Cells were cultured in MSCGM, and media was changed every 2 days. At each time point, cells were harvested.

### 3.2.6. Cell harvest and lysis for total c-Met analysis

Cells were harvested by washing culture flasks with sterile Dulbecco's phosphate buffered saline (DPBS, without calcium or magnesium; Cellgro® Mediatech, Inc., #21-031-CV, Manassas, VA), and then detaching hMSCs from the flask with 6 mL of 0.25% Trypsin Ethylenediaminetetraacetic acid (Trypsin EDTA; Cellgro® Mediatech, Inc., #25-053-CI, Manassas, VA). Trypsin EDTA was inactivated by pipetting the cell solution into 5 mL of DMEM with 10% FBS in a drop-wise fashion. Cells were then centrifuged at 1,000 rpm for 5 minutes. Media was aspirated, and cell pellets were then washed by resuspending them in 1 mL of phosphate buffered saline (PBS, pH 7.2-7.4). Washed cells were then re-centrifuged at 1,000 rpm for 5 minutes to reform the pellet.

For cell lysis, lysis buffer was prepared with a composition of 1% NP-40 (EMD/Calbiochem, Rockland, MA; #492016), 20 mM Tris (pH 8.0; Sigma Aldrich, St. Louis, MO), 137 mM sodium chloride (NaCl; Sigma Aldrich), 10% glycerol, 2 mM EDTA (Sigma Aldrich), 1 mM sodium orthovanadate ($Na_3VO_4$, Sigma, #S6508), 10 μg/mL Aprotinin (Sigma, #A6279), and 10 μg/mL Leupeptin (Sigma, #L8511). As samples were being harvested over multiple time points, total cell lysates were stored at -80°C until all samples were collected.

### 3.2.7. Assaying Total c-Met by ELISA

Prior to ELISA analysis, samples were thawed and protein quantification was acquired using a NanoDrop™ 2000 spectrophotometer system (Manufactured by NanoDrop Products, Wilmington, DE; supplied by Thermo Scientific, Waltham, MA). Based on the protein quantifications, calculations were made to determine the appropriate volume needed for 40 μg of each sample.

Samples were then tested by an enzyme-linked immunosorbent assay (ELISA), using a DuoSet® ELISA kit for human total c-Met (R&D Systems, Minneapolis, MN; #DYC358-2). All formulations for buffers and reagents were detailed by the manufacturer, and prepared fresh in the lab. All antibodies and standards were provided by the manufacturer. Briefly, the predetermined wells of a 96-well plate were treated with 100 μL of mouse anti-human Total HGF-R/c-Met capture antibody (2.0 μg/mL), and allowed

to incubate overnight at room temperature. The next day, the wells were aspirated and rinsed 3 times with wash buffer (0.05% Tween 20 in PBS). Wells were then treated with 300 μL of block buffer (1% Bovine serum albumin, 0.05% sodium azide) for 2 hours at room temperature. After blocking, wells were rinsed 3 times with wash buffer. After washing, samples and standards were added to the predetermined wells, and incubated for 2 hours at room temperature. Samples were prepared by adding the appropriate volume for 40 μg of each sample to sample buffer, for a total of 100 μL. Standards were run in duplicate, and were prepared by making a seven-point standard curve using 2-fold serial dilutions with a high standard concentration of 8000 pg/mL reconstituted in sample buffer. After sample/standard incubation, wells were again rinsed 3 times with wash buffer. Wells were then treated with 100 μL of biotinylated goat anti-human HGF-R/c-Met detection antibody (100 ng/mL), and allowed to incubate for 2 hours at room temperature. After detection antibody, the wells were washed 3 times with wash buffer, and then immediately treated with 100 μL of streptavidin-conjugated horseradish peroxidase enzyme for 20 minutes at room temperature. After 20 minutes, wells were treated with 100 μL of substrate solution (1:1 ratio of hydrogen peroxide and tetramethylbenzidine) for another 20 minutes at room temperature. After substrate solution, wells were treated with stop solution (2 N sulfuric acid), and then imaged for optical density using a microplate reader.

### 3.2.8. Quantifying Total c-Met Expression

To quantify total c-Met expression, ELISA plates were analyzed by a microplate reader (VICTOR$^{3}{}_{TM}$ Wallac 1420 Multilabel Counter, manufactured by Perkin Elmer®, Waltham, MA; #1420-011) to determine the optical density of wells at both 450 nm and 540 nm wavelengths. To correct for optical imperfections in the plate, the 540 nm readings were subtracted from the corresponding 450 nm readings. As recommended by the manufacturer, a standard curve was established by plotting the log of the seven-point HGF-R/c-Met standard concentrations versus the log of the corresponding corrected optical densities, and a linear best fit line was determined by regression analysis. Assuming a good fit, the equation for the best fit line of the standard curve was used to back-calculate the concentration of total c-

Met detected in each sample well. Concentrations for each well were then normalized to the dilutions of each sample, which were required to bring each of the sample volumes to 100 µL during the ELISA procedure. Total c-Met expression was presented in ng/mL concentrations, and samples were compared.

#### 3.2.9. Statistics

Data are reported as mean ± standard error of the mean as multiple observations were made for each sample. For growth kinetics experiments, differences between groups at each time point were determined using a Student's unpaired t-test with significance established for p-values $\leq 0.05$. For total c-Met expression, differences between groups were determined by one-way analysis of variance (ANOVA). A *post hoc* Tukey test was then used to perform multiple pair-wise comparisons. Differences were considered significant for p-values $\leq 0.05$.

### 3.3. Results

#### 3.3.1. Effects of reduced-$O_2$ on hMSC growth kinetics

By tracking and comparing the population doublings (PDs) of hMSCs grown in normal-$O_2$ and reduced-$O_2$ over time, we examined the effect of reduced-$O_2$ conditioning on the growth kinetics of hMSCs. Cells were cultured as indicated in the methods and PDs were calculated over a number of passages, until senescence of the hMSCs in their respective $O_2$ conditions. By calculating the cumulative PDs over each passage, we found normal-$O_2$ hMSCs expanded by an average 7.35 ± 0.53 PDs by passage 11 (Figure 3.1A). Normal-$O_2$ hMSCs reached peak exponential growth by passage 8, with slight increases in PDs before senescence at passage 11 or 12. However, reduced-$O_2$ hMSCs expanded by an average 17.27 ± 1.78 PDs by passage 16, reaching peak exponential growth by passage 14 or 15. In addition, cells cultured in reduced-$O_2$ hMSCs had significantly higher cumulative PDs compared to normal-$O_2$ hMSCs from passage 5 through passage 12, indicating a marked difference in population expansion over the same time course. Furthermore, reduced-$O_2$ hMSCs continued expanding well

beyond passage 12 (past the point of comparison to normal-$O_2$ hMSCs), indicating an increase in longevity or delay in senescence.

By analyzing the individual PDs at each passage, it is possible to analyze trends in growth rate for both oxygen conditions from one passage to another. PDs were highest for both normal-$O_2$ and reduced-$O_2$ hMSCs at passage 3, which declined for both oxygen conditions over successive passages (Figure 3.1B). The rate of PD decline was more rapid for normal-$O_2$ hMSCs, with sustained growth between passages 4 and 6, and then a significant decrease at passage 7. Reduced-$O_2$ hMSCs appeared to respond to their environment for a slight increase in PDs between passages 4 and 7, with sustained growth between passages 8 and 12, with a steady decline over passages 13-16. While both oxygen conditions showed a drop in PD after passage 3, the normal-$O_2$ PD decline is more rapid than reduced-$O_2$ PDs. Highlighting this difference, reduced-$O_2$ PDs trend upward from passage 5 to passage 7, and reduced-$O_2$ PDs are significantly higher than normal-$O_2$ PDs at passages 5, 6, 7, and 8. Reduced-$O_2$ hMSCs continue doubling well past normal-$O_2$ senescence at passage 11, and reduced-$O_2$ conditioning appears to sustain a steady growth rate of hMSCs for a significantly longer period of time (Figure 3.1).

### 3.3.2. Effects of reduced-$O_2$ on total c-Met expression

Previous analyses for the effects of reduced-$O_2$ conditioning on c-Met expression in hMSCs have used qualitative methods to study the effect in short periods of exposure.[1,11] We improved upon these studies by quantifying total c-Met expression by ELISA over a time-course of 14 days (normalizing total c-Met expression to total protein for each sample). Quantitative measures allowed for statistical analysis to determine real differences among compared groups. First, we quantified c-Met from hMSCs that had been conditioned in reduced-$O_2$ for 1, 3, 7, 10, or 14 days (Figure 3.2). Trends indicated a steady expression of c-Met from day 1 (34.51 ± 5.12 ng/mL, n=6) to day 3 (35.22 ± 9.87 ng/mL, n=13). However, there was a sharp increase in c-Met by day 7 (85.46 ± 23.18 ng/mL, n=9), which was nearly 2.5 times the expression found at day 1. Total c-Met expression was sustained out to day 10 (77.86 ± 21.31ng/mL, n=11), but then decreased to baseline levels by day 14 (34.90 ± 5.22 ng/mL, n=8). Total c-

Met expression at days 7 and 10 were both significantly higher than days 1, 3, or 14 ($p < 0.01$), but there was no significant difference in expression between day 7 and day 14. In addition, there was no significant difference in c-Met expression at days 1, 3, or 14 (Figure 3.2).

Based on the results for expression of c-Met in hMSCs conditioned in reduced-$O_2$, we narrowed our time-frame for analyzing c-Met in hMSCs cultured in normal-$O_2$ to include days 3, 7, and 10 (Figure 3.3). Trends indicated a relatively low expression of c-Met at day 3 (24.53 ± 8.70 ng/mL, n=6), followed by a sharp c-Met increase at day 7 (52.41 ± 10.69 ng/mL, n=8). Day 10 expression (33.88 ± 4.64 ng/mL, n=3) showed a decrease in c-Met from day 7. Statistical analysis showed that c-Met expression at day 7 was significantly higher than both days 3 and 10 ($p < 0.01$), and that there was no significant difference in expression between days 3 and 10.

In a comparison between c-Met expression levels of hMSCs conditioned at either reduced-$O_2$ or normal-$O_2$, the trend of a significant increase at day 7 and a tapered decline at day 10 is observed in both groups (Figure 3.4). In comparison of both conditions at day 3, reduced-$O_2$ hMSCs appeared to show more c-Met expression, but statistical analysis showed there was no significant difference between reduced-$O_2$ and normal-$O_2$ hMSCs. There was a significant increase of c-Met expression in reduced-$O_2$ hMSCs compared to normal-$O_2$ hMSCs at days 7 and 10 ($p < 0.01$). At day 7, reduced-$O_2$ c-Met expression (85.46 ± 23.18 ng/mL, n=9) was over 1.5 times as much as normal-$O_2$ c-Met expression (52.41 ± 10.69 ng/mL, n=8). At day 10, reduced-$O_2$ c-Met expression (77.86 ± 21.31ng/mL, n=11) was over 2 times as much as normal-$O_2$ c-Met expression (33.88 ± 4.64 ng/mL, n=3).

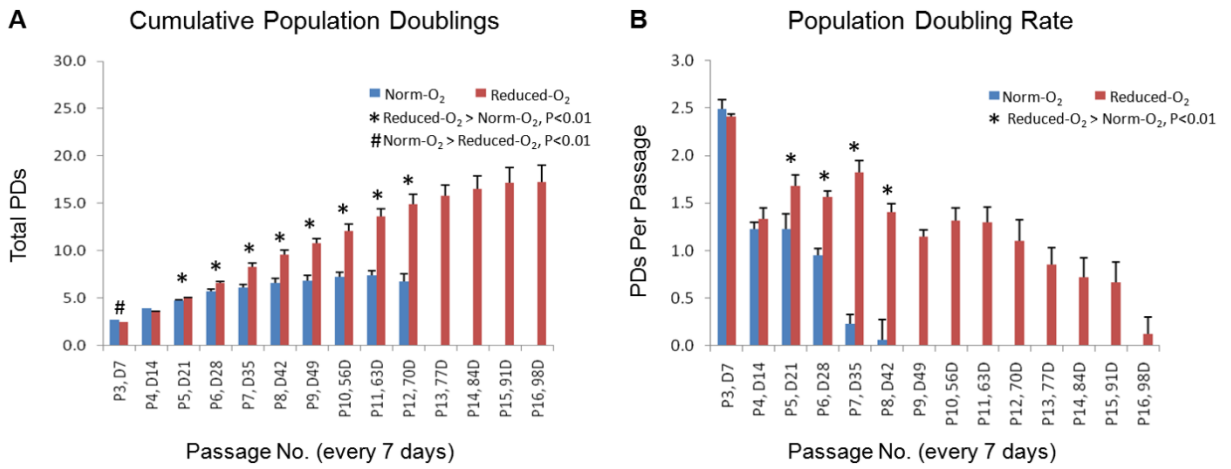


**Figure 3.1. Effects of oxygen concentration on hMSC growth kinetics.** (A) Conditioning hMSCs in reduced-$O_2$ significantly increased cumulative population doublings from passage 5 to passage 12, and extended proliferative capacity out to passage 16. (B) Both oxygen conditions caused a decrease in hMSC doubling at passage 4. Normal-$O_2$ hMSCs showed a short-term maintenance of doubling rate to passage 6, followed by a sharp decline to passage 8. Reduced-$O_2$ hMSCs adapted for a gradual increase in doubling rate to passage 7, and then a prolonged decline in doubling rate to passage 16. Differences were evaluated using a Student's unpaired t-test at each passage, and were considered significant for p-values $\leq 0.05$. Error bars indicate standard error.

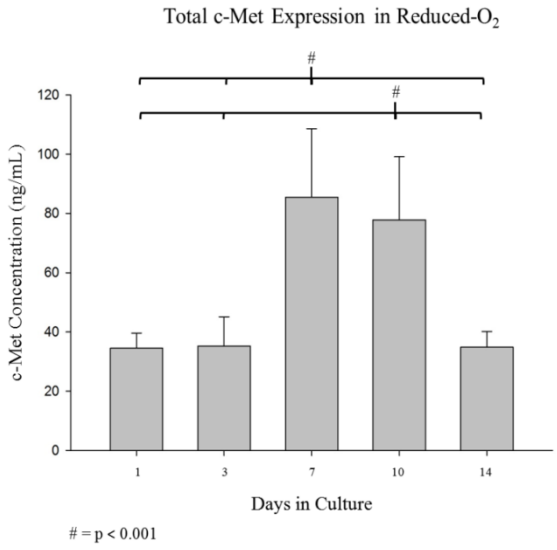


**Figure 3.2. Total c-Met expression of hMSCs cultured in reduced-$O_2$ over a period of days.** Total c-Met expression was compared for hMSCs cultured in reduced-$O_2$ for 1, 3, 7, 10, and 14 days. Total c-Met expression was steady between day 1 (n=6) and day 3 (n=13). Reduced-$O_2$ conditioning of hMSCs significantly increased total c-Met expression at day 7 (n=9). Increased c-Met persisted at day 10 (n=11), and then decreased back to baseline by day 14 (n=8). Differences were evaluated across different time points, using a one-way ANOVA with a Tukey *post-hoc* test, and were considered significant for p-values $\leq 0.05$. Error bars indicate standard error. Samples were normalized to total protein.

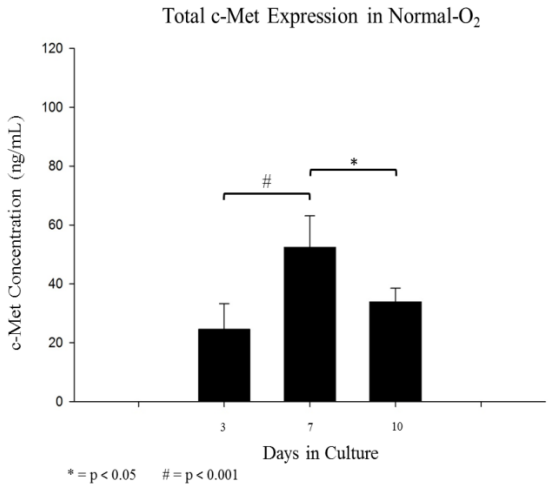


**Figure 3.3. Total c-Met expression of hMSCs cultured in normal-$O_2$ over a period of days.** Total c-Met expression was compared for hMSCs cultured in normal-$O_2$ for 3, 7, and 10 days. Expression of total c-Met significantly increased from day 3 (n=6) to day 7 (n=8), and then decreased back to baseline by day 10 (n=3). Differences were evaluated using a one-way ANOVA with a Tukey post-hoc test, and were considered significant for p-values $\leq 0.05$. Error bars indicate standard error.

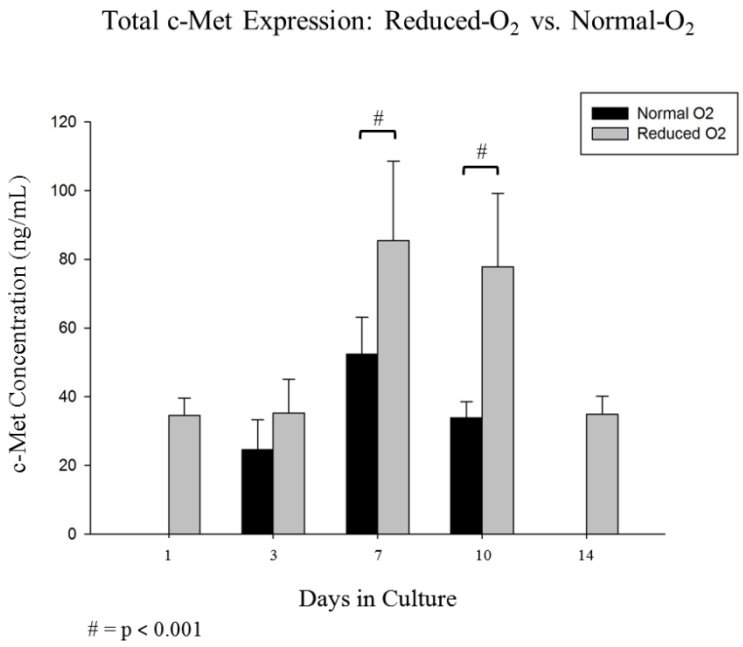


**Figure 3.4. Comparing total c-Met expression of hMSCs cultured in reduced-$O_2$ versus normal-$O_2$.** In a comparison of the data, both oxygen conditions significantly increased total c-Met expression at day 7. However, the increased total c-Met in reduced-$O_2$ conditions was significantly higher than the increased total c-Met in normal-$O_2$. Both oxygen conditions also caused a decline of c-Met expression after day 7. However, reduced-$O_2$ could sustain elevated c-Met expression through day 10. Differences were evaluated using a one-way ANOVA with a Tukey post-hoc test, and were considered significant for p-values $\leq 0.05$. Error bars indicate standard error.

### 3.4. Discussion

In consideration of the lower physiological oxygen tensions in both the bone marrow niche and the myocardial infarct microenvironment, studying how marrow-derived hMSCs respond in low oxygen concentrations may be of great importance for better understanding the innate properties of hMSCs and how they will respond in oxygen deprived tissues. More important to our overall goal of using hMSCs as a cell therapy to regenerate the injured heart, delivered cells must be able to endure the transition from the "normal"/atmospheric 20% $O_2$ to a much lower oxygen tension of 0.4-1.7% $O_2$. Studies in cellular homeostasis with respect to reduced-$O_2$ and hypoxic environments have shown that decreases in $O_2$ availability will increase cellular acidosis, oxidative stress, and reactive oxygen species; all of which impair normal cell biology and decrease viability.[18-22] Therefore, it is likely that hMSCs cultured at 20% $O_2$ *in vitro* will undergo significant physiological duress when transplanted into the reduced-$O_2$ environment of an infarct, which would hinder their longer-term survival, retention, and therapeutic function *in vivo*. By culturing hMSCs in reduced-$O_2$ *in vitro* prior to transplantation into MIs *in vivo*, it may be possible to condition cells to develop the appropriate machinery or functionality to adequately adapt to oxygen deficient tissues.[20-22]

Several groups have begun to study the effects of culturing hMSCs in reduced-$O_2$ conditions, finding that various reduced-$O_2$ concentrations and exposure durations can cause changes in several physiological processes such as growth kinetics, cell signaling, growth factor secretion, and therapeutic potential.[1,2,9,11] However, discrepancies in the literature and an incomplete understanding of reduced-$O_2$ effects lends to the argument that more research is necessary to learn how hMSCs respond in oxygen poor environments, to possibly uncover untapped mechanisms that may improve cell survival or cardiac differentiation. The goal of this study was to investigate the growth kinetics and c-Met expression of hMSCs after being cultured in a controlled reduced-$O_2$ conditioning system, to understand how prolonged reduced-$O_2$ exposure effects hMSC proliferation and the expression of a receptor believed to enhance cardiogenic differentiation.[16,17] A reliable reduced-$O_2$ culturing environment was implemented in the laboratory, using a dedicated incubator with a controlled system that regulated the gas composition for 2% $O_2$. With

the exception of feeding and passaging periods, this system allowed for constant reduced-$O_2$ exposure ideal for longer-term studies and for comparisons to 20% $O_2$ cultured hMSCs. Growth kinetics were evaluated by calculating and compiling population doublings (PDs) over successive passages. Total c-Met expression was determined as a function of concentration, calculated by measurements of optical density by means of ELISA.

The results of our growth kinetics study indicate that prolonged conditioning in 2% $O_2$ significantly increased hMSC PDs from 7.35 ± 0.53 to 17.27 ± 1.78 ($p < 0.01$; Figure 3.1A). In addition, 2% $O_2$ conditioning sustained hMSC growth to passage 16 versus only passage 12 in 20% $O_2$, with significantly higher cumulative population doublings between the two oxygen conditions from passage 5 to passage 12 ($p < 0.01$; Figure 3.1A). Overall, our results are consistent with previous studies that indicate 2% $O_2$ can increase hMSC growth kinetics with prolonged reduced-$O_2$ conditioning.[3,4] We designed our study with similar parameters as these previous studies with respect to $O_2$ concentration, feeding regimen, and passaging times; however, we calculated population doublings as a more definitive indicator of fold-expansion, and we continued our study until the cells in both $O_2$ concentrations reached senescence. Our analysis further suggests that long-term conditioning in 2% $O_2$ can increase hMSC proliferation and extend their longevity, which could be further confirmed by cell cycle analysis and molecular characterization in future studies. Cell cycle analysis would help to determine if the reduced-$O_2$ conditioning caused more hMSCs to enter the S-phase, or caused hMSCs to complete the cell cycle at a faster rate, or generated a sub-population of highly proliferative hMSCs. Molecular characterization may help to determine if additional factors such as increased cytokine/paracrine signaling or telomerase activation is responsible for the increased proliferation.

On a critical note, our results may also be consistent with previous studies that indicate short-term exposure to reduced-$O_2$ may decrease hMSC growth kinetics.[6,23] After only 7 days in culture at passage 3, hMSCs in 20% $O_2$ showed significantly more growth with 2.67 ± 0.02 PDs compared to hMSCs in 2% $O_2$ with only 2.46 ± 0.03PDs ($p < 0.01$, Figure 3.1 A and B). Additionally, our results show that reduced-$O_2$ conditioned hMSCs may undergo a prolonged lag phase between passages 3 and 5, before showing a

significantly higher PD compared to normal-$O_2$ hMSCs at passages 5 through 12 (Figure 3.1B). This prolonged lag phase has also been acknowledged by another study that shares our findings that longer-term reduced-$O_2$ conditioning increases hMSC growth kinetics.[3] These differences in our own results illustrate how the length of reduced-$O_2$ exposure duration can affect the interpretation of how reduced-$O_2$ affects hMSC growth kinetics. However, it appears that the initial exposure to 2% $O_2$ may cause a decrease or lag in hMSC growth, but prolonged reduced-$O_2$ conditioning can significantly increase the growth of hMSCs for a significantly longer period of time. Observational assessment of the cells did not indicate an increase in cell death during the lag phase in reduced-$O_2$ culture, but cell viability assays were not performed during this period. Response mechanisms involved in the lag phase, growth phase, or "switch" between phases remains unknown. It also remains unclear whether the effects in growth kinetics are a positive response to a MSC-niche oxygen environment or a stress response to low oxygen tension.

What is clear about our observations is that hMSCs need time to respond to the reduced-$O_2$ environment, and hMSCs appear to thrive in reduced-$O_2$ once they have adapted accordingly. Therefore, it is likely that hMSCs cultured at 20% $O_2$ *in vitro* are unequipped and unprepared to respond to reduced-$O_2$ conditions when transplanted into MIs *in vivo*, which contributes to their poor survival. Conditioning hMSCs in reduced-$O_2$ *in vitro* prior to implantation may allow them to develop the appropriate cellular machinery with which to adapt more readily to the reduced-$O_2$ environment of an MI. Concomitantly, our observations suggest that reduced-$O_2$ conditioning can dramatically increase the sheer number of hMSCs, as we saw the PDs increase from $7.35 \pm 0.53$ to $17.27 \pm 1.78$. This provides new optimism for expanding hMSCs for their use as a potential cell therapy to replace the estimated 1 billion cardiomyocytes lost during an MI (Figure 3.5).

The results of our total c-Met expression study indicate that continued exposure in 2% $O_2$ can significantly increase c-Met expression in hMSCs (Figures 3.2 and 3.4). Analysis of a time-course study on reduced-$O_2$ conditioned hMSCs found that c-Met expression remained fairly constant from day 1 to day 3, but then significantly increased at day 7. Increased c-Met expression was maintained through day 10, but then significantly decreased by day 14. These data suggest that the duration of reduced-$O_2$

exposure may play a role in regulating c-Met expression levels in hMSCs, with a significant upregulation between days 3-10.

To further understand reduced-$O_2$ effects on c-Met expression, we also performed a condensed time-course study on normal-$O_2$ conditioned hMSCs to evaluate the c-Met expression profile within the 3-10 day timeframe (Figures 3.3 and 3.4). Normal-$O_2$ conditioned hMSCs expressed relatively low levels of c-Met at day 3, a significant increase of c-Met at day 7, and then a significant decrease of c-Met by day 10. These results indicate that normal-$O_2$ conditioned hMSCs show a similar c-Met expression profile compared to reduced-$O_2$ conditioned hMSCs. Both conditions show low expression before day 7, a significant increase of expression at day 7, and then a decrease in expression after day 7. However, reduced-$O_2$ conditioned hMSCs appear to sustain high levels of c-Met expression from day 7 to day 10 before dropping off at day 14, and normal-$O_2$ conditioned hMSCs show a significant decrease in c-Met by day 10.

In comparing the c-Met expression levels of hMSCs conditioned in both oxygen concentrations at these three time points, reduced-$O_2$ hMSCs showed significantly more c-Met expression than normal-$O_2$ hMSCs at days 7 and 10, but not at day 3 (Figure 3.4). As a whole, our analysis indicates that culturing hMSCs for 7 days in either oxygen condition can increase c-Met expression; however, reduced-$O_2$ conditioning elicits significantly more c-Met expression compared to normal-$O_2$ conditioning at 7 days. In our analysis, samples were normalized to total protein to compare different batches of cells across controlled time points; therefore, results do not reflect c-Met concentrations based on total cell number or cell confluence. During sample collection, cells were trypsinized from culture flasks to prepare total cell lysates. To our knowledge, after a thorough literature search, the trypsinization process does not appear to remove or detriment the integrity of the c-Met receptor. However, it is unclear whether the increase in c-Met corresponds with cells entering a particular phase of the cell cycle. While a direct link between cell cycle and c-Met expression has not been established, it has been reported that HGF can act as a potent mitogen in some cell types (e.g. neuronal and endothelial cells),[24,25] and that HGF signaling may help to mediate c-Met expression in a positive feedback loop.[26]

In further consideration, while we did not find statistical difference in c-Met expression at day 3 for hMSCs cultured in normal-$O_2$ (24.53 ± 8.70 ng/mL) or reduced-$O_2$ (35.22 ± 9.87 ng/mL). Previous studies have argued that culturing hMSCs in reduced-$O_2$ increases c-Met expression after exposure durations of only 16-72 hours, using qualitative techniques such as Western blotting and densitometry.[1,11] However, our quantitative analysis suggests that there is no statistical difference in c-Met expression at these early time points, and that true differences in c-Met expression are only realized at longer conditioning durations.

In considering the role of HGF/c-Met signaling for the activation of cardiac differentiation pathways, our results suggest that we can leverage reduced-$O_2$ conditioning to increase c-Met expression, which may allow for increased HGF/c-Met interaction and downstream cardiac-pathway activation. Significant increases of c-Met expression at days 7 and 10 suggest that there may be a finite window of opportunity for using HGF to initiate the cardiac program in hMSCs. Optimal timing is a common theme for scientists who study cardiac differentiation strategies in all stem cell types, regardless of chemical or mechanical induction methods. Based on the results of this study, we incorporated a 7 day reduced-$O_2$ culturing period into our conditioning regimen, prior to HGF treatment for the induction of cardiac differentiation.

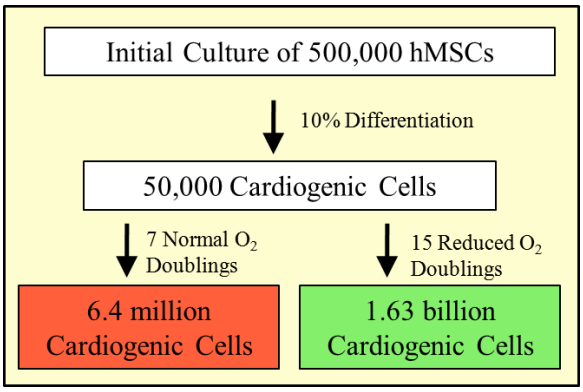


**Figure 3.5. Cardiogenic cell expansion in reduced-$O_2$ conditions.** In consideration of our results showing that reduced-$O_2$ conditioning can significantly increase hMSC growth kinetics, it may be possible to leverage these effects for the expansion of cardiogenic cells. During a typical initial seeding, 500,000 hMSCs are plated in a T-75 flask. As a conservative estimate, a strategy or conditioning regimen allowing for 10% cardiac differentiation would produce 50,000 cardiogenic cells. If the sub-population of cardiogenic cells could be purified and expanded over 15 doublings in reduced-$O_2$, it may be possible to produce over 1.5 billion cardiogenic cells.

## 3.5. References


1 Rosova, I., Dao, M., Capoccia, B., Link, D. & Nolta, J. A. Hypoxic Preconditioning Results in Increased Motility and Improved Therapeutic Potential of Human Mesenchymal Stem Cells. *Stem Cells*, (2008).

2 Hu, X. *et al.* Transplantation of hypoxia-preconditioned mesenchymal stem cells improves infarcted heart function via enhanced survival of implanted cells and angiogenesis. *J Thorac Cardiovasc Surg* **135**, 799-808, (2008).

3 Grayson, W. L., Zhao, F., Izadpanah, R., Bunnell, B. & Ma, T. Effects of hypoxia on human mesenchymal stem cell expansion and plasticity in 3D constructs. *J Cell Physiol* **207**, 331-339, (2006).

4 Grayson, W. L., Zhao, F., Bunnell, B. & Ma, T. Hypoxia enhances proliferation and tissue formation of human mesenchymal stem cells. *Biochem Biophys Res Commun* **358**, 948-953, (2007).

5 Robert M. Berne, M. N. L., Bruce M. Koeppen, Bruce A. Stanton 1014 (Mosby, an affiliate of Elsevier, Inc., St. Louis, MO, 2004).

6 Hung, S. C. *et al.* Short-term exposure of multipotent stromal cells to low oxygen increases their expression of CX3CR1 and CXCR4 and their engraftment in vivo. *PLoS ONE* **2**, e416, (2007).

7 Potier, E. *et al.* Hypoxia affects mesenchymal stromal cell osteogenic differentiation and angiogenic factor expression. *Bone* **40**, 1078-1087, (2007).

8 Chacko, S. M. *et al.* Myocardial oxygenation and functional recovery in infarct rat hearts transplanted with mesenchymal stem cells. *Am J Physiol Heart Circ Physiol* **296**, H1263-1273, (2009).

9 Lennon, D. P., Edmison, J. M. & Caplan, A. I. Cultivation of rat marrow-derived mesenchymal stem cells in reduced oxygen tension: effects on in vitro and in vivo osteochondrogenesis. *J Cell Physiol* **187**, 345-355, (2001).

10 Kanichai, M., Ferguson, D., Prendergast, P. J. & Campbell, V. A. Hypoxia promotes chondrogenesis in rat mesenchymal stem cells: a role for AKT and hypoxia-inducible factor (HIF)-1alpha. *J Cell Physiol* **216**, 708-715, (2008).

11 Chacko, S. M. *et al.* Hypoxic preconditioning induces the expression of prosurvival and proangiogenic markers in mesenchymal stem cells. *Am J Physiol Cell Physiol* **299**, C1562-1570, (2010).

12 Okuyama, H. *et al.* Expression of vascular endothelial growth factor receptor 1 in bone marrow-derived mesenchymal cells is dependent on hypoxia-inducible factor 1. *J Biol Chem* **281**, 15554-15563, (2006).

13 Malladi, P., Xu, Y., Chiou, M., Giaccia, A. J. & Longaker, M. T. Effect of reduced oxygen tension on chondrogenesis and osteogenesis in adipose-derived mesenchymal cells. *Am J Physiol Cell Physiol* **290**, C1139-1146, (2006).

14 Lee, J. H. & Kemp, D. M. Human adipose-derived stem cells display myogenic potential and perturbed function in hypoxic conditions. *Biochem Biophys Res Commun* **341**, 882-888, (2006).

15 Gnecchi, M. *et al.* Evidence supporting paracrine hypothesis for Akt-modified mesenchymal stem cell-mediated cardiac protection and functional improvement. *Faseb J* **20**, 661-669, (2006).

16 Forte, G. *et al.* Hepatocyte growth factor effects on mesenchymal stem cells: proliferation, migration, and differentiation. *Stem Cells* **24**, 23-33, (2006).

17 Roggia, C., Ukena, C., Bohm, M. & Kilter, H. Hepatocyte growth factor (HGF) enhances cardiac commitment of differentiating embryonic stem cells by activating PI3 kinase. *Exp Cell Res* **313**, 921-930, (2007).

18 Mekhail, K., Khacho, M., Gunaratnam, L. & Lee, S. Oxygen sensing by H+: implications for HIF and hypoxic cell memory. *Cell Cycle* **3**, 1027-1029, (2004).

19 Gustafsson, A. B. & Gottlieb, R. A. Autophagy in ischemic heart disease. *Circ Res* **104**, 150-158, (2009).

20 Peterson, K. M., Aly, A., Lerman, A., Lerman, L. O. & Rodriguez-Porcel, M. Improved survival of mesenchymal stromal cell after hypoxia preconditioning: role of oxidative stress. *Life Sci* **88**, 65-73, (2011).

21 Suzuki, K. *et al.* Dynamics and mediators of acute graft attrition after myoblast transplantation to the heart. *Faseb J* **18**, 1153-1155, (2004).

22 Wang, Z. J. *et al.* Lipopolysaccharides can protect mesenchymal stem cells (MSCs) from oxidative stress-induced apoptosis and enhance proliferation of MSCs via Toll-like receptor(TLR)-4 and PI3K/Akt. *Cell Biol Int* **33**, 665-674, (2009).

23 Salim, A., Nacamuli, R. P., Morgan, E. F., Giaccia, A. J. & Longaker, M. T. Transient changes in oxygen tension inhibit osteogenic differentiation and Runx2 expression in osteoblasts. *J Biol Chem* **279**, 40007-40016, (2004).

24 Ebens, A. *et al.* Hepatocyte growth factor/scatter factor is an axonal chemoattractant and a neurotrophic factor for spinal motor neurons. *Neuron* **17**, 1157-1172, (1996).
25 Bussolino, F. *et al.* Hepatocyte growth factor is a potent angiogenic factor which stimulates endothelial cell motility and growth. *The Journal of cell biology* **119**, 629-641, (1992).
26 Rappolee, D. A., Iyer, A. & Patel, Y. Hepatocyte growth factor and its receptor are expressed in cardiac myocytes during early cardiogenesis. *Circulation research* **78**, 1028-1036, (1996).

## CHAPTER 4: Effects of reduced-$O_2$ and HGF on expression of cardiac-specific markers in hMSCs

### 4.1. Introduction

Since the 1990's, bone marrow derived cells have been studied extensively for their multipotent ability to become a number of different cell types for therapeutic tissue regeneration applications.[1-5] Based on these early successes of using bone marrow cells (BMCs) in a variety of organ systems, there was a natural progression to explore the use of these cells for cardiac therapy. Orlic *et al.*'s seminal study in 2001 isolated $Lin^-/c\text{-}kit^+$ BMCs from male GFP-transgenic mice and delivered them to MIs in female mice to show a significant increase in ventricular function.[6] Most notably, they also tracked the male GFP-labeled cells and found that delivered BMCs expressed cardiac-specific markers such as cardiac myosin, MEF2C, and Nkx2.5 *in vivo*. From their results, they concluded that delivered BMCs could regenerate new myocardium, which contributed to the increases they observed in ventricular function. The study sparked optimism that BMCs could be used as a cardiac cell therapy to regenerate diseased myocardium, which evoked enormous scientific interest from researchers in the field. The study also sparked controversy as some researchers could not reproduce Orlic *et al.*'s findings,[7,8] while others reported measured successes showing BMCs could partially differentiate towards a cardiac lineage *in vitro*,[9-17] express cardiac-specific markers *in vivo*,[13,18-20] and improve cardiac function.[13,18,20-25]

After Orlic *et al.*'s landmark study, there was a strong focus from the scientific community to determine mechanisms that would transdifferentiate BMCs into cardiomyocytes *in vitro*. There were several reasons for these efforts. One major concern was that BMCs were a mixed population of cells that contained a variety of multipotent cells capable of differentiating into alternative cell types such as osteocytes and adipocytes,[26] which would be extremely detrimental in the cardiac environment. The prospect of differentiating BMCs to a cardiomyocyte lineage *in vitro* and then separating the generated cardiomyocytes from the mixed batch of cells for a more pure population was a goal to alleviate this safety concern. In addition, many were eager to differentiate BMCs into mature, functional cardiomyocyte phenotypes *in vitro*, in order to study electrophysiological and mechanical properties of the newly generated cardiomyocytes.

In the effort to transdifferentiate BMCs to cardiomyocytes *in vitro*, several strategies or combinations of strategies were investigated. Some groups isolated subpopulations of BMCs such as c-kit$^+$ cells,[9] marrow stromal cells,[11,12] and mesenchymal stem cells (MSCs)[10,15,16,20,27] prior to treatment, hoping to select for a population of BMCs that were more apt for cardiac differentiation. In addition, some groups used co-culture strategies with rat neo-natal cardiomyocytes to show that a low percentage of marrow-derived cells could partially differentiate towards a cardiomyocyte lineage by expressing cardiac-specific markers[9,12,14] and displaying inward rectifying currents[9]. Other groups have experimented with cytokine treatments (i.e. retinoic acid, TGF-β, FGF-2, HGF, and PDGF) to show partial cardiac differentiation by gene and protein expression.[16,17,28] Treatment of marrow stromal cells with the DNA demethylation agent 5-azacytidine induced about 30% differentiation, showing cardiac marker expression, propagation of action potentials, and spontaneous contraction.[11] Some studies have combined co-culture with rat neo-natal cardiomyocytes with cytokine treatments such as BMP4/TGF-β,[9] dimethyl sulfoxide,[14] or 5-azacytidine[14] to show little or no effect on cardiac differentiation. Our lab has used mechanical manipulation to make hMSC spheroids, which shows that 57% of the hMSCs can differentiate towards a cardiac lineage detected by sarcomeric α-Actinin expression within 2 weeks (Figure 4.1).[13] Patch-clamping analysis of our "cardiogenic" cells indicate that 16% of the differentiated hMSCs display large L-type $Ca^{2+}$ currents, indicating that some of the differentiated hMSCs may be capable of producing cardiac-specific action potentials.[13] The combination of cardiac protein expression and L-type $Ca^{2+}$ currents suggest that these cells are partially differentiated to a cardiac lineage, but are not fully differentiated cardiomyocytes.

Despite these successes, the current BMC and MSC differentiation techniques are insufficient because only a low percentage of cells differentiate and only partial differentiation has been achieved. Co-culture experiments can be problematic because of the challenging nature of trying to extract out the differentiated marrow-derived cells from the mix of rat neo-natal cardiomyocytes and undifferentiated cells. On a related note, the characterization of differentiated marrow-cells in co-culture experiments has come under scrutiny, questioning whether "new" cardiomyocytes can be fully distinguished from neo-

natal cardiomyocytes. Cytokine treatments try to apply factors previously described in the developmental or embryonic literature, but the methods of application range dramatically. Some groups use a "kitchen sink" approach,[28] while others use a more limited approach with finite concentrations and arbitrary time points. Unfortunately, most cytokine treatments have resulted in low-percentage cardiac differentiation, with only a limited number of cardiac genes and proteins being evaluated. Methods using 5-azacytidine are problematic because the chemical inhibits methyltransferases, which decreases DNA methylation in an uncontrolled manner, affecting DNA replication and RNA transcription in a random fashion with unpredictable results.[29] Mechanical differentiation techniques often require tedious techniques that demand skillful implementation. For instance, our spheroid method uses a tedious hanging-drop technique (Figure 4.1, A), in which hanging cell suspensions must be carefully manipulated and fed for three days before being plated for cellular outgrowth. Unfortunately, mechanical manipulation methods have also shown low-percentage cardiac differentiation, with a limited breadth of marker expression and only a small percentage of cells showing L-type calcium-channel currents.

For the purpose of exploring novel methods that will initiate cardiac-specific differentiation of hMSCs and improve upon current limitations,[30] we developed a simplistic *in vitro* conditioning regimen based on aspects described in the MSC literature. As discussed in Chapter 3, some studies report that reduced-$O_2$ conditioning can increase MSC differentiation potential,[31-33] and we have shown that conditioning hMSCs in reduced-$O_2$ for 7 days can significantly increase the expression of the c-Met receptor. The c-Met receptor is a disulfide-linked heterodimeric transmembrane protein encoded by the c-met proto-oncogene,[34] which exhibits tyrosine-kinase activity to recruit different signal transducers and adaptors that have been shown to affect ERK/MAPK and PI3K.[16] Although the c-Met receptor was originally discovered in a chemical-carcinogen treated osteogenic sarcoma cell line in 1984,[35] c-Met was only recently discovered in hMSCs in 2004.[36] The c-Met receptor only elicits intracellular signaling for biological processes when it interacts with hepatocyte growth factor (HGF).

HGF is a pleiotropic cytokine involved in a number of biological processes in embryogenesis and organ system maintenance. HGF has been shown to be involved developmental processes in kidney

tubulogenesis,[37] angiogenesis,[38] and mammary gland formation.[39] In addition, HGF can affect motility and morphogenesis of endothelial cells,[40] act as a chemoattractant for both motor neuron axons[41] and myoblast precursors,[42] and play a role in kidney and liver regeneration.[43,44] In cardiac applications, HGF has been shown to be involved in developmental cardiogenesis,[45] and has shown cardioprotective effects in ischemic myocardium.[46] With respect to cardiac differentiation, Roggia *et al.* found that HGF can increase cardiac marker expression of cardiomyocyte-differentiated embryonic stem cells, and increase the number of beating embryoid bodies.[47] In addition, Forte *et al*. suggest that treating mouse MSCs with human HGF can induce cardiac gene and protein expression.[16] Both studies suggest that HGF/c-Met signaling activates the downstream effectors phophatidylinositol 3-kinase (PI3K) and Akt, which activate cardiac transcription factors to initiate a cardiac program (Figure 4.2).

We hypothesize that employing a conditioning regimen of reduced-$O_2$ culturing and HGF treatment will have a combined effect to express cardiac-specific markers in hMSCs *in vitro*. In Chapter 4, we will investigate the expression of cardiac genes and proteins in reduced-$O_2$/HGF treated hMSCs. Based on our rationale and analysis in Chapter 3, we used our 2% $O_2$ culturing system to implement the reduced-$O_2$ component in our combined conditioning regimen. Studies focusing on HGF/c-Met signaling and cardiac differentiation of hMSCs have previously used HGF concentrations in the range of 20-25 ng/mL.[16,48] And based on the previous study using human HGF to induce cardiac marker expression in mouse MSCs,[16] we supplemented DMEM/L-Glutamine medium with 20 ng/mL human HGF in our combined conditioning regimen. To our knowledge, the effects of a combined reduced-$O_2$/HGF conditioning regimen on cardiac marker expression in hMSCs have not been reported.

### 4.1.1. Determining the effect of reduced-$O_2$/HGF conditioning on cardiac gene transcription of hMSCs *in vitro*

Based on the literature for developmental cardiomyogenesis and embryonic stem cells, cardiac gene induction can occur within the first 3 to 7 days of differentiation.[47,49-51] However, a definitive understanding of the order and timing of signaling events, transcription factor interaction, and regulatory

mechanisms required for cardiac differentiation of embryonic stem cells is still unknown. The processes involved in the cardiac differentiation in MSCs are even more equivocal. However, based on the previous MSC studies showing partial cardiac differentiation and the developmental biology literature regarding the interaction of cardiac transcription factors, we have pieced together a basic pathway for the role of HGF/c-Met signaling in cardiomyogenesis (Figure 4.2).

To determine the effect of reduced-$O_2$/HGF conditioning on the cardiac gene expression of hMSCs *in vitro*, we investigated treated hMSCs for the expression of gene transcripts corresponding with factors outlined in our basic cardiac pathway. To do this, cells were first cultured in reduced-$O_2$ for 7 days to increase c-Met expression, then treated for another 7 days with 20 ng/mL human HGF before being harvested for total RNA isolation. cDNA was then synthesized from mRNA, and then cardiac-specific gene expression was detected by reverse transcription polymerase chain reaction (RT-PCR).

The DMEM/HGF treatment media differs from traditional media used to culture hMSCs, which is typically a growth medium consisting of a DMEM/L-Glutamine base supplemented with 10% fetal bovine serum. The growth medium we used is a proprietary formulated mesenchymal stem cell growth medium (MSCGM; Lonza Inc.). Although some studies have indicated that cells can have unique responses when cultured in low-serum or serum-deprived media, the DMEM/HGF treatment we chose helps to assure that the changes we observe are HGF dependent.

In order to better understand the effects of our reduced-$O_2$/HGF treatment, we had to consider the differences in oxygen concentration, HGF supplementation, and serum deprivation. To parse out the effects of these different treatment factors, we formulated 6 treatment conditions that were tested in an initial screen for gene expression of key cardiac genes (MEF2C, Nkx2.5, GATA-4, sarcomeric α-Actinin, and CaCNA1C). The formulated treatment groups used in our initial screen are outlined in Table 4.1.

For further characterization, we then screened reduced-$O_2$/HGF conditioned hMSCs for a more inclusive set of cardiac genes with unique primers for myosin heavy chain, myosin light chain, troponin, and additional L-type calcium subunits. Having already parsed the effects of oxygen concentration and media treatments in our initial panel of cardiac genes, we limited our treatment comparisons in this

experiment. For further analysis, we compared only reduced-$O_2$/HGF conditioned hMSCs and traditionally cultured hMSCs, grown in normal-$O_2$ with growth media (MSCGM).

### 4.1.2. Determining the effect reduced-$O_2$/HGF conditioning on cardiac protein translation of hMSCs *in vitro*

To complement the results for cardiac gene transcription, we investigated the effects of reduced-$O_2$/HGF conditioning on the cardiac protein expression of hMSCs *in vitro*. We hypothesized that only a sub-population of reduced-$O_2$/HGF conditioned hMSCs may express cardiac proteins, and we were also interested in visualization the localization of protein expression in differentiating cells. Therefore, we used immunocytochemistry (ICC) as a more appropriate method to detect low protein expression (either due to low expression across the cell field, or only a small percentage of cells expressing protein), which may be undetectable by Western blot analysis on large batches of cells.

In this experiment, we used 2 formats to accommodate the ICC protocols established in the Gaudette Lab. Cells were seeded onto either 24-well plate tissue culture plastic, or sterile glass coverslips that were pre-fitted into 24-well plates. Cells were conditioned as previously described in our cardiac gene analysis (Section 4.1.1) before being fixed. Cells were fixed in cold methanol (stored in -20ºC) and ICC was performed using cardiac-specific primary antibodies for MEF2C, Nkx2.5, GATA-4, sarcomeric α-Actinin, and Cav1.2 (L-type calcium channel marker). Then appropriate specific fluorescent secondary antibodies were applied. Cells were then counterstained for Hoechst 33342 nuclear dye, and analyzed by fluorescence microscopy for expression and subcellular localization. In this analysis, we limited our treatment comparisons to include only reduced-$O_2$/HGF conditioned hMSCs and traditionally cultured hMSCs, grown in normal-$O_2$ with growth medium.

### 4.1.3. Evaluating the role of HGF/c-Met signaling on cardiac marker expression

To further assess our hypothesis that HGF/C-Met signaling is involved in the activation of downstream cardiac-marker expression in hMSCs, we investigated two possible control mechanisms in

our proposed pathway (Figure 4.2). Previous studies suggest HGF/c-Met signaling activates different adapter proteins (e.g. Gab-1, SHC, and GRB2) to activate effectors such as PI3K and Akt, which further activates downstream cardiac transcription factors such as MEF2C, Nkx2.5, and GATA-4 to initiate cardiac differentiation.[16,47] To test this, we treated reduced-$O_2$/HGF conditioned hMSCs with two independent small-molecule inhibitors to evaluate their effects on downstream cardiac gene transcription.

In this study, we tested small-molecule inhibitor PHA-665752, which has previously been shown to inhibit c-Met phosphorylation and decrease c-Met dependent cell processes such as motility and proliferation.[52,53] Independently, we also tested small-molecule inhibitor LY294002, which has previously been shown to completely inhibit PI3K by competitively inhibiting its ATP binding site.[54] LY294002 has been used on several cell types including stem cells to show complete but reversible inhibition of PI3K, subsequent dephosphorylation of downstream effectors such as Akt, and loss of PI3K-dependent cellular activity.[33,47,54-56]

Both small-molecule inhibitors were tested separately with concentrations comparable to those reported in the literature. Inhibitor treatments were applied to cells for 2 hours before the addition of HGF (20 ng/mL). This treatment process was repeated every 24 hours for 7 days. On the 7$^{th}$ day, cells were harvested for RNA isolation, cDNA synthesis, and RT-PCR analysis for cardiac-specific genes.

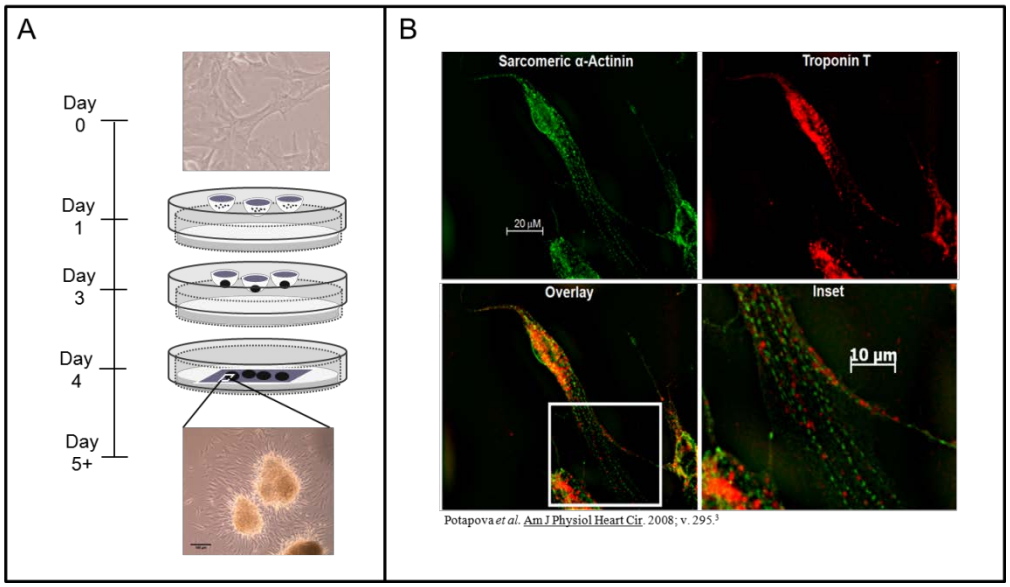


**Figure 4.1. Cardiogenic cells differentiated from hMSC spheroids.** (A) We previously used the hanging drop technique to form hMSC spheroids. Cell suspensions were hung from petri dish lids and fed every 24 hours from day 0 to day 3. By day 3, hMSCs aggregated to form spheroids, which were then plated onto tissue culture surfaces. Spheroids were cultured for cellular outgrowth for 7-10 days after plating. (B) Some of the cells growing out from the spheroid showed to be cardiogenic cells, characterized by positive expression of cardiac-specific proteins sarcomeric α-Actinin (green) and troponin T (red), as well as L-type calcium channel currents (figure modified from Rosen *et al*. Stem Cells, 2007; complete data shown in this manuscript).[57]

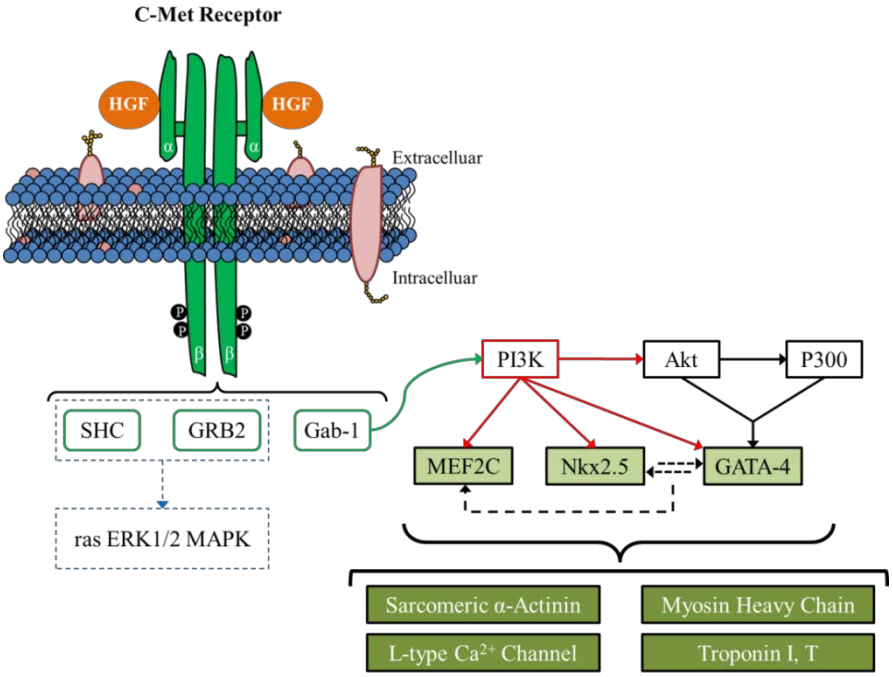


**Figure 4.2. Proposed signaling pathway for HGF/c-Met involvement in the cardiac differentiation program.** Based on previous studies regarding HGF/c-Met signaling on effector proteins, as well as signaling mechanisms involved in developmental and stem cell cardiomyogenesis, we propose the above pathway for how HGF/c-Met signaling can initiate or contribute to the cardiac program in hMSCs.

| # | Name | Description |
|---|---|---|
| 1 | Normal-$O_2$/MSCGM | Traditional hMSC culture conditions, atmospheric $O_2$ (20%) and growth media |
| 2 | Normal-$O_2$/DMEM | Atmospheric $O_2$ (20%) and DMEM (without FBS or HGF) |
| 3 | Normal-$O_2$/HGF | Atmospheric $O_2$ (20%) and DMEM supplemented with 20 ng/mL HGF |
| 4 | Reduced-$O_2$/MSCGM | 2% $O_2$ and growth media |
| 5 | Reduced-$O_2$/DMEM | 2% $O_2$ and DMEM (without FBS or HGF) |
| 6 | Reduced-$O_2$/HGF | 2% $O_2$ and DMEM supplemented with 20 ng/mL HGF |

**Table 4.1. Table of conditioning regimens.** MSCGM (Mesenchymal Stem Cell Growth Media; proprietary formulation from Lonza, Inc.); DMEM (Dulbecco's Modified Eagle's Medium); FBS (fetal bovine serum); HGF (hepatocyte growth factor). Reduced-$O_2$/HGF conditions highlighted in yellow, other listed conditions tested as controls.

## 4.2 Materials and Methods

### 4.2.1. Human mesenchymal stem cell culture

Human mesenchymal stem cells (hMSCs) isolated from adult bone marrow were purchased from Lonza, Inc. (Walkersville, MD; # PT-2501). Cryo-preserved vials arrived as passage-2 hMSCs, which had been pre-characterized by the manufacturer (Appendix A). Upon thawing, hMSCs were plated as passage-3 with a seeding density of 500,000 cells per T-75 flask. New vials were plated and expanded using mesenchymal stem cell growth medium (MSCGM; Lonza's proprietary hMSC growth media, # PT-3001). Multiple flasks originating from the same vial were segregated to either normal-$O_2$ (20%) or reduced-$O_2$ (2%) conditions (as previously described in the Chapter 3). Cells were maintained at 37°C, growth media was changed every 2 days, and cells were passaged when growth reached 80-90% confluency. Successive cell-passages were maintained in their pre-designated oxygen concentrations, and passage 4-8 hMSCs were used for experimentation.

### 4.2.2. Media Treatments

Based on preliminary studies done on the c-Met receptor for HGF, media treatments were preceded by a 7-day growth period to increase c-Met expression. Therefore, cells passaged for media treatment experimentation were initially seeded and cultured in MSCGM for 7 days in their respective $O_2$ concentrations, as described previously in the methods for hMSC culture (Section 4.2.1). On the $7^{th}$ day, MSCGM was removed, and appropriate media treatments were applied. MSCGM groups received fresh MSCGM, DMEM groups received DMEM (with L-glutamine and 4.5 g/L glucose; Lonza, Inc.), and HGF groups received DMEM supplemented with 20 ng/mL human HGF (PeproTech, Rocky Hill, NJ; # 100-39). Treatment media was changed every 24 hours for another 7 days, and then cells were harvested or fixed for experimentation. A treatment timeline is shown in Figure 4.3.

### 4.2.3. Inhibitor Treatment

Small-molecule inhibitors were applied independently during the media treatment phase of our conditioning regimen (Figure 4.3). Inhibitor media was made using DMEM supplemented with either 5 µM PHA665752 (CalBiochem®, now part of EMD Chemicals, Philadelphia, PA; #448102) or 50 µM LY294002 (Gibco®, part of Invitrogen, Camarillo, CA; #PHZ1144). Inhibitor media was made fresh at each application, and then applied to cells for 2 hours. After 2 hours, an appropriate volume of HGF solution (Peprotech) was spiked into the applied inhibitor media to bring the HGF concentration to 20 ng/mL. This inhibitor treatment process was repeated every 24 hours, for 7 days.

### 4.2.4. RNA Isolation

RNA was isolated using a NucleoSpin® RNA/Protein total RNA and protein isolation kit (Macherey-Nagel, Bethlehem, PA; # 740933). Reagent preparation and RNA isolation were completed using the guidelines and protocols set by the manufacturer. The kit was used to isolate RNA and protein from the same sample. RNA purity was aided by filtration with a nucleic acid column, followed by rDNase treatment and a series of washes per the manufacturer's protocol. RNA samples were collected and stored at -80°C until processing.

### 4.2.5. cDNA Synthesis

Complementary DNA (cDNA) was synthesized using a SuperScript™ First-Strand Synthesis System kit (Invitrogen, Carlsbad, CA; #11904-018). All of the following reagents were prepared and supplied in the Invitrogen kit. The kit is designed with SuperScript™ II Reverse Transcriptase enzyme and RNaseOUT™ Recombinant RNase Inhibitor components, to reduce RNase H activity and safeguard against target RNA degradation. To make cDNA, 5 µg of total RNA from each sample used. Sample volume was combined with 0.5 mM dNTPs, 0.5 µg of Oligo(dT) primers, and RNase-free water for a total volume of 10 µL. The mix was incubated at 65°C for 5 minutes, and then chilled on ice for 1 minute. A second reaction mix was prepared with 1X RT Buffer (20 mM Tris-HCl pH 8.4, 50 mM KCl),

5 mM $MgCl_2$, 0.01 M DTT, and 40 units of RNaseOUT™. Chilled samples were treated with 9 µL of the second mix, and then incubated at 42°C for 2 minutes. After 2 minutes incubation, 1 µL (50 units) of SuperScript™ RT enzyme was added to each mix, and then placed back into 42°C for 50 minutes. Reactions were then terminated by incubating them at 70°C for 15 minutes. After termination, reactions were chilled on ice and collected by brief centrifugation. Prior to RT-PCR, all reactions were treated with 1 µL (2 units) of RNase H and incubated at 37°C for 20 minutes.

#### 4.2.6. RT-PCR

Gene transcription was detected by reverse transcription polymerase chain reaction (RT-PCR), using AccuStart™ Taq polymerase reagents from Quanta Biosciences (Gaithersberg, MD; # 95061-250), and deoxyribonucleotides (dNTPs) from Promega Corporation (Madison, WI; # C114G). Each RT-PCR reaction mixture was prepared with 1x PCR Reaction Buffer (2.5 µL; Quanta Biosciences), 1.5 mM magnesium chloride (0.75 µL; Quanta Biosciences), 200 mM dNTPs (0.5 µL; Promega Corporation), 0.5 units of Taq polymerase (0.1 µL; Quanta Biosciences), 10 pM primer solution (mixture of forward and reverse primers, custom made), 240 ng of sample cDNA, and enough RNase-free water to bring each reaction to a final volume of 25 µL (Gibco, Camarillo, CA; # 10977-015). Preparations were run on a thermocycler for 30-35 cycyles.

RT-PCR products were separated onto a 2% agarose gel by electrophoresis, and gene expression was determined by band detection at the appropriate size (bp) of the amplicon. Qualitative analysis of gene expression was compared against the sample's internal expression for glyceraldehyde-3-phosphate dehydrogenase (GAPDH) and across treatments. RT-PCR primers for cardiac-specific genes were either custom designed or adopted from previous studies (Table 4.2), to include genes for early-stage cardiac transcription factors, sarcomeric proteins, and L-type $Ca^{2+}$ channel subunits. All RT-PCR primers were specialty ordered through and manufactured by Eurofins MWG Operon (Huntsville, AL).

Total RNA from human heart (Clontech, Mountain Veiw, CA; #636532) was synthesized for human cardiac cDNA using the same methods described above (Section 4.2.5). Human cardiac cDNA provided

a positive control for cardiac gene expression, and was reported in all RT-PCR studies. Negative, "no-template" controls were included in all RT-PCR studies, but not reported.

### 4.2.7. Immunocytochemistry

For protein analysis by immunocytochemistry (ICC), hMSCs were plated in 24-well tissue culture plates with a seeding density of ~12,000 cells/well. Conditioning treatments were applied as described in Section 4.2.2, with a 7-day growth phase and a 7-day media treatment phase. After conditioning, cells were washed with phosphate-buffered saline (PBS), and then fixed with cold methanol (Sigma Aldrich, St. Louis, MO; #M-3641) for 20 minutes at -20°C. After fixation, wells were washed 3 times with PBS and plates were kept in 4°C before being processed.

For the ICC procedure, samples were acclimated to room temperature for 3 minutes in fresh PBS composed of: deionized water supplemented with 8.0 g/L sodium chloride (Sigma-Aldrich, #S9888), 0.2 g/L potassium chloride (Sigma-Aldrich, #P-4504), 1.44 g/L sodium phosphate dibasic (Sigma-Aldrich, #S7907), and 0.24 g/L potassium phosphate monobasic (Sigma-Aldrich #P-5379). The samples were then washed twice (5 minutes each) on a rotator with a solution of PBS with 0.05% Tween 20 (Sigma-Aldrich #P1379). Cells being analyzed for cardiac transcription factors were then permeablized with 1.5 N hydrochloric acid for 20 minutes at room temperature, and cells being analyzed for sarcomeric proteins were permeablized with Triton X-100 (Sigma-Aldrich, #T-8787) for 20 minutes at room temperature. Samples were then washed 3 times in PBS (5 minutes each), and then blocked for an hour at room temperature with 1.5% serum in PBS (Normal Goat Serum, Invitrogen, # 016201; or Normal Rabbit Serum, Dako, # X0902). After blocking, samples were treated with primary antibody for MEF2C (Sigma Aldrich, # HPA005533), Nkx2.5 (Santa Cruz Biotechnology, Santa Cruz, CA; # SC-8697), GATA-4 (Millipore, Billerica, MA; # P43694), Cav1.2 (Millipore, #Q01815), or sarcomeric α-actinin (Sigma-Aldrich, # A7811) in PBS with 1.5% serum (of secondary antibody host), overnight at $4^{o}$C. After primary antibody incubation, samples were washed 3 times (5 minutes each) before being treated with secondary antibody (Invitrogen Alexa Fluor 488 Rabbit anti-Goat, # A11078; Invitrogen Alexa Fluor 488 Goat anti-

Rabbit, # A11008; or Invitrogen Alexa Fluor 488 Rabbit anti-Mouse, # A11059) in PBS with 1.5% serum (of the secondary antibody host), at room temperature for 1 hour. The samples were then washed 2 times in PBS (5 minutes each) on a rotator, and then counterstained with Hoechst 33342 nuclear dye (Sigma-Aldrich, # H3570) at a concentration of 1:6000 in PBS. The samples were then washed 2 final times in PBS (5 minutes each). Once washes were removed, samples were covered with fresh PBS and stored at 4$^{o}$C until they were imaged.

### 4.2.8. Microscopy and post-processing

Immunostained samples were observed and analyzed using two different inverted, fluorescent microscope systems. The first was a Leica DMIL microscope, fitted with a Leica DFC420C camera, used in conjunction with the Leica Application Suite software (Leica Microsystems Inc., Buffalo Grove, IL). The second was an Olympus IX81 microscope, fitted with an Olympus Q-Color 5 camera, used in conjunction with the Olympus Slidebook software (Olympus America Inc., Center Valley, PA). Images were post-processed for scale and re-sizing, using Image J software (National Institutes of Health, Bethesda, MD).

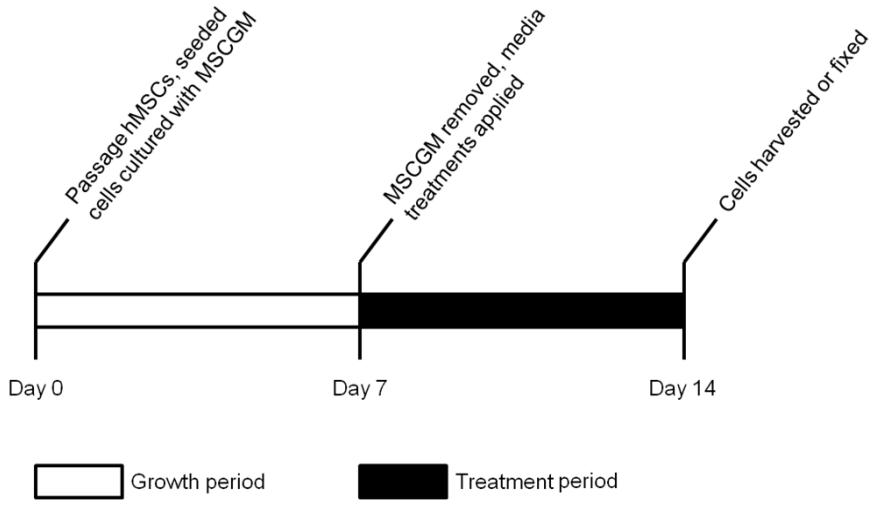


**Figure 4.3. Conditioning timeline.** In our combined conditioning regimen, hMSCs were first cultured for a growth period: cells were seeded at day 0, cultured in their respective oxygen conditions, and fed every other day with MSCGM for 7 days. After the 7-day growth period, hMSCs were then cultured for a treatment period: MSCGM was removed, cells were fed with designated treatment media, and media was changed every 24 hours for another 7 days.

| Gene | Forward primer sequence (5'-3') | Reverse primer sequence (5'-3') | Binding position | Length (bp) | Annealing Temp (°C) | Description |
|---|---|---|---|---|---|---|
| MEF2C | CGC TCT TCA CCT TGG TTC AG | TGG TGG TAC GGT CTC TAG GA | 1421-1611 | 191 | 51 | Myocyte Enhancement Factor 2 C |
| Nkx 2.5 | CTT CTA TCC ACG TGC CTA CAG CGA | CCG GTT CTG GAA CCA GAT CTT GAC | 449-743 | 295 | 60 | Cardiac transcription factor |
| GATA-4 | GCG GCC TCT ACC ACA AGA TG | GTC TGG CAG TTG GCA CAG GA | 1276-1381 | 106 | 56 | Cardiac transcription factor |
| ACTN2 | CAA GCA CAC GAA CTA CAC GAT GGA | GAT GAA GGA TTG GAA GGT GAC GGT | 2334-2649 | 316 | 57 | Sarcomeric α-Actinin |
| MYHCβ | GAT CAT CAA GGC CAA GGC TAA C | GAT CAG TGC CTC CTT CTC ATC C | 3766-3949 | 184 | 56 | Myosin Heavy Chain Beta |
| MYLC2A | ACA GAG TTT ATT GAG GTG CCC C | AAG GTG AAG TGT CCC AGA GG | 563-944 | 381 | 61 | Myosin Light Chain 2A |
| MYLC2V | TAT TGG AAC ATG GCC TCT GGA T | GGT GCT GAA GGC TGA TTA CGT T | 407-788 | 382 | 61 | Myosin Light Chain 2V |
| cTnT | GGC AGC GGA AGA GGA TGC TGA A | GAG GCA CCA AGT TGG GCA TGA ACG A | 147-298 | 150 | 60 | Troponin T, type 2 |
| cTnI | CCC TGC ACC AGC CCC AAT CAG A | CGA AGC CCA GCC CGG TCA ACT | 182-414 | 250 | 60 | Troponin I, type 3 |
| CACNα1C | TCT TTC ACC CCA ATG CCT AC | TGC TGG AAC ATC TGC TAT GC | 864-1241 | 377 | 59 | L-Type $Ca^{2+}$ α1C subunit, cardiac |
| CACNα1D | GCA AGA TGA CGA GCC TGA G | ATG GTT ATG ATG GTT ATG ACA C | 5164-5407 | 244 | 60 | L-Type $Ca^{2+}$ α1D subunit, cardiac |
| CACNα1S | GGT GGA GGC TGC GAT GGA | ATG GCT GTT GCT ATG GTT GCT | 4989-5262 | 274 | 60 | L-Type $Ca^{2+}$ α1S subunit, skeletal |
| GAPDH | ATC ACC ATC TTC CAG GAG CGA | TTC TCC ATG GTG GTG AAG ACG | 322-422 | 101 | 52 | glyceraldehyde-3-phosphate dehydrogenase |

**Table 4.2. Table of primers and conditions for RT-PCR.** This table specifies forward and reverse primers used for semi-quantitative RT-PCR of cardiac transcription factors, sarcomeric proteins, and L-type calcium channel subunits. Primers were either custom designed, or adopted from previous work in the literature: MYLC2A, MYLC2V, cTnT, and cTnI from Kehat *et al.*[50]; CACNα1D and CACNα1S from Heubach *et al.*[58]

## 4.3. Results

### 4.3.1. Effects of reduced-$O_2$/HGF conditioning on cardiac gene expression in hMSCs

To determine if reduced-$O_2$/HGF conditioning of hMSCs *in vitro* can elicit the expression of cardiac-specific genes, we evaluated our treated hMSCs for gene transcripts corresponding with cardiac transcription factors, sarcomere components, and L-type calcium channel subunits. Due to the variables of our conditioning regimen, we ran an initial screen for a short-list of cardiac genes on 6 different combinations of oxygen-level/media treatments (normal-$O_2$/MSCGM, normal-$O_2$/DMEM, normal-$O_2$/HGF, reduced-$O_2$/MSCGM, reduced-$O_2$/DMEM, and reduced-$O_2$/HGF; Table 4.1). Human cardiac cDNA, synthesized from human heart total RNA purchased from Clontech, was used as a positive control. Our initial screen shows that a combined conditioning regimen of reduced-$O_2$ and HGF can increase both the relative amount and breadth of cardiac-specific genes (Figure 4.4). Traditionally cultured hMSCs grown in normal-$O_2$/MSCGM conditions only showed low-level expression of L-type $Ca^{2+}$ channel subunit marker, CaCNA1C. DMEM treatment (alone, without serum) of normal-$O_2$ hMSCs did not express any cardiac genes, including a loss of expression of CaCNA1C. Treating normal-$O_2$ hMSCs with HGF elicited MEF2C expression, and also appeared to increase CaCNA1C signal. Treatment with reduced-$O_2$ and MSCGM appeared to increase MEF2C and CaCNA1C expression, and also showed very low levels of sarcomeric α-Actinin. DMEM treatment of reduced-$O_2$ hMSCs maintained MEF2C and low-level α-Actinin expression, but decreased CaCNA1C. Reduced-$O_2$/HGF conditioning showed an increase in MEF2C, α-Actinin, and CaCNA1C expression, while also eliciting expression for Nkx2.5 and GATA-4 cardiac transcription factors. Results indicate that HGF can elicit cardiac-specific genes in both normal-$O_2$ and reduced-$O_2$ conditions, but HGF treatment in reduced-$O_2$ appears to increase the magnitude and degree of cardiac gene expression. Results also indicate that reduced-$O_2$ conditions, either with or without growth media, can also elicit increases in cardiac gene expression for MEF2C, α-Actinin, and CaCNA1 (but not Nkx2.5 or GATA-4).

Further cardiac gene characterization was compared between reduced-$O_2$/HGF conditioned hMSCs and traditionally cultured hMSCs grown in normal-$O_2$/MSCGM. Again, human cardiac cDNA was

included in our analysis for a positive control. Reduced-$O_2$/HGF conditioned hMSCs showed positive expression for myosin heavy chain beta (MHCβ), myosin light chain 2A (MYLC2A), cardiac troponin T (cTnT), cardiac troponin I (cTnI), and L-type $Ca^{2+}$ channel subunit marker CaCNA1D (Figure 4.5). Normal-$O_2$/MSCGM hMSCs did not express any of the expanded cardiac-specific genes. Reduced-$O_2$/HGF conditioned hMSCs showed cardiac gene expression that was qualitatively much lower than the human cardiac positive control. Results also indicate that reduced-$O_2$/HGF conditioned hMSCs do not express CaCNA1S, a marker for L-type $Ca^{2+}$ channel subunit protein Cav1.1. The Cav1.1 subunit is highly associated with and expressed in skeletal muscle, with minor signals detected in other tissues such as heart, lung, brain, and kidney.[59] Our results would agree with this analysis, in that CaCNA1S is only slightly expressed in human cardiac muscle. In addition, the lack of CaCNA1S expression in the reduced-$O_2$/HGF conditioned hMSCs suggests that either there is not enough CaCNA1S transcript to be detected, or they are expressing a more definitive cardiac phenotype.

### 4.3.2. Effects of reduced-$O_2$/HGF conditioning on cardiac protein expression in hMSCs

To complement our cardiac gene analysis, we used immunocytochemistry (ICC) to detect cardiac protein expression and localization. Results indicate that reduced-$O_2$/HGF conditioned hMSCs can elicit cardiac-specific protein expression for MEF2C, Nkx2.5, GATA-4, sarcomeric α-Actinin, and the L-type $Ca^{2+}$ channel subunit Cav1.2 (Figure 4.6). Observational analysis shows that expression for MEF2C, Nkx2.5, and GATA-4 transcription factors localize to the nucleus, sarcomeric α-Actinin appears to localize in the cytoplasm, and Cav1.2 appears to localize throughout the cell membrane. This data suggests that some of the detected cardiac genes are being translated into cardiac-specific proteins, and that the cardiac proteins appear to be localizing to appropriate cellular regions based on their known functions.

ICC for Nkx2.5, GATA-4, sarcomeric α-Actinin, and Cav1.2 was also done on traditionally cultured hMSCs grown in normal-$O_2$/MSCGM (Figure 4.7). Results indicate that untreated, normal-$O_2$/MSCGM hMSCs do not show protein expression for Nkx2.5, GATA-4, or sarcomeric α-Actinin. Some of the

untreated, normal-$O_2$/MSCGM hMSCs do express low-levels of Cav1.2, appearing to localize on the cell membrane.

### 4.3.3. Applying small-molecule inhibitors to evaluate the effects of HGF/c-Met signaling on cardiac gene expression

To assess the role of HGF/c-Met signaling in the activation of downstream cardiac gene transcription in hMSCs, we tested the effects of two small-molecule inhibitors on our reduced-$O_2$/HGF conditioned hMSCs. Both small-molecule inhibitors were tested independently, and were chosen based on their targeted effector proteins involved in our proposed HGF/c-Met signaling pathway (Figure 4.8). As described in the methods, inhibitors were applied during the media-treatment phase of the conditioning regimen. Either 5 μM of PHA665752 or 50 μM of LY294002 were applied to cells for 2 hours before supplementing the inhibitor media with 20 ng/mL HGF. Inhibitors were applied in this fashion every 24 hours, for the duration of the 7 day media-treatment phase, to compare against reduced-$O_2$/HGF hMSCs that were also treated for 7 days.

Our results show that both PHA665752 and LY294002 were ineffective in decreasing MEF2C gene expression (Figure 4.9). However, both inhibitors were independently effective in decreasing gene expression for Nkx2.5, sarcomeric α-Actinin, MHCβ, cTnT, and cTnI. Reduced-$O_2$/HGF conditioned cells treated with 5 μM PHA665752 appeared to express low-levels of sarcomeric α-Actinin, cTnT, and cTnI. This data may correlate with preliminary ELISA studies, showing that 5 μM PHA665752 could significantly decrease, but not completely mitigate, c-Met phosphorylation in reduced-$O_2$ hMSCs (Figure 4.10); indicating that PHA665752 can decrease c-Met phosphorylation to attenuate expression of cardiac genes. In addition, treatment with 50 μM LY294002 attenuated the expression of cardiac genes in reduced-$O_2$/HGF conditioned hMSCs.

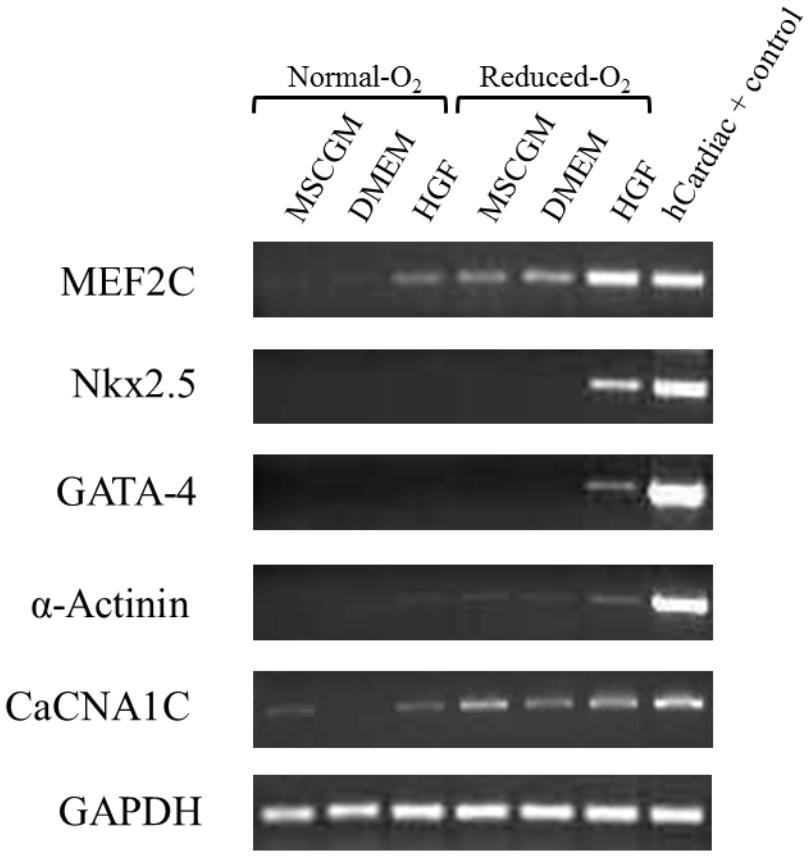


**Figure 4.4. Effects of different conditioning regimens on cardiac gene transcription.** In a preliminary screen, all six oxygen/media treatment combinations were compared for gene expression of cardiac transcription factors (MEF2C, Nkx2.5, and GATA-4), sarcomeric protein (α-Actinin), and an L-type calcium channel marker (CaCNA1C). HGF treatment in both $O_2$ conditions increased MEF2C, CaCNA1C. Reduced-$O_2$ conditioning with MSCGM or DMEM also increased MEF2C and CaCNA1C, and elicited low-level α-Actinin expression. Reduced-$O_2$/HGF conditioning appeared to increase MEF2C, α-Actinin, and CaCNA1C signal, as well as elicit gene expression of both Nkx2.5 and GATA-4.

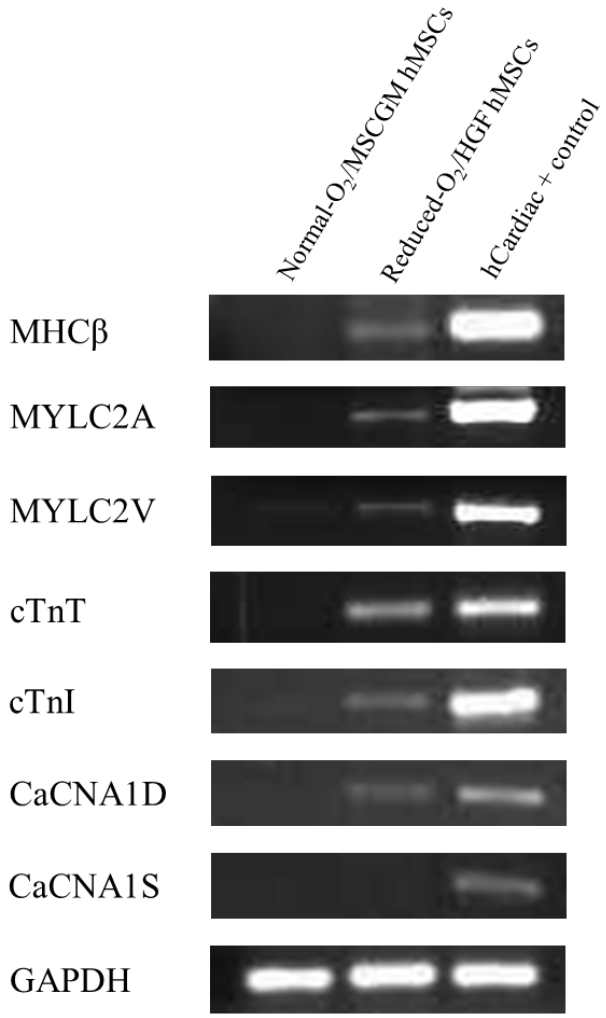


**Figure 4.5. Effects of reduced-O2/HGF conditioning on expression of an expanded set of cardiac genes.** In a secondary screen for cardiac gene expression, we compared traditionally cultured normal-$O_2$/MSCGM hMSCs versus reduced-$O_2$/HGF conditioned hMSCs. Reduced-$O_2$/HGF conditioned hMSCs showed low-level expression for MHCβ, MYLC2A, MYLC2V, cTnT, cTnI, and CaCNA1D, but no expression of CaCNA1S. Normal-$O_2$/MSCGM hMSCs did not show expression for any of the cardiac genes in the second screen.

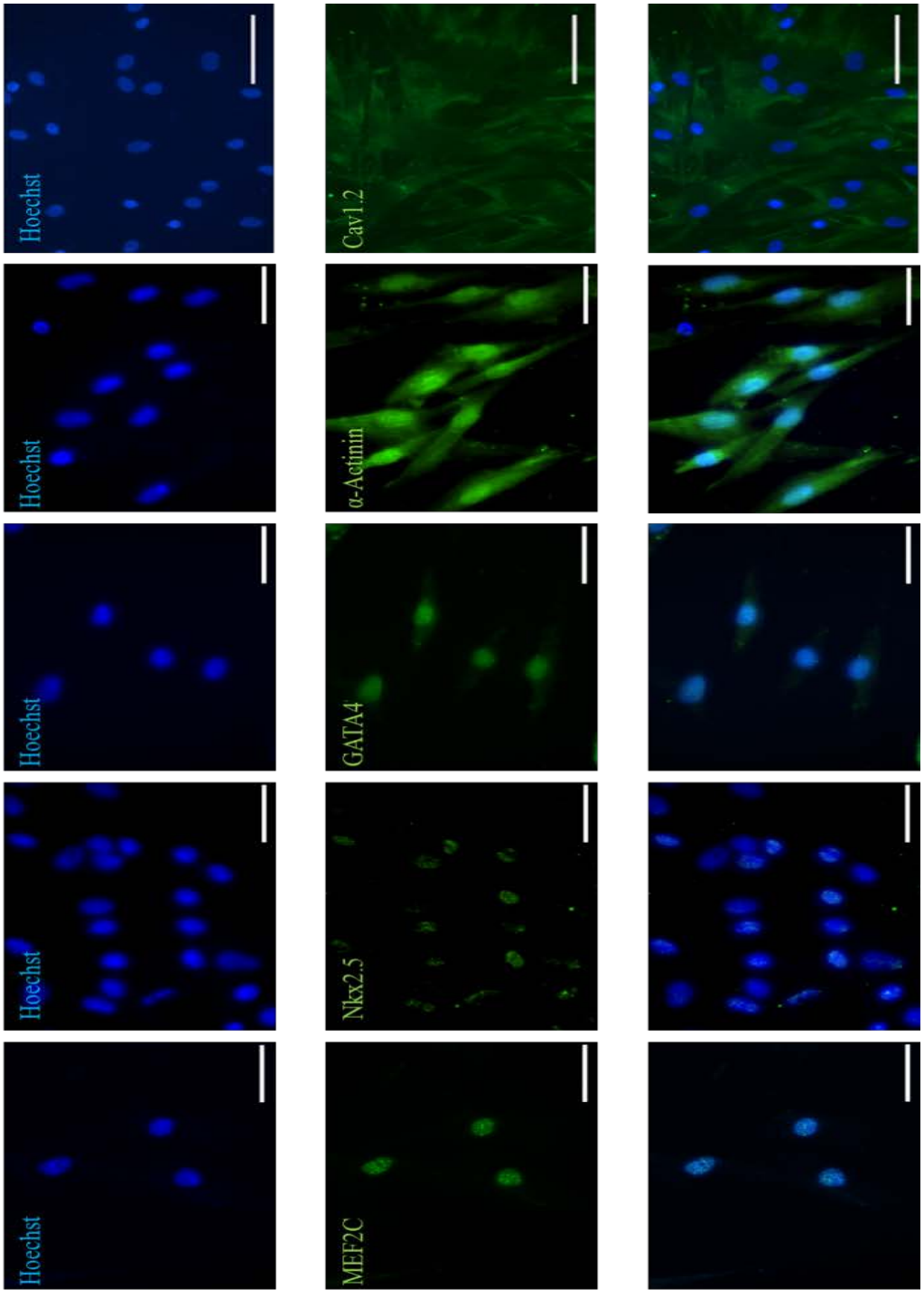


**Figure 4.6. Cardiac-marker protein expression in reduced-O2/HGF conditioned hMSCs.** Cardiac protein detection by immunocytochemistry showed that reduced-$O_2$/HGF conditioned hMSCs express MEF2C, Nkx2.5, GATA-4 cardiac transcription factors localized to cell nuclei, sarcomeric α-Actinin in the cytoplasm, and L-type calcium channel subunit Cav1.2 on the cell membrane. Scale bars = 50 μm.

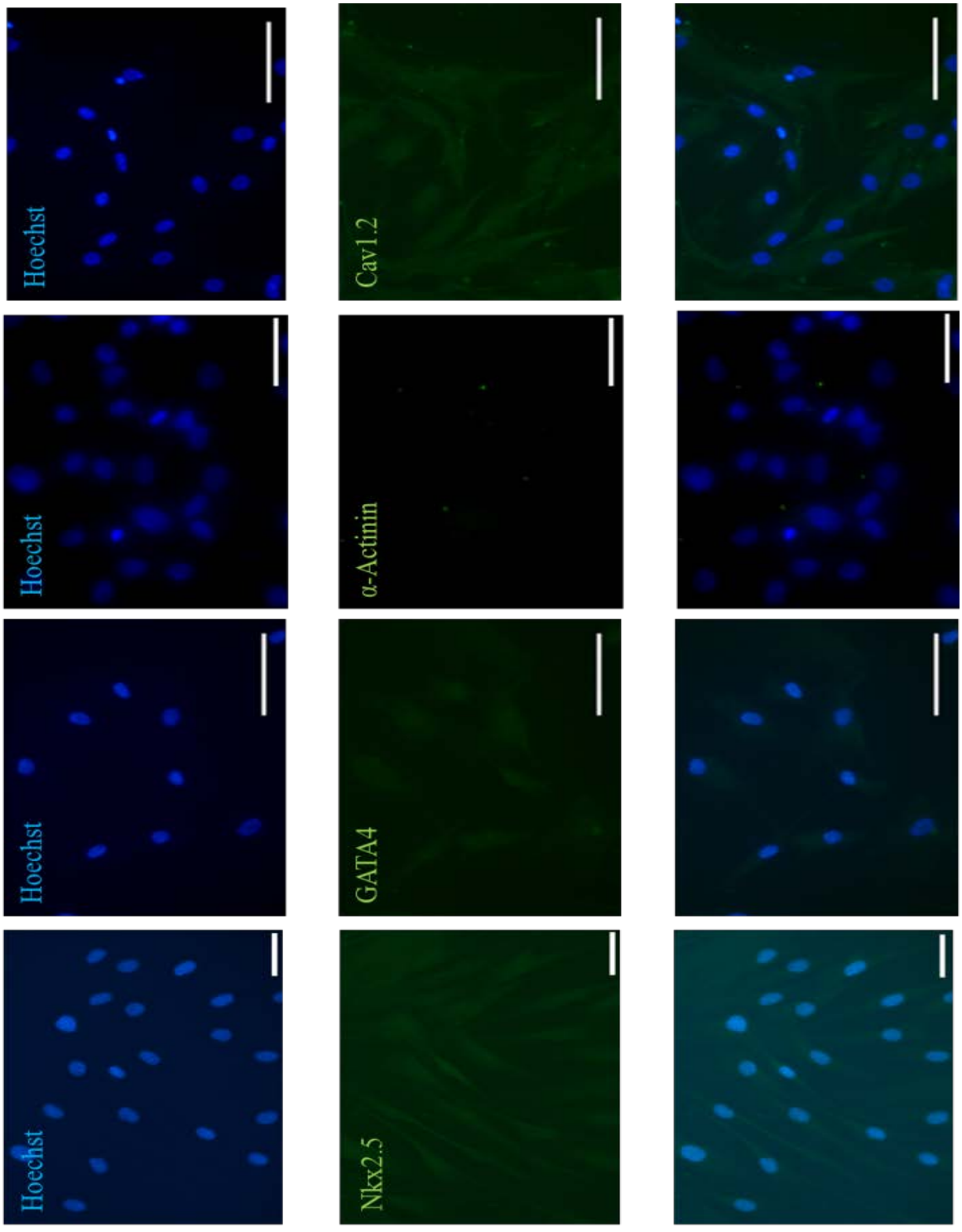


**Figure 4.7. Cardiac-marker protein expression in normal-$O_2$/MSCGM conditioned hMSCs.** Cardiac protein detection by immunocytochemistry showed that hMSCs grown in normal-$O_2$/MSCGM conditions did not express Nkx2.5, GATA-4, or sarcomeric α-Actinin. They did show low-level expression L-type calcium channel subunit Cav1.2. MEF2C was not tested. Scale bars = 50 μm.

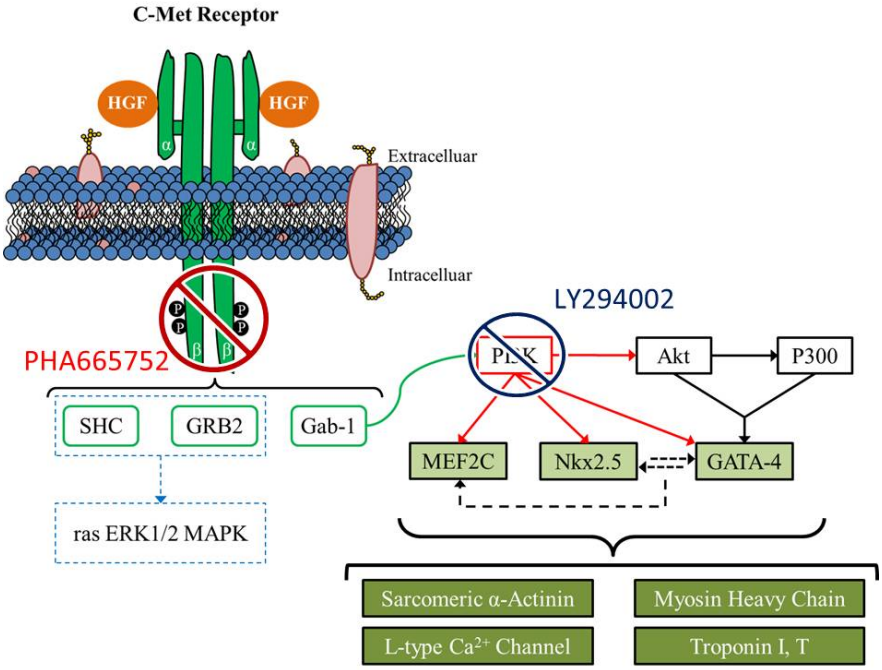


**Figure 4.8. Small-molecule inhibition of proposed HGF/c-Met cardiac signaling pathway.** Two small-molecule inhibitors were tested independently to evaluate the involvement of HGF/c-Met signaling in cardiac differentiation of hMSCs. PHA665752 inhibits c-Met phosphorylation, and LY294002 competitively inhibits ATP binding of PI3K.

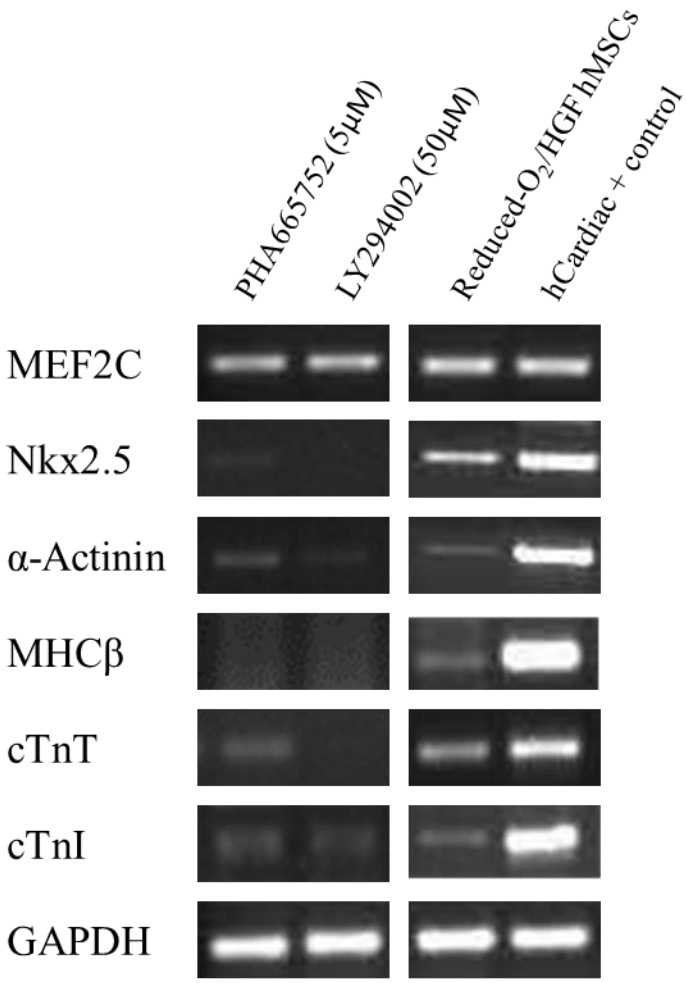


**Figure 4.9. Small-molecule inhibitor analysis on cardiac gene expression.** Reduced-$O_2$/HGF conditioned hMSCs treated with 5 μM PHA665752 retained MEF2C expression, but showed a loss of expression for Nkx2.5 and MHCβ, and lowered expression for α-Actinin, cTnT, and cTnI. Reduced-$O_2$/HGF conditioned hMSCs treated with 50 μM LY294002 also retained MEF2C expression, but showed a loss of all other cardiac genes.

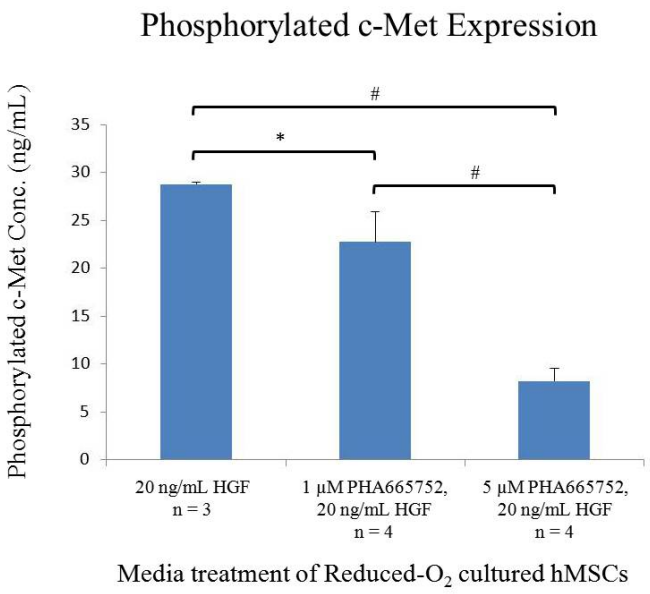


**Figure 4.10. Preliminary data showing effects of PHA665752 on c-Met phosphorylation.** Prior to small-molecule inhibitor analysis on gene expression, we ran a preliminary study to evaluate the effects of two different concentrations of PHA665752 on phosphorylated c-Met expression in hMSCs. Both 1 µM and 5 µM concentrations of PHA665752 showed to significantly decrease c-Met phosphorylation, however the 5 µM concentration showed a more drastic decrease. The 5 µM concentration treatment still indicates a low concentration of phosphorylated c-Met. Since the 5 µM concentration was used in our small-molecule inhibitor analysis on gene expression, it may be possible that the lowered c-Met phosphorylation can elicit low-level cardiac gene expression. Differences were evaluated using a Student's unpaired t-test at each passage, and were considered significant for p-values $\leq 0.05$. Error bars indicate standard error.

## 4.4. Discussion

Current methods for differentiating hMSCs towards a cardiac lineage have significant limitations. Techniques for mechanical or chemical induction are complex and tedious, signaling mechanisms remain undefined, and only a small percentage of hMSCs have been shown to express a limited number of cardiac-specific markers. To improve upon these limitations, we developed a simplistic regimen combining reduced-$O_2$ conditioning with HGF treatment. The conditions for this regimen were based on MI environmental cues for low-oxygen tension and increased HGF release;[60,61] as well as the previous studies showing that reduced-$O_2$ conditioning could increase signaling and survival factors in hMSCs,[48,62,63] and the studies showing that HGF is involved in cardiomyogenesis.[16,45,47] In Chapter 3, we showed that culturing hMSCs in reduced-$O_2$ for 7 days could significantly increase the expression for the c-Met receptor. In our conditioning regimen, we incorporate a growth-phase for the increase of c-Met, and then a media-treatment phase for the addition of HGF (in serum-free medium). In this chapter, we sought to investigate the effects of reduced-$O_2$/HGF conditioning on cardiac-marker expression of hMSCs *in vitro*.

While it has been reported that HGF is not required for heart development,[45] knockout mice for HGF and the c-Met receptor are lethal during the second half of the gestation period (E12-E18) due to complications with placental formation and liver development.[42,64,65] Although the details of heart development defects are not fully understood in HGF/c-Met knockout mice, these deficiencies reportedly contribute to cardiac arrhythmias.[64] Although HGF and the c-Met receptor may not be required for heart development, it is speculated that HGF/c-Met may aid in the autoregulation and maintenance of early myocardial cells, as well as provide autocrine/paracrine signaling factors that support cardiac development.[45] This analysis compliments the previously discussed stem cell studies, in which HGF/c-Met signaling has also shown to improve cardiac differentiation in human ESCs and induce cardiac specific marker expression in mouse MSCs.[16,47] HGF/c-Met signaling may play a critical role in early cardiomyogenesis by providing necessary paracrine factors that support and drive the cardiac differentiation program. While the specific role of HGF/c-Met signaling in cardiac development and

differentiation is not completely understood, it is possible that the absence of HGF or c-Met could compromise early cardiac gene transcription. This would be largely detrimental, as previous studies report knockout mice that are deficient for early cardiac genes required for heart development (e.g. Nkx2.5) become lethal by gestation days E9-E11.[66,67]

Our results showed that a combined conditioning regimen of reduced-$O_2$/HGF could elicit the expression of several cardiac genes and proteins in hMSCs. In our combined regimen, we examined the effects of treating cells with 20 ng/mL HGF; a concentration we chose based on what was previously reported in the literature on mouse MSCs.[16] However, it is possible that 20 ng/mL may not be the optimum concentration for eliciting cardiac specific markers in hMSCs. Future titration studies would be useful to determine if higher or lower concentrations of HGF could elicit more expression of cardiac markers, or possibly further differentiate hMSCs towards a more mature cardiac phenotype. In addition, we only looked at reduced-$O_2$/HGF conditioned cells that were treated for 7 days. This is to say that we did not evaluate conditioned cells for shorter or longer durations. Therefore, it is possible that some of the effects we see in cardiac gene and protein expression could be due to timing between the different $O_2$ groups. By looking at different time points in both $O_2$ conditions, it may be possible that normal-$O_2$ cultured cells can elicit similar cardiac gene expression. Analysis at different time points may also provide more information as to a timeline of cardiac gene transcription, and whether longer conditioning durations can further differentiate cells into mature cardiac phenotypes.

In further consideration of our reduced-$O_2$/HGF conditioning regimen, we chose to condition hMSCs for long durations in the reduced-$O_2$ environment; with thawed cells being maintained in reduced-$O_2$ throughout their growth, and then an additional 2 weeks in reduced-$O_2$ during the conditioning treatment. Our rationale for choosing longer-term reduced-$O_2$ exposure was to pre-condition cells for implantation into the oxygen-poor infarct environment. However, in our analysis of cardiac gene and protein expression, we did not analyze the effects of short term reduced-$O_2$ conditioning. It is possible that short term reduced-$O_2$ durations could provide a necessary signaling cascade for cardiac differentiation; and then transitioning cells from reduced-$O_2$ back to normal-$O_2$ would prevent increased growth/proliferation

(as observed in our growth kinetics study, Chapter 2). In consideration of cellular processes, it may be necessary attenuate the proliferation effects observed in reduced-$O_2$ conditioning to allow for further cardiac differentiation. However, it may also be possible that longer-term reduced-$O_2$ exposure can provide a supporting signaling cascade necessary to elicit cardiac specific markers.

Comparatively, our combined reduced-$O_2$/HGF conditioning regimen of hMSCs showed an increased breadth of cardiac-specific marker expression than we previously achieved in our hanging-drop differentiation method (e.g. Nkx2.5, Gata-4, and MEF2C gene and protein expression). In further consideration of the hanging drop method, it may be possible that spheroid formation is also causing a reduced-$O_2$ microenvironment in which cells are secreting/receiving signaling factors. It may even be possible that spheroid formation is creating a reduced-$O_2$/HGF microenvironment that helps to elicit cardiac makers in hMSCs, which drives some of the spheroid cells towards a cardiogenic lineage.[13]

In a qualitative assessment by immunocytochemistry, it appeared that many of the reduced-$O_2$/HGF conditioned cells could express cardiac specific proteins (e.g. MEF2C, Nkx2.5, and α-Actinin). This would suggest that increases in cardiac gene expression are most likely due to more hMSCs becoming cardiogenic, rather than stronger cardiac gene expression in a small sub-population of cardiogenic cells in a mixed batch of hMSCs. From our qualitative ICC assessment, it also appears that a greater number of hMSCs from our reduced-$O_2$/HGF conditioning method can express cardiac specific proteins, as compared with our previously described "hanging drop" method. However, we did not take cell counts to determine the number cardiogenic cells in this study, and a comparative quantitative analysis would be needed to determine if reduced-$O_2$/HGF conditioning was more efficient for producing cardiogenic cells than spheroid formation.

Using small-molecule inhibitors to target specific control points in our proposed HGF/c-Met pathway, we showed that decreases in c-Met or PI3K activation could attenuate cardiac gene expression. These results would suggest that the HGF/c-Met pathway and the PI3K effector protein are instrumental in initiating the cardiac-program in marrow-derived hMSCs. The c-Met inhibitor (5 μM PHA665752) was effective for decreasing most of the cardiac genes we screened, with low expression of α-Actinin, cTnT,

and cTnI. The PI3K inhibitor (50 μM LY294002) was effective for attenuating most of the cardiac genes we screened, as well. However, neither inhibitor could effectively decrease the expression of MEF2C. These results would suggest other signaling mechanisms besides HGF/c-Met and PI3K are involved in MEF2C gene transcription. In our analysis, inhibitor concentrations were chosen based on concentrations previously reported in the literature. In preliminary studies, we tried to analyze the inhibitor concentrations to determine if the inhibitors could mitigate the phosphorylation of effector molecules. In our analysis of PHA665752, we found that both 1 μM and 5 μM concentrations of inhibitor could significantly decrease c-Met phosphorylation. However, 1 μM still showed a high level of c-Met phosphorylation which could potentially allow for downstream signaling. The 5 μM concentration showed a more drastic decrease, but could not completely inhibit c-Met phosphorylation. This may account for why we still see slight expression of α-Actinin, cTnT, and cTnI in the PHA665752 treated cells. Complications due to biochemical processing prevented us from completing an analysis on the effects that the PI3K inhibitor (50 μM LY294002) had on decreasing phosphorylation of Akt. Therefore, it is unclear whether the 50 μM concentration was effective for mitigating PI3K and its downstream signaling events. However, we did observe that 50 μM LY294002 could attenuate the expression of cardiac genes. Further titration experiments are needed to determine if different/increased doses of these inhibitors can decrease the phosphorylation of effector molecules, decrease MEF2C gene expression, and completely abate cardiac gene expression.

## 4.5. References


1 Jiang, Y. *et al.* Pluripotency of mesenchymal stem cells derived from adult marrow. *Nature* **418**, 41-49, (2002).

2 Lagasse, E. *et al.* Purified hematopoietic stem cells can differentiate into hepatocytes in vivo. *Nat Med* **6**, 1229-1234, (2000).

3 Wang, X. *et al.* Kinetics of liver repopulation after bone marrow transplantation. *The American journal of pathology* **161**, 565-574, (2002).

4 Brazelton, T. R., Rossi, F. M., Keshet, G. I. & Blau, H. M. From marrow to brain: expression of neuronal phenotypes in adult mice. *Science (New York, N.Y* **290**, 1775-1779, (2000).

5 Weimann, J. M., Charlton, C. A., Brazelton, T. R., Hackman, R. C. & Blau, H. M. Contribution of transplanted bone marrow cells to Purkinje neurons in human adult brains. *Proc Natl Acad Sci U S A* **100**, 2088-2093, (2003).

6 Orlic, D. *et al.* Bone marrow cells regenerate infarcted myocardium. *Nature* **410**, 701-705, (2001).

7 Balsam, L. B. *et al.* Haematopoietic stem cells adopt mature haematopoietic fates in ischaemic myocardium. *Nature* **428**, 668-673, (2004).

8 Murry, C. E. *et al.* Haematopoietic stem cells do not transdifferentiate into cardiac myocytes in myocardial infarcts. *Nature* **428**, 664-668, (2004).

9 Lagostena, L. *et al.* Electrophysiological properties of mouse bone marrow c-kit+ cells co-cultured onto neonatal cardiac myocytes. *Cardiovasc Res* **66**, 482-492, (2005).

10 Beeres, S. L. *et al.* Human adult bone marrow mesenchymal stem cells repair experimental conduction block in rat cardiomyocyte cultures. *J Am Coll Cardiol* **46**, 1943-1952, (2005).

11 Makino, S. *et al.* Cardiomyocytes can be generated from marrow stromal cells in vitro. *J Clin Invest* **103**, 697-705, (1999).

12 Xu, M. *et al.* Differentiation of bone marrow stromal cells into the cardiac phenotype requires intercellular communication with myocytes. *Circulation* **110**, 2658-2665, (2004).

13 Potapova, I. A. *et al.* Enhanced recovery of mechanical function in the canine heart by seeding an extracellular matrix patch with mesenchymal stem cells committed to a cardiac lineage. *Am J Physiol Heart Circ Physiol* **295**, H2257-2263, (2008).

14 Koninckx, R. *et al.* Human bone marrow stem cells co-cultured with neonatal rat cardiomyocytes display limited cardiomyogenic plasticity. *Cytotherapy*, 1-15, (2009).

15 Poh, K. K. *et al.* Repeated direct endomyocardial transplantation of allogeneic mesenchymal stem cells: safety of a high dose, "off-the-shelf", cellular cardiomyoplasty strategy. *Int J Cardiol* **117**, 360-364, (2007).

16 Forte, G. *et al.* Hepatocyte growth factor effects on mesenchymal stem cells: proliferation, migration, and differentiation. *Stem Cells* **24**, 23-33, (2006).

17 Xaymardan, M. *et al.* Platelet-derived growth factor-AB promotes the generation of adult bone marrow-derived cardiac myocytes. *Circ Res* **94**, E39-45, (2004).

18 Amado, L. C. *et al.* Cardiac repair with intramyocardial injection of allogeneic mesenchymal stem cells after myocardial infarction. *Proc Natl Acad Sci U S A* **102**, 11474-11479, (2005).

19 Yoon, Y. S. *et al.* Clonally expanded novel multipotent stem cells from human bone marrow regenerate myocardium after myocardial infarction. *J Clin Invest* **115**, 326-338, (2005).

20 Toma, C., Pittenger, M. F., Cahill, K. S., Byrne, B. J. & Kessler, P. D. Human mesenchymal stem cells differentiate to a cardiomyocyte phenotype in the adult murine heart. *Circulation* **105**, 93-98, (2002).

21 Potapova, I. A. *et al.* Replacing damaged myocardium. *J Electrocardiol* **40**, S199-201, (2007).

22 Assmus, B. *et al.* Transplantation of Progenitor Cells and Regeneration Enhancement in Acute Myocardial Infarction (TOPCARE-AMI). *Circulation* **106**, 3009-3017, (2002).

23 Janssens, S. *et al.* Autologous bone marrow-derived stem-cell transfer in patients with ST-segment elevation myocardial infarction: double-blind, randomised controlled trial. *Lancet* **367**, 113-121, (2006).

24 Lunde, K. *et al.* Intracoronary injection of mononuclear bone marrow cells in acute myocardial infarction. *N Engl J Med* **355**, 1199-1209, (2006).

25 Schachinger, V. *et al.* Improved clinical outcome after intracoronary administration of bone-marrow-derived progenitor cells in acute myocardial infarction: final 1-year results of the REPAIR-AMI trial. *European heart journal* **27**, 2775-2783, (2006).

26 Pittenger, M. F., Mosca, J. D. & McIntosh, K. R. Human mesenchymal stem cells: progenitor cells for cartilage, bone, fat and stroma. *Curr Top Microbiol Immunol* **251**, 3-11, (2000).

27 Potapova, I. *et al.* Functional Regeneration of the Canine Ventricle Using Adult Human Mesenchymal Stem Cells Committed In Vitro to a Cardiac Lineage. *Circ Res* **99**, E19, (2006).
28 Behfar, A. *et al.* Guided cardiopoiesis enhances therapeutic benefit of bone marrow human mesenchymal stem cells in chronic myocardial infarction. *J Am Coll Cardiol* **56**, 721-734, (2010).
29 Ye, N. S. *et al.* Proteomic profiling of rat bone marrow mesenchymal stem cells induced by 5-azacytidine. *Stem cells and development* **15**, 665-676, (2006).
30 Marban, E. & Malliaras, K. Boot camp for mesenchymal stem cells. *J Am Coll Cardiol* **56**, 735-737, (2010).
31 Lennon, D. P., Edmison, J. M. & Caplan, A. I. Cultivation of rat marrow-derived mesenchymal stem cells in reduced oxygen tension: effects on in vitro and in vivo osteochondrogenesis. *J Cell Physiol* **187**, 345-355, (2001).
32 Lee, J. H. & Kemp, D. M. Human adipose-derived stem cells display myogenic potential and perturbed function in hypoxic conditions. *Biochem Biophys Res Commun* **341**, 882-888, (2006).
33 Kanichai, M., Ferguson, D., Prendergast, P. J. & Campbell, V. A. Hypoxia promotes chondrogenesis in rat mesenchymal stem cells: a role for AKT and hypoxia-inducible factor (HIF)-1alpha. *J Cell Physiol* **216**, 708-715, (2008).
34 Bottaro, D. P. *et al.* Identification of the hepatocyte growth factor receptor as the c-met proto-oncogene product. *Science (New York, N.Y* **251**, 802-804, (1991).
35 Cooper, C. S. *et al.* Molecular cloning of a new transforming gene from a chemically transformed human cell line. *Nature* **311**, 29-33, (1984).
36 Neuss, S., Becher, E., Woltje, M., Tietze, L. & Jahnen-Dechent, W. Functional expression of HGF and HGF receptor/c-met in adult human mesenchymal stem cells suggests a role in cell mobilization, tissue repair, and wound healing. *Stem Cells* **22**, 405-414, (2004).
37 Santos, O. F. *et al.* Involvement of hepatocyte growth factor in kidney development. *Developmental biology* **163**, 525-529, (1994).
38 Bussolino, F. *et al.* Hepatocyte growth factor is a potent angiogenic factor which stimulates endothelial cell motility and growth. *The Journal of cell biology* **119**, 629-641, (1992).
39 Yang, Y. *et al.* Sequential requirement of hepatocyte growth factor and neuregulin in the morphogenesis and differentiation of the mammary gland. *The Journal of cell biology* **131**, 215-226, (1995).
40 Birchmeier, C., Birchmeier, W., Gherardi, E. & Vande Woude, G. F. Met, metastasis, motility and more. *Nat Rev Mol Cell Biol* **4**, 915-925, (2003).
41 Ebens, A. *et al.* Hepatocyte growth factor/scatter factor is an axonal chemoattractant and a neurotrophic factor for spinal motor neurons. *Neuron* **17**, 1157-1172, (1996).
42 Bladt, F., Riethmacher, D., Isenmann, S., Aguzzi, A. & Birchmeier, C. Essential role for the c-met receptor in the migration of myogenic precursor cells into the limb bud. *Nature* **376**, 768-771, (1995).
43 Matsumoto, K. & Nakamura, T. Hepatocyte growth factor: renotropic role and potential therapeutics for renal diseases. *Kidney Int* **59**, 2023-2038, (2001).
44 Michalopoulos, G. K. & DeFrances, M. C. Liver regeneration. *Science (New York, N.Y* **276**, 60-66, (1997).
45 Rappolee, D. A., Iyer, A. & Patel, Y. Hepatocyte growth factor and its receptor are expressed in cardiac myocytes during early cardiogenesis. *Circulation research* **78**, 1028-1036, (1996).
46 Duan, H. F. *et al.* Treatment of myocardial ischemia with bone marrow-derived mesenchymal stem cells overexpressing hepatocyte growth factor. *Molecular therapy : the journal of the American Society of Gene Therapy* **8**, 467-474, (2003).
47 Roggia, C., Ukena, C., Bohm, M. & Kilter, H. Hepatocyte growth factor (HGF) enhances cardiac commitment of differentiating embryonic stem cells by activating PI3 kinase. *Exp Cell Res* **313**, 921-930, (2007).
48 Rosova, I., Dao, M., Capoccia, B., Link, D. & Nolta, J. A. Hypoxic Preconditioning Results in Increased Motility and Improved Therapeutic Potential of Human Mesenchymal Stem Cells. *Stem Cells*, (2008).
49 Xu, C., Police, S., Rao, N. & Carpenter, M. K. Characterization and enrichment of cardiomyocytes derived from human embryonic stem cells. *Circ Res* **91**, 501-508, (2002).
50 Kehat, I. *et al.* Human embryonic stem cells can differentiate into myocytes with structural and functional properties of cardiomyocytes. *J Clin Invest* **108**, 407-414, (2001).
51 He, J. Q., Ma, Y., Lee, Y., Thomson, J. A. & Kamp, T. J. Human embryonic stem cells develop into multiple types of cardiac myocytes: action potential characterization. *Circ Res* **93**, 32-39, (2003).

52 Smolen, G. A. *et al.* Amplification of MET may identify a subset of cancers with extreme sensitivity to the selective tyrosine kinase inhibitor PHA-665752. *Proceedings of the National Academy of Sciences of the United States of America* **103**, 2316-2321, (2006).
53 Christensen, J. G. *et al.* A selective small molecule inhibitor of c-Met kinase inhibits c-Met-dependent phenotypes in vitro and exhibits cytoreductive antitumor activity in vivo. *Cancer research* **63**, 7345-7355, (2003).
54 Vlahos, C. J., Matter, W. F., Hui, K. Y. & Brown, R. F. A specific inhibitor of phosphatidylinositol 3-kinase, 2-(4-morpholinyl)-8-phenyl-4H-1-benzopyran-4-one (LY294002). *The Journal of biological chemistry* **269**, 5241-5248, (1994).
55 Shoba, L. N., Newman, M., Liu, W. & Lowe, W. L., Jr. LY 294002, an inhibitor of phosphatidylinositol 3-kinase, inhibits GH-mediated expression of the IGF-I gene in rat hepatocytes. *Endocrinology* **142**, 3980-3986, (2001).
56 Liu, H. *et al.* Hypoxic preconditioning advances CXCR4 and CXCR7 expression by activating HIF-1alpha in MSCs. *Biochemical and biophysical research communications* **401**, 509-515, (2010).
57 Rosen, A. B. *et al.* Finding fluorescent needles in the cardiac haystack: tracking human mesenchymal stem cells labeled with quantum dots for quantitative in vivo three-dimensional fluorescence analysis. *Stem Cells* **25**, 2128-2138, (2007).
58 Heubach, J. F. *et al.* Electrophysiological properties of human mesenchymal stem cells. *J Physiol* **554**, 659-672, (2004).
59 James Kew, C. D. 568 (Oxford University Press Inc., USA, New York, 2010).
60 Chacko, S. M. *et al.* Myocardial oxygenation and functional recovery in infarct rat hearts transplanted with mesenchymal stem cells. *Am J Physiol Heart Circ Physiol* **296**, H1263-1273, (2009).
61 Sato, T. *et al.* Sequential changes of hepatocyte growth factor in the serum and enhanced c-Met expression in the myocardium in acute myocardial infarction. *Jpn Circ J* **63**, 906-908, (1999).
62 Gnecchi, M. *et al.* Evidence supporting paracrine hypothesis for Akt-modified mesenchymal stem cell-mediated cardiac protection and functional improvement. *Faseb J* **20**, 661-669, (2006).
63 Chacko, S. M. *et al.* Hypoxic preconditioning induces the expression of prosurvival and proangiogenic markers in mesenchymal stem cells. *Am J Physiol Cell Physiol* **299**, C1562-1570, (2010).
64 Schmidt, C. *et al.* Scatter factor/hepatocyte growth factor is essential for liver development. *Nature* **373**, 699-702, (1995).
65 Uehara, Y. *et al.* Placental defect and embryonic lethality in mice lacking hepatocyte growth factor/scatter factor. *Nature* **373**, 702-705, (1995).
66 Copp, A. J. Death before birth: clues from gene knockouts and mutations. *Trends in genetics : TIG* **11**, 87-93, (1995).
67 Lyons, I. *et al.* Myogenic and morphogenetic defects in the heart tubes of murine embryos lacking the homeo box gene Nkx2-5. *Genes Dev* **9**, 1654-1666, (1995).

## CHAPTER 5: Evaluate regional cardiac function of cell-treated Myocardial Infarcts

### 5.1. Introduction

Although we have investigated the effects of reduced-$O_2$/HGF conditioning on cardiac-specific marker expression of hMSCs *in vitro*, we were also interested in delivering reduced-$O_2$/HGF conditioned hMSCs to acute MIs *in vivo* to assess the potential effects on cardiac function. Current cell therapy strategies for cardiac regeneration aim to overcome the chief limitation of current MI treatments by replacing necrotic cardiomyocytes with viable cells that can restore cardiac mechanical function. Several different cell types (e.g. skeletal myoblasts,[1,2] embryonic stem cells,[3] bone marrow cells,[4,5] mesenchymal stem cells,[6-8] etc.) have been delivered to diseased hearts in clinical and pre-clinical studies to show improvement in cardiac mechanical function. While there have been some initial studies to correlate the engraftment of varying numbers of implanted cells,[9] conclusive evidence of a correlation between the number of regenerated striated cardiomyocytes and improvements in regional mechanical function has not been established. This leads to a fundamental question of whether the delivered cells can increase active function by adding contractile elements, or improving electrical communication between native cardiomyocytes, or they simply improve passive function by increasing the compliance within the region of the developed scar.[10,11] Using techniques to study regional mechanical cardiac function, however, it is possible to study defined regions of interest within the heart. And by using a high spatial-resolution imaging technique called high density mapping (HDM), it is possible to determine area deformation within small infarct regions with a high degree of accuracy, precision, and repeatability.[12,13] By correlating measured changes in heart-surface deformation with measured intracavitary pressure over the course of a heartbeat, we used HDM to calculate regional stroke work and systolic area contraction as indicators of active function in MIs treated with reduced-$O_2$/HGF conditioned hMSCs.

As previously described, bone marrow derived MSCs are a sub-population of BMCs that have been studied as a cell therapy in several *in vivo* applications. In addition to their multipotent ability to differentiate into different cell types,[14,15] MSCs have also shown to improve wound healing and tissue function by homing to injury sites,[16-18] secreting tissue-protective cytokines,[19-21] promoting

angiogenesis,[20,22,23] and mediating inflammation.[24,25] Just as BMCs, MSCs have been transplanted into infarcted hearts to show improvements in cardiac function in animal studies and human clinical trials.[6-8,23,26] Possible mechanisms for the enhanced function may be due to increasing myocyte content through MSC-cardiomyocyte differentiation,[6,27,28] or limiting native myocyte loss through protective MSC signaling that promotes cardiomyocyte survival and maintains cardiomyocyte contractility.[19,20,25,29-32] Despite these successes using MSCs for cardiac cell therapy, complete restoration of normal cardiac mechanical function has not yet been achieved, and it remains unclear whether short-term improvements in function will persist longer term.

For any of the cell types used in cardiac cell therapy, one of the chief limitations that needs to be addressed is the survival of the implanted cells.[33] In the dynamic environment of the infarcted heart, decreased blood supply causes ischemia, which reduces oxygen tensions to the range of 0.4-1.7% $O_2$.[34] Reduced oxygen tension in MIs is a major factor contributing to the low survival of implanted cells, as a result of increased oxidative stress that has shown to trigger autophagy and apoptosis mechanisms in both native myocytes and delivered MSCs.[35-37] If delivered MSCs cannot survive, they cannot sustain delivery of cardioprotective factors nor regenerate enough infarcted myocardium for long-term functional improvement. One of the main reasons implanted MSCs experience increased oxidative stress is because they have been cultured and prepared at atmospheric 20% $O_2$ *in vitro* prior to delivery, and they do not have the appropriate cellular machinery to adapt to reduced oxygen tensions in an MI. Conditioning MSCs in reduced-$O_2$ prior to implantation can enhance redox mechanisms,[37] which may enable them to adapt more readily to the reduced-$O_2$ MI environment. *In vitro* studies have shown that conditioning MSCs in reduced-$O_2$ can increase migration,[38,39] prosurvival markers,[38,40,41] proangiogenic markers,[20,41] and cardioprotective factor secretion.[40,41] When implanted into MIs *in vivo*, reduced-$O_2$ preconditioned MSCs showed increased recruitment to the infarct,[39,42] increased MSC survival,[43] and increased angiogenesis.[42,43] In addition, reduced-$O_2$ conditioned MSCs showed therapeutic benefit in MIs by reducing infarct size,[42,43] increasing wall thickness,[42] and improving global cardiac function indices such as increased systolic pressure,[43] decreased end-diastolic pressure,[43] increased fractional shortening,[42] and

increased ejection fraction.[42] While these results are encouraging, only a limited number of studies have been performed using reduced-$O_2$ conditioned MSCs to treat the infarcted heart. Continued investigation is needed to confirm these outcomes and to further understand the therapeutic potential of delivering reduced-$O_2$ conditioned MSCs to MIs.

In contribution to this body of literature, we designed our *in vivo* study to compare the functional outcomes of MIs treated with unconditioned hMSCs, reduced-$O_2$ conditioned hMSCs, and reduced-$O_2$/HGF conditioned hMSCs. Furthermore, we sought to analyze the regional cardiac mechanics of the cell-treated infarcts, which is more definitive than global heart measures for understanding the function within the implant regions. As described previously, MIs generally occur within small regions of the heart. By using specialized techniques for determining the mechanical function in these defined regions, it is possible to study the effects of dysfunction and treatment within infarct areas. As discussed in Sections 2.6 and 2.10, several techniques have been developed for studying regional cardiac mechanics (e.g. echocardiography, MRI, NOGA, sonomicrometry, and HDM). In our study, we used HDM to determine regional function across the infarcted area for a whole field analysis with high spatial resolution. In this system, silicon carbide particles (40 μm in diameter) were applied directly to the epicardial surface, which created a densely speckled contrast on the heart when illuminated with white light. Using a high speed camera to capture images of the speckled surface over the course of a heartbeat, HDM uses a sub-pixel algorithm to interpolate discrete signals with respect to sampling rate and time. By dividing a region of interest into subimages, HDM detects sub-pixel motion to determine the displacement of each subimage between consecutive images through Fourier transform.[12] Using a phase-correlation algorithm to increase computational efficiency beyond the capabilities of conventional particle tracking or digital correlation techniques, displacements can be determined at hundreds of locations to provide a whole field measurement.[13] With a demonstrated accuracy of 0.09 pixels and precision of 0.04 pixels,[12] HDM is an ideal system for studying regional cardiac mechanics in treated and untreated infarct regions within the rat heart.

### 5.1.1. Evaluating regional cardiac function of MIs treated with conditioned hMSCs

To determine whether reduced-$O_2$/HGF conditioned hMSCs can improve cardiac function, we delivered pre-conditioned cells to rat MIs *in vivo*. During the initial procedure, MIs were induced in the left ventricle (LV) of male athymic rats by temporarily ligating the left anterior descending coronary artery for 1 hour. LVs were reperfused for 15 minutes following ligation, and then 1 million cells were delivered to the infarct region by intramyocardial injection. Following the initial procedure, rats were maintained for either 1 week or 1 month time points. At the end of the survival periods, we performed a second procedure to record functional data from the infarct region using HDM, before sacrificing the animals and excising the hearts for histological analysis. From the collected data, we calculated regional stroke work (RSW) and systolic area contraction (SAC) to compare MI treatments.

For both the 1 week and 1 month groups, we compared the functional data of MIs treated with DMEM (delivery media), unconditioned hMSCs, reduced-$O_2$ conditioned hMSCs, and reduced-$O_2$/HGF conditioned hMSCs. For reference, we also performed HDM on normal, non-infarcted rat hearts.

Our analysis shows that all cell treatments can improve regional mechanical function of MIs, and that improved function could be sustained from 1 week to 1 month in each treatment. However, reduced-$O_2$/HGF conditioned hMSCs could significantly improve function compared to both unconditioned hMSCs and reduced-$O_2$ conditioned hMSCs.

## 5.2. Materials and Methods

### 5.2.1. Surgical Procedures and Infarct Model

To determine the effect of implanted cells on the regional mechanical function of an MI, we developed an infarct model in athymic rats. All animals used in this study received humane care in compliance with the "Guide for the Care and Use of Laboratory Animals" prepared by the National Academy of Sciences and published by the National Institutes of Health (NIH publication no. 85-23, revised 1985). The Institutional Animal Care and Use Committee (IACUC) at Worcester Polytechnic Institute reviewed and approved the protocols followed in this study (IACUC # 10-20).

Seven-ten week old male Rowett nude athymic rats (Charles River Laboratories, Wilmington, MA; Strain code: 316, RNU), weighing 250-350 grams, were anesthetized with an intraperotineal injection of Ketamine (100 mg/kg; Manufactured by Bioniche Teoranta, Galway, Ireland; Distributed by Vedco Inc, St. Joseph, MO) and Xylazine (10 mg/kg; Manufactured by IVX Animal Health Corporation, St. Joseph, MO). Rats were then intubated with a 16 gauge angiocatheter and maintained under general anesthesia using inhalational isofluorane. A digital pulse-oximeter was used to monitor $pO_2$ and heart rate, which was maintained between 200-250 beats per minute. A left-side thoracotomy between the 4$^{th}$ and 5$^{th}$ intercostal spaces was performed to access the thoracic cavity and expose the left ventricle (LV), and the pericardium was resected.

Myocardial infarcts were induced by temporary suture ligation of the left anterior descending (LAD) coronary artery for 1 hour. After 1 hour, suture ligations were removed and hearts were allowed to reperfuse for 15 minutes. After reperfusion, cells were delivered to the infarct region by intramyocardial injection. Infarct regions were identified by a discoloration of the ischemic tissue, which showed to be a pale pink color that was distinct from the red color of the surrounding healthy myocardium. For all procedures, a suspension of 1 million cells in 50 μL of DMEM was delivered using a Hamilton surgical syringe (Hamilton Company, Reno, NV; #80601), by making five 10 μL injections in the pale-colored infarct region. Following cell delivery, the chest wall was closed with biodegradable suture (4-0 Vicryl; Ethicon, Guaynabo, Puerto Rico; #J304H), and animals were observed until normal vital signs were recovered. The animals were then maintained under vivarium staff care for the duration of the survival periods.

Following the 1-week and 1-month recovery periods, the animals were returned to the operating room, anesthetized, intubated, and maintained under general anesthesia as described in the initial procedure. Hearts were again exposed by making a left-side thoracotomy between the 4$^{th}$ and 5$^{th}$ intercostal space to access the thoracic cavity, and any developed adhesions in the thoracic cavity were carefully dissected. A pressure transducer (Millar Instruments, Houston, TX; Model #: SPR-524) was placed into the LV by implantation through the apex of the heart. Once pressure recordings from the

transducer were confirmed, functional data was recorded using the HDM system. After data acquisition, rats were euthanized with Beuthanasia-D (0.25 mL/kg; Schering-Plough Animal Health, Kenilworh, NJ), and hearts were excised for histological analysis.

### 5.2.2. Cell preparation and delivery

In preparing hMSCs for *in vivo* delivery, the same general cell culture techniques and specialized conditioning treatments were used as previously described in Chapter 4 (Section 4.2.2, Table 4.1, and Figure 4.3). Briefly, cryovials of cells were thawed, counted, and split into T-75 flasks for growth in either normal-$O_2$ or reduced-$O_2$ conditions. Flasks were seeded and fed every other day with growth medium (MSCGM) for 7 days. After the 7$^{th}$ day, growth media was removed and different media treatments were applied. Media treatments were changed every day for another 7 days. However, on the 6$^{th}$ day of the initial growth-media treatment, hMSCs were fed with MSCGM supplemented with an 8.2 nM concentration of 655 ITK$^{TM}$ quantum dot nano-particles (Invitrogen, #Q21321MP). Quantum dots are passively endocytosed by hMSCs and can be used as a cell-tracking technique, which will be discussed further in Chapter 6. After a 24-hour incubation in quantum dot supplemented MSCGM, cells were washed twice with sterile PBS (without calcium or magnesium; Cellgro, Manassas, VA; # 21-031-CV), and then treated for media conditioning. Quantum dot cell-loading was assessed the 7$^{th}$ day of the initial growth-media treatment, to ensure sufficient loading and uniformity in all flasks across $O_2$/media treatments.

After hMSCs were media-conditioned for 7 days, cells were removed from their designated $O_2$ incubators, washed with sterile PBS, and then detached from culture plates with 0.25% trypsin (Cellgro). Cells were exposed to 5% fetal bovine serum media to deactivate trypsin, then immediately centrifuged at 1,000 rpm for 5 minutes. After centrifugation, the excess media/trypsin solution was aspirated, and the cell pellets were resuspended in 1 mL of sterile DMEM (Lonza, Inc.). Cells were counted using a hemocytometer, cell concentrations were determined, and then 1 million cells were aliquoted from the cell suspension into another sterile conical tube. The 1 million-cell aliquot was centrifuged again at 1,000

rpm for 5 minutes, and the old DMEM was aspirated. The 1 million-cell pellet was resuspended in 50 μL of fresh sterile DMEM, transferred into sterile 0.5-mL microcentrifuge tube, which was then sealed and transported to the operating room.

Just prior to cell implantation, a sterile 27-gauge surgical needle (Becton Dickenson) was fixed to 100μL-Hamilton surgical syringe. The syringe was back-filled with ~30 μL of sterilized mineral oil to account for dead-space in the needle flange. Once the syringe was prepared, the 50 μL cell suspension was uncapped, mixed by gentle pipetting, and then drawn into the syringe for delivery.

### 5.2.3. Measurement of regional mechanical function

Regional function was determined by high-density mapping (HDM), as previously described in the analysis of rabbit, porcine, and canine hearts.[6,44-47] After the LV was exposed and the pressure transducer was implanted during the terminal procedure, gross anatomical observations were made to determine a region of interest (ROI) for analysis (Figure 5.1). Once the ROI was identified, silicon carbide particles (~40 μm in diameter) were applied to the epicardial surface of the heart to create a unique random light intensity pattern. A complementary metal-oxide semiconductor camera (CMOS camera; Photron, San Diego, CA) was then focused onto the ROI (Figure 5.1). The camera system settings were adjusted to acquire 8-bit grayscale images with a 1280 x 1024 pixel resolution, at a frame rate of 250 Hz for 4 seconds. Synchronous LV pressure readings were digitally recorded from the Millar pressure transducer that was connected to an analog-to-digital converter (National Instruments, Austin, TX; Model #: PCI-6023E). Both the CMOS camera and the pressure transducer were connected to a single data acquisition board, and were triggered simultaneously using an external TTL trigger.

### 5.3.4. Image post-processing

As described in the chapter introduction, HDM uses a sub-pixel phase correlation algorithm to obtain displacements of the epicardial surface at multiple locations within the ROI. To do this, the ROI was divided into subimages by configuring the HDM software to analyze a 64 x 64 pixel subimage size. By

analyzing the coordinate pixel-shifts of the unique light intensity distribution over consecutive images, *u* and *v* displacements of each subimage could be calculated from one frame to the next (Figure 5.2A). Based on the calculated displacements of 4 adjacent subimages, changes in area in successive frames were computed using Green's theorem (Figure 5.2B):

$$A = \frac{1}{2}\sum_{i=1}^{4}(x_i y_{i+1} - x_{i+1} y_i)$$

where *i* indicates the subimage, and *x* and *y* indicate subimage coordinates. Then by normalizing the initial area to 1, changes in area were then used to calculate area stretch ratios over the cardiac cycle. Combining these area calculations with synchronous pressure measurements, regional area work loops were created for each sampled heartbeat (Figure 5.3). Regional stroke work (RSW) was calculated by integrating area with respect to pressure over one cardiac cycle:

$$RSW = \int A \cdot dP$$

We report RSW both with and without normalization to pressure. RSW with normalization to pressure is reported as a unitless value, whereas RSW without normalization to pressure is reported in mm Hg. RSW is an index of the amount of work being performed by the ROI. Since the integral is path-dependent, a positive value for RSW (counter-clockwise work loop) indicates that the region is contracting in synchrony with normal myocardium and performing work. A negative value for RSW (clockwise work loop) indicates that the region is non-synchronous with normal myocardium, and that the surrounding myocardium is performing work on the ROI. Systolic area contraction (SAC) of the ROI was calculated as the difference between end-diastolic area (EDA) and end-systolic area (ESA), with end-diastolic area normalized to 1, and then reported as percent normalized contraction based on the following equation:

$$SAC = \left(\frac{EDA - ESA}{EDA}\right) \times 100 = \left(\frac{1 - ESA}{1}\right) \times 100$$

### 5.3.5. Statistics

RSW and SAC values were determined for 4 individual heartbeats in each rat, and then average RSW and SAC values were calculated. Averaged RSW and SAC values for rats in each treatment group were then averaged again, and data are reported as mean ± standard error of the mean. One-way analysis of variance (ANOVA) was used to determine RSW and SAC differences in treatment groups at the 1-week and 1-month time points. ANOVA was also used to determine if the values for RSW and SAC were different between the 1-week and 1-month treatment groups. A *post hoc* Tukey test was then used to perform multiple pair-wise comparisons. Differences were considered significant for p-values $\leq 0.05$.

RSW and SAC values for normal, non-infarcted hearts were determined in the same manner as the other treatment groups. In a separate analysis, RSW and SAC values for normal heart were determined to be significantly higher than all other treatment groups by one-way ANOVA. For reference, normal heart data is included on our graphical representations.

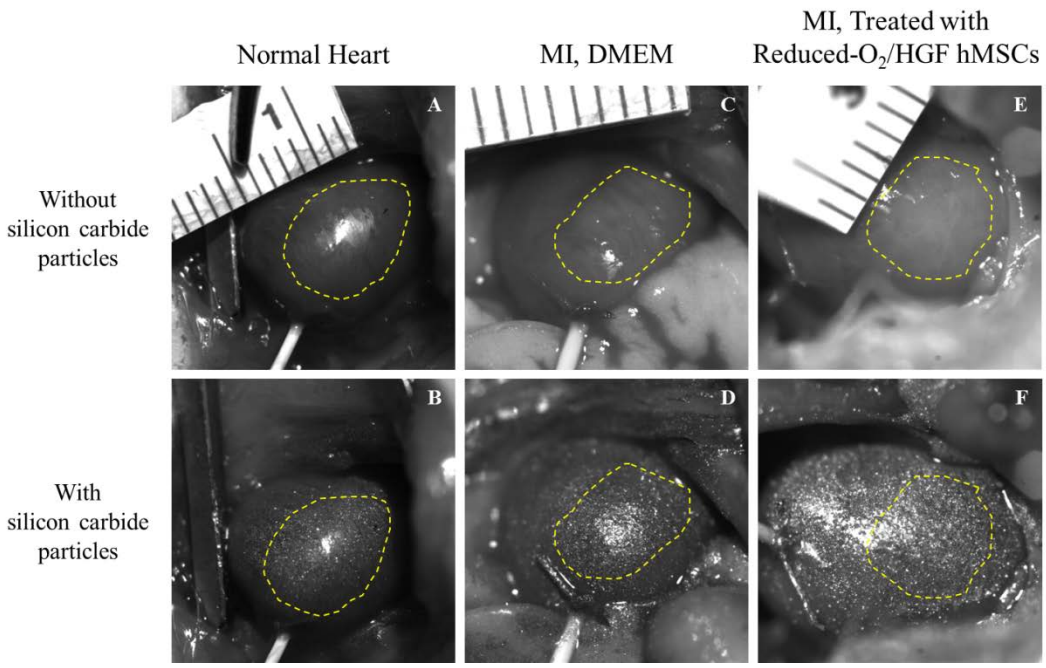


**Figure 5.1. Identifying regions of interest in vivo.** During terminal surgeries, hearts were exposed by left thoracotomy and any adhesions were removed. Rib spreaders were used for better access to the left ventricle (LV), and regions of interest (ROIs) were selected before the application of silicon carbide particles and retro-reflective beads (A, C, and E). Normal hearts without infarct presented with healthy, red-colored, contracting myocardium and ROIs were focused anywhere on the LV (A). Infarcted hearts, whether treated with media or cells, presented with a pale, discolored region in the LV, and ROIs were focused within these defect areas (C and E). Once ROIs were chosen, silicon carbide particles and retro-reflective beads were applied, and high-speed cameras were focused onto the epicardial surface (B, D, and F). During analysis, sub-regions within ROIs could be analyzed, and border-zone regions could be neglected.

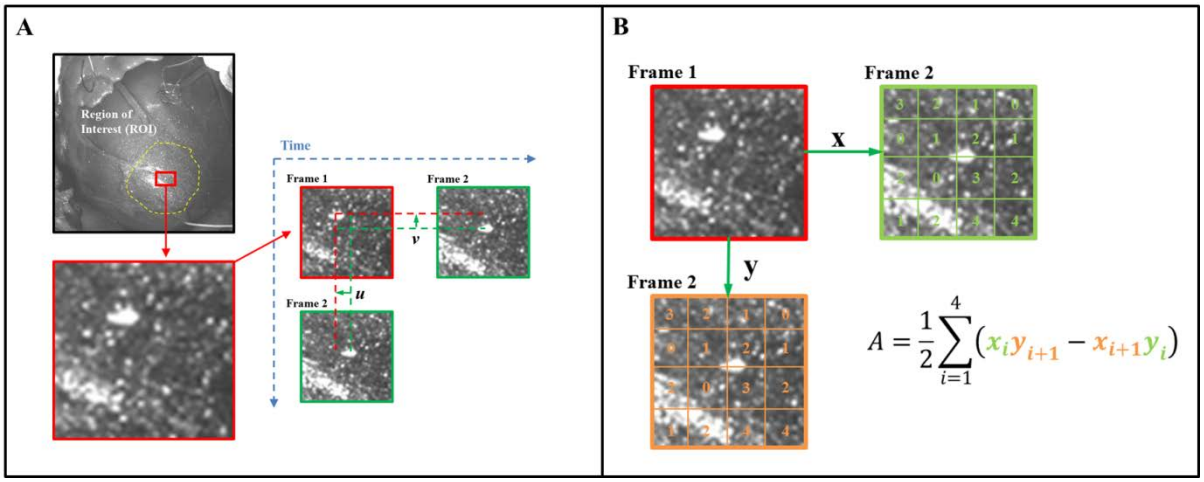


**Figure 5.2. Using High Density Mapping (HDM) to determine regional mechanical function.** HDM was used to determine deformations of the epicardial surface of rat hearts *in vivo*. (A) ROIs with a unique light intensity distribution was selected, for analysis in a series of subsequent images. The ROI was divided into sub-images, and a Fourier transform was used to determine the *x* and *y* coordinates of the light intensity peak in each sub-image. The coordinates for each sub-image were compared to the coordinates for the same sub-image in subsequent images, and resulting displacements were determined. (B) The area of each set of 4 adjacent sub-images was computed, and all areas were summed to find the total change in area across frames.

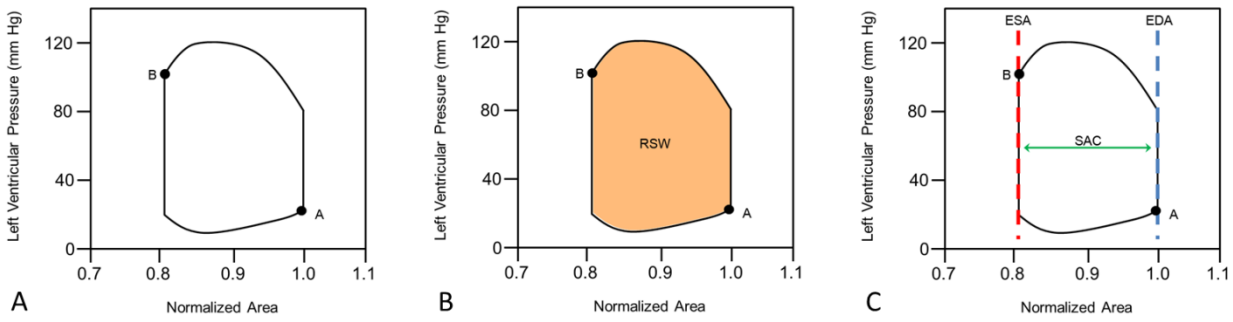


**Figure 5.3. Schematics of pressure-area work loops.** (A) By correlating computed area changes with pressure changes recorded from the left ventricular cavity, we could establish pressure-area work loops for each cardiac cycle. Within each pressure-area work loop, we could identify end-diastole (point A) and end-systole (point B), and end-diastolic areas were always normalized to 1. (B) Regional stroke work (RSW) was calculated by integrating the area with respect to pressure; positive work was shown by counter-clockwise progression of pressure-area points, and negative work was shown by clockwise progression of pressure-area points. Positive work indicates that ROIs were contracting in contribution to total work in the heart, whereas negative work indicates that work was being done on the ROI by surrounding myocardium. (C) Systolic area contraction (SAC) was calculated by finding the difference between the end-diastolic area (EDA, area at end-diastole) and the end-systolic area (ESA, area at end-systole).

## 5.3. Results

After 1-week and 1-month survival periods, pressure recordings and HDM were used to study ROIs within left ventricular infarcts. Infarct regions were identified based on gross anatomical observations of the LV, where necrotic MI regions produced a white-colored scar area that contrasted with the red/pink color of healthy myocardium (Figure 5.4). A high speed CMOS camera was focused onto the MI regions, and data was acquired at 250 frames/second for 4 seconds, with 1280x1024 pixel resolution. In post-procedure analysis, the HDM program was used to correlate cumulative area stretch ratios with intracavitary pressure measurements, to produce area work loops for each analyzed heartbeat (Figure 5.4). RSW and SAC were calculated as described in the methods (Figure 5.3). Four heartbeats were analyzed and averaged for each animal, and then values for animals in the same treatment group were averaged. Regional cardiac mechanical data is reported as mean ± standard error of the mean, and results are summarized in in Table 5.1.

### *Regional Stroke Work*

In analyzing the regional mechanical data without normalization to pressure after 1 week, the mean RSW of DMEM treated MIs was 0.97 ± 0.44 mm Hg (n = 7; Figure 5.5). Treating MIs with traditional, normal-$O_2$/MSCGM hMSCs significantly increased infarct function with a mean RSW of 3.37 ± 0.47 mm Hg (n = 9; $p \leq 0.001$). MIs treated with reduced-$O_2$/MSCGM hMSCs significantly increased infarct function compared to both DMEM ($p \leq 0.01$) and normal-$O_2$/MSCGM hMSC treatments, with a mean RSW of 5.44 ± 0.31 mm Hg (n = 8; $p \leq 0.001$). Furthermore, MIs treated with reduced-$O_2$/HGF hMSCs showed to significantly increase regional mechanical function compared to all other MI treatment groups, with a mean RSW of 7.48 ± 0.30 (n = 10). While all MI groups resulted in significantly decreased function compared to normal non-infarcted hearts (RSW: 21.482 ± 1.71 mm Hg, n = 6), MIs treated with reduced-$O_2$/HGF hMSCs was effective in restoring ~35% of normal regional work after 1 week (as compared to the normal-heart analysis).

After 1 month, the mean RSW of DMEM treated MIs was 2.54 ± 0.35 mm Hg (n = 7; Figure 5.6). The mean RSW of MIs treated with traditional normal-$O_2$/MSCGM hMSCs was 4.08 ± 0.89 mm Hg (n = 7), and the mean RSW of MIs treated with reduced-$O_2$/MSCGM hMSCs was 4.98 ± 0.52 mmHg (n = 6). Our analysis indicates that there was no significant difference in RSW at 1 month across the following MI-treatment groups: DMEM, normal-$O_2$/MSCGM hMSCs, or reduced-$O_2$/MSCGM hMSCs. MIs treated with reduced-$O_2$/HGF hMSCs had a mean RSW of 7.44 ± 0.79 (n = 6), which was significantly higher than DMEM ($p \leq 0.001$) or normal-$O_2$/MSCGM hMSC treatments ($p \leq 0.01$), but showing no significant difference compared to the reduced-$O_2$/MSCGM hMSC treatment. Compared to normal non-infarcted heart function, all MI treatments showed significantly decreased RSW at 1 month.

In a comparison of individual treatment groups at 1-week versus 1-month, there was no significant difference in RSW for any MI treatment between time points (Figure 5.7). Our results indicate that 1-week improvements in RSW could be sustained out to 1 month.

***Normalized Regional Stroke Work***

Since different treatment conditions contributed to LV pressure variation (Figure 5.4), we also analyzed RSW with normalization to pressure (Figure 5.8). After 1 week, the mean normalized RSW of DMEM treated MIs was 0.011 ± 0.004 (n = 7). MIs treated with traditional normal-$O_2$/MSCGM hMSCs resulted in a mean normalized RSW of 0.035 ± 0.006 (n = 9), which again showed a significant increase in function compared to DMEM treatment. MIs treated with reduced-$O_2$/MSCGM conditioned hMSCs had a mean normalized RSW of 0.046 ± 0.003 (n = 8), which also showed a significant increase in function compared to DMEM. However, our analysis indicates there was no statistical difference between MIs treated with normal-$O_2$/MSCGM hMSCs or reduced-$O_2$/MSCGM hMSCs. The mean normalized RSW for MIs treated with reduced-$O_2$/HGF conditioned hMSCs was 0.069 ± 0.004 (n = 10), and again showed to significantly increase regional function compared to all other MI treatment groups. Again, all MI treatments at 1 week showed significantly decreased work compared to normal non-infarcted hearts, with a mean normalized RSW of 0.160 ± 0.008 (n = 6). However, in normalizing for

pressure, our analysis indicates that reduced-$O_2$/HGF conditioned hMSCs may be able to restore normal regional work upwards of ~43% after 1 week.

After 1 month, the mean normalized RSW of DMEM treated MIs was 0.021 ± 0.002 (n = 7; Figure 5.9). The mean normalized RSW of MIs treated with traditional normal-$O_2$/MSCGM hMSCs was 0.034 ± 0.007 (n = 7), and the mean normalized RSW of MIs treated with reduced-$O_2$/MSCGM hMSCs was 0.038 ± 0.005 (n = 6). As with non-normalized RSW, our analysis showed there was no significant difference in normalized RSW for MIs treated with DMEM, normal-$O_2$/MSCGM hMSCs, or reduced-$O_2$/MSCGM hMSCs at 1 month. MIs treated with reduced-$O_2$/HGF hMSCs had a mean normalized RSW of 0.07 ± 0.008 (n = 6). Reduced-$O_2$/HGF hMSCs significantly increased normalized RSW compared to DMEM ($p \leq 0.001$), normal-$O_2$/MSCGM hMSCs ($p \leq 0.01$), and reduced-$O_2$/MSCGM hMSCs ($p \leq 0.01$). As with non-normalized RSW, all MI treatments at 1 month showed significantly decreased normalized RSW compared to normal non-infarcted heart function.

In a comparison of individual treatment groups at 1-week versus 1-month, there was no significant difference in normalized RSW for any MI treatment between time points (Figure 5.10). Our results indicate that 1-week improvements in normalized RSW could be sustained out to 1 month.

***Systolic Area Contraction***

By taking the difference of the normalized area at end-diastole and end-systole, SAC was calculated as a measure of contractile shortening in the region of interest. At 1 week, DMEM treated MIs resulted in a mean SAC of 1.04 ± 0.48% (n = 7; Figure 5.11). MIs treated with normal-$O_2$/MSCGM hMSCs had a mean SAC of 3.76 ± 0.85% (n = 9), which was nearly statistically different than the DMEM treatment ($p = 0.055$). Treatment with reduced-$O_2$/MSCGM hMSCs resulted in a mean SAC of 5.39 ± 0.66% (n = 8), which was significantly different than the DMEM treatment ($p \leq 0.01$), but not statistically different than normal-$O_2$/MSCGM hMSCs. MIs treated with reduced-$O_2$/HGF hMSCs resulted in a mean SAC of 8.93 ± 0.63% (n = 10). Treatment with reduced-$O_2$/HGF hMSCs showed a significant increase in SAC compared to DMEM ($p \leq 0.001$), normal-$O_2$/MSCGM hMSCs ($p \leq 0.001$), and reduced-$O_2$/MSCGM

hMSCs ($p \leq 0.01$). All MI treatment groups resulted in significantly decreased SAC values compared to normal non-infarcted hearts (19.53 ± 1.18%, n = 6). Treatment with reduced-$O_2$/HGF hMSCs may be able to restore contractility to ~46% of normal heart function.

At 1 month, the mean SAC of DMEM treated MIs was 1.97 ± 0.42% (n = 7; Figure 5.12). Treatment with normal-$O_2$/MSCGM hMSCs resulted in a mean SAC of 5.99 ± 1.11% (n = 7), which was significantly higher than the DMEM treatment ($p \leq 0.05$). MIs treated with reduced-$O_2$/MSCGM hMSCs showed a mean SAC of 4.51 ± 0.89% (n = 6), which showed no statistical difference to either DMEM or normal-$O_2$/MSCGM hMSCs. Treatment with reduced-$O_2$/HGF hMSCs resulted in a mean SAC of 10.63 ± 1.56% (n = 6), which was significantly higher than DMEM ($p \leq 0.001$), normal-$O_2$/MSCGM hMSCs ($p \leq 0.05$), and reduced-$O_2$/MSCGM hMSCs ($p \leq 0.01$). All MI treatment groups at 1 month indicated significantly decreased SAC values compared to normal non-infarcted heart function.

In a comparison of individual treatment groups at 1-week versus 1-month, there was no significant difference in SAC for any MI treatment between time points (Figure 5.13). Our results indicate that 1-week improvements in SAC could be sustained out to 1 month.

| Time Point | Group | n | RSW | Normalized RSW | SAC |
|---|---|---|---|---|---|
| | Normal Heart | 6 | 21.48 ± 1.71 | 0.16 ± 0.008 | 19.53 ± 1.18 |
| **1 Week** | MI, DMEM | 7 | 0.97 ± 0.44 | 0.011 ± 0.004 | 1.04 ± 0.48 |
| | MI, Normal-$O_2$/MSCGM | 9 | 3.37 ± 0.47 | 0.035 ± 0.006 | 3.76 ± 0.85 |
| | MI, Reduced-$O_2$/MSCGM | 8 | 5.44 ± 0.31 | 0.046 ± 0.003 | 5.39 ± 0.66 |
| | MI, Reduced-$O_2$/HGF | 10 | 7.48 ± 0.30 | 0.069 ± 0.004 | 8.93 ± 0.63 |
| **1 Month** | MI, DMEM | 7 | 2.54 ± 0.35 | 0.021 ± 0.002 | 1.97 ± 0.42 |
| | MI, Normal-$O_2$/MSCGM | 7 | 4.08 ± 0.89 | 0.034 ± 0.007 | 5.99 ± 1.11 |
| | MI, Reduced-$O_2$/MSCGM | 6 | 4.99 ± 0.52 | 0.038 ± 0.005 | 4.51 ± 0.89 |
| | MI, Reduced-$O_2$/HGF | 6 | 7.44 ± 0.79 | 0.07 ± 0.008 | 10.63 ± 1.56 |

**Table 5.1. Summary of Mechanical Data.** RSW (Regional stroke work; measured in mm Hg). Normalized RSW is unitless. SAC (systolic area contraction; percent normalized area). DMEM (Dulbecco's Modified Eagles Medium). MSCGM (Mesenchymal Stem Cell Growth Media; proprietary of Lonza Inc.). HGF (hepatocyte growth factor). MI (myocardial infarct).

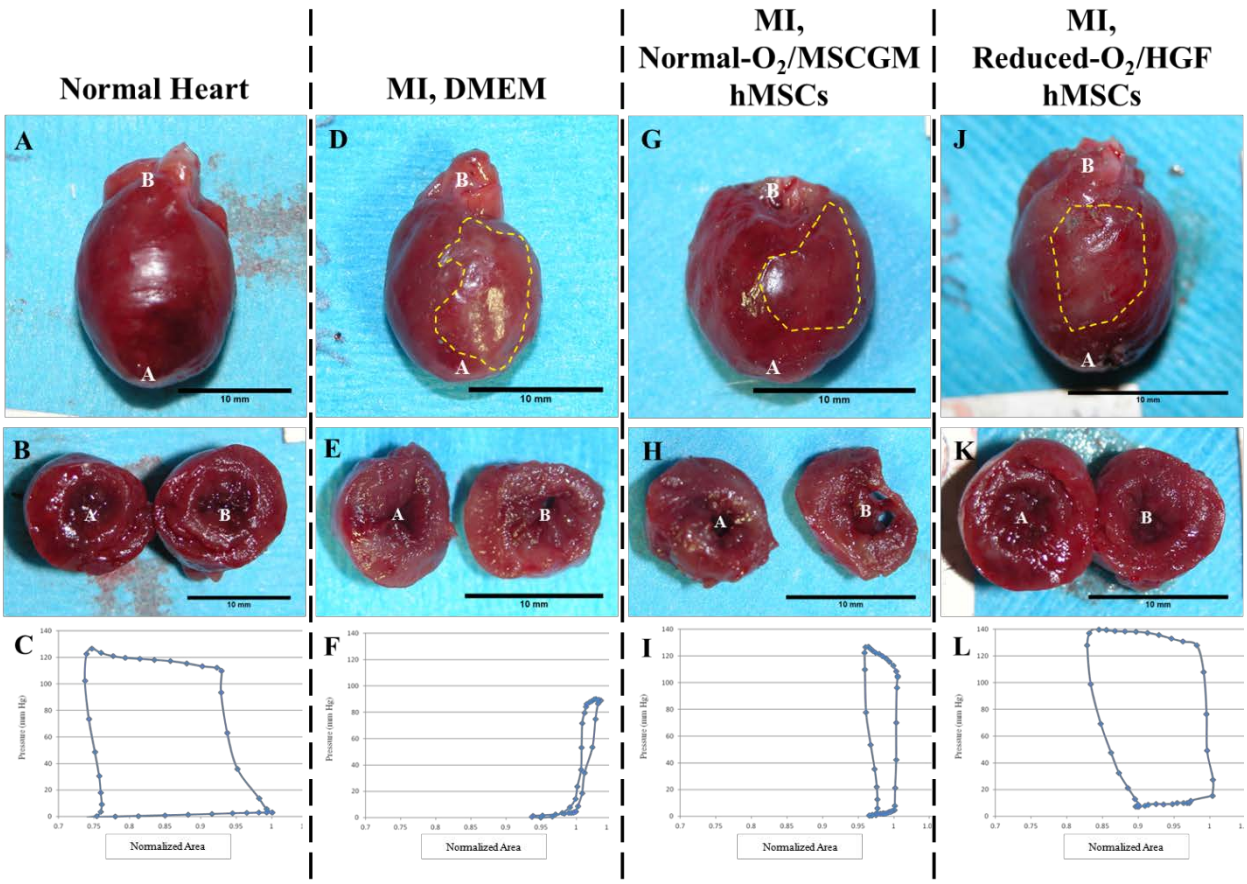


**Figure 5.4. Gross anatomy and corresponding pressure-area work loops.** Once terminal procedures were completed, hearts were excised (A, D, G, J) and left ventricular defect areas were re-identified (marked with yellow, dotted line). Hearts were bisected between the base (marked "B") and apex (marked "A"), generally cutting through the identified defect region (B, E, H, K). Some of the cross-sections of bisected hearts also showed necrotic areas within the mid-myocardium. Mechanical data was analyzed by HDM to establish pressure-area work loops that correspond to each heart (C, F, I, L).

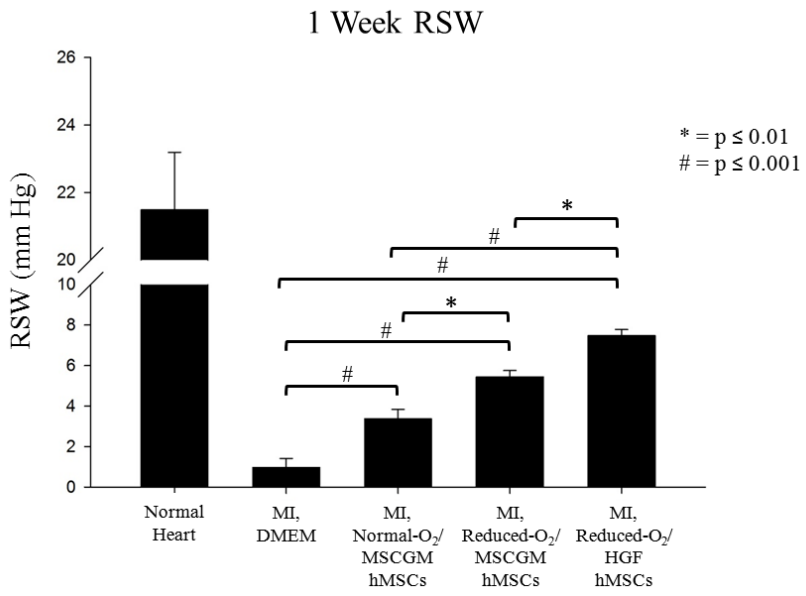


**Figure 5.5. Regional stroke work (RSW, mm Hg) after 1-week survival.**

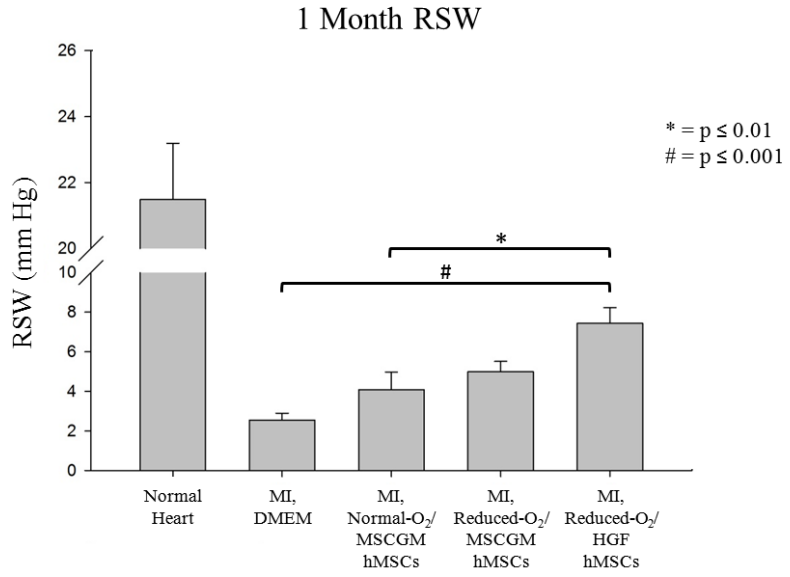


**Figure 5.6. Regional stroke work (RSW, mm Hg) after 1-month survival.**

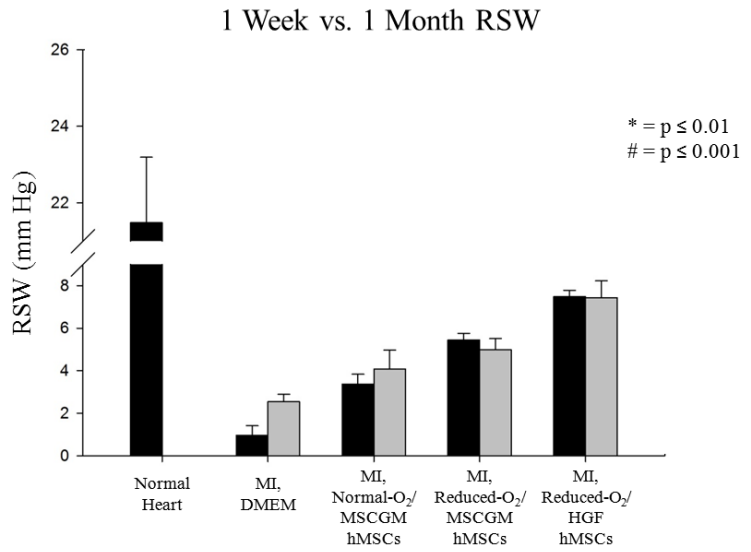


**Figure 5.7. Comparison of regional stroke work at 1-week and 1-month survival time points.**

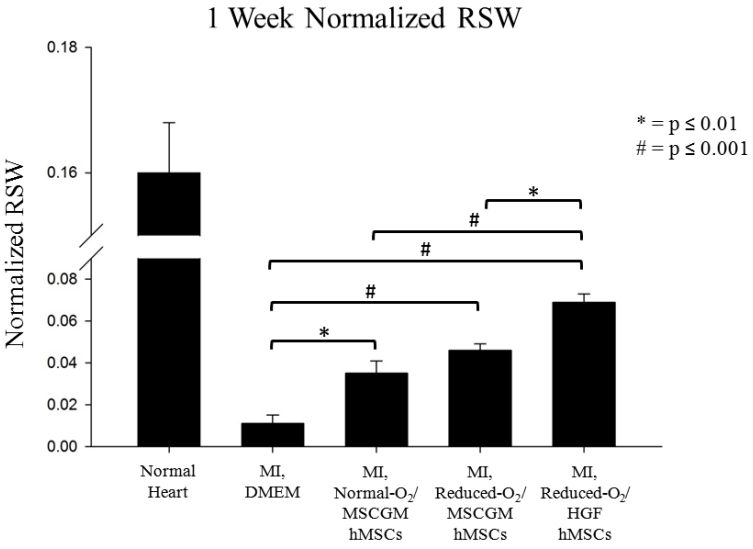


**Figure 5.8. Normalized regional stroke work after 1 week survival.**

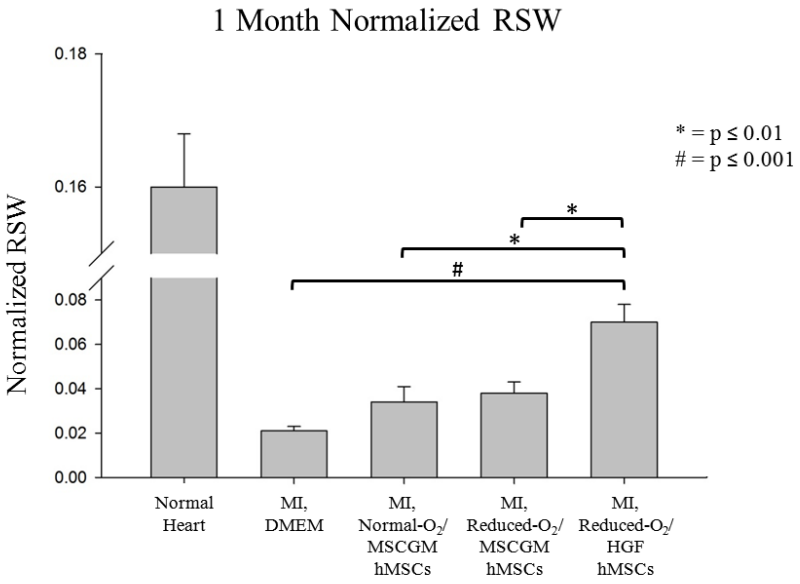


**Figure 5.9. Normalized regional stroke work after 1-month survival**

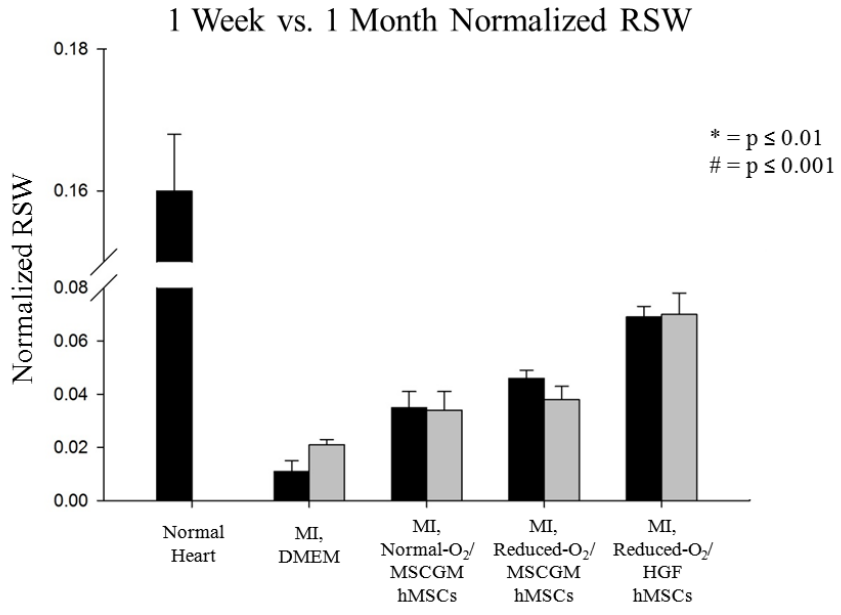


**Figure 5.10. Comparison of normalized regional stroke work at 1-week and 1-month survival time points.**

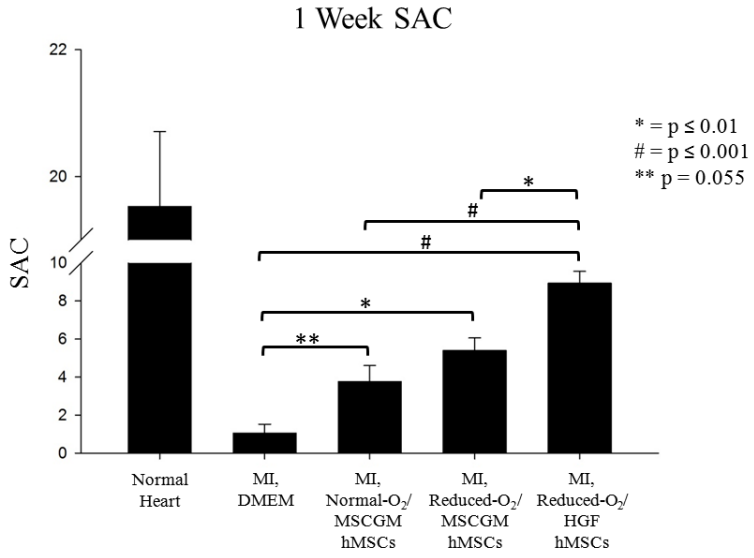


**Figure 5.11. Systolic area contraction (SAC) after 1-week survival.**

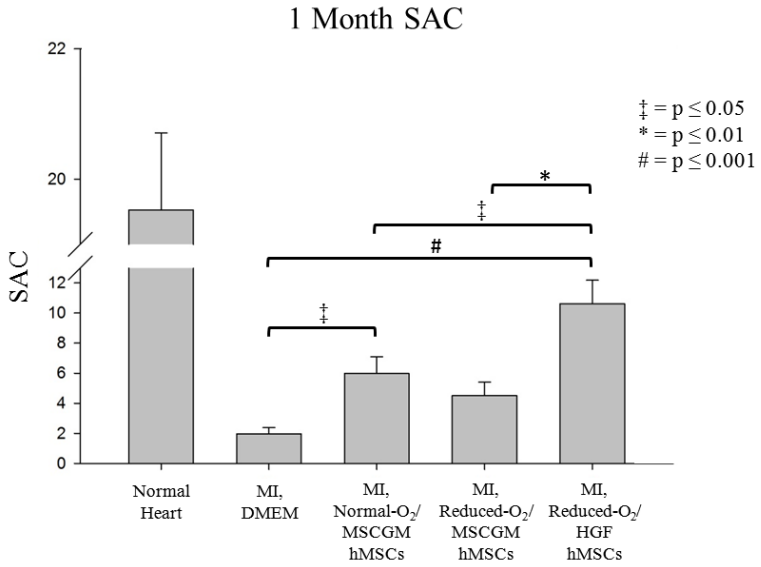


**Figure 5.12. Systolic area contraction (SAC) after 1-month survival.**

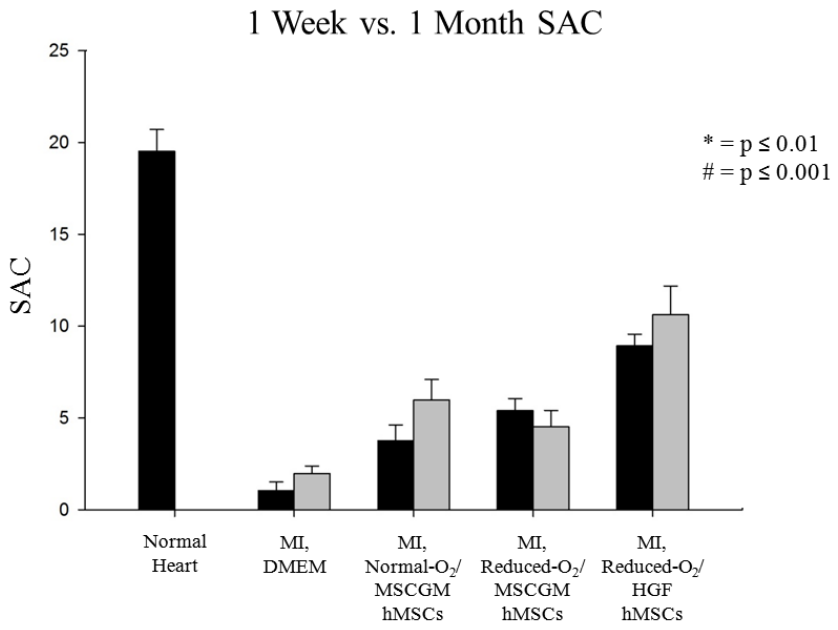


**Figure 5.13. Comparison of systolic area contraction (SAC) at 1-week and 1-month survival time points.**

## 5.4. Discussion

In this study, we implanted reduced-$O_2$/HGF conditioned hMSCs to rat MIs *in vivo* to study the effects on regional cardiac mechanics. We found that reduced-$O_2$/HGF conditioned hMSCs could significantly improve regional stroke work and systolic area contraction at both 1-week and 1-month time points, compared to MIs treated with DMEM, normal-$O_2$/MSCGM hMSCs, or reduced-$O_2$/MSCGM hMSCs. While treating MIs with reduced-$O_2$/HGF conditioned hMSCs could not restore regional mechanical function to the levels observed in healthy non-infarcted hearts, our results suggest that our novel treatment regimen could pre-condition hMSCs to be more effective *in vivo* than conventional hMSCs.

More work is necessary to understand the possible mechanisms responsible for the increases in regional mechanical function. In Chapter 6, we will evaluate the retention of reduced-$O_2$/HGF hMSCs, and their expression of cardiac-specific proteins *in vivo*. Previous qualitative studies suggest that increased cell retention can increase cardiac function, however, a quantitative correlation between cell number and function has not been determined. Logically, it would make sense that the engraftment of more cells could increase function by improving the passive mechanics of an MI, delivering more cardioprotective factors for native myocyte survival, and limiting infarct size. As another mechanism lending to the observed increases in mechanical function, it may be possible that some of the implanted cells differentiate further *in vivo* for a more mature cardiomyocyte phenotype. This would suggest that implanted cells may be able to fully differentiate in contractile cells, to increase cardiac mechanics through active function, after 2 months *in vivo*.[6]

While our functional results are promising, there are several factors to consider in the design of future *in vivo* studies. In our experimental design, we treated acute MIs 15 minutes after the removal of a temporary ligation. Previous studies have shown that delivering cells 1 week after an MI can enhance cell survival and functional outcomes. In future studies, it may be more appropriate to deliver cells at the 1-week post-infarct time point. Also in our studies, we only delivered 1 million cells to the infarct region. While it remains unclear as to the optimal cell number for implantation, it is unlikely that the 1 million

delivered cells can repopulate or regenerate the 1 billion cardiomyocytes lost during an MI. Furthermore, more cells will be needed in order to achieve similar levels of functional recovery in adult humans that we observed in rats. By delivering more redcued-$O_2$/HGF hMSCs to the infarcts, it may be possible to further enhance functional recovery. On a related note, there is a need to improve cell delivery techniques that will allow for better cell engraftment. In our study, we delivered cells by the standard IM injection technique, which is prone to high levels of cell loss. New delivery techniques must be developed to limit cell loss, so that more cells can be retained for contribution to functional outcomes.

## 5.5. References


1 Taylor, D. A. *et al.* Regenerating functional myocardium: improved performance after skeletal myoblast transplantation. *Nat Med* **4**, 929-933, (1998).

2 Murry, C. E., Wiseman, R. W., Schwartz, S. M. & Hauschka, S. D. Skeletal myoblast transplantation for repair of myocardial necrosis. *J Clin Invest* **98**, 2512-2523, (1996).

3 Laflamme, M. A. *et al.* Cardiomyocytes derived from human embryonic stem cells in pro-survival factors enhance function of infarcted rat hearts. *Nat Biotechnol* **25**, 1015-1024, (2007).

4 Lunde, K. *et al.* Intracoronary injection of mononuclear bone marrow cells in acute myocardial infarction. *N Engl J Med* **355**, 1199-1209, (2006).

5 Janssens, S. *et al.* Autologous bone marrow-derived stem-cell transfer in patients with ST-segment elevation myocardial infarction: double-blind, randomised controlled trial. *Lancet* **367**, 113-121, (2006).

6 Potapova, I. A. *et al.* Enhanced recovery of mechanical function in the canine heart by seeding an extracellular matrix patch with mesenchymal stem cells committed to a cardiac lineage. *Am J Physiol Heart Circ Physiol* **295**, H2257-2263, (2008).

7 Hare, J. M. *et al.* A randomized, double-blind, placebo-controlled, dose-escalation study of intravenous adult human mesenchymal stem cells (prochymal) after acute myocardial infarction. *J Am Coll Cardiol* **54**, 2277-2286, (2009).

8 Grauss, R. W. *et al.* Mesenchymal stem cells from ischemic heart disease patients improve left ventricular function after acute myocardial infarction. *Am J Physiol Heart Circ Physiol* **293**, H2438-2447, (2007).

9 Wolf, D. *et al.* Dose-dependent effects of intravenous allogeneic mesenchymal stem cells in the infarcted porcine heart. *Stem cells and development* **18**, 321-329, (2009).

10 Gaudette, G. R. & Cohen, I. S. Cardiac regeneration: materials can improve the passive properties of myocardium, but cell therapy must do more. *Circulation* **114**, 2575-2577, (2006).

11 Wall, S. T., Walker, J. C., Healy, K. E., Ratcliffe, M. B. & Guccione, J. M. Theoretical impact of the injection of material into the myocardium: a finite element model simulation. *Circulation* **114**, 2627-2635, (2006).

12 Kelly, D. J., Azeloglu, E. U., Kochupura, P. V., Sharma, G. S. & Gaudette, G. R. Accuracy and reproducibility of a subpixel extended phase correlation method to determine micron level displacements in the heart. *Med Eng Phys* **29**, 154-162, (2007).

13 Gaudette, G. R., Todaro, J., Krukenkamp, I. B. & Chiang, F. P. Computer aided speckle interferometry: a technique for measuring deformation of the surface of the heart. *Ann Biomed Eng* **29**, 775-780., (2001).

14 Pittenger, M. F., Mosca, J. D. & McIntosh, K. R. Human mesenchymal stem cells: progenitor cells for cartilage, bone, fat and stroma. *Curr Top Microbiol Immunol* **251**, 3-11, (2000).

15 Potapova, I. *et al.* Functional Regeneration of the Canine Ventricle Using Adult Human Mesenchymal Stem Cells Committed In Vitro to a Cardiac Lineage. *Circ Res* **99**, E19, (2006).

16 Sasaki, M. *et al.* Mesenchymal stem cells are recruited into wounded skin and contribute to wound repair by transdifferentiation into multiple skin cell type. *J Immunol* **180**, 2581-2587, (2008).

17 Ye, J., Lee, S. Y., Kook, K. H. & Yao, K. Bone marrow-derived progenitor cells promote corneal wound healing following alkali injury. *Graefes Arch Clin Exp Ophthalmol* **246**, 217-222, (2008).

18 Hale, S. L., Dai, W., Dow, J. S. & Kloner, R. A. Mesenchymal stem cell administration at coronary artery reperfusion in the rat by two delivery routes: a quantitative assessment. *Life Sci* **83**, 511-515, (2008).

19 Wang, M., Crisostomo, P. R., Herring, C., Meldrum, K. K. & Meldrum, D. R. Human progenitor cells from bone marrow or adipose tissue produce VEGF, HGF, and IGF-I in response to TNF by a p38 MAPK-dependent mechanism. *Am J Physiol Regul Integr Comp Physiol* **291**, R880-884, (2006).

20 Sadat, S. *et al.* The cardioprotective effect of mesenchymal stem cells is mediated by IGF-I and VEGF. *Biochem Biophys Res Commun* **363**, 674-679, (2007).

21 Neuss, S., Becher, E., Woltje, M., Tietze, L. & Jahnen-Dechent, W. Functional expression of HGF and HGF receptor/c-met in adult human mesenchymal stem cells suggests a role in cell mobilization, tissue repair, and wound healing. *Stem Cells* **22**, 405-414, (2004).

22 Wu, Y., Chen, L., Scott, P. G. & Tredget, E. E. Mesenchymal stem cells enhance wound healing through differentiation and angiogenesis. *Stem Cells* **25**, 2648-2659, (2007).

23 Hu, X. *et al.* Optimal temporal delivery of bone marrow mesenchymal stem cells in rats with myocardial infarction. *Eur J Cardiothorac Surg* **31**, 438-443, (2007).

24 Pittenger, M. Sleuthing the source of regeneration by MSCs. *Cell stem cell* **5**, 8-10, (2009).

25 Guo, J., Lin, G. S., Bao, C. Y., Hu, Z. M. & Hu, M. Y. Anti-inflammation role for mesenchymal stem cells transplantation in myocardial infarction. *Inflammation* **30**, 97-104, (2007).
26 Amado, L. C. *et al.* Cardiac repair with intramyocardial injection of allogeneic mesenchymal stem cells after myocardial infarction. *Proc Natl Acad Sci U S A* **102**, 11474-11479, (2005).
27 Toma, C., Pittenger, M. F., Cahill, K. S., Byrne, B. J. & Kessler, P. D. Human mesenchymal stem cells differentiate to a cardiomyocyte phenotype in the adult murine heart. *Circulation* **105**, 93-98, (2002).
28 Behfar, A. *et al.* Guided cardiopoiesis enhances therapeutic benefit of bone marrow human mesenchymal stem cells in chronic myocardial infarction. *J Am Coll Cardiol* **56**, 721-734, (2010).
29 Wang, M. *et al.* STAT3 mediates bone marrow mesenchymal stem cell VEGF production. *J Mol Cell Cardiol* **42**, 1009-1015, (2007).
30 Wang, Y., Ahmad, N., Wani, M. A. & Ashraf, M. Hepatocyte growth factor prevents ventricular remodeling and dysfunction in mice via Akt pathway and angiogenesis. *J Mol Cell Cardiol* **37**, 1041-1052, (2004).
31 Guo, Y. *et al.* Locally overexpressing hepatocyte growth factor prevents post-ischemic heart failure by inhibition of apoptosis via calcineurin-mediated pathway and angiogenesis. *Arch Med Res* **39**, 179-188, (2008).
32 Giordano, F. J. *et al.* A cardiac myocyte vascular endothelial growth factor paracrine pathway is required to maintain cardiac function. *Proc Natl Acad Sci U S A* **98**, 5780-5785, (2001).
33 Zhang, M. *et al.* Cardiomyocyte grafting for cardiac repair: graft cell death and anti-death strategies. *J Mol Cell Cardiol* **33**, 907-921, (2001).
34 Chacko, S. M. *et al.* Myocardial oxygenation and functional recovery in infarct rat hearts transplanted with mesenchymal stem cells. *Am J Physiol Heart Circ Physiol* **296**, H1263-1273, (2009).
35 Gustafsson, A. B. & Gottlieb, R. A. Autophagy in ischemic heart disease. *Circ Res* **104**, 150-158, (2009).
36 Wang, Z. J. *et al.* Lipopolysaccharides can protect mesenchymal stem cells (MSCs) from oxidative stress-induced apoptosis and enhance proliferation of MSCs via Toll-like receptor(TLR)-4 and PI3K/Akt. *Cell Biol Int* **33**, 665-674, (2009).
37 Peterson, K. M., Aly, A., Lerman, A., Lerman, L. O. & Rodriguez-Porcel, M. Improved survival of mesenchymal stromal cell after hypoxia preconditioning: role of oxidative stress. *Life Sci* **88**, 65-73, (2011).
38 Rosova, I., Dao, M., Capoccia, B., Link, D. & Nolta, J. A. Hypoxic Preconditioning Results in Increased Motility and Improved Therapeutic Potential of Human Mesenchymal Stem Cells. *Stem Cells*, (2008).
39 Hu, X. *et al.* Hypoxic preconditioning enhances bone marrow mesenchymal stem cell migration via Kv2.1 channel and FAK activation. *American journal of physiology. Cell physiology* **301**, C362-372, (2011).
40 Gnecchi, M. *et al.* Evidence supporting paracrine hypothesis for Akt-modified mesenchymal stem cell-mediated cardiac protection and functional improvement. *Faseb J* **20**, 661-669, (2006).
41 Chacko, S. M. *et al.* Hypoxic preconditioning induces the expression of prosurvival and proangiogenic markers in mesenchymal stem cells. *Am J Physiol Cell Physiol* **299**, C1562-1570, (2010).
42 Tang, Y. L. *et al.* Hypoxic preconditioning enhances the benefit of cardiac progenitor cell therapy for treatment of myocardial infarction by inducing CXCR4 expression. *Circ Res* **104**, 1209-1216, (2009).
43 Hu, X. *et al.* Transplantation of hypoxia-preconditioned mesenchymal stem cells improves infarcted heart function via enhanced survival of implanted cells and angiogenesis. *J Thorac Cardiovasc Surg* **135**, 799-808, (2008).
44 Gaudette, G. R. *et al.* Determination of regional area stroke work with high spatial resolution in the heart. *Cardiovascular Engineering: An International Journal* **2**, 129-137, (2002).
45 Azeloglu, E. U. *et al.* High resolution mechanical function in the intact porcine heart: mechanical effects of pacemaker location. *J Biomech* **39**, 717-725, (2006).
46 Kochupura, P. V. *et al.* Tissue-engineered myocardial patch derived from extracellular matrix provides regional mechanical function. *Circulation* **112**, I144-149, (2005).
47 Kelly, D. J. *et al.* Increased Myocyte Content and Mechanical Function Within a Tissue-Engineered Myocardial Patch Following Implantation. *Tissue Eng Part A*, (2009).

## CHAPTER 6: Determine retention and cardiac differentiation of delivered cells

### 6.1. Introduction

Cellular therapy for cardiac applications has the potential for regenerating new myocardium for the restoration of healthy, functional tissue in diseased hearts. One of the main goals of cardiac cell therapy is to deliver viable, contractile cells that will contribute to active mechanical function, evoking a new optimism for treating the millions of people suffering from myocardial infarction (MI) and heart failure (HF).[1,2] As discussed in Chapter 2, several cell types have been investigated for the use in cardiomyoplasty.[1,3] Regardless of the chosen cell type, however, one of the most significant hurdles that remains in cardiac cell therapy is improving the retention and survival of implanted cells.[4,5] The infarcted heart is a dynamic environment: undergoing ischemia, inflammation, and cellular turnover while still being mechanically stretched by healthy, myocardium in the board-zone of the infarct. All of these factors have been shown to detriment the engraftment and survival of both native cardiomyocytes and delivered cells.[5-12] And if implanted cells cannot adhere and sustain healthy function, they will not be able to deliver therapeutic factors or contribute to active contraction to restore normal heart function. To overcome this hurdle, different strategies have been investigated to improve the retention and viability. Some groups have tried to improve retention and viability by developing and evaluating new methods of cell delivery. While other groups have devised *in vitro* strategies, either by cellular pre-conditioning methods to bolster delivered-cell resistance to apoptosis, or by increasing cell recruitment to injury sites when implanted *in vivo*.

In the evaluation of cardiomyoplasty techniques, the current methods for mesenchymal stem cell (MSC) delivery include intravenous (IV),[13,14] intracoronary (IC),[15] and intramyocardial (IM) injection,[15] as well as cell-seeded biomaterial scaffold implantation.[16-18] However, the current methods are inefficient, demonstrating low cell retention in the diseased heart or poor integration with native myocardium. Though IV delivery was identified as the least invasive technique, only 1% of the delivered MSCs migrated to the heart, while a majority of the cells were found to reside in the lungs.[13] The IC infusion technique was used in conjunction with angioplasty, in an attempt to improve targeted delivery

to the heart. However, only 3% of the delivered MSCs were found to engraft in the heart, while a majority of the cells exited the heart through the bloodstream into pulmonary circulation.[15] IM implantation is the most invasive of the injection techniques, but allows for direct, localized delivery controlled by the surgeon. Unfortunately, IM injection only increased engraftment to 11%, largely due to cell death and extravasation after needle retraction.[15] Cell-dosage and timing of treatment are also confounding factors with the injection techniques. Wolf *et al*. showed that engraftment percentage may depend significantly on the number of MSCs delivered, although the reported engraftment assessment still only estimated 1-3% retention (based on measurements of body weight and heart weight).[19] In a study to evaluate the optimal temporal delivery post-MI, Hu *et al*. determined that delivery at 1-week improved retention compared to either 1-hour or 2-week delivery time points.[20] However, this temporal assessment was based on limited histological evidence, and a full assessment of retention was not performed. The argument for delivery after 1-week post-MI is further strengthened by work which shows that apoptosis indices are significantly reduced at 7 days.[5]

To overcome the poor engraftment of injection techniques, cell-graft constructs or cell-seeded biomaterials have also been investigated for more efficient delivery of cells. Materials such as collagen,[16,17] fibrin,[21] gelatin,[22] alginate,[23] and extracellular matrix[18] have been cell-seeded and implanted in the heart. Oftentimes, the use of biomaterials adds another layer of complexity to the process. Cells need time to adhere onto the material and seeding efficiencies may be difficult to determine, therefore making it difficult to determine the number of cells being delivered to the heart upon implantation. Despite these challenges, scaffold-based cell delivery has been shown to increase cell engraftment in the heart to ~23%.[17] However, delivered cells tend to be retained within the scaffold volume, instead of integrating and coupling with native myocardium.[24] As cell-seeded biomaterials are typically implanted onto the epicardial surface of the heart, less than 1% of delivered cells have been found to traverse to the endocardium where most MIs occur.[17] Although biomaterial delivery increases the engraftment of implanted cells, it remains unclear whether the cells can incorporate into diseased regions for therapeutic or regenerative effects.

In addition to technical delivery approaches, others have explored biological approaches to increasing the retention of delivered cells. The biological approaches have been aimed at enhancing the resistance to apoptosis once cells are implanted in the MI or increasing cell recruitment to the infarct site. Some groups have genetically modified MSCs for the increase of both Akt and ILK,[25-27] which have been shown to block or inhibit stress- and anoikis-related apoptotic pathways. These studies showed that Akt or ILK transfected cells could improve cardiac function and angiogenesis in MIs, with a cell retention increase of ~2.5-4 times that of non-transfected MSCs. However, retention studies were performed with limited histological analysis, and total cell engraftment was not assessed. Beyond genetic modification, reduced-$O_2$ conditioning of MSCs has also been shown to increase prosurvival factors such as Akt, HIF-1α, survivin, and additional growth factors.[9,27-29] In addition, reduced-$O_2$ conditioning has been shown to increase the expression of MSC proteins that play a role in cell migration and homing to injured myocardium.[28-32] Reduced-$O_2$ conditioning increased MSC retention by ~3 times that of unconditioned MSCs,[32] and decreased delivered-MSC apoptosis by ~25%.[9] However, total cell engraftment of reduced-$O_2$ conditioned MSCs has not been analyzed. Additionally, the c-Met receptor has been shown to play a critical role in MSC motility and migration to injured tissue sites,[30,33] which is attributed to increases of HGF in these compromised regions. HGF has been shown to play roles in cardiomyogenesis,[34,35] cardiac cell survival,[36,37] and cardioprotective effects in ischemic myocardium.[38] In addition, HGF has also been shown to signaling for increased cell survival, retention, and myogenicity in other cell types used in cardiac repair (e.g. skeletal myoblasts).[39]

In contribution to this body of literature, we determined the retention of our implanted reduced-$O_2$/HGF conditioned hMSCs after 1 week. For comparison, we also determined the retention of implanted normal-$O_2$/MSCGM hMSCs at the same time point. To further characterize the fate of reduced-$O_2$/HGF conditioned hMSCs *in vivo*, we also stained histological sections to determine if our conditioned cells expressed cardiac-specific markers. To aid us in our analysis of delivered-cell retention and differentiation, we used a novel cell-tracking technique using quantum dot nanoparticles (QDs), which was previously developed in our lab.[40] Cells were passively loaded with QDs prior to

implantation *in vivo*. QDs are endocytosed by hMSCs, presenting as a punctate signal that resides within the cytoplasm (Figure 6.1). During histological analysis, delivered cells were identified by co-localizing QD-signal with nuclei counter-stained with Hoechst dye. Following 1-week survival periods, excised hearts were sectioned from base to apex, and sequential sections were analyzed.

### 6.1.1. Determining the retention of reduced-$O_2$/HGF conditioned hMSCs delivered to a myocardial infarct

As discussed above, cell retention is a major limitation of current cardiac cell therapy applications. However, limited analysis has shown that conditioning MSCs in reduced-$O_2$ can increase cell retention within an MI. An increase in cell retention suggests that reduced-$O_2$ conditioned MSCs may have more appropriate cellular mechanisms conducive for better survival in the dynamic MI environment, by being able to adapt to oxygen deprived tissues and oxidative stress to overcome associated apoptosis mechanisms.[11,41] In addition, we showed that reduced-$O_2$ conditioning of hMSCs can increase c-Met receptor expression (Chapter 3). Increased c-Met has been shown to improve hMSC motility and migration to injury sites,[30] which may also play a role in increased hMSC retention.[29]

In our analysis, we determined the cell retention of reduced-$O_2$/HGF hMSCs compared to normal-$O_2$/MSCGM hMSCs after 1 week. To determine these outcomes, cell-treated infarcted hearts from our 1-week *in vivo* studies were excised for histology. Three hearts from both treatment groups were bisected between the apex and base, at the approximate midline of the infarct, and then fixed in 4% paraformaldehyde. Cryosections (~8 μm thick) were made from the mid-infarct, out to either the base or the apex. Sections were pre-screened under a fluorescent microscope for QD signal, to determine the range of the cell-implant region. Positive sections were counter-stained with Hoechst nuclear dye, and then analyzed by fluorescent-detection microscopy. QD-positive cells were then counted in every 20$^{th}$ section.

### 6.1.2. Determining the cardiac-specific protein expression of reduced-$O_2$/HGF conditioned hMSCs delivered to a myocardial infarct

The ultimate goal of cardiomyoplasty is to replace diseased myocardium with new, contractile cells that can regenerate active mechanical function. The hope is that delivered cells can fully differentiate into mature cardiomyocyte phenotypes that integrate with healthy native myocardium. Therefore, we sought to determine the expression of cardiac-markers of reduced-$O_2$/HGF conditioned hMSCs after 1 week *in vivo*. As discussed in Chapter 3, some studies report that reduced-$O_2$ conditioning can increase MSC differentiation potential.[42-44] Also in Chapter 3, we showed that conditioning hMSCs with reduced-$O_2$/HGF could increase cardiac gene and protein expression *in vitro*. And when implanted into MIs *in vivo*, reduced-$O_2$/HGF conditioned hMSCs significantly improved regional mechanical function after 1 week, with increases in systolic area contraction that would suggest there may be myocardial shortening within our analyzed regions of interest. To determine if reduced-$O_2$/HGF conditioned cells express cardiac markers *in vivo*, sequential cryosections (~8 μm) from the hearts in our retention study were pre-screened for under a fluorescent microscope for QD-signal (cell tracking nanoparticles). QD-positive sections were then immunostained for cardiac-specific sarcomeric α-actinin and myosin heavy chain. Cryosections were then counterstained with Hoechst nuclear dye, and then analyzed by fluorescent-detection microscopy for protein expression and localization.

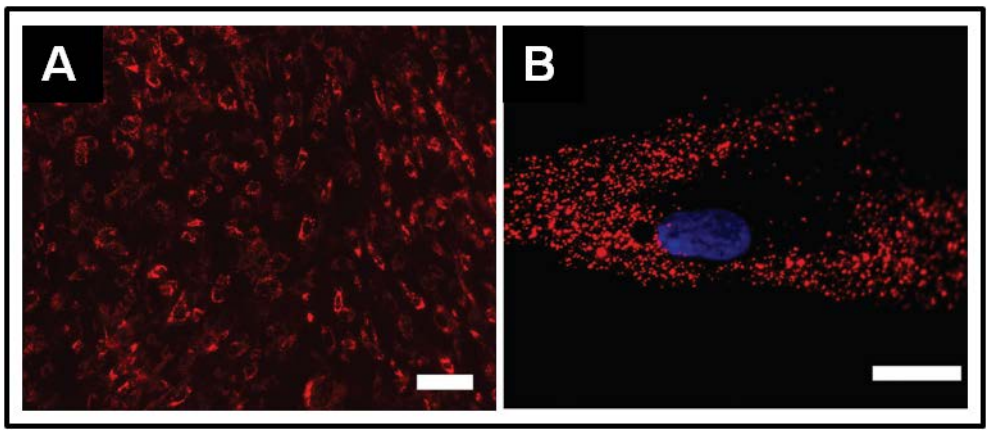


**Figure 6.1. Quantum-dot loading of hMSCs for cell-tracking *in vivo*.** (A) Quantum-dot (QD) nano-particles are endocytosed by hMSCs with high efficiency (scale bar = 100 μm). (B) Delivered hMSCs are identified by co-localizing cytoplasmic QD-signal with Hoechst-stained nuclei (scale bar = 25 μm). Figure adapted from Rosen *et al*., 2007.[40]

## 6.2. Materials and Methods

### 6.2.1. Quantum-Dot loading of hMSCs

In order to track delivered cells to determine cell retention and cardiac differentiation, hMSCs were pre-loaded with quantum dot nanoparticles (QDs; Invitrogen, #Q21321MP) prior to implantation. In preparation for *in vivo* delivery, hMSCs were treated with MSCGM supplemented with an 8.2 nM concentration of 655 ITK$^{TM}$ QDs on day 6 of the growth-media phase. QDs are passively endocytosed by hMSCs and reside in the cellular cytoplasm (Figure 6.1). Quantum dot cell-loading was assessed the 7$^{th}$ day of the initial growth-media treatment, to ensure sufficient loading and uniformity in all flasks across $O_2$/media treatments. After a 24-hour incubation in quantum dot supplemented MSCGM, cells were washed twice with sterile PBS (without calcium or magnesium; Cellgro, Manassas, VA; # 21-031-CV), and then treated for media conditioning.

Upon implantation, hMSCs retain QDs for the duration of several weeks. In the event of cell disruption, QDs are washed away through the lymphatic system. During histological analysis, QD-signal can be viewed under fluorescent-microscopy without additional histological staining techniques, and can be clearly distinguished from autofluorescence of native and diseased myocardium.

### 6.2.2. Histological Preparation

Excised hearts were bisected between the apex and base, with a midline cut through the infarct area (Figure 6.2). Hearts were fixed in 4% paraformaldehyde for 24 hours, then transferred to 30% sucrose and stored at 4°C until being processed for sectioning. For sectioning, each half of the rat heart was embedded in freezing O.C.T. Compound (Sakura Finetek USA Inc., Torrance, CA). Eight µm cryosections were cut from the embedded apex and base segments using a Leica CM3050 cryostat (-20°C specimen temperature; Leica Microsystems, Bannockburn, IL). Sections were cut from the midline bisect to the end of both the apex and base, so that each heart was fully sectioned (Figure 6.2). Sections were collected on positively-charged glass slides (3 sections/slide; VWR® Micro Slides; VWR International,

West Chester, PA). Slides were placed in slide boxes organized by experiment, and then stored in a freezer (≤ -20°C) to preserve the heart tissue sections.

### 6.2.3. Cell Retention Analysis

In this analysis, infarcted hearts treated reduced-$O_2$/HGF conditioned hMSCs (n = 3) were compared to infarcted hearts treated with normal-$O_2$/MSCGM conditioned hMSCs (n = 3) at the 1-week survival point. Cryosectioned heart slides were pre-screened for QD-signal prior to cell retention analysis. To do this, slides were removed from the freezer and immediately analyzed with an upright fluorescent microscope (Leica DMLB2) for the presence of QDs within the tissue. Starting with the first slide originating from the midline bisect, every 20$^{th}$ slide in both the apex and base directions were pre-screened in this fashion. After all slides were pre-screened, the established range of QD-positive slides was then analyzed for cell retention.

The range of QD-positive slides (every 20$^{th}$ slide from the midline, out to the last QD-positive slide in both the apex and base) was stained with Hoechst nuclear dye (1:6000 in PBS; Invitrogen Molecular Probes, Eugene, OR; # H3570), washed 3 times in PBS, and then coverslipped with Cytoseal-60$^{TM}$ mounting media (Richard Allan Scientific, Kalamazoo, MI). Each heart section was then analyzed with the Leica DMLB2 fluorescent microscope, systematically acquiring 40x images of QD-signal regions throughout entire sections. During data acquisition, pictures for each "40x area" were captured for both Hoechst-signal and QD-signal. Hoechst and QD images were then overlapped using Image J software (National Institutes of Health, Bethesda, MD). Implanted cells were identified by co-localizing QD-signal with Hoechst-stained nuclei.

Images were analyzed and QD-positive cells were counted by three individuals. Total QD-positive cell counts were calculated from each individual, and then an average QD-positive cell count was determined for each heart section (mean ± standard deviation). Total QD-positive cell counts from each section were plotted against location in the heart (from apex to base), and linear interpolation was used to estimate the number of QD-positive cells present in the sections between those analyzed. From these

interpolations, the total numbers of QD-positive hMSCs were approximated for each heart, and the two treated MI groups were compared.

### 6.2.4. Immunohistochemistry

For immunohistochemical analysis for cardiac-specific marker expression in implanted reduced-$O_2$/HGF conditioned hMSCs, sequential cryosections were stained from the same hearts used in our cell retention analysis. Prior to immunocytochemistry, heart sections were again pre-screened on an upright microscope (Leica DMLB2) for the presence of QD-signal. Sections showing positive signal were then processed for immunostaining of cardiac-specific sarcomeric α-Actinin and myosin heavy chain (MHC).

Slides were first rehydrated at room temperature for 3 minutes in PBS. Sections being prepared for sarcomeric α-Actinin were permeablized with cold acetone at -20°C for 10 minutes. Sections being prepared for MHC were permeablized with cold methanol at -20° for 20 minutes. The sections were then washed 3 times (5 minutes each) on a rotator with a solution of PBS with 0.05% Tween 20 (Sigma-Aldrich #P1379). Sections were blocked for an hour at room temperature with 1.5% serum in PBS (Normal Goat Serum, Invitrogen, # 016201; or Normal Rabbit Serum, Dako, # X0902). After blocking, sections were treated with primary antibody for sarcomeric α-actinin (Sigma-Aldrich, # A7811) or MHC (Chemicon, part of Millipore; # MAB1552) in PBS with 1.5% serum (of secondary antibody host), overnight at 4$^{o}$C. After primary antibody incubation, sections were washed 3 times (5 minutes each) before being treated with secondary antibody (Invitrogen Alexa Fluor 488 Rabbit anti-Goat, # A11078; Invitrogen Alexa Fluor 488 Goat anti-Rabbit, # A11008; or Invitrogen Alexa Fluor 488 Rabbit anti-Mouse, # A11059) in PBS with 1.5% serum (of the secondary antibody host), at room temperature for 1 hour. The sections were then washed 2 times in PBS (5 minutes each) on a rotator, and then counterstained with Hoechst 33342 nuclear dye (Sigma-Aldrich, # H3570) at a concentration of 1:6000 in PBS. The slides were then washed 3 final times in PBS (5 minutes each), and then coverslipped with Cytoseal-60$^{TM}$. Sections were then analyzed using a confocal microscope, for co-localization of QD-positive cells with either sarcomeric α-Actinin or MHC signal.

### 6.2.5. Microscopy and post-processing

For pre-screening and cell retention analysis, sections were analyzed using a Leica DMLB2 fluorescent microscope, fitted with a Leica DFC480 camera, used in conjunction with the Leica Application Suite software (Leica Microsystems Inc., Buffalo Grove, IL). Immunohistochemistry analysis was performed using a Leica TCS SP5 Spectral Confocal based on a Leica DM16000 Inverted research microscope, equipped with Leica Application Suite AF software. Images were post-processed for scale and re-sizing, using Image J software (National Institutes of Health, Bethesda, MD).

### 6.2.6. Statistical Analysis

Data for cell retention analysis is reported as mean ± standard deviations as multiple observations were made for each sample. Differences between the 2 treated-MI groups were determined using a Student's unpaired t-test with significance established for p-values $\leq 0.05$.

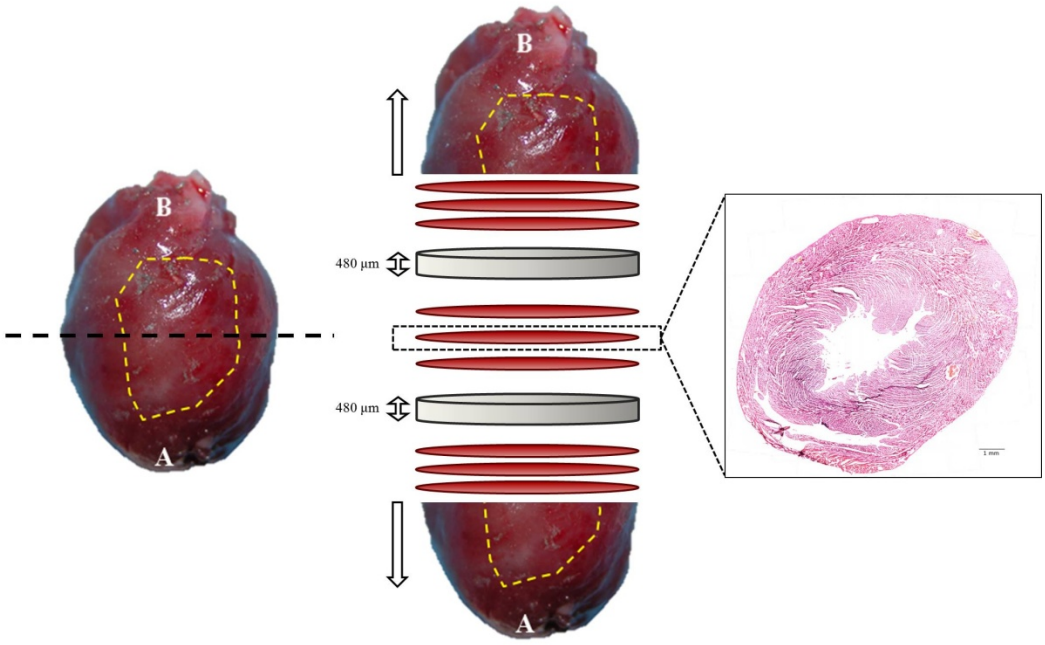


**Figure 6.2. Schematic of histological preparation.** For histological analysis, hearts were excised and bisected between the base ("B") and the apex ("A"). Apexes and bases were frozen in O.C.T media, and 8 µm cryosections were cut from the midline out to each end. Three sections were collected onto each slide. Every 20$^{th}$ slide was analyzed for cell retention, leaving 480 µm of tissue between each analyzed slide. Subsequent slides were analyzed by immunohistochemistry for cardiac-specific proteins.

## 6.3. Results

For our histological analysis, excised hearts were bisected within the myocardial infarct (MI) region, and then 8 μm cryosections were cut from the midline to ends of both the apex and base, so that each heart was fully sectioned (Figure 6.2). Prior to cell retention or immunohistochemical analysis, selected slides were pre-screened under an upright fluorescent microscope to identify quantum-dot (QD) loaded hMSCs. For cell retention studies, MIs treated reduced-$O_2$/HGF conditioned hMSCs (n = 3) were compared to MIs treated with normal-$O_2$/MSCGM conditioned hMSCs (n = 3) at the 1-week survival time point. Every 20$^{th}$ slide in both the apex and base directions were pre-screened and then counter-stained with Hoechst nuclear dye, and then QD-positive cells were counted in each section. With about 480 μm of tissue being skipped between slides, a linear interpolation was used between counted sections for a total cell count of QD-positive hMSCs. For immunohistochemical studies, cryosections from infarcted hearts treated reduced-$O_2$/HGF conditioned hMSCs were stained for cardiac-specific markers. Sequential sections from the cell retention study were used, and QD-positive cells were identified and analyzed for marker expression with a confocal microscope.

### 6.3.1. Cell retention of reduced-$O_2$/HGF conditioned hMSCs implanted into a myocardial infarct after 1 week

To analyze cell retention, hMSCs were loaded with QD-nanoparticles prior to implantation in order to track delivered cells within the myocardium. During cell preparation, quantum dot cell-loading was assessed to ensure sufficient loading and uniformity in all flasks across $O_2$/media treatments. During implantation, 1 million QD-loaded cells were delivered to each heart. Delivered cells were identified in analyzed cryosections by co-localizing QD-signal with Hoechst counterstained nuclei. Qualitative analysis indicated that there were more QD-positive cells in MIs treated with reduced-$O_2$/HGF conditioned hMSCs compared to MIs treated with traditional normal-$O_2$/MSCGM hMSCs (Figure 6.3). For a more quantitative analysis, every 20$^{th}$ slide was analyzed in 3 hearts treated with reduced-$O_2$/HGF hMSCs and 3 hearts treated with normal-$O_2$/MSCGM hMSCs. QD-positive cells were counted in each

section by 3 individuals, and then averaged cell numbers were calculated for every analyzed section throughout each heart. Plotting average cell number over the distance in each heart, results indicated that there were more QD-positive cells in MIs treated with reduced-$O_2$/HGF conditioned hMSCs compared to MIs treated with traditional normal-$O_2$/MSCGM hMSCs (Figure 6.4). Assuming a linear interpolation for QD-positive cells in the tissue between analyzed cryosections, total QD-positive cell counts were calculated in each heart. Cell counts for the hearts in each group were averaged, and the two treated MI groups were compared using a Student's t-test. Results showed that 13.5% of the reduced-$O_2$/HGF hMSCs were retained (135,216 ± 42,044 cells), which was significantly higher than the 3.9% retention of the normal-$O_2$/MSCGM hMSCs (38,952 ± 30,261 cells; $p < 0.02$; Figure 6.5).

### 6.3.2. Cardiac differentiation of reduced-$O_2$/HGF conditioned hMSCs *in vivo*

To determine cardiac-marker expression *in vivo*, sequential cryosections from infarcted hearts treated reduced-$O_2$/HGF conditioned hMSCs were stained for either sarcomeric α-Actinin or myosin heavy chain (MHC), and then counterstained with Hoechst nuclear dye. Again, delivered cells were identified by co-localizing QD-signal with Hoechst stained nuclei. Our results indicate that some of implanted reduced-$O_2$/HGF hMSCs can express sarcomeric α-Actinin (Figure 6.6) and MHC (Figure 6.7) after 1 week, though co-localization of the two cardiac proteins was not determined. In addition, we found a number of retained reduced-$O_2$/HGF hMSCs that do not express either cardiac-specific protein. In further analysis of immunostained sections, reduced-$O_2$/HGF hMSCs showing positive cardiac-marker expression tended to reside near or within MI border-zone regions.

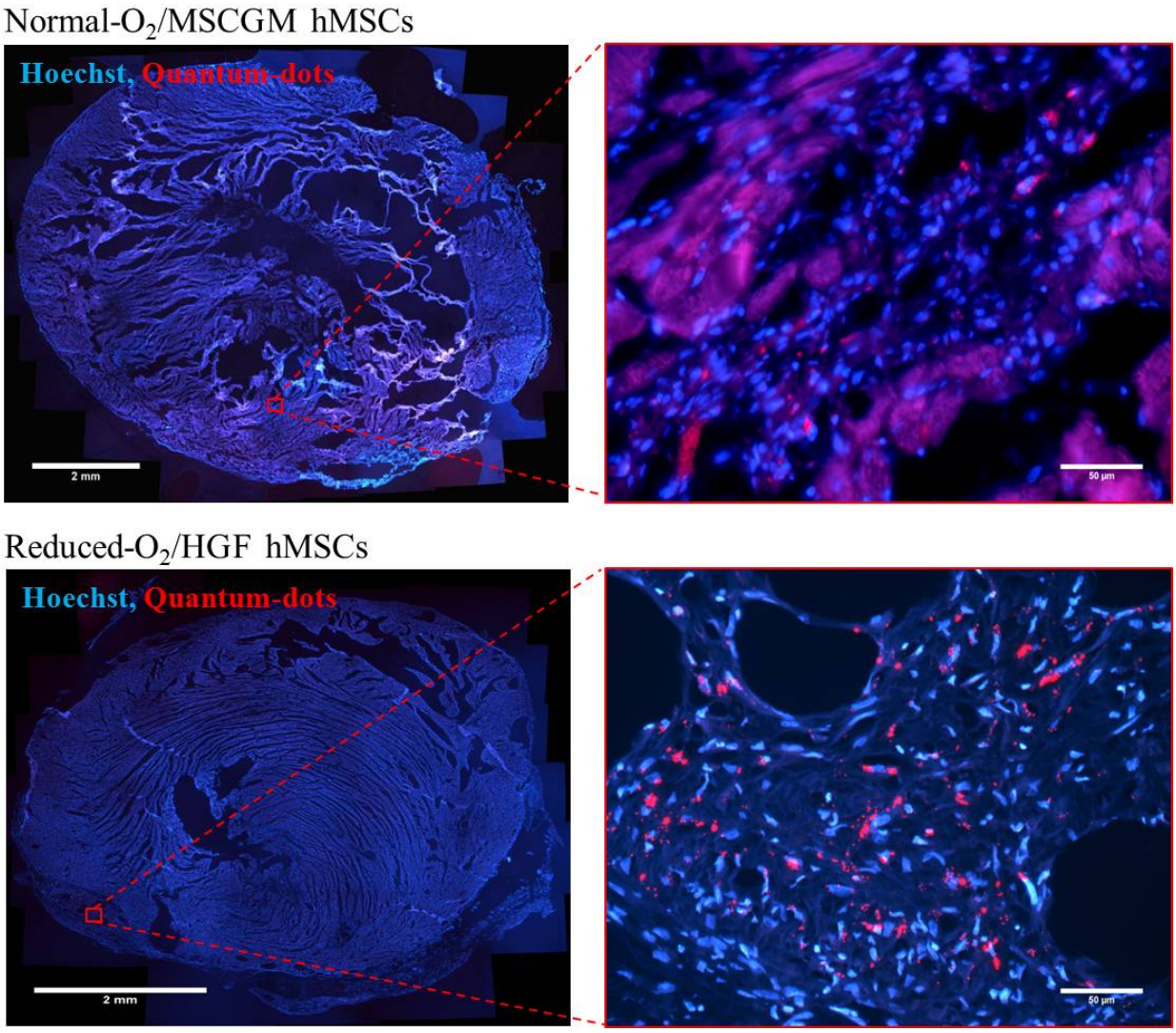


**Figure 6.3. Representative histological sections for cell retention analysis.** For cell retention analysis, infarcted hearts treated with normal-$O_2$/MSCGM hMSCs were compared to infarcted hearts treated with reduced-$O_2$/HGF hMSCs. Cryosections were counterstained with Hoechst nuclear dye. Whole sections were scanned QD-signal, and then regions of QD-signal were analyzed at a higher magnification to count QD-positive cells. The representative images in this figure illustrate our qualitative results, indicating a higher retention of reduced-$O_2$/HGF hMSCs than normal-$O_2$/MSCGM hMSCs, depicted by a higher QD-signal content.

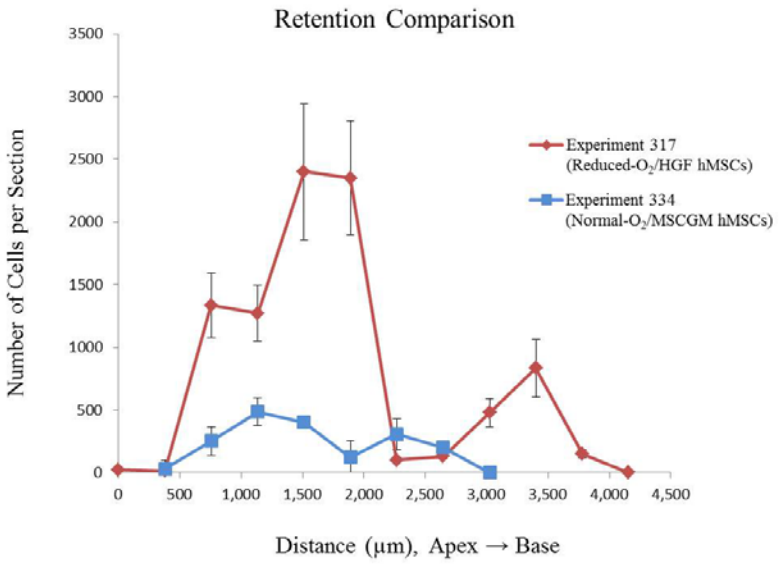


**Figure 6.4. Representative cell retention data.** For a quantitative assessment, QD-positive cells were counted in 3 infarcted hearts treated with normal-$O_2$/MSCGM hMSCs and 3 infarcted hearts treated with reduced-$O_2$/HGF hMSCs. For each heart, QD-positive hMSCs were counted in every 20$^{th}$ slide, throughout the entire heart (apex to base). Each slide was counted by 3 individuals, and cell counts were summed and plotted over the cryosection distance. The representative data in this graph depicts one heart treated with normal-$O_2$/MSCGM hMSCs versus one heart treated with reduced-$O_2$/HGF hMSCs. Overall, it appears that more reduced-$O_2$/HGF hMSCs were retained at throughout the analyzed hearts. Data is reported as mean ± standard deviation. Individual hearts from each group were not intended to be compared head-to-head, therefore statistical analysis was not performed in this comparison.

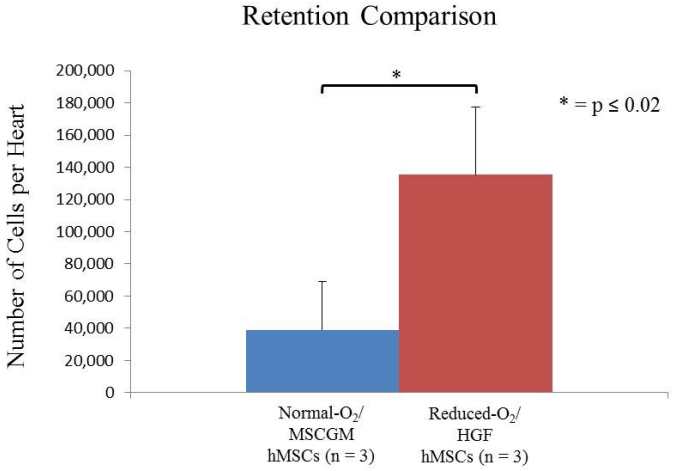


**Figure 6.5. Compiled cell retention analysis.** Using a linear interpolation between counted cryosections, a total QD-positive cell count was determined for each heart. Total QD-positive cell counts for hearts in both groups were averaged, respectively. Our quantitative analysis shows a significantly higher retention of reduced-$O_2$/HGF hMSCs than normal-$O_2$/MSCGM hMSCs. Differences were evaluated using a Student's unpaired t-test, and were considered significant for p-values $\leq 0.05$. Error bars indicate standard deviation.

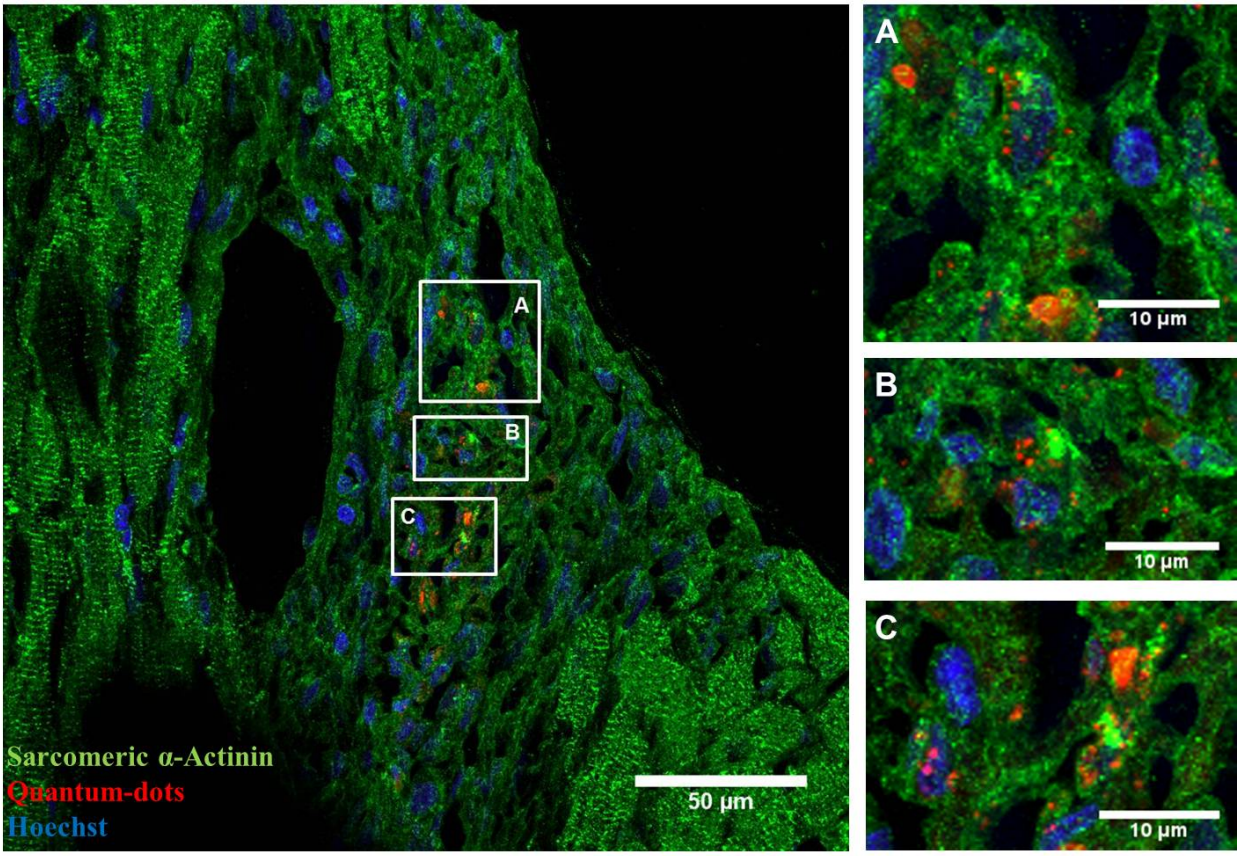


**Figure 6.6. Sarcomeric α-Actinin expression of implanted reduced-$O_2$/HGF conditioned hMSCs.**

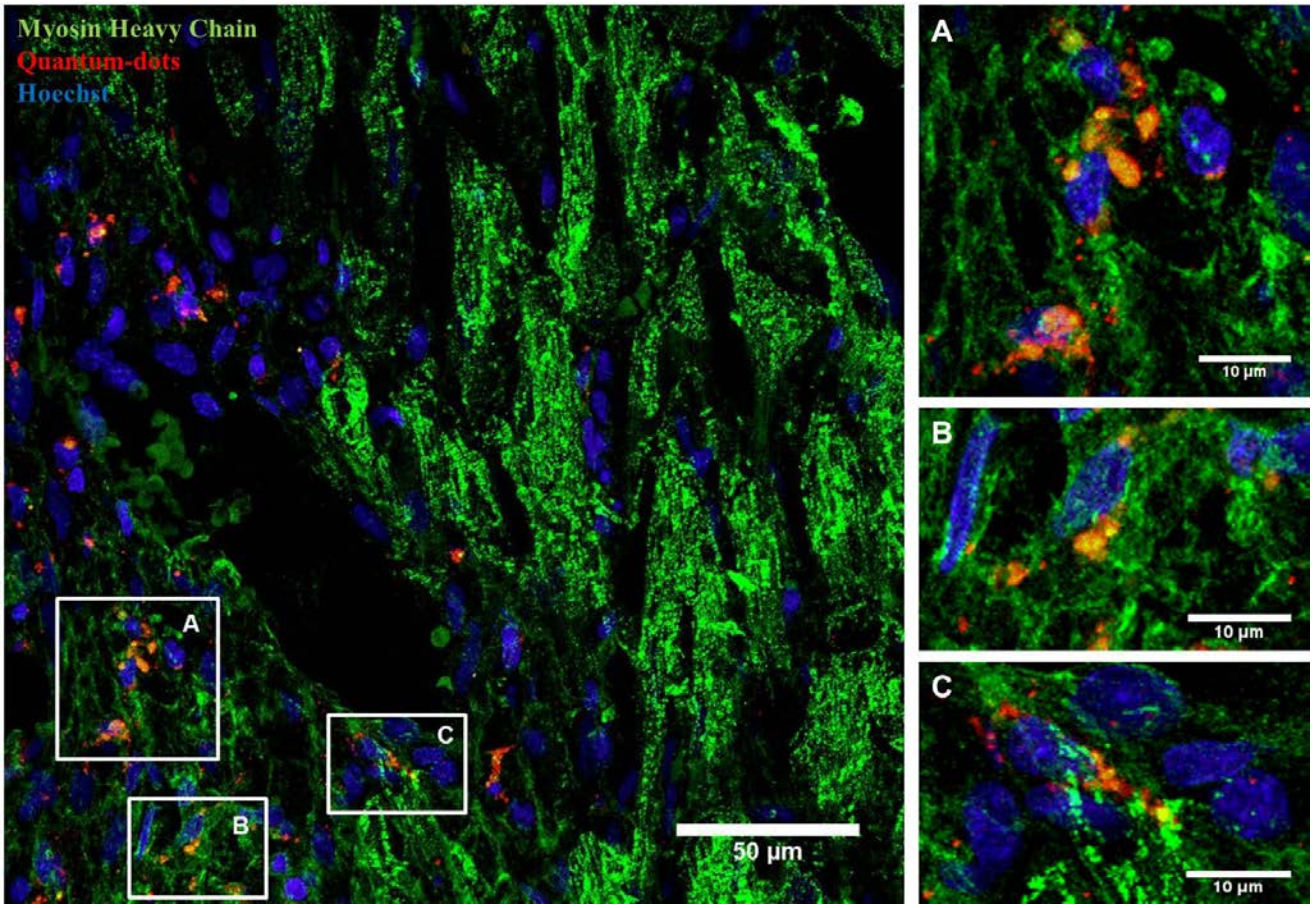


**Figure 6.7. Myosin Heavy Chain expression of implanted reduced-$O_2$/HGF conditioned hMSCs.**

## 6.4. Discussion

To account for the possible mechanisms responsible for the increases in regional mechanical function observed in Chapter 5, we also evaluated delivered-cell retention and cardiac-specific marker expression *in vivo*. In a comparative study of cell-treated MIs at 1-week, there was a significantly higher retention of reduced-$O_2$/HGF hMSCs than traditionally cultured normal-$O_2$/MSCGM hMSCs. During cell delivery, we made 5 IM injections of (10 µL each) to implant 1 million cells within the infarcted myocardium. In our retention study, we analyzed every 20$^{th}$ slide in each heart, leaving ~480 µm of sectioned tissue between analyzed slides for additional assays (e.g. immunohistochemistry of implanted cells). To determine total cell retention, we assumed a linear interpolation between analyzed cryosections to account for delivered cells in the unanalyzed tissue. Given that our delivery method consisted of 5 injection locations that were chosen randomly within the infarct region, a linear interpolation model may not be optimum for determining delivered cells in unanalyzed tissue (and ultimately, total cell retention). However, a preliminary analysis of sequential slides revealed that cryosections immediately before and after the analyzed sections were found to contain similar numbers of QD-loaded hMSCs to the sections that were counted. However, we also knew that the number of delivered cells had to increase/decrease throughout the 480 µm of unanalyzed tissue, depending on the differences in cell counts at each analyzed section. In our assumption, we also neglected to consider the phenomena of delivered-cell proliferation and migration. However, we made sure to section each heart entirely from base to apex, and analyze cryosections through the entire distance of the infarct region. Of the cryosections that were analyzed, whole-section scans were made to identify and count multiple regions of QD-loaded cells. While there were definite increases/decreases of QD-loaded cells from one analyzed section to another, we were confident that we could identify multiple injection sites, and our preliminary analysis of sequential sections gave us confidence that a linear interpolation would provide a reasonably accurate assessment.

Previous studies suggest that increased retention of delivered cells can further enhance cardiac function, by adding more elements that contribute to both passive and active mechanics. In addition, a higher retention of cells would tend to suggest an increased delivery of signaling factors that would limit

infarct size and cardiomyocyte death. These may be contributing factors for the realized improvements in regional mechanical functional. In a future study, an assessment of delivered-cell retention could also be done in the 1-month hearts to investigate whether delivered cells are retained longer-term. It may be possible that there are less hMSCs in 1-month hearts than 1-week hearts, which may suggest that cells are lost over time but serve a short-term benefit for lasting functional recovery. It is also possible that there are more hMSCs in 1-month hearts due to delivered-cell proliferation. However, if more cells are present at 1-month, our functional results indicate that they did not significantly affect regional mechanics. Alternatively, it may be possible that there are a similar number of hMSCs in 1-month and 1-week hearts, foregoing mechanisms of cell death or proliferation. In this case, delivered hMSCs may serve a more long-term functional role by fully differentiating into contractile cardiomyocytes or by supporting native cardiomyocytes in a cardioprotective capacity.

Our immunohistochemical analysis of cell-treated hearts at 1-week showed that some of the implanted reduced-$O_2$/HGF hMSCs appeared to stain positive for sarcomeric α-Actinin and myosin heavy chain. However, it is unclear whether the proteins are arranged in a typical sarcomeric phenotype. The data would suggest that these cells have the appropriate cellular machinery to form contractile elements. However, it is possible that they still are only partially differentiated *in vivo*. There is a possibility that our QD-loaded cells have fused with native cardiomyocytes *in vivio*, as reported in previous studies.[45-47] In our confocal microscopy analysis, however, the inset regions we analyzed indicated α-actinin and myosin heavy chain staining was co-localized with Hoechst-stained nuclei surrounded by quantum dot signal. It is still possible that our delivered cells fused with native cardiomyocytes and have become integrated within the myocardium, but our analysis would also strongly suggest that our delivered cells are expressing cardiac specific markers independently of surrounding myocytes.

Further analysis on 1-month hearts may reveal whether implanted cells can display mature cardiac phenotypes with more time *in vivo*. In addition, it remains unclear how many of the delivered reduced-$O_2$/HGF hMSCs express these markers. Even with Figures 6.6 and 6.7, there is evidence of QD-loaded hMSCs that do not express sarcomeric α-Actinin or myosin heavy chain. In future histological analysis, it

may be possible to count the number of hMSCs expressing cardiac-specific proteins. In addition, it may be possible to correlate the number of cardiogenic hMSCs with the observed increases in regional mechanical function. In doing this, it may be possible to gauge how many regenerated or new cardiomyocytes are needed in order to achieve quantifiable improvements in cardiac function.

## 6.5. References


1 Guyette, J. P., Cohen, I. S. & Gaudette, G. R. Strategies for regeneration of heart muscle. *Crit Rev Eukaryot Gene Expr* **20**, 35-50, (2010).

2 Gaudette, G. R. & Cohen, I. S. Cardiac regeneration: materials can improve the passive properties of myocardium, but cell therapy must do more. *Circulation* **114**, 2575-2577, (2006).

3 Schuldt, A. J., Rosen, M. R., Gaudette, G. R. & Cohen, I. S. Repairing damaged myocardium: evaluating cells used for cardiac regeneration. *Curr Treat Options Cardiovasc Med* **10**, 59-72, (2008).

4 Proulx, M. K. *et al.* Fibrin microthreads support mesenchymal stem cell growth while maintaining differentiation potential. *J Biomed Mater Res A* **96**, 301-312, (2011).

5 Zhang, M. *et al.* Cardiomyocyte grafting for cardiac repair: graft cell death and anti-death strategies. *J Mol Cell Cardiol* **33**, 907-921, (2001).

6 Reinecke, H., Zhang, M., Bartosek, T. & Murry, C. E. Survival, integration, and differentiation of cardiomyocyte grafts: a study in normal and injured rat hearts. *Circulation* **100**, 193-202, (1999).

7 Chang, S. A. *et al.* Impact of Myocardial Infarct Proteins and Oscillating Pressure on the Differentiation of Mesenchymal Stem Cells: Effect of Acute Myocardial Infarction on Stem Cell Differentiation. *Stem Cells*, (2008).

8 Uchiyama, T., Engelman, R. M., Maulik, N. & Das, D. K. Role of Akt signaling in mitochondrial survival pathway triggered by hypoxic preconditioning. *Circulation* **109**, 3042-3049, (2004).

9 Hu, X. *et al.* Transplantation of hypoxia-preconditioned mesenchymal stem cells improves infarcted heart function via enhanced survival of implanted cells and angiogenesis. *J Thorac Cardiovasc Surg* **135**, 799-808, (2008).

10 Vanhoutte, D., Schellings, M., Pinto, Y. & Heymans, S. Relevance of matrix metalloproteinases and their inhibitors after myocardial infarction: a temporal and spatial window. *Cardiovasc Res* **69**, 604-613, (2006).

11 Suzuki, K. *et al.* Dynamics and mediators of acute graft attrition after myoblast transplantation to the heart. *Faseb J* **18**, 1153-1155, (2004).

12 Robey, T. E., Saiget, M. K., Reinecke, H. & Murry, C. E. Systems approaches to preventing transplanted cell death in cardiac repair. *J Mol Cell Cardiol* **45**, 567-581, (2008).

13 Kraitchman, D. L. *et al.* Dynamic imaging of allogeneic mesenchymal stem cells trafficking to myocardial infarction. *Circulation* **112**, 1451-1461, (2005).

14 Barbash, I. M. *et al.* Systemic delivery of bone marrow-derived mesenchymal stem cells to the infarcted myocardium: feasibility, cell migration, and body distribution. *Circulation* **108**, 863-868, (2003).

15 Hou, D. *et al.* Radiolabeled cell distribution after intramyocardial, intracoronary, and interstitial retrograde coronary venous delivery: implications for current clinical trials. *Circulation* **112**, I150-156, (2005).

16 Thompson, C. A. *et al.* Percutaneous transvenous cellular cardiomyoplasty. A novel nonsurgical approach for myocardial cell transplantation. *Journal of the American College of Cardiology* **41**, 1964-1971, (2003).

17 Simpson, D., Liu, H., Fan, T. H., Nerem, R. & Dudley, S. C., Jr. A tissue engineering approach to progenitor cell delivery results in significant cell engraftment and improved myocardial remodeling. *Stem Cells* **25**, 2350-2357, (2007).

18 Potapova, I. A. *et al.* Enhanced recovery of mechanical function in the canine heart by seeding an extracellular matrix patch with mesenchymal stem cells committed to a cardiac lineage. *Am J Physiol Heart Circ Physiol* **295**, H2257-2263, (2008).

19 Wolf, D. *et al.* Dose-dependent effects of intravenous allogeneic mesenchymal stem cells in the infarcted porcine heart. *Stem cells and development* **18**, 321-329, (2009).

20 Hu, X. *et al.* Optimal temporal delivery of bone marrow mesenchymal stem cells in rats with myocardial infarction. *Eur J Cardiothorac Surg* **31**, 438-443, (2007).

21 Christman, K. L. *et al.* Injectable fibrin scaffold improves cell transplant survival, reduces infarct expansion, and induces neovasculature formation in ischemic myocardium. *Journal of the American College of Cardiology* **44**, 654-660, (2004).

22 Ozawa, T. *et al.* Optimal biomaterial for creation of autologous cardiac grafts. *Circulation* **106**, I176-182, (2002).

23 Leor, J. *et al.* Bioengineered cardiac grafts: A new approach to repair the infarcted myocardium? *Circulation* **102**, III56-61, (2000).

24 Davis, M. E., Hsieh, P. C., Grodzinsky, A. J. & Lee, R. T. Custom design of the cardiac microenvironment with biomaterials. *Circulation research* **97**, 8-15, (2005).

25 Song, S. W. *et al.* Integrin-linked kinase is required in hypoxic mesenchymal stem cells for strengthening cell adhesion to ischemic myocardium. *Stem Cells* **27**, 1358-1365, (2009).
26 Noiseux, N. *et al.* Mesenchymal stem cells overexpressing Akt dramatically repair infarcted myocardium and improve cardiac function despite infrequent cellular fusion or differentiation. *Mol Ther* **14**, 840-850, (2006).
27 Gnecchi, M. *et al.* Evidence supporting paracrine hypothesis for Akt-modified mesenchymal stem cell-mediated cardiac protection and functional improvement. *Faseb J* **20**, 661-669, (2006).
28 Liu, H. *et al.* Hypoxic preconditioning advances CXCR4 and CXCR7 expression by activating HIF-1alpha in MSCs. *Biochemical and biophysical research communications* **401**, 509-515, (2010).
29 Chacko, S. M. *et al.* Hypoxic preconditioning induces the expression of prosurvival and proangiogenic markers in mesenchymal stem cells. *Am J Physiol Cell Physiol* **299**, C1562-1570, (2010).
30 Rosova, I., Dao, M., Capoccia, B., Link, D. & Nolta, J. A. Hypoxic Preconditioning Results in Increased Motility and Improved Therapeutic Potential of Human Mesenchymal Stem Cells. *Stem Cells*, (2008).
31 Hung, S. C. *et al.* Short-term exposure of multipotent stromal cells to low oxygen increases their expression of CX3CR1 and CXCR4 and their engraftment in vivo. *PLoS ONE* **2**, e416, (2007).
32 Tang, Y. L. *et al.* Hypoxic preconditioning enhances the benefit of cardiac progenitor cell therapy for treatment of myocardial infarction by inducing CXCR4 expression. *Circ Res* **104**, 1209-1216, (2009).
33 Forte, G. *et al.* Hepatocyte growth factor effects on mesenchymal stem cells: proliferation, migration, and differentiation. *Stem Cells* **24**, 23-33, (2006).
34 Roggia, C., Ukena, C., Bohm, M. & Kilter, H. Hepatocyte growth factor (HGF) enhances cardiac commitment of differentiating embryonic stem cells by activating PI3 kinase. *Exp Cell Res* **313**, 921-930, (2007).
35 Rappolee, D. A., Iyer, A. & Patel, Y. Hepatocyte growth factor and its receptor are expressed in cardiac myocytes during early cardiogenesis. *Circulation research* **78**, 1028-1036, (1996).
36 Kitta, K. *et al.* Hepatocyte growth factor induces GATA-4 phosphorylation and cell survival in cardiac muscle cells. *J Biol Chem* **278**, 4705-4712, (2003).
37 Kitta, K., Day, R. M., Ikeda, T. & Suzuki, Y. J. Hepatocyte growth factor protects cardiac myocytes against oxidative stress-induced apoptosis. *Free radical biology & medicine* **31**, 902-910, (2001).
38 Duan, H. F. *et al.* Treatment of myocardial ischemia with bone marrow-derived mesenchymal stem cells overexpressing hepatocyte growth factor. *Molecular therapy : the journal of the American Society of Gene Therapy* **8**, 467-474, (2003).
39 Hill, E., Boontheekul, T. & Mooney, D. J. Designing scaffolds to enhance transplanted myoblast survival and migration. *Tissue Eng* **12**, 1295-1304, (2006).
40 Rosen, A. B. *et al.* Finding fluorescent needles in the cardiac haystack: tracking human mesenchymal stem cells labeled with quantum dots for quantitative in vivo three-dimensional fluorescence analysis. *Stem Cells* **25**, 2128-2138, (2007).
41 Peterson, K. M., Aly, A., Lerman, A., Lerman, L. O. & Rodriguez-Porcel, M. Improved survival of mesenchymal stromal cell after hypoxia preconditioning: role of oxidative stress. *Life Sci* **88**, 65-73, (2011).
42 Lennon, D. P., Edmison, J. M. & Caplan, A. I. Cultivation of rat marrow-derived mesenchymal stem cells in reduced oxygen tension: effects on in vitro and in vivo osteochondrogenesis. *J Cell Physiol* **187**, 345-355, (2001).
43 Lee, J. H. & Kemp, D. M. Human adipose-derived stem cells display myogenic potential and perturbed function in hypoxic conditions. *Biochem Biophys Res Commun* **341**, 882-888, (2006).
44 Kanichai, M., Ferguson, D., Prendergast, P. J. & Campbell, V. A. Hypoxia promotes chondrogenesis in rat mesenchymal stem cells: a role for AKT and hypoxia-inducible factor (HIF)-1alpha. *J Cell Physiol* **216**, 708-715, (2008).
45 Alvarez-Dolado, M. *et al.* Fusion of bone-marrow-derived cells with Purkinje neurons, cardiomyocytes and hepatocytes. *Nature* **425**, 968-973, (2003).
46 Nygren, J. M. *et al.* Bone marrow-derived hematopoietic cells generate cardiomyocytes at a low frequency through cell fusion, but not transdifferentiation. *Nat Med* **10**, 494-501, (2004).
47 Laflamme, M. A. & Murry, C. E. Regenerating the heart. *Nat Biotechnol* **23**, 845-856, (2005).

# CHAPTER 7: Conclusions and Future Work

## 7.1. Conclusions

This body of work aims to forward the approach of using exogenous hMSCs as a cell therapy for the dysfunctional heart. Since 2001, several preclinical and clinical studies have shown that hMSCs derived from adult bone marrow may have a limited capacity to regenerate myocardium and restore cardiac function. However, it remains unclear whether delivered hMSCs simply supply the heart with therapeutic signaling factors for cardioprotection, or whether hMSCs can fully differentiate into mature phenotypes that contribute to active mechanical function. Several differentiation strategies have been investigated to show that hMSCs can at least partially differentiate towards a cardiomyocyte lineage both *in vitro* and *in vivo*, showing cardiac-specific marker expression and calcium channel currents. Furthermore, partially-differentiated cardiogenic hMSCs have been implanted into canine hearts *in vivo* to show improved cardiac function compared undifferentiated, fully multipotent hMSCs.[1,2] These results demonstrate a unique paradigm in cell therapy, in which the implantation of partially-differentiated cells may have a greater capacity for mature, organ-specific phenotypes and functional roles.

Conditioning primitive hMSCs to adopt cardiac-specific genes and proteins will provide cells with the appropriate cellular machinery to further differentiate into mature phenotypes *in vivo*. In addition, the conditioned hMSCs with cardiogenic phenotype may be able to respond and adapt to cardiac microenvironmental cues for better retention, integration, and contribution to function. In 2008, our lab showed how mechanical manipulation of hMSCs by hanging drops could partially differentiate hMSCs towards a cardiac lineage and improve mechanical function of MIs *in vivo*.[1] Most recently, Behfar *et al*. showed that conditioning hMSCs with a "kitchen sink" cocktail of cytokines could induce cardiopoiesis, also expressing cardiac-markers *in vitro* and improving MI function *in vivo*.[3] Recent reviews suggest that conditioning hMSCs towards a cardiac lineage prior to implantation may improve both direct and indirect mechanisms of cardiac repair.[4-6] However, current strategies for cardiac differentiation of hMSCs are insufficient. Mechanical and chemical induction methods are technically challenging and tedious, while

several of the cardiac-differentiation mechanisms of these techniques remain undefined. These limitations contribute to the fact that current cardiac-differentiation strategies for hMSCs result in only a small number of cells becoming cardiogenic. Exploring new hMSC conditioning regimens may help to overcome the limitations of current differentiation methods. A simplistic strategy with fewer steps and factors may be more clinically applicable due to the ease of implementation; and a better understanding of how these simpler strategies induce cardiac-mechanisms may allow for an increased number of cardiogenic cells or degree of cardiac differentiation.

In this thesis we introduced a novel *in vitro* conditioning regimen, carefully designed to incorporate environmental cues found in MIs *in vivo* (e.g. decreased oxygen tension[7] and increased cell-signaling factors[8-10]). We exploited these cues for a simple strategy using reduced-$O_2$ culturing and HGF treatment to initiate cardiac differentiation of hMSCs *in vitro*. For the basis of this work, we hypothesized that applying a combined conditioning treatment of reduced-$O_2$ and HGF to hMSCs *in vitro* will enhance cardiac-specific gene and protein expression. Additionally, we hypothesized that the transplantation of conditioned hMSCs into an *in vivo* MI model will result in differentiation of delivered hMSCs and improved cardiac mechanical function. To test these hypotheses, we formulated three major objectives. In the first objective, we evaluated the effects of reduced-$O_2$ conditioning on hMSC growth kinetics and c-Met receptor expression. In the second objective, we determined the effects of reduced-$O_2$/HGF conditioning on cardiac-specific marker expression in hMSCs. And in the final objective, we implanted reduced-$O_2$/HGF conditioned hMSCs into MIs *in vivo* to evaluate regional cardiac mechanics, as well as delivered-cell retention and cardiac-marker expression.

In our initial studies, we showed that conditioning hMSCs in reduced-$O_2$ can significantly increase the number of population doublings and the number of passages compared to hMSCs traditionally grown in ambient oxygen conditions. Our analysis suggests that hMSCs may respond more positively to low-oxygen niche environments, and that hMSCs grown in reduced-$O_2$ are healthier, less inclined to senesce, and possibly more plastic or "stem-like" in their propensity to proliferate. Our initial studies also showed that hMSCs conditioned in reduced-$O_2$ could significantly increase expression of the c-Met receptor after

7 days in culture. As c-Met has been previously implicated in cardiomyogenesis,[11,12] our results suggest that there may be a finite window for initiating the cardiac program in hMSCs. This is an ongoing theme for scientists who study cardiac differentiation strategies in all stem cell types. Trying to find the optimum treatment to initiate cardiac differentiation is often highly dependent on timing, whether delivering certain growth factors by a chemical induction or forming embryoid bodies by a mechanical induction.

By exploiting the effects of conditioning hMSCs in reduced-$O_2$ to increase the expression of c-Met, we then investigated the effects of reduced-$O_2$/HGF conditioning on cardiac-specific marker expression in hMSCs *in vitro*. Our results showed that a combined conditioning regimen of reduced-$O_2$/HGF could elicit the expression of several cardiac genes and proteins in hMSCs, with an increased breadth of cardiac-specific marker expression than we previously achieved in our hanging-drop differentiation method. However, we did not analyze the effects of short term reduced-$O_2$ conditioning. It is possible that short term reduced-$O_2$ durations could provide a necessary signaling cascade for cardiac differentiation. In consideration of cellular processes, it may be necessary attenuate the proliferation effects of reduced-$O_2$ conditioning (described in Chapter 2), as proliferation often offsets the cellular processes needed for differentiation. Short-term exposure to reduced-$O_2$ may initiate necessary cardiac signaling events, but then transitioning the cells back to a less proliferative normal-$O_2$ environment may allow for further cardiac differentiation.

Using small-molecule inhibitors to target specific control points in our proposed HGF/c-Met pathway, we showed that decreases in c-Met or PI3K activation could attenuate cardiac gene expression. These results would suggest that the HGF/c-Met pathway and the PI3K effector protein are instrumental in initiating the cardiac-program in marrow-derived hMSCs.

We then implanted conditioned hMSCs to MIs *in vivo* and found that reduced-$O_2$/HGF conditioned hMSCs could significantly improve regional stroke work and systolic area contraction at 1-week and 1-month time points, compared to MIs treated with DMEM, normal-$O_2$/MSCGM hMSCs, or reduced-$O_2$/MSCGM hMSCs. To account for the possible mechanisms responsible for the increases in regional

mechanical function, we also evaluated delivered-cell retention and cardiac-specific marker expression *in vivo*. In a comparative study of MI treated hearts, there was a significantly higher retention of reduced-$O_2$/HGF conditioned hMSCs than traditionally cultured normal-$O_2$/MSCGM hMSCs. It is possible that the significant increases in cell retention of reduced-$O_2$/HGF conditioned hMSCs could account for the increases in cardiac mechanical function. With higher cell retention, it likely that delivered cells can attenuate scar formation and increase passive cardiac mechanics.[4,5] In addition, a significantly higher retention of delivered cells can supply more paracrine factors and cytokines to the infarcted heart, which may provide necessary signaling factors for native myocyte proliferation or native stem cell recruitment/differentiation.

However, our immunohistochemical analysis showed that some of the implanted reduced-$O_2$/HGF hMSCs stained positive for sarcomeric α-Actinin and myosin heavy chain. These results suggest that some of our implanted cells may be further differentiating towards a cardiomyocyte phenotype. Further analysis is needed to determine whether these cells are displaying sarcomere formation and spacing, as an indication of mature cardiomyocyte differentiation. Although these results are encouraging, only a small percentage of the delivered cells appear display cardiac protein expression indicative of sarcomere formation. Therefore, it may be unlikely that the increases we observed in cardiac mechanical function can be attributed to our delivered cells becoming functional, contractile cardiomyocytes. It is more likely that our delivered cells increased myocyte content in infarcted hearts by delivering signaling factors that either served a cardioprotective role to enhance the cell survival of native myocytes, or induced native myocytes to proliferate, or recruited native stem cells to differentiate into new myocytes.

As a whole, these data suggest that reduced-$O_2$/HGF conditioned hMSCs may be able to differentiate to a contractile cardiac phenotype, which may be capable of contributing active mechanical function in the diseased heart. With respect to the overall goal of cardiomyoplasty, this data adds support for the argument that conditioned “cardiogenic” hMSCs may be better than unconditioned hMSCs for replacing necrotic myocardium and restoring cardiac function. In a qualitative assessment by immunocytochemistry, it appears that our conditioning regimen can increase the number of hMSCs that

express cardiac specific markers. However, conditioned hMSCs do not show sarcomere formation *in vitro*, which suggests that they are partially differentiated "cardiogenic" cells. In consideration of using reduced-$O_2$/HGF conditioned hMSCs as a potential cardiac cell therapy, it may be more advantageous to implant partially differentiated cardiogenic cells *in vivo* rather than fully differentiated cardiac cells. Partially differentiated cardiogenic cells are more likely to adapt to specific cardiac regions (e.g. ventricle, atrium, epicardium, or endocardium) for more site-appropriate cardiac cell types; whereas fully differentiated cardiac cells may cause functional complications (e.g. arrhythmias) if implanted in the wrong regions of the heart. In further consideration of being able to deliver enough cells to regenerate the lost cardiomyocytes resulting from an MI, our results from Chapter 3 would indicated that reduced-$O_2$ conditioning can significantly increase the expansion of hMSCs. Combined with our reduced-$O_2$/HGF conditioning regimen, it is likely that we can generate billions of cardiogenic hMSCs for a potential cardiac cell therapy. At this point, it is unclear whether our partially differentiated cardiogenic cells can maintain cardiac-specific marker expression over successive cell passages. Therefore, it is likely that we would first have to expand the hMSCs in reduced-$O_2$ and growth medium, and then apply our reduced-$O_2$/HGF conditioning regimen for cardiogenic differentiation. Additionally, further analysis would be needed to determine whether late-passage hMSCs can still be conditioned for cardiac-specific marker expression.

With this being said, many fundamental scientific questions remain unanswered. It is still unclear whether enough hMSCs are being retained to regenerate an entire infarct. Likewise, it remains uncertain if enough hMSCs can fully differentiate to a mature cardiomyocyte phenotype, to significantly increase enough contractile mass to restore healthy cardiac function. As of yet, there have not been any studies to correlate increased myocyte content with improvements in function. Furthermore, additional studies are needed to determine if cardiogenic hMSCs are incorporating with host tissue for synchronous electrical and mechanical function. These questions necessitate further investigation.

## 7.2. Future Work

In order to address some of these outstanding questions regarding the use of hMSCs as a cardiac cell therapy, several aspects can be investigated in future *in vitro* and *in vivo* studies. Despite the reported successes of partially differentiating hMSCs toward a more cardiogenic phenotype, it remains unclear if hMSCs can fully differentiate into mature cardiomyocytes. And while reduced-$O_2$/HGF treated hMSCs show an increased breadth and expression of cardiac-specific genes and proteins, they do not demonstrate a striated contractile phenotype *in vitro*. In addition, it remains unclear if reduced-$O_2$/HGF conditioned hMSCs can fully differentiate into cardiomyocytes *in vivo* to contribute to active contraction, and whether the determined increases in function can be sustained longer-term.

Our small-molecule inhibitor experiments suggest that both c-Met and PI3K signaling are involved in cardiac differentiation of hMSCs. However, a complete picture of the signaling events required to drive the cardiac program in hMSCs remains largely undefined. Behfar *et al*. have also done some preliminary work to suggest that transforming growth factor β1, bone morphogenetic protein-4, Activin A, retinoic acid, insulin-like growth factor-1, fibroblast growth factor-2 (FGF-2), alpha-thrombin, and interleukin-6 (IL-6) may also be involved in the cardiac-pathway of hMSCs.[3] In consideration of these findings, we concede that there may be several key signaling events taking place in our system in addition to the HGF/c-Met pathway. In also considering that conditioned hMSCs have been shown to increase the secretion of prosurvival and growth factors,[13-15] it is likely that secreted factors may also have autocrine effects on the hMSCs. We have done some preliminary studies on the supernatants of reduced-$O_2$/HGF conditioned hMSCs, to quantify some of the cytokines involved in the Behfar study by ELISA. In our preliminary studies, we have found that reduced-$O_2$/HGF conditioned hMSCs can significantly increase the secretion of Activin A, FGF-2, and IL-6 compared to hMSCs grown in normal-$O_2$ or reduced-$O_2$ conditions (data not shown). This preliminary data suggests that reduced-$O_2$/HGF conditioning may elicit additional autocrine signaling cascades that may also contribute to the cardiac program in hMSCs. More work is needed to evaluate reduced-$O_2$/HGF conditioned hMSCs for the additional cytokines implicated in the Behfar study. An understanding of these factors and subsequent autocrine signaling pathways may

help to clarify the mechanisms involved in cardiac differentiation of hMSCs. Furthermore, it may be possible to exploit one or more of these factors to generate cardiogenic hMSCs with more mature myocyte phenotypes.

With induction timing playing an intricate role in cardiogenesis,[16-18] it is possible that reduced-$O_2$/HGF conditioning for 7 days is not a sufficient amount of time for complete cardiac differentiation in hMSCs. One simple future study would be to condition hMSCs with reduced-$O_2$/HGF for longer time points over the course of a month, to evaluate the presence of additional sarcomeric proteins and phenotypic presentation. From our *in vitro* differentiation study, we showed that reduced-$O_2$/HGF conditioned hMSCs can express markers corresponding with the L-type calcium channel. Another potential study would be to evaluate the functionality of the L-type calcium channel in reduced-$O_2$/HGF conditioned hMSCs using calcium dye imaging or patch clamping techniques. In addition, reduced-$O_2$/HGF hMSCs could be screened for additional cardiac ion-channel markers expression and functionality. Another potential *in vitro* aspect would be to investigate the effects of either mechanical or electrophysiological stimulation on redueced-$O_2$/HGF conditioned hMSCs. Previous studies have shown that inducing mechanical stretch or electrophysiological stimulation on cells *in vitro* can elicit functional properties similar to those generated *in vivo*.[19-21] In-house systems are readily available for these studies, such as the Flexcell® equibiaxial-stretch cell culturing system for mechanical stimulation, or the C-Pace™ electric pulse system for continuous electrical stimulation. Cells could be stimulated using parameters similar to *in vivo* conditions, and then cells could be evaluated for viability, orientation, cardiac-marker expression, and phenotypic presentation.

For *in vivo* analysis, there are several future work studies that can be generated from our initial experiments. Logically, we would want to analyze the 1-month excised hearts for cell retention and cardiomyocyte marker expression, and compare them with our 1-week results. Histochemical trichrome techniques could be used to determine the infarct size of 1-week and 1-month hearts; and it may be possible to determine MI volume by using a similar linear interpolation model to the one we used in our cell retention study. In addition, cryosections from 1-week and 1-month hearts treated with reduced-

$O_2$/HGF hMSCs can be stained for more cardiac markers (e.g. troponin I, connexin 43, and ventricular myosin light chain). Advanced multi-stain immunohistochemical techniques can also be applied to determine if implanted reduced-$O_2$/HGF hMSCs can express two or more cardiac markers in combination.

From a functional standpoint, immunostained cryosections could also be analyzed to count the number of cardiac-positive hMSCs in both 1-week and 1-month hearts. In doing this, it may be possible to correlate the number of delivered cardiogenic cells with functional increases observed at the 1-week and 1-month time points. Furthermore, additional *in vivo* studies can be designed to analyze the functional and histological effects of cell-treated MIs for longer survival time points. All of these functional studies would most likely require the development of novel analytical techniques (e.g. image analysis methods, correlation algorithms, or longer-term cell tracking systems). However, they would advance the field by beginning to address some of the outstanding limitations regarding cell therapy for cardiac applications.

## 7.3. References


1 Potapova, I. A. *et al.* Enhanced recovery of mechanical function in the canine heart by seeding an extracellular matrix patch with mesenchymal stem cells committed to a cardiac lineage. *Am J Physiol Heart Circ Physiol* **295**, H2257-2263, (2008).

2 Potapova, I. *et al.* Functional Regeneration of the Canine Ventricle Using Adult Human Mesenchymal Stem Cells Committed In Vitro to a Cardiac Lineage. *Circ Res* **99**, E19, (2006).

3 Behfar, A. *et al.* Guided cardiopoiesis enhances therapeutic benefit of bone marrow human mesenchymal stem cells in chronic myocardial infarction. *J Am Coll Cardiol* **56**, 721-734, (2010).

4 Gaudette, G. R. & Cohen, I. S. Cardiac regeneration: materials can improve the passive properties of myocardium, but cell therapy must do more. *Circulation* **114**, 2575-2577, (2006).

5 Cohen, I. S. & Gaudette, G. R. Regenerating the heart: new progress in gene/cell therapy to restore normal mechanical and electrical function. *Dialogues in Cardiovascular Medicine* **14**, 19, (2009).

6 Marban, E. & Malliaras, K. Boot camp for mesenchymal stem cells. *J Am Coll Cardiol* **56**, 735-737, (2010).

7 Chacko, S. M. *et al.* Myocardial oxygenation and functional recovery in infarct rat hearts transplanted with mesenchymal stem cells. *Am J Physiol Heart Circ Physiol* **296**, H1263-1273, (2009).

8 Vanhoutte, D., Schellings, M., Pinto, Y. & Heymans, S. Relevance of matrix metalloproteinases and their inhibitors after myocardial infarction: a temporal and spatial window. *Cardiovasc Res* **69**, 604-613, (2006).

9 Sutton, M. G. & Sharpe, N. Left ventricular remodeling after myocardial infarction: pathophysiology and therapy. *Circulation* **101**, 2981-2988, (2000).

10 Chang, S. A. *et al.* Impact of Myocardial Infarct Proteins and Oscillating Pressure on the Differentiation of Mesenchymal Stem Cells: Effect of Acute Myocardial Infarction on Stem Cell Differentiation. *Stem Cells*, (2008).

11 Roggia, C., Ukena, C., Bohm, M. & Kilter, H. Hepatocyte growth factor (HGF) enhances cardiac commitment of differentiating embryonic stem cells by activating PI3 kinase. *Exp Cell Res* **313**, 921-930, (2007).

12 Rappolee, D. A., Iyer, A. & Patel, Y. Hepatocyte growth factor and its receptor are expressed in cardiac myocytes during early cardiogenesis. *Circulation research* **78**, 1028-1036, (1996).

13 Sadat, S. *et al.* The cardioprotective effect of mesenchymal stem cells is mediated by IGF-I and VEGF. *Biochem Biophys Res Commun* **363**, 674-679, (2007).

14 Kanichai, M., Ferguson, D., Prendergast, P. J. & Campbell, V. A. Hypoxia promotes chondrogenesis in rat mesenchymal stem cells: a role for AKT and hypoxia-inducible factor (HIF)-1alpha. *J Cell Physiol* **216**, 708-715, (2008).

15 Chacko, S. M. *et al.* Hypoxic preconditioning induces the expression of prosurvival and proangiogenic markers in mesenchymal stem cells. *Am J Physiol Cell Physiol* **299**, C1562-1570, (2010).

16 Xu, C., Police, S., Rao, N. & Carpenter, M. K. Characterization and enrichment of cardiomyocytes derived from human embryonic stem cells. *Circ Res* **91**, 501-508, (2002).

17 Sartiani, L. *et al.* Developmental changes in cardiomyocytes differentiated from human embryonic stem cells: a molecular and electrophysiological approach. *Stem Cells* **25**, 1136-1144, (2007).

18 Kehat, I. *et al.* Human embryonic stem cells can differentiate into myocytes with structural and functional properties of cardiomyocytes. *J Clin Invest* **108**, 407-414, (2001).

19 Shimko, V. F. & Claycomb, W. C. Effect of Mechanical Loading on Three-Dimensional Cultures of Embryonic Stem Cell-Derived Cardiomyocytes. *Tissue Eng*, (2007).

20 McMahon, L. A., Campbell, V. A. & Prendergast, P. J. Involvement of stretch-activated ion channels in strain-regulated glycosaminoglycan synthesis in mesenchymal stem cell-seeded 3D scaffolds. *J Biomech* **41**, 2055-2059, (2008).

21 Kawano, S., Otsu, K., Shoji, S., Yamagata, K. & Hiraoka, M. Ca(2+) oscillations regulated by Na(+)-Ca(2+) exchanger and plasma membrane Ca(2+) pump induce fluctuations of membrane currents and potentials in human mesenchymal stem cells. *Cell Calcium* **34**, 145-156, (2003).